UNIVERSITAT POLITÈCNICA DE VALÈNCIA

PROGRAMA DE DOCTORADO

CIENCIA TECNOLOGÍA Y GESTIÓN ALIMENTARIA

DOCTORAL THESIS

Development and characterization of corn starch films by blending with more hydrophobic compounds

Rodrigo Ortega Toro

Supervisors:

Dra. Amparo Chiralt Boix, prof.

Dr. Pau Talens Oliag, prof.

Valencia, June 2015

Dra. AMPARO CHIRALT BOIX, CATEDRÁTICA DE UNIVERSIDAD Y Dr. PAU TALENS OLIAG, PROFESOR TITULAR DE UNIVERSIDAD DEL DEPARTAMENTO DE TECNOLOGÍA DE ALIMENTOS DE LA UNIVERSITAT POLITÈCNICA DE VALÈNCIA

CONSIDERAN: que la memoria titulada **Development and Characterization of corn starch films by blending with more hydrophobic compounds** que, para aspirar al grado de Doctor, presenta D. Rodrigo Ortega Toro, realizada bajo su dirección en el Instituto Universitario de Ingeniería de Alimentos para el Desarrollo (IuIAD) de la Universitat Politècnica de València, reúne las condiciones adecuadas para su presentación como tesis doctoral, por lo que **AUTORIZAN** al interesado su presentación en ese doctorado.

Valencia, 12 de Mayo de 2015

Fdo: Dra. Amparo Chiralt Boix
Directora de la tesis

Fdo: Dr. Pau Talens Oliag
Director de la tesis

This work has been founded by the Ministerio de Economía y Competitividad (Spain) through the Projects AGL2010-20694, AGL2013-42989-R, and the Santiago Grisolía grant GRISOLIA/2012/001 of Generalitat Valenciana.

A mi Padre

A mi Madre

A mi familia

AGRADECIMIENTOS

Gracias a todos los que de alguna forma me han acompañado día a día y también gracias a aquellos que en la distancia me han dado aliento para dar lo mejor de mí a cada instante.

Gracias especiales a Amparo y Pau por abrirme las puertas del grupo de investigación y darme su confianza, sin su apoyo este gran proyecto no se hubiera iniciado. Amparo, gracias porque con tu dedicación y el gran conocimiento que siempre transmites eres el mejor ejemplo a seguir. Pau, muchas gracias porque aparte de ser supervisor de esta tesis, en muchas ocasiones has actuado como un amigo aportándome las palabras y los consejos que necesitaba.

Gracias a mis compañeros (as) de laboratorio por darme anécdotas que recordaré durante toda mi vida. Gracias en especial a María José y a Alberto porque me apoyaron desde el inicio, cuando llegue al IuIAD… y me dieron las pautas adecuadas para continuar mi trabajo.

A los estudiantes de máster a quienes tuve la oportunidad de orientar en su trabajo final Jessica, Sofía, Amparo e Iris, gracias por su importante contribución.

Gracias a Sofi por darme amor, paz y alegría durante estos años. Gracias por apoyarme incondicionalmente y mostrarme lo importante que es amar conservar el equilibrio.

Desidero ringraziare Mario, Gabriella, Giovanna e Piero per avermi aiutato nel lavoro svolto all'Istituto per i Polimeri, Compositi e Biomateriali (IPCB) di Napoli (Italia). Il periodo trascorso all'IPCB ha rappresentato una esperienza che mi ha arricchito molto, caratterizzata da episodi molto belli e che, sicuramente, avranno un grande impatto sulla mia vita personale e professionale. Grazie a tutti i ragazzi dell'IPCB-CNR.

Para finalizar, quiero agradecer a mis padres, los he sentido muy cerca siempre. Gracias mamá por guiar mis primeros pasos hacia la ciencia y el arte. Gracias papá por apoyarme en cada momento de mi vida, gracias por enseñarme a ser un hombre responsable y a conservar la calma en momentos de inquietud.

Gracias a todos por todo… porque todo ha sido necesario para que se diera este momento.

DEVELOPMENT AND CHARACTERIZATION OF CORN STARCH FILMS BY BLENDING WITH MORE HYDROPHOBIC COMPOUNDS

ABSTRACT

Different strategies were used to improve physical properties of corn starch based films, with glycerol (30%) as plasticizer, based on increasing their hydrophobic character in order to reduce the materials' water sensitivity. Starch was blended with different components (surfactants and more hydrophobic polymers), with and without compatibilizers, to obtain blend films through different processing techniques (casting, melt blending, compression molding and extrusion). Bilayer film formation by compression molding with starch and poly(ε-caprolactone) (PCL) was also studied.

The addition of surfactants to starch films obtained by casting gave rise to a decrease in water vapor permeability (WVP), but an increase in the film fragility was observed. Surfactants with lower hydrophilic-lipophilic balance (HLB), solid at room temperature, promoted a fine microstructure in the matrix with smaller lipid particle, which enhanced water vapor barrier properties.

Thermo-processing was used to obtain the other films due to its broader industrial application. Starch blends with hydroxypropyl methylcellulose (HPMC) showed an HPMC dispersed phase in the starch matrix and better water barrier properties, but they were more permeable to oxygen, especially when they contained citric acid (CA) as compatibilizer. CA induced cross-linking in the polymeric matrix, thus slightly increasing film hardness, but decreasing its extensibility.

The incorporation of PCL in different ratios to starch films obtained by compression molding gave rise to polymer phase separation, although a small PCL miscibility in the starch rich phase was detected, which reduced the glass transition

temperature of the starch phase. The structural heterogeneity and lack of interfacial adhesion between polymers gave rise to fragile films. Nevertheless, small amounts of PCL (10%) reinforced the matrix (increase in the elastic modulus). When the PCL ratio increased, WVP was reduced but oxygen permeability increased. The incorporation of CA as compatibilizer of these blends provoked an increase in the water solubility of the films, by hydrolysis, and improved the mechanical properties of the films when PCL ratio was low (10%), but it did not affect the film barrier properties. The incorporation of polyethylene glycol (PEG 4000) to the blends with a low proportion of PCL did not imply an improvement in the film properties, since it promoted phase separation. Starch-PCL blends with 1:0.05 mass ratio, without compatibilizer, were quite homogenous and exhibited good mechanical properties and stability.

In order to incorporate greater amounts of PCL, thus improving film hydrophobicity and stability, PCL was chemically modified by grafting glycidyl methacrylate or glycidyl methacrylate and maleic anhydride (PCL_{-g}), to be used as compatibilizers. Films with 20 % PCL and 2.5 or 5 % of PCL_{-g} showed very good mechanical and barrier properties and stability, inhibiting starch retrogradation. Their barrier properties met the food packaging requirements for a wide number of food products.

Bilayer films obtained by compression molding of starch (or starch with 5% PCL) and PCL layers showed very low WVP and oxygen permeability and adequate mechanical properties. The adhesion of bilayers was greatly improved by the application of ascorbic acid and, especially, potassium sorbate, as aqueous solutions, at the interface before compression molding. These compounds, in turn, imparted antioxidant and antimicrobial properties, respectively, to the films, thus improving their potential use as active packaging material for food uses.

DESARROLLO Y CARACTERIZACIÓN DE PELÍCULAS DE ALMIDÓN DE MAÍZ POR MEZCLADO CON COMPUESTOS MÁS HIDROFÓBICOS

RESUMEN

Se han utilizado diversas estrategias para mejorar las propiedades físicas de films a base de almidón de maíz, con glicerol (30 %) como plastificante, basadas en el incremento de su carácter hidrofóbico, para reducir su sensibilidad al agua. El almidón se mezcló con diferentes compuestos (surfactantes y polímeros más hidrofóbicos), con y sin compatilizadores, para la obtención de films mixtos por diferentes técnicas de procesado (casting, mezclado en fundido, moldeo por compresión y extrusión). Se estudió también la formación de films bicapa almidón-poli-ε-caprolactona (PCL) mediante moldeo por compresión.

La adición de surfactantes a los films de almidón elaborados por casting dio lugar a una disminución de su permeabilidad al vapor de agua (WVP), pero aumentó su fragilidad. Los surfactantes con menor balance hidrófilo-lipófilo (HLB), y sólidos a temperatura ambiente, proporcionaron una microestructura de los films con menor tamaño de partícula, que potenció las propiedades barrera al vapor de agua.

Por su mayor aplicabilidad industrial, se emplearon técnicas de termo-procesado para la obtención del resto de films estudiados. Los obtenidos por mezcla con hidroxipropil metilcelulosa (HPMC) presentaron una fase dispersa de HPMC en la matriz de almidón y mejores propiedades barrera al vapor de agua, pero fueron algo más permeables al oxígeno, sobre todo cuando se incorporó ácido cítrico (CA) como compatibilizador. Este provocó entrecruzamiento en la matriz polimérica, incrementado ligeramente su dureza y reduciendo su extensibilidad.

La incorporación de PCL en diferentes proporciones a los films de almidón obtenidos por termo-compresión, dio lugar a la separación de fases polímericas, detectándose una pequeña miscibilidad de la PCL en la fase rica en almidón que redujo la temperatura de

transición vítrea de la fase amilácea. La heterogeneidad de su estructura y la falta de adhesión entre fases dio lugar a films demasiado frágiles, aunque en pequeña proporción (10%), la PCL reforzó la matriz (aumentó el módulo de elasticidad). Al aumentar la proporción de PCL, disminuyó la WVP de los films, pero aumentó la permeabilidad al oxígeno. La incorporación de CA como compatibilizador de estas mezclas aumentó la solubilidad en agua de los films por efecto de hidrólisis y supuso una mejora en las propiedades mecánicas de los films con baja proporción de PCL (10 %), pero no afectó a sus propiedades barrera. La incorporación de polietilenglicol (PEG 4000) a las mezclas con baja proporción de PCL no mejoró las propiedades de los films, potenciando la separación de fases. Las mezclas almidón:PCL con proporción másica 1:0.05, sin compatibilizador, fueron bastante homogéneas y exhibieron buen comportamiento mecánico y estabilidad.

Para incorporar una mayor proporción de PCL, y mejorar la hidrofobicidad y estabilidad de los films, se modificó la PCL por reacción con glicidil metacrilato o anhídrido maleico y glicidil metacrilato (PCL_{-g}), para su uso como compatibilizadores. Los films con 20% de PCL y 2.5 y 5 % de los PCL_{-g} presentaron muy buenas propiedades mecánicas y de barrera al vapor de agua y a los gases y buena estabilidad al inhibir la retrogradación del almidón. Sus propiedades de barrera cumplieron con los requisitos de envasado de un número importante de productos alimentarios.

La obtención de films bicapa por termo-compresión a partir de almidón (o almidón con 5% PCL) y PCL proporcionó un material con muy baja permeabilidad al vapor de agua y al oxígeno y buenas propiedades mecánicas. La adhesión entre las capas mejoró en gran medida con la incorporación de ácido ascórbico, y sobre todo de sorbato potásico, en la interfase en forma de disolución acuosa antes de la termo-compresión. Estos compuestos impartieron, a su vez, propiedades antioxidantes y antimicrobianas, respectivamente, a los films, mejorando su uso potencial para el envasado activo de alimentos.

DESENVOLUPAMENT I CARACTERITZACIÓ DE PEL•LÍCULES DE MIDÓ DE DACSA PER MESCLAT AMB COMPOSTOS MÉS HIDROFÒBICS

RESUM

S'han utilitzat diverses estratègies per a millorar les propietats físiques de films a base de midó de dacsa, amb glicerol (30 %) com plastificant, basades en l'increment del seu caràcter hidrofòbic, per a reduir la seua sensibilitat a l'aigüa. El midó es va mesclar amb diferents compostos (surfactants i polímers més hidrofòbics), amb i sense compatibilitzadors, per l'obtenció de films mixtos mitjançant diferents tècniques de processat (càsting, mesclat en fos, modelatge per compressió i extrusió). Es va estudiar també la formació de films bicapa midó-poli-e-caprolactona (PCL) mitjançant modelatge per compressió.

L'addició de surfactants als films de midó elaborats per càsting va donar lloc a una disminució de la seua permeabilitat al vapor d'aigüa (WVP), però va augmentar la seua fragilitat. Els surfactants amb menor balanç hidròfil-lipòfil (HLB), i sòlids a temperatura ambient, varen proporcionar una microestructura dels films amb menor grandària de partícula, que varen potenciar les propietats barrera al vapor d'aigüa. Per la seua major aplicabilitat industrial, es van emprar tècniques de termo-processat per l'obtenció de la resta de films estudiats. Aquells obtinguts per mescla amb hidroxipropil-metilcellulosa (HPMC) varen presentar una fase dispersa de HPMC en la matriu de midó i millors propietats barrera al vapor d'aigüa, però varen ser un poc més permeables a l'oxigen, sobretot quan es va incorporar àcid cítric (CA) com compatibilitzador. Aquest va provocar entrecreuament en la matriu polimérica, incrementant lleugerament la seua duresa i reduïnt la seua extensibilitat.

La incorporació de PCL en diferents proporcions als films de midó obtinguts per termo-compressió, va donar lloc a la separació de fases polimèriques, detectant-se una xicoteta miscibilitat de la PCL en la fase rica en midó que va reduir la temperatura de

transició vítria de la fase amilàcea. L'heterogeneïtat de la seua estructura i la falta d'adhesió entre fases va donar lloc a films massa fràgils, encara que en xicoteta proporció (10%), la PCL va reforçar la matriu (augmentant el mòdul d'elasticitat). Al augmentar la proporció de PCL, va disminuir la WVP dels films, però va augmentar la permeabilitat a l'oxigen. La incorporació de CA com compatibilitzador d'aquestes mescles va augmentar la solubilitat en aigüa dels films per efecte d'hidròlisi i va suposar una millora en les propietats mecàniques dels films amb baixa proporció de PCL (10 %), però no va afectar les propietats barrera. La incorporació de polietilenglicol (PEG 4000) a les mescles amb baixa proporció de PCL no va millorar les propietats dels films, potenciant la separació de fases. Les mescles midó:PCL amb proporció màssica 1:0.05, sense compatibilitzador, varen ser prou homogènies i varen exhibir un bon comportament mecànic i una bona estabilitat.

Per a incorporar una major proporció de PCL i millorar l'hidrofobicitat i estabilitat dels films, es va modificar la PCL per reacció amb glicidil metacrilat o anhídrid maleic i glicidil metacrilat (PCL_{-g}), per al seu ús com compatibilitzadors. Els films amb 20% de PCL i 2.5 i 5 % dels PCL_{-g} varen presentar molt bones propietats mecàniques i de barrera al vapor d'aigüa i als gasos i bona estabilitat al inhibir la retrogradació del midó. Les seues propietats de barrera varen complir amb els requisits d'envasament d'un nombre important de productes alimentaris.

L'obtenció de films bicapa per termo-compressió a partir de midó (o midó amb 5% PCL) i PCL va proporcionar un material amb molt baixa permeabilitat al vapor d'aigüa i al oxigen i bones propietats mecàniques. L'adhesió entre les capes va millorar en gran mesura amb l'incorporació d'àcid ascòrbic, i sobretot de sorbat de potassi, en la interfase en forma de dissolució aquosa abans de la termocompressió. Aquestos compostos varen impartir, a la vegada, propietats antioxidants i antimicrobianes, respectivament, als films, millorant el seu ús potencial per a l'envasament actiu d'aliments.

TABLE OF CONTENTS

PREFACE

DISSERTATION OUTLINE

This Doctoral Thesis is structured in five sections: Introduction, Objectives, Chapters, General Discussion and Conclusions. The Introduction section discusses the state of the art concerning thermoplastic starch-based films. The Objectives section presents general and specific objectives of the Thesis. The Chapters section is organized into seven chapters, presented as a collection of scientific publications. In the General Discussion section, a global discussion of the most relevant results obtained in this Doctoral Thesis is given. Finally, the most important conclusions are presented.

The Chapters section is organised as follows:

Chapter 1, entitled "*Effect of the incorporation of surfactants on the physical properties of corn starch films*", analyses the effect of surfactant addition on structural, mechanical, optical and barrier properties of film-forming dispersions and starch-based films obtained by casting from the aqueous dispersions. Subsequently, taking into account the potential industrial application, thermal processing has been tried, but it was dismissed due to the high crystallization rate of these surfactants during the cooling step which gave rise to very brittle films. Then, blends of starch with other thermoplastic polymers more hydrophobic than starch were considered as a better strategy.

In this sense, hydroxypropyl methylcellulose is a biodegradable polymer, less water sensitive than starch and can be processed by thermal methods. So, in **Chapter 2** the "*Properties of starch–hydroxypropyl methylcellulose based films obtained by compression moulding*" were studied. To overcome the low interfacial adhesion between these polymers, citric acid was added as compatibilizer agent to improve the blend properties. An extensive characterization was carried out for these blends.

Blending of starch with biodegradable polymers from natural sources is interesting, but their principal drawback is their low degradation temperature as compared with biodegradable polymers from synthesis. This characteristic limits their thermal processing by compression moulding or extrusion. Therefore, in **Chapter 3,** starch blending with a synthetic biodegradable polymer (poly(ε-caprolactone)-PCL) was studied. "*Physical and structural properties, and thermal behaviour of starch-poly(ε-caprolactone) blend films for food packaging*" were studied. These materials were obtained by melt blending and compression moulding and were extensively characterised. Despite the fact that starch-PCL blends have been widely reported in literature, knowing how they behave in the process conditions used in the thesis was considered necessary. These blends showed some desirable characteristics, but poor interfacial adhesion between these non-compatible polymers. In this way, in the subsequent chapters different strategies to overcome this drawback were analysed.

In **Chapter 4**, the "*Influence of citric acid on the properties and stability of starch-poly(ε-caprolactone) based films*" was studied. The obtained results point to enhanced interactions between PCL and starch chains in films with citric acid, although this only quantitatively benefits the film properties at a low PCL ratio. In **Chapter 5,** "*starch-based films obtained by compression moulding: effect of a low proportion of poly(ε-caprolactone) and/or polyethylene glycol*" was studied. In this work, it was observed that starch films could incorporate 5% PCL without a notable polymer phase separation, leading to more stretchable and stable films, without the beneficial effects of PEG. So, other strategies are necessary in order to achieve better results.

The chemical modification of PCL to obtain compatibilizers (grafted Poly(ε-caprolactone) -PCL_{-g}) for starch and PCL blends was studied in **Chapter 6,** entitled "*Enhancement of interfacial adhesion between starch and poly(ε-caprolactone):*

Strategies of chemical compatibilization". Starch-PCL blend films with different ratios of grafted PCL were obtained by using extrusion and compression moulding. The compatibilizer developed was efficient and, as a result, some physical properties of the blend films were improved, especially the barrier and mechanical properties.

Finally, in **Chapter 7**, another strategy was used to improve the functionality of starch-PCL films: the development of a bilayer material with starch and PCL layers. Chapter 7, entitled "*Active bilayer films of thermoplastic starch and poly(ε-caprolactone) obtained by compression moulding*", shows the results of this study. Active compounds (antimicrobials or antioxidants) were added at the interface in order to impart active properties to the final material. All bilayers showed good barrier properties to water vapour and oxygen and good mechanical performance.

DISSEMINATION OF RESULTS

This Doctoral Thesis is formed by 7 scientific articles, 4 published in international journals, 2 Accepted in international journals and 1 under revision for patent before publication.

- ✓ **Ortega-Toro, R.**, Jiménez, A., Talens, P., & Chiralt, A. (2014). Effect of the incorporation of surfactants on the physical properties of corn starch films. *Food Hydrocolloids*, 38, 66-75.

- ✓ **Ortega-Toro, R**., Jiménez, A., Talens, P., & Chiralt, A. (2014). Properties of starch–hydroxypropyl methylcellulose based films obtained by compression molding. *Carbohydrate Polymers*, 119, 155-165.

- ✓ **Ortega-Toro, R.**, Contreras, J., Talens, P., & Chiralt, A. (2015). Physical and structural properties and thermal behaviour of starch-poly(ε-caprolactone) blend films for food packaging. *Food Packaging and Shelf Life*, doi:10.1016/j.fpsl.2015.04.001.

- ✓ **Ortega-Toro, R.**, Collazo-Bigliardi, S., Talens, P., & Chiralt, A. (2015). Influence of citric acid on the properties and stability of starch-polycaprolactone based films. *Journal of Applied Polymer Science*. DOI: 10.1002/app.42220.

- ✓ **Ortega-Toro, R.**, Muñoz, A., Talens, P., & Chiralt, A. (2015). Improvement of properties of glycerol plasticized starch films by blending with a low ratio of polycaprolactone and/or polyethylene glycol. *Food Hydrocolloids*. Accepted Manuscript.

- ✓ **Ortega-Toro, R.**, Santagata, G., d'Ayala, G., G., Cerruti, P., Talens, P., Chiralt, A., & Malinconico, M. (2015). Enhancement of interfacial adhesion between Starch and Poly(ε-caprolactone): strategies of chemical compatibilization. *Carbohydrate Polymers*, Under per rev.

- ✓ **Ortega-Toro, R.**, Morey, I., Talens, P., & Chiralt, A. (2015). Active bilayer films of thermoplastic starch and polycaprolactone obtained by compression molding. *Carbohydrate Polymers*, 127, 282–290.

INTERNATIONAL CONFERENCES:

- ✓ **Oral communication**. **Ortega-Toro, R.,** Jiménez, A., Talens, Pau., & Chiralt, A. *Films de almidón termoplástico. Influencia de la incorporación de hidroxipropil metilcelulosa y ácido cítrico*. Seminario internacional de empaques biodegradables. June, 2013. Popayán, Colombia

- ✓ **Poster presentation**. **Ortega-Toro, R.,** Jiménez, A., Talens, P. & Chiralt, A. *Efecto de tensoactivos sobre las propiedades estructurales y de barrera de películas a base de almidón*. Congreso Iberoamericano de Ingeniería de Alimentos. (CIBIA 9). January, 2014. Valencia-Spain.

- ✓ **Poster presentation**. **Ortega-Toro, R.,** Talens, P. & Chiralt, A. *Películas a base de almidón e hidroxipropil-metilcelulosa. Influencia del ácido cítrico como agente de entrecruzamiento*. Congreso Iberoamericano de Ingeniería de Alimentos. (CIBIA 9). January, 2014. Valencia-Spain.

- ✓ **Poster presentation. Ortega-Toro, R.**, Collazo-Bigliardi, S., Contreras, J., Talens, P., & Chiralt, A. *Structural properties of starch and Polycaprolactone based films*. II Congreso Internacional de Investigación e Innovación en Ingeniería, Ciencia y Tecnología de Alimentos (IICTA). May, 2014. Medellín-Colombia

- ✓ **Poster presentation. Ortega-Toro, R.**, Muñoz, A., Talens, P., & Chiralt, A. *Efecto de la incorporación de policaprolactona y polietilenglicol en las propiedades ópticas y de barrera al vapor de agua de películas a base de almidón*. International conference on Food Innovation (FoodInnova). October, 2014. Concordia-Entre Ríos-Argentina.

- ✓ **Oral communication (Key note). Ortega-Toro, R.**, Santagata, G., Gómez d'Ayala, G., Cerruti, P., Talens, P., Chiralt, A., & Malinconico, M. *Enhancement of interfacial adhesion between Starch and Poly(ε-caprolactone): strategies of chemical compatibilization*. Eurofillers and Polymer Blends. April, 2015. Montpellier, France.

PREDOCTORAL STAY AT FOREIGN INSTITUTION

Institute for Polymers, Composites and Biomaterials. Consiglio Nazionale delle Ricerche (Naples, Italy), from September 2014 to November 2014 under the supervision of Dr. Mario Malincónico.

I. INTRODUCTION

Nomenclature

APP	Ammonium Polyphosphate
ATBC	Acetyl Tributyl Citrate
C.F.	Cooling Fast
C.S.	Cooling Slow
CA	Citric Acid
CF	Cotton Fibre
CG	Carrageenan
CH	Chitosan
CHT	Chitin
CHNC	Chitin Nanocrystal
CHNF	Chitin Nanofibres
CMC	Carboxymethyl cellulose
CNT	Carbon Nanotube
DGEBA	Bisphenol A Diglycidyl Ether
Eq. RH	Equilibrium Relative Humidity
ESO	Epoxidized Soybean Oil
Et3N	Triethylamine
Flax-Psil	Flax treated with Phosphorous-Silane
-g-	Grafted
GP	Grease Proof
Gly	Glycerol
GlyPh	Glycerol Phosphate
GPOE	Glycidyl Methacrylate Grafted Poly (Ethylene Octane)
Lotader 3210	Random terpolymer of Ethylene, Butyl Acrylate (6%) and Maleic Anhydride (3%)
Lotader 3410	Poly(Ethylene-co-Butyl Acrylate-co-Maleic Anhydride) Terpolymer
LPB	Liquid Packaging Board
LS	Calcium Lignosulfonate
MA	Maleic Anhydride
MalA	Maleic acid
MaA	Malic Acid
MS	Magnesium Stearate
MTPS	Modified Thermoplastic Starch
N.R.	Not Reported
MMT	Montmorillonite
PCL_{-g}	Poly(ε-caprolactone) grafted
PU2	Poly(ε-caprolactone) Diol Reacted with Isocyanate
PU3	Poly(ε-caprolactone) Triol Reacted with Isocyanate
PU4	Poly(ε-caprolactone) Tetrol Reacted with Isocyanate
SA	Stearic Acid
SBC	Starch based coating
SHP	Sodium Hypophosphite
TA	Tartaric Acid
T_g	Glass transition temperature
$T_{g\alpha}$	T_g from Starch-Rich Zone
$T_{g\beta}$	T_g from Glycerol-Rich Zone
T_m	Melting temperature
T_{max}	Maximum temperature of degradation
TN	Talc Nanoparticles
TPS	Thermo Plastic Starch
VTMS	Vinyltrimethoxysilane
WF	Wood Fibre

I.1. THERMOPLASTIC STARCH BASED FILMS. STRATEGIES TO IMPROVE THEIR FUNCTIONAL PROPERTIES

The industry of conventional plastics has grown considerably since the 1950`s, when crude oil and its large-scale industrial use for synthetic polymers was discovered (Shen *et al.*, 2009). In 2014, the global annual production of conventional plastics was 300 million tonnes (European Bioplastics Association, 2014). Different processes to obtain plastic products were developed in line with the growth of this industry: extrusion, injection moulding (injection compression moulding, lost-core process, gas-assisted injection moulding, co-injection moulding, two-shot injection moulding), thermoforming, blow moulding, rotational moulding (centrifugal casting) and foaming (Harper, 2004). Currently, despite the significant expansion of the plastics industry, the massive use of plastics has generated serious problems derived from waste accumulation and pollution problems (Shen *et al.*, 2009), and declining crude oil reserves. All these aspects and the growing environmental social awareness make it necessary to look for alternative materials to substitute, at least partially, synthetic plastics. Nowadays, bioplastics seem to be the best option.

According to European Bioplastics Association, bioplastics are plastics that are biobased, biodegradable or both. These materials can be biobased non-biodegradable plastics (biobased polyethylene, biobased polyethylene terephthalate, biobased polyamides and materials such as starch-polyolefin blends, etc.) and biobased biodegradable and compostable plastics (thermoplastic starch, poly(ε-caprolactone), polylactic acid and polyhydroxy alkanoate, etc) (European Bioplastics Association, 2013). They are of particular relevance because they allow a sustainable production, are environmentally friendly and completely biodegradable. In 2013, the target biodegradable plastics were polylactic acid

(PLA) (30.3%), biodegradable starch blends (30.1%), biodegradable polyesters (28.7%) and polyhydroxyalkanoate (PHA) (5.6%) (Figure I.1) (European Bioplastics Association, 2014).

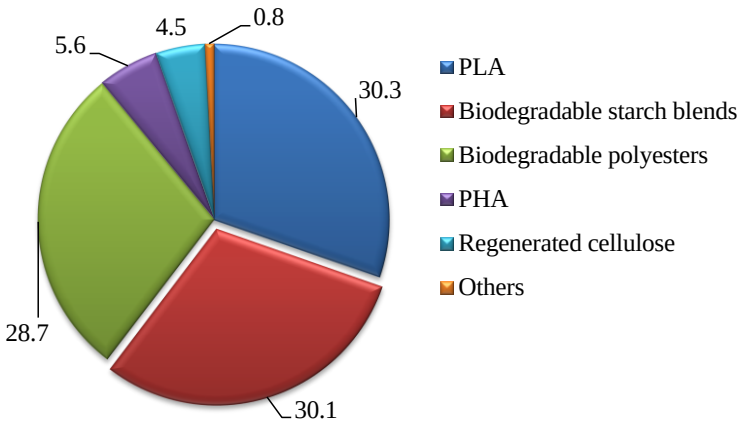

Figure I.1.-Global production of bioplastics in 2013
[Source: European Bioplastics Association, 2014]

Starch-based plastics occupy a relevant position amongst the bio-based materials. It has had a relevant role in the last few decades in several applications and has recently been a frontrunner in bio-based materials. The global production of starch-based plastics in 2013 was 668 kilo tons (kt), with an estimated growth of 94.3% (1298 kt *per annum*) for the period 2013-2020 (Shen *et al*., 2009). Starch has several advantages, such as its low cost, renewability, sustainable production and good processability by means of conventional techniques (Shen *et al*., 2009; Jiménez *et al*., 2012; Cai *et al*., 2014; Garcia *et al*., 2014; Lopez *et al*., 2014; Soares *et al*., 2014; Alves *et al*., 2015). However, it also exhibits some drawbacks, such as brittleness, a highly hydrophilic nature and retrogradation throughout time (López *et al*., 2013; Taghizadeh & Favis, 2013; B *et al*., 2014; Ortega-Toro *et al*.,

2014; Salaberria *et al*., 2014). Different strategies aimed to improved the properties of the starch based materials has been used, such as the use of thermo-mechanical processing, plasticizers, chemical modification, incorporation of fillers, additives or blending with other polymers. This allows us to obtain a wide range of materials with diverse properties, enabling a broad scale of applications. The most common process used for obtaining thermoplastic starch are compression moulding, extrusion, co-extrusion, injection moulding and blow extrusion. Properties of strach products obtained by these differetn techniques by using differetn formulation starteties are summarized in Tables A.I.1 to A.I.5 (see appendix A), where references of the different studies are also given.

Nowadays, there are several starch-based materials on the market. The global leaders in this field are: Novamont (Italy), Rodenburg (Netherlands), Biotec (Deutschland), Limagrain (France), Livan (Canada), Cereplast (Unites States of America), Plantic (Australia) and Biop (Deutschland). Usually, commercial materials developed by these companies are starch-based blends with other polymers, such as poly(ε-caprolactone) (PCL), polyvinyl alcohol (PVOH), polybutylene succinate (PBS), PLA, poly(butylene succinate-co-butylene adipate) (PBSL), poly(butylene adipate-co-terephthalate) (PBAT), PHA, polyhydroxybutyrate (PHB), polypropylene (PP) and polyethylene (PE). Packaging and agriculture are the predominant applications of starch based plastics. In some cases, conventional materials can be substituted wholly or partially by starch plastics (Shen *et al*., 2009). However, despite technological advances and the successful commercialization of some these materials, the optimization of process and the improvement of physicochemical characteristics are necessary to reduce the production costs and find new applications.

The different methods used to obtain starch-based plastics are described below as well the relationship between starch properties and process conditions and the

different strategies used for their improvement. The role of starch-based materials in food packaging and the potential replacement of conventional plastics are also analysed.

I.1.1. Methods for obtaining starch-based materials. Influence on their properties.

Starch granules can vary in shape, size, structure and chemical composition, depending on the origin of the starch (Smith, 2001). Chemically, native starch is composed of two main macromolecular components: amylose and amylopectin (Figure I.2). Amylose is a nearly linear polymer of α-1,4 anhydroglucose units that has excellent film-forming ability. Meanwhile, amylopectin is a highly branched polymer of short α-1,4 chains linked by α-1,6 glucosidic branching points occurring every 25-30 glucose units (Durrani & Donald, 1995; Liu, 2005). Physically, native starches take the form of granules where both amylose and amylopectin are structured by hydrogen-bonding, containing crystalline and non-crystalline regions in alternating layers (Jenkins *et al*., 1993). In fact, most native starches are semi-crystalline, having a crystallinity of about 20-45% (Whistler *et al*., 1984). Amylose and the branching points of amylopectin form the amorphous regions while the short-branched chains in the amylopectin are the main crystalline components in granular starch. So, the higher content of amylopectin in native starch means greater crystallinity (Cheetham & Tao, 1998). The ratio of amylose/amylopectin depends on the source and age of the starch. Starch generally contains 20 to 25 % amylose and 75 to 80 % amylopectin (Brown & Poon, 2005). For instance, wheat, corn and potato starch contain 20-30% amylose, while its content in waxy starches is lower than 5% and in high-amylose starches is as high as 50-80 % (Liu, 2005).

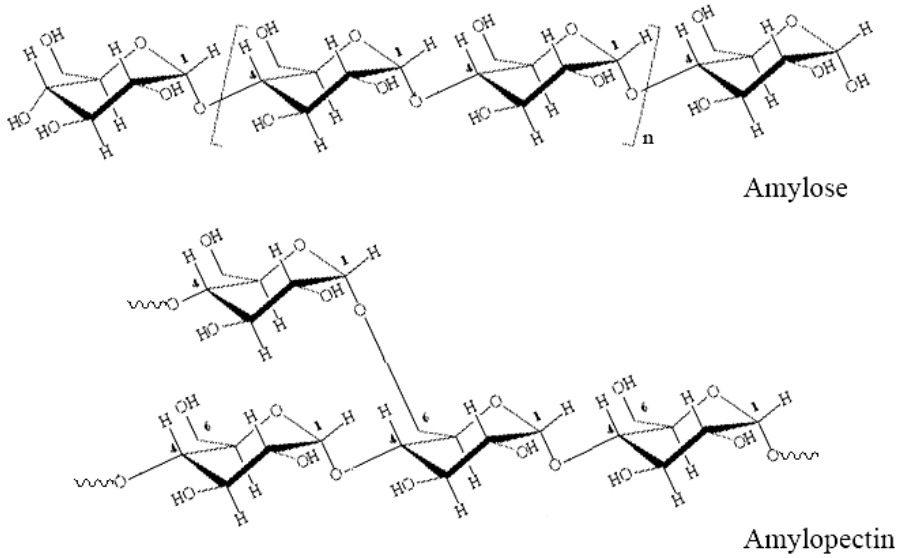

Figure I.2.-Chemical structure of starch: amylose and amylopectin.

Starch granules are not soluble in cold water due to the fact that strong hydrogen bonds hold the starch chains together. However, when starch is heated in water, the crystalline structure is disrupted and water molecules interact with the hydroxyl groups of amylose and amylopectin, producing the partial solubilisation of starch (Hoover, 2001). Heating starch suspensions in an excess of water or of another solvent able to form hydrogen bonding (e.g. liquid ammonia, formamide, formic acid, chloroacetic acid and dimethyl sulfoxide) and at high temperatures (between 65-100 ºC approximately depending on the type of starch) provokes an irreversible gelatinization (destructuration) process. This process is highly affected by the kind of solvent and the starch/solvent ratio. This process introduces irreversible changes in starch granules, such as the loss of crystallinity, water absorption and the swelling of the granules (Zhong *et al*., 2009, Carvalho, 2008).

Although native starch is not a thermoplastic material, it can be processed like conventional polymers if it is treated properly. Carvalho (2008) described thermoplastic starch (TPS) as an amorphous or semi-crystalline material composed of gelatinized or destructurized starch containing one or a mixture of plasticizers. The native granular structure of starch is disrupted and converted into TPS by processing under high temperature and shear conditions in the presence of plasticizers (Ma *et al*., 2009; Pinto *et al*., 2009, Castillo *et al*., 2013), in a similar way to common synthetic polymers. TPS can be repeatedly softened and hardened so that it can be moulded/shaped by the action of heat and shear forces, thus allowing its processing to be conducted with the techniques commonly used in the plastics industry.

Properties of the starch materials are affected by the type of starch, chemical modifications and processing conditions (Chaudhary *et al*., 2008) while TPS materials exhibit some disadvantages such as their strong hydrophilic character and poor mechanical and barrier properties as compared to synthetic polymers (Curvelo *et al*., 2001; Avérous & Boquillón, 2004; Ma *et al*., 2009; Castillo *et al*., 2013). Different approaches to overcome these limitations have been tested. For instance, TPS matrices have been strengthened with organic or mineral fillers (Cyras *et al*., 2008). These fillers reinforce polymeric matrices and led to films with better properties due to the synergistic effect between the components (Wilhelm *et al*., 2003).

In general, the processing of starch is more complicated and difficult to control than that of conventional polymers, due to the fact that its properties make its processing difficult: high glass transition temperature, high viscosity, water evaporation, fast retrogradation, etc. However, with a proper formulation and suitable processing conditions, many of these drawbacks can be overcome. Formulation developments include different strategies: 1) the adding of appropriate

plasticizers and lubricants (Moscicki *et al*., 2012; López *et al*., 2013; Yu *et al*., 2013); 2) the use of modified starch in which the hydroxyls have been replaced by ester or ether groups (e.g. carboxymethyl starch and hydroxypropylated starch); 3) the blending of starch with hydrophobic polymers (e.g. PLA, PCL or cellulose) (Martin & Avérous, 2001; Sarazin *et al*., 2008; Brandelero *et al*., 2011) with the appropriate compatibilizers; 4) the use of starch-graft-hydrophobic polymer, such as starch-graft-PLA, starch-graft-PCL, etc. or 5) the blending of starch with nanoclays to form starch nanocomposites (Liu *et al*., 2009).

Actually, rigid and flexible films, foams and cushioning materials containing starch have also been developed using different methods (Maningat *et al.,* 2009) with the same technologies used for synthetic polymers, such as compression and injection moulding, extrusion, blowing, etc. (Zhai *et al*., 2003; Avérous & Boquillon, 2004; Teixeira *et al.,* 2007; Sarazin *et al*., 2008; López *et al*., 2013). This allows the use of the actual machinery, making it easier to process and lowering the industrial sector investment (Castillo *et al*., 2013).

I.1.1.1. Compression moulding

In this method, the moulding material, generally preheated, is first placed in an open, heated mould cavity. The mould is closed with a top force or plug member and pressure is applied to force the material into contact with every part of the mould, while heat and pressure are maintained until the moulding material has cured. The process employs thermosetting resins in a partially cured stage, either in the form of granules, putty-like masses, or preforms (Kim *et al*., 2011). Advanced composite thermoplastics can also be compression moulded with unidirectional tapes, woven fabrics, randomly oriented fibre mat or chopped strand (Kim *et al.*, 2011). The advantage of compression moulding is its ability to mould large, fairly intricate parts. It is one of the cheapest moulding methods as compared with others,

such as transfer moulding and injection moulding. Moreover, it wastes relatively little material, which is an advantage when working with expensive compounds. It would significantly reduce the cycle time of intermediate preparation (Memon & Nakai, 2013). However, compression moulding often provides poor product consistency and difficulty in controlling flashing, and it is not suitable for some types of materials. It is also suitable for ultra-large basic shape production in sizes beyond the capacity of extrusion techniques (Todd *et al*., 1993). Hulleman *et al*. (1999) showed that the amount of B-type crystallinity is the major factor influencing the mechanical behaviour of compression-moulded, glycerol-plasticised potato starches. The changes in the process parameters, such as temperature and water content during moulding, allowed the amount of B-type crystallinity to be varied and, thus, the properties of these materials. When melting was completed, as concluded from the thermal analysis, still residual, birefringent granules were present in the materials moulded at relatively high temperatures, suggesting the continued presence of a high degree of structural order within the granules. The measured mechanical properties of the plasticized potato starches correlated well with the amount of B-type crystallinity.

I.1.1.2. Extrusion process

It is probably the most important processing method for thermoplastics and is used to produce films and sheets. The extrusion of high amylose starch can be more difficult than the processing of normal thermoplastic starches, partly due to the high die pressures required because of the high melt viscosity (Shogren & Jasberg, 1994). This has been attributed to the high melting temperatures of amylose at low moisture content (Shogren, 1992). An increase in the amylose content relative to that of normal starch is, however, interesting, since high amylose materials exhibited greater strength and toughness (Van Soest & Borger, 1997). Thuwall *et*

al. (2006a) concluded that thermoplastic high amylose potato starch (HAP) is quite suitable for extrusion although it is more difficult to process than thermoplastic starch based on native potato starch (e.g. a higher moisture content and a higher extrusion temperature is required with HAP). The higher melt viscosities might also be a result of a more entangled structure in the amylose which then would partly account for the greater tensile strength of the HAP-material. Here it was found that the high amylose material could be successfully extruded at a temperature of 160 ºC if the starch has 45 parts of glycerol per 100 parts of starch and the moisture content is 30%. The extrusion was facilitated by a higher compression ratio of the screw, increased flow rate and smaller die gap. Most studies on the processing of high amylose starches have been carried out on corn starches (Willet *et al*., 1995; Van Soest & Essers; 1997; Thuwall *et al*., 2006a). The extrusion processing of starch or starch-containing resins has been used in conjunction with injection moulding or post-extrusion equipment to make films, sheets and ribbons with many of the functional properties typical of petroleum-based plastics (Otey *et al*., 1980; Doane, 1992; Moscicki *et al*., 2012; Yu *et al*., 2013).

Krishna *et al*. (2012) demonstrated the potential production of fish gelatine films using extrusion and compression processes by means of solid and liquid feeds which are mixed within the barrel. Blends of glycerol and gelatine were obtained and only 20-25% glycerol with respect to gelatine allows the continuous extrusion of gelatine sheets. The authors observed significant differences in physical properties upon comparing extruded films with solution cast films. The thickness of the extruded films was four to five times higher than solution cast films at the same glycerol concentrations; extruded films were more flexible than solution cast films, with an elongation nearly 7–10 times higher. The extrusion processing of fish gelatine films did not affect water vapour barrier properties to a great extent.

Different authors have reported the compatibility of PLA and starch matrices in extrusion processes (Martin & Avérous, 2001; Huneault & Li, 2007). Sarazin *et al*. (2008) reported significant improvements in the impact and elongation at break properties of PLA through the addition of thermoplastic wheat starch as well as PCL. An elongation at break for PLA/PCL/TPS 40/10/50 of 55% was achieved, as compared to 5% for the pure PLA. When high glycerol contents are present in the TPS phase and PCL is added to modify the ductility of the PLA, synergies come into play which allows the ternary PLA/PCL/TPS blend properties to exceed that observed with any of the binary pairs.

I.1.1.3. Reactive extrusion (REX)

Chemical changes to starch or starch-based materials during extrusion processing of food products have also been widely investigated and reviewed (Hablot *et al*., 2013). It is a type of extrusion process in which individual components are first bonded by a chemical reaction. Twin-screw extruders are particularly suitable for the reactive extrusion process due to their excellent mixing properties (Xie *et al*., 2006; Raquez *et al.*, 2008a; Moad, 2011). According to Moad, (2011) twin-screw extruders, in particular, can be used to produce modified starches in a continuous process with a more consistent product quality. The extruder has the advantage of being an excellent mixing device and is particularly suitable for processing highly viscous fluids (such as gelatinized starch). Thus, with the use of REX, starch modification can be performed in a homogeneous medium. The extruder also displays good heat transfer and plug flow characteristics. Variations in screw design offer good control over residence times and residence time distributions, and provide opportunities for adding (or removing) reagents and additives, such as processing aids and stabilizers, during the process.

I.1.1.4. Co-extrusion

It is defined as simultaneous extrusion from a single die of two or more homogeneous plastic layers (films) which form a laminar structure with varying degrees of adhesion. Each material needs its own independent extruder, but a single die can supply more than one layer of the same product. The final product consists of independent layers of material in different forms. The main considerations for successful co-extrusion are design of structure, selection of polymers with required physical properties, design of equipment for predicted structure and feasibility study (commercial consideration) (Djordjevic, 2001). Co-extrusion has major advantages over single extrusion and lamination in the case of sheet and film or for other products, such as no post-treatment, no additional handling labour and fewer quality problems, fewer problems with regard to adhesion and appearance, flexibility of thickness and location of layers and low cost. Polymers can be selected to satisfy criteria such as moisture, gas or aroma barrier, chemical resistance, high/low temperature resistance, glossy or dull surface, mechanical strength and crack-resistant surface, recycling, etc. (Djordjevic, 2001).

However, there are some inherent problems with the multiphase nature of the flow during co-extrusion operations, such as non-uniform layer distribution, encapsulation, and interfacial instabilities, which are critical since they directly affect the quality and functionality of the multilayer products. The layer encapsulation phenomena correspond to the surrounding of the more viscous polymer by the less viscous one (Yu, 2009). For the co-extrusion process, starch can be processed as a powder (dry blend) or as granules. In the latter case, the dry blend is extruded, granulated after air-cooling, and then equilibrated at a given relative humidity and temperature. Some authors (Martin *et al.* 2001; Martin & Avérous, 2002) have examined the use of coextruded sheet processing to produce polyester/thermoplastic wheat starch/polyester multilayer films. It was found that

adhesion strength between the layers and stability of the interface were crucial properties in controlling the final performance properties of the films.

I.1.1.5. Injection moulding

Prior to thermoplastic processing such as injection moulding, starch is extruded and gelatinized to form a thermoplastic material that can be subsequently processed into viable products. Different extrusion processing conditions will alter the transformation of the starch during the preparation of the thermoplastic starch resin, which ultimately affects the mechanical properties of the finished product. Screw speed is a particularly useful processing variable, since it is readily altered during extrusion operation, controls the amount of work done on the material during processing, affects the extent of degradation of starch and alters the rheology of starch melts (Chaudhary *et al*., 2008). The injection moulding is a process by which a hot polymer melt is injected into an empty, cold cavity of a desired shape and is allowed to solidify under high holding pressure (Abbés *et al*., 1998). The injection moulding cycle can be divided into three steps: filling, packing, and cooling. At the beginning of the injection moulding cycle, the molten polymer, which is maintained at a uniform temperature inside the barrel of the injection machine, is pushed through the sprue, runner, gate and then into the cavity. This is done under controlled ram speed or controlled hydraulic pressure, depending on the control scheme of the injection unit. Before the cavity is completely filled, the process control scheme switches over to pack/hold pressure control to avoid a pressure rise at the end of filling, which can damage the mould. As the plastic begins to cool, the newly moulded part shrinks. So, more material is packed into the cavity under high pressure to compensate for the increasing density of the polymer melt resulting from increasing pressure and decreasing temperature. After the solidification of polymer at the entrance of the mould, the holding

pressure is removed and the part remains in the mould to cool. When the part is sufficiently cool, to avoid significant deformations, the mould opens and ejects the solid part (Abbés *et al*., 1998). Polymers, commonly thermoplastic (at least 90%), are the basic components of items produced by injection moulding. Currently, the plastics industry supplies a wide variety of polymeric materials. Both, amorphous (e.g. polyurethane (PU), polyvinyl chloride (PVC)) and semi-crystalline (e.g. nylon; PE) polymers may be thermoplastic; they differ from each other in terms of behaviour during the injection moulding process and characteristics of the finished products. The amorphous polymers have an injection moulding behaviour of soften on heating and poor lubricity. On the other hand, the semi-crystalline polymers have melt on heating behaviour, good lubricity and marked and anisotropic shrinkage (Zema *et al*., 2012). According to Abbés *et al*. (1998), many studies have been reported using potato starch (around 15% water content) for obtaining oral capsules as an alternative system to gelatine dip-moulded capsules. One of the problems encountered in the injection moulding of thermoplastic starch is the high pressure used to fill the mould cavity (Abbés *et al.*,1998).

I.1.1.6. Film blowing

It is the most popular method of polymer processing, commonly used in the manufacturing of packaging materials (Della *et al*., 1995; Funke *et al*., 1998; Moscicki *et al*., 2012). The preparation of films based on thermoplastic starch by using the film-blowing technique is a challenging technology. However, most of the studies on film blowing have been conducted on blends of thermoplastic starch with other biodegradable and non-biodegradable polymers where TPS is usually the minor component. Film blowing is a commonly-used method for producing self-supporting plastic films. An empty tube is extruded and then expanded by increasing the pressure inside the tube. The tensile properties of the melt are of

great importance for the final result in both melt calendering and film blowing. Poor melt tenacity has been identified as one of the potential limitations when extruding (or processing) thermoplastic starch, i.e. starch blended with plasticizer and water, at elevated temperatures (Thunwall *et al*., 2006a). Thunwall *et al*. (2006b) recently identified factors influencing the melt tenacity of thermoplastic starch and indicated some ways of improving it, where the high plasticizer content and a material system based on oxidized and hydroxypropylated starch seemed here to be favourable. In several studies on the film blowing of starch-containing materials, rather moderate quantities of starch have either been introduced into a synthetic polymeric system (Otey *et al*., 1980; Jana & Maiti, 1999; Fishman *et al*., 2006) or been used together with a biodegradable polymer, such as PVOH, PCL or polyester (Halley *et al*., 2001; Matzinos *et al*., 2002). It can be concluded that films based on such blends can be produced by film blowing. Zullo & Iannace, (2009) reported studies where particular TPS were blended with PCL to adjust the rheological properties of the melt before the film blowing process. Moreover, blends of PCL/starch/ low density polyethylene (LDPE) were prepared with the aim of increasing the mechanical properties of PCL/starch and making the LDPE films partially biodegradable (Matzinos *et al*., 2002). More recently, McGlashan & Halley (2003) employed nanoclays to improve the film properties of mixtures of starch and aliphatic polyesters. With the clay, was added the film was more transparent and the process of film blowing was more stable; the exfoliation of nanoclay prevented the migration of the plasticizer. Recent studies (Thunwall *et al*., 2008) regarding the film blowing process of TPS were conducted on potato starch with differ amylose content and modified potato starches. The increases in amylose content produced greater stiffness and higher melt viscosity; thus, the material was difficult to process and required a higher amount of plasticizers, water and glycerol (Zullo & Iannace, 2009).

I.1.2. Effect of production method on the physical properties of starch-based films

Although the method used in the film production affects its functional properties, the plasticizer content, botanical source of starch, amylose:amylopectin ratio and the equilibrium relative humidity of the films are also influential.

TPS-based films obtained by compression moulding presented a high degree of rigidity and low deformation. Elastic modulus (EM) and elongation at break (E) varied over a wide range between 1049 MPa (2.4% elongation) (Lopez *et al*., 2014-corn starch, 30% glycerol and equilibrium relative humidity (Eq. RH) 60%) and 268 MPa (28% elongation) (Ortega-Toro *et al*., 2014-corn starch, 30% glycerol and Eq. RH 53%) as compared with the TPS films obtained by other methods, where the values reported were between 45 MPa (47% elongation) (Thuwall *et al*., 2006a-potato starch, 45% glycerol and Eq. RH 50%) and 40 MPa (48% elongation) (Müller *et al*., 2014-corn starch, 36% glycerol and Eq. RH 50%) for extrusion and injection, respectively. According to Lopez *et al*. (2014) the formation of a dense and rigid matrix could be attributed to compression process conditions, where high temperature, pressure and shear force during moulding lead to the approximation of the starch chains. Compression moulding facilitates the evaporation of water during the process, unlike extrusion and injection that have different temperature profiles throughout the equipment and the process occurs in more closed systems, limiting water evaporation. This causes the approximation of starch chains and leads to the compaction of the polymeric matrix, increasing its rigidity and strength. The plasticizer content (glycerol and water) also affects the mechanical properties. A high content of plasticizer promotes an increase in elongation and a decrease in rigidity.

The mechanical and structural properties of the films directly influence their barrier properties. More compact films give rise to a lower water vapour permeability

(WVP) and manufacturing defects, such as pores and cracks, increase the WVP values (Brandelero *et al*., 2011). TPS-based films obtained by extrusion presented higher values of WVP as compared with the films prepared by compression moulding; e.g. 20% of glycerol-sorghum starch extruded films have values of 6.4 $x10^{-4}$ $g \cdot day^{-1} \cdot Pa^{-1} \cdot m^{-1}$ (Rodríguez-Castellanos *et al*., 2013) whereas 30% of glycerol-corn starch thermo-compressed films show 1.11-1.16 $x10^{-4}$ $g \cdot day^{-1} \cdot Pa^{-1} \cdot m^{-1}$ (Ortega-Toro *et al*., 2014; López *et al*., 2015). Other factors, such as process temperature and pressure, plasticizer content, film thickness and storage conditions will also affect the values. Versino *et al*., (2015) reported still lower values (1.30 $x10^{-5}$ $g \cdot day^{-1} \cdot Pa^{-1} \cdot m^{-1}$) of WVP for 30% glycerol-cassava starch obtained by compression moulding. This coincides with the influence of the botanical source and the amylose-amylopectin ratio on the values of barrier properties.

As far as the thermal degradation of starch materials is concerned, thermal gravimetric analysis (TGA) data reported by different authors provide information on the thermal stability of TPS materials obtained by extrusion (Hablot *et al*., 2013), injection (Salaberria *et al*., 2014) or compression moulding (Lomelí-Ramírez *et al*., 2014; Prachayawarakorn *et al*., 2010; B. *et al*., 2014; Ferreira *et al*., 2014; Versino *et al*., 2015). In every case, thermograms exhibited two mass losses, the initial step at around 100-200 ºC corresponding to water loss and the possible volatilization of the plasticizer and the next step, observed between 281ºC-305ºC, associated with the starch decomposition. The thermal stability of the starch-based materials depends on the molecular structure of starch. Manufacturing processes performed at high temperatures and pressures could degrade the starch chains, at least partially, giving rise to starch-based films with a low degradation temperature.

Another important factor is the botanic source of the starch. Castaño *et al*. (2014) studied the physical properties of thermoplastic starch films of *Aesculus*

Hippocastanum seed starch (AH), and *Araucaria Araucana* seed starch (AA). The materials were processed under the same conditions. The starch was blended with glycerol (30%) at 120 ºC for 15 min and injection moulded at 130 ºC in cylinder, 55 ºC of mould temperature, and 300 bar of injection pressure. The authors found that AH starch-based films exhibit a degradation temperature (T_{max}) which is 5 ºC lower than AA starch-based films.

I.1.3. Strategies to improve functional properties of the starch based materials.

Much research has been focussed on developing suitable solutions for improving the properties of starch-based materials, considering their biodegradable nature, ready availability and low cost. Different approaches are described below.

I.1.3.1. Starch modification

A frequent strategy used to enhance the TPS properties is chemical modification. The most-commonly employed methods of bringing about chemical modification in starch molecules are esterification, etherification, acetylation, hydroxypropylation and oxidation (López *et al*., 2013; Olsson *et al*., 2014). Maleated thermoplastic starch has been reported as an excellent option for improving blends using hydrophobic polymers, such as PLA or PBAT (Raquez *et al*., 20008a, b; Shin *et al*., 20011; Wootthikanokkhan *et al*., 2012). The chemical modification of starch chains (surface chemical modification) reduces the hydrophilic nature of the chain without changing the bulk composition and properties of TPS (Belhassen *et al*., 2014). The increase in the amylose content has also been considered interesting because of the increased strength and toughness of the resulting films, as compared with native starch films (Thuwall *et al*., 2006a).

López *et al*. (2013) mixed native and acetylated corn starches with glycerol by means of blown extrusion. The obtained films presented different properties, those containing the lowest acetylated:native starch ratio (10:70, with 20% glycerol) being the strongest films. At low concentrations, acetylated starch can reinforce the film matrix. Nevertheless, at a low glycerol content, when the ratio of acetylated starch was higher (80:5 with 15% glycerol), the water vapour and gas barrier properties were improved with respect to the other formulations.

Olsson *et al*., 2014 used hydroxypropylated and oxidized potato starch, Sodium Montmorillonite (Na-MMT), polyethylene glycol (PEG), citric acid (CA) and glycerol to obtain a TPS coating. This was applied to the surface of grease proof (GP) and liquid packaging board (LPB) sheets giving rise to barrier properties comparable with those of two commercial latex-based barrier dispersions. This starch-based dispersion was an efficient barrier to oxygen on GP paper and also exhibited good barrier properties in a multi-layer film with polyethylene.

Esterification through the reaction with an anhydride is a suitable option for enhancing the starch blends with hydrophobic polymers. Raquez et al. (2008a) developed maleated-TPS (modified thermoplastic starch: MTPS) by reaction with maleic anhydride (MA) as the esterification agent. Figure I.3 shows the reaction mechanism, according to Raquez *et al.* (2008a). A free carboxylic group at the C6 position of glucose units was observed in modified TPS. This characteristic could promote transesterification reactions between MTPS and biodegradable polyesters (Raquez *et al*., 2008b). Shin *et al.* (20011) modified starch by reaction with MA before its blend with PLA. The interfacial adhesion was enhanced by the presence of PLA grafted (-g-) to starch (PLA-g-TPS) copolymers that were formed at the polymer interface. Tensile strength (TS) and elongation at breack point showed a significant decrease when the proportion of MTPS increased in the blend, which was attributed to the increase in the PLA crystallinity after the addition of MTPS.

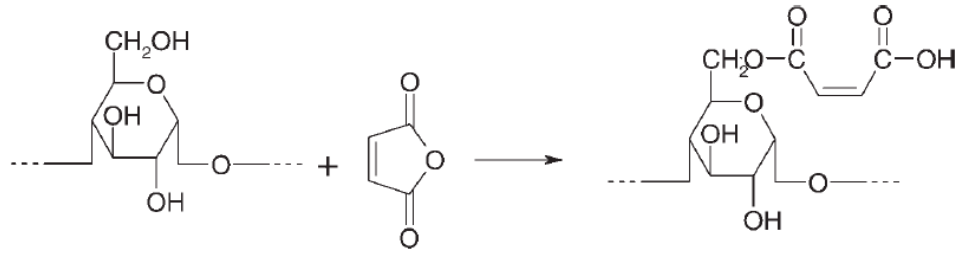

Figure I.3.-Esterification reactions of starch backbone with maleic anhydride (Raquez *et al.* (2008a).

In the same way, Wootthikanokkhan *et al*. (2012) studied the influence of processing conditions on the properties of PLA-MTPS blends. The MTPS was prepared by mixing cassava starch with glycerol and MA, and the films were obtained by compression moulding. A decrease in EM, TS and E was observed after the addition f MTPS to the matrix. Likewise, TS and EM increased when the blending temperature rose, at the expense of E. This may be due to hydrolysis and trans-esterification processes that occur during the blending process.

The surface chemical modification of starch chains is another promising method. Belhassen *et al*. (2014) improved the elastic modulus and the tension strength of the TPS through melt reactive blending with epoxidized soybean oil (ESO). However, the film elongation was adversely affected. A ring opening condensation reaction between the epoxide of the ESO and the hydroxyl groups of starch and glycerol was confirmed. Otherwise, Thuwall *et al*. (2006) studied the effect of the increase in amylose content on TPS films of potato starch and found a significant enhancement of the mechanical properties. However, extrusion was more difficult for high amylose TPS material than for TPS because of its high melt viscosity. This phenomenon has been attributed to the high melting temperatures of amylose at low moisture contents and the more entangled structure in the amylose as compared to that of amylopectin.

I.1.3.2. Organic and inorganic fillers

The term "fillers" refer to solid additives that are incorporated into a plastic matrix (Harper, 2004). The use of fillers is an interesting, alternative means of reinforcing starch-based composites, thus principally improving the mechanical (modulus and tensile strength) and thermal properties, while reducing costs. The adequate interaction between the filler and the polymer matrix is fundamental in order to obtain good materials. In this sense, particle size, particle shape and the distribution of sizes and surface chemistry of the particles are relevant characteristics (Harper, 2004).

Thermoplastic starch has been reinforced with organic fillers obtained from natural sources, such as sisal (Campos *et al*., 2012), wood (Müller *et al*., 2014), flax (Bocz *et al*., 2014), coconut (Lomelí-Ramírez *et al*., 2014) or cotton fibres (Prachayawarakorn *et al.,* 2010), chitin, (Salaberria *et al*., 2014), cassava bagasse (Teixeira *et al*., 2012; Versino *et al*., 2015), lignin (Privas *et al*., 2013) and rice bran (Cano *et al.,* 2014).

Prachayawarakorn *et al.,* (2010) obtained good mechanical, thermal, water absorption and biodegradable properties, reinforcing a thermoplastic rice starch matrix with 10g cotton fibres/100g polymer, using chemically modified PE with MA (PE-g-MA) and Vinyltrimethoxysilane (VTMS) as compatibilizers. The increase in the thermal stability of TPS through the addition of cotton fibres was remarkable. Campos *et al*. (2012) studied the effect of UV-C irradiation of the TPS biocomposites with sisal bleached fibres. The addition of 20g sisal/100g TPS-PCL led to an increase in EM from 62.2 to 103 MPa and TS from 1.7 to 3.8 MPa; however, the elongation decreases by up to 32%. Müller *et al*. (2014) incorporated wood micro-fibres into TPS with 36% of glycerol; this resulted in increased stiffness and strength, the effect being more marked for the highest fibre ratio. However, the elongation at break point decreased considerably, from 48% to 2%

with 4g fibre/100g polymer matrix. Similarly, Bocz *et al*. (2014) studied the incorporation of chopped flax fibre into PLA/TPS biocomposites. Glycerol phosphate (GlyPh), a plasticizer of TPS with flame retardant potential, and Phosphorus-silane (PSil), applied as a surface-treating agent of the fibres, were successfully combined. GlyPh promoted the decrease in the glass transition temperature (T_g) of starch from 253 ºC (TPS reference) to 200 ºC in the case of TPS-GlyPh. Lomelí-Ramírez *et al*. (2014) incorporated green coconut fibre into cassava starch. Thermal studies showed that thermal stability was enhanced as a consequence of the increase in fibre ratio. Dynamic mechanical thermal analysis (DMTA) showed an increase in the storage modulus, higher T_g values and lower damping modulus (tan δ) when the fibre content was raised.

Teixeira *et al*. (2012) studied the incorporation of cassava bagasse into thermoplastic cassava starch. The first one formulated a bio-composite by blending TPS or TPSb (TPS with cassava bagasse) with PLA (80:20); CA and stearic acid (SA) were also added. The formulations with TPSb films exhibited similar TS, but higher EM and lower E than TPS films. Versino *et al*. (2015) also studied the use of cassava root peel and bagasse as natural fillers of TPS. The addition of bagasse (1.5g bagasse/100g polymer) increased the EM and the TS of TPS composites by 260% and 128%, respectively. No notable changes in the water vapour permeability (1.30×10^{-5} $g \cdot day^{-1} \cdot Pa^{-1} \cdot m^{-1}$) of TPS were observed as a result of the increase in the filler content. Versino *et al*. (2015) reported phase separation for the starch films equilibrated at 60% relative humidity, through the two temperatures of the relaxation processes (observed by DMTA) associated with glass transition: the first one at a lower temperature ($T_{g\beta}$) attributed to a glycerol-rich phase (-45 ºC) and the second one ($T_{g\alpha}$) attributed to a starch-rich phase (27 ºC). The incorporation of 1.5% of bagasse promotes the $T_{g\alpha}$ increase up to 46 ºC, which was associated with stronger hydrogen bond interactions between the reinforcing

materials and starch. The double glass transition has also been reported by other authors (Salaberria *et al*., 2014), who studied chitin nanocrystals and nanofibres as nanosized fillers in TPS. The thermal and mechanical properties were better when chitin nanofibres were incorporated into biocomposites than when the films were prepared with nanocrystals. The incorporation of calcium lignosulfonate (LS), on a nanometric scale, into TPS was studied by Privas *et al*., 2013. The incorporation of 2 g LS/100g TPS-Lotader 3210 (Lotader 3210: Random Terpolymer of Ethylene, Butyl Acrylate and Maleic Anhydride) promoted a decrease of about 22% in the oxygen permeability.

Of the organic fillers, lipids have also been used to improve the properties of starch films on the basis of their potential to increase the hydrophobicity of the polymer matrix, thus increasing the water resistance of the films. A significant number of the studies have been carried out for emulsion-based films where lipids are dispersed as droplets or particles of different sizes, depending on the interactions among components and the homogenization method used for blending. Although there are some studies (García *et al*., 2000; Salgado *et al*., 2013) where lipids and polymers are dry blended (by using roll mills or extruders), most of them used the casting method to prepare the films, with the subsequent step of the evaporation of a great amount of solvent. This implies a previous step of component homogenization where the order and conditions in which compounds are blended may have a great influence on the film's microstructure and properties. The incorporation of lipids into hydrocolloid matrices generally improves their resistance to moisture action, in comparison with lipid-free films, but other properties may be negatively affected, due to the lack of compatibility with starch. Essential oils and their components are especially relevant lipids, widely used as fillers of hydrocolloid films, since they can act as antioxidants and antimicrobials, thus imparting bioactivity to the film (Bonilla *et al*. 2013).

In some cases, the incorporation of lipids (essential oils, oleic acid or α-tocopherol, etc.) into biopolymer matrices gives rise to less stretchable, less resistant films, as observed by different authors (Fabra *et al.*, 2008; Jiménez *et al.*, 2013a). These results have been related with the heterogeneous structure of the film matrix where lipids interrupt the continuity of the polymer network, thus implying a reduction of the matrix cohesion forces. In starch matrices, lipid incorporation greatly affects the film's nanostructure, since complexes of amylose helical forms and lipids are formed, affecting the crystalline structure of the films and their mechanical behaviour (Jiménez *et al*., 2012; Jiménez *et al*., 2013b).

In recent years, inorganic nanofillers, such as nanoclay, Na-MMT, talc nanoparticles (TN), and carbon nanotube (CNT) have grown in importance as fillers of starch films (Müller *et al*., 2012; Taghizadeh & Favis, 2013; B *et al*., 2014; Olsson *et al*., 2014; López *et al*., 2015). Clays are an attractive option due to their availability, low cost, and significant effect on the improvement of mechanical and barrier properties of the films. Recently, attention has focused on montmorillonite (MMT) minerals to develop nanocomposites. Müller *et al*. (2012) achieved a WVP reduction of about 63% with the addition of 4g MMT/ 100g polymer to TPS films, due to the formation of an intercalated composite. B *et al.* (2014) studied TPS/PLA/Na-MMT nanocomposites and found an improvement in the EM, TS, and E as a result of the addition of 1g Na-MMT/100g polymer (TPS-PLA, 60:40). Another option for reinforcing TPS is talc nanoparticles. Talc is a phyllosilicate with a layered structure that consists of octahedral brucite [$Mg(OH)_2$] sheets sandwiched between two tetrahedral silica [Si_2O_5] sheets. López *et al*. (2015) incorporated talc nanoparticles into thermoplastic corn starch and found that the addition of 5g nanofiller/100g polymer promoted an increase in EM (~39%) and TS (~49%) and a decrease in E (~4.8), WVP (~25%) and O_2P (~27%) with respect to the TPS films of reference.

Finally, CNT constitute a promising alternative for the generation of novel material, improving the morphology and mechanical properties. Taghizadeh & Favis (2013) dispersed CNT into PCL/TPS systems and studied the localization of CNT in the polymer matrix. They found that CNT migrate to the interface, react with thermoplastic starch and then are subsequently drawn into the low viscosity TPS phase, enhancing the interfacial interactions between both polymers.

I.1.3.3. Blends with biodegradable and compostable plastics

Thermo-mechanical processes, such as extrusion, converts starch into a thermoplastic material, which offers a route for successful blends of starch with other bioplastics to form materials with improved properties.

I.1.3.3.1. Blends with natural biopolymers

What has not been extensively studied is thermo-mechanical blending with natural biopolymers, such as cellulose, proteins and lignin. The main reason is because most natural biopolymers have thermal degradation temperatures lower or close to their glass transition temperature, i.e. the cellulose T_g is 230 ºC and its thermal decomposition starts at 225 ºC (Mark, 1999). In contrast, the T_g of native corn starch is ~223 ºC (Mark, 1999) and its thermal degradation starts at ~270 ºC with T_{max} at ~333 ºC (Wang & Xie, 2010).

However, natural biopolymers, such as chitosan (CH), chitin (CHT), hydroxypropyl methylcellulose (HPMC) and gelatine (Figure I.4), have been processed satisfactorily by conventional methods. Thermoplastic corn starch and CH/CHT were obtained by melt mixing and thermo-compression at 140 ºC (Lopez *et al*., 2014).

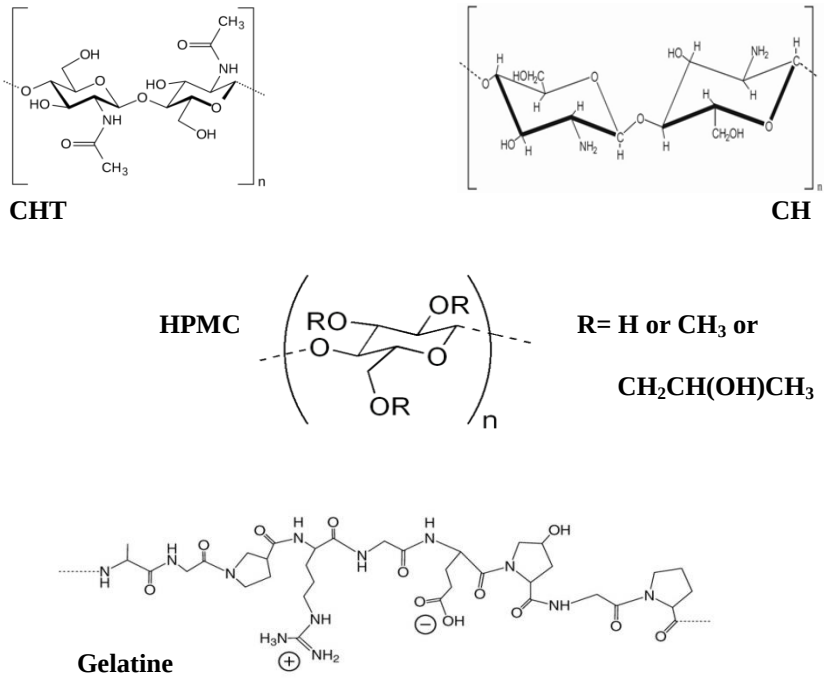

Figure I.4.-Chemical structure of some natural biodegradable polymers.

Authors did not incorporate more than 10g biopolymer/ 100g native starch. In general, the addition of CHT (10% with respect to native starch) implied better mechanical and barrier properties of the films than when CH was added. As regards TPS-CHT10 films, a decrease of ~56% in WVP with respect to the TPS reference was obtained. Soares *et al*. (2013) studied blend films of TPS/PLA (70:30), obtaining sheets by thermo-compression and, afterwards, adding a coating of CH by spraying and immersion. Coating by spraying was more efficient than when the immersion method was used. The CH coating promoted an increase in TS (~54%) and EM (~86%), but a decrease in E (~86%) and WVP (~28%) with respect to the reference TPS/PLA blend film. Subsequently, Soares *et al*. (2014)

tried to enhance these formulations by changing the post compression-moulding drying conditions from 150 ºC to room temperature. To do this, they applied slow (180 min) and fast (20 min) cooling rates and then spray-coated with CH. The mechanical properties did not improve with the slow cooling; however, the WVP decreased by ~43% with respect to the same formulation when fast cooling was employed.

Lopez *et al*. (2014) used thermo-compression to obtain films of thermoplastic corn starch with chitosan/chitin with uniform thickness and good appearance. The clarity of TPS films decreased as the chitosan content rose while water vapour permeability was reduced. The addition of these biopolymers to TPS increased the tensile strength and elastic modulus and decreased the elongation at break, while TPS films with chitosan reduced *S. aureus* and *E. coli* growth in the contact zone, in line with the antimicrobial properties of chitosan.

Fakhouri *et al*. (2013) studied the influence of processing methods on the properties of starch/gelatine type-A films at different starch:gelatine ratios: 4:1, 1:1 and 1:4. Authors compared films obtained by casting (70 ºC), pressing (90 ºC), pressing followed by blowing (90, 100 and 110 ºC, in zones 1 to 3) and extrusion (110, 100, 100 and 95 ºC, in zones 1 to 4) followed by blowing. Blends prepared by casting had the lowest WVP and those obtained by pressing and blowing exhibited surface cracks, the lowest TS values and the highest WVP. Blends obtained by extrusion and blowing had the greatest water solubility (%).

I.1.3.3.2. Blends with synthetic biodegradable polymers

Synthetic biopolymers (Figure I.5), unlike natural biopolymers, can be processed over a wide range of temperatures-pressures without damaging their molecular structure or properties. Currently, thermo-processed blend films with TPS and

synthetic biodegradable polymers have been widely documented, although one of the first studies into starch blends with a synthetic polymer (PVOH), was carried out by solution casting Otey *et al*. (1974).

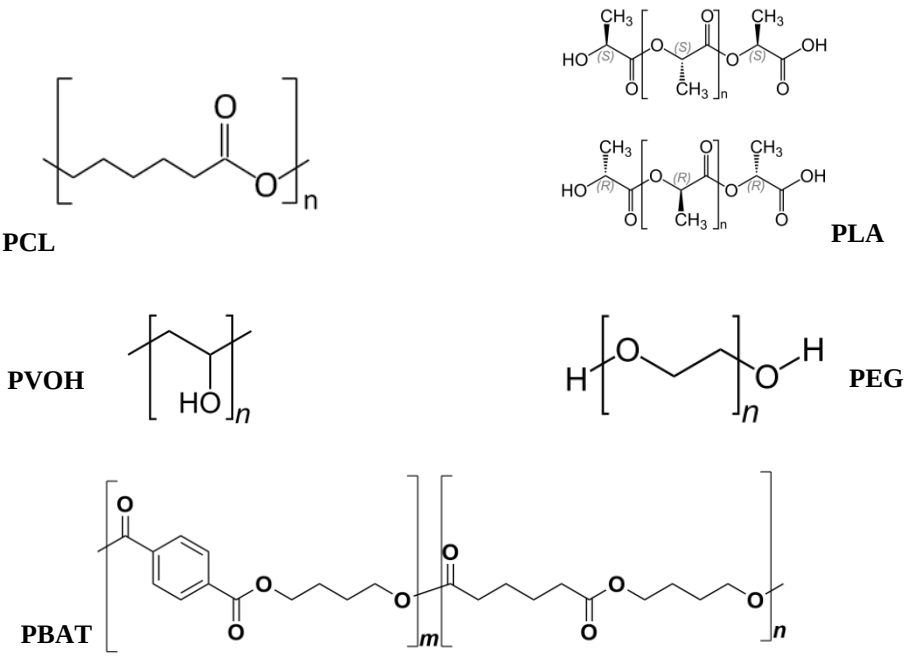

Figure I.5.-Chemical structure of some synthetic biodegradable polymers.

The physical properties of blend film formulations including PCL (Sugih *et al*., 2009; Campos *et al*., 2012; Taghizadeh & Favis, 2013; Cai *et al*., 2014), PLA (Sarazin *et al*., 2008; Shi *et al*., 2011; Wootthikanokkhan *et al*., 2012; Abdillahi *et al*., 2013; B *et al*., 2014; Bocz *et al*., 2014; Soares *et al*., 2013, 2014), PVOH (Katerinopoulou *et al*., 2014,), PBAT (Brandelero *et al*., 2010, 2011; Olivato *et al*., 2012a; Hablot *et al*., 2013; Shirai *et al*., 2013; García *et al*., 2014), poly(butylene succinate-co-adipate) (PBSA) (Jbilou *et al*., 2013), PU (Zhang *et al*., 2012) and

PEG (Yu *et al*., 2013) have been studied, as has their relevance for packaging applications. The most recent works are commented on below.

Li & Favis (2010) studied coalescence, dynamic and static mechanical properties and interfacial interactions of films with PCL/TPS at different ratios. Glycerol was used as plasticizer at 38% and 42% (w/w) with respect to TPS. These blends showed a highly interactive system and the tensile properties demonstrated ductility at very high levels of TPS (> 50%). High glycerol content promoted an increase in molecular mobility which in turn promoted compatibility between TPS/PCL due to hydrogen bond formation (Matzinos *et al*., 2002; Rodriguez-Gonzalez *et al*., 2004). Other authors (Cai *et al*., 2014) studied the structure, thermal properties, morphology and crystallization in TPS/PCL blends (at 0:10, 2:10, 4:10 and 6:10 ratios) obtained by compression moulding. Results revealed that the addition of TPS gave rise to a decrease in thermal stability and a good dispersion of the polymers, although weak interfacial adhesion was observed. Different strategies have been developed for the purposes of enhancing TPS/PCL blends, including the use of a third polymer, such as PLA, in the formulation. Ternary blends of TPS/PLA/PCL with different glycerol contents (24 and 36% with respect to TPS), obtained by extrusion, have been studied by Sarazin *et al*. (2008). In the ternary system, the impact and elongation at break of PLA was improved. The three components were mutually immiscible; however, a good PCL dispersion was observed in PLA, which enhanced the ductility of the ternary blends as compared to TPS/PLA blends. On the other hand, a high content of glycerol promoted synergies in such a way that the properties of ternary blends exceed the properties of binary blends in every case. In the ternary system, the increase in glycerol led to a rise in E (~66%), but a slight decrease in EM (~14%).

Other polymers, such as PU, have offered interesting results when blending with starch. Unlike PCL or PLA, cyanate groups (NCO) in PU can form a covalent bond

with -OH groups of starch. Zhang *et al*. (2012) synthesized PU by means of chemical reactions using PCL-diol, PCL-triol or PCL-tetrol and 4, 4'-methylenedi-p-phenyl diisocyanate. The products obtained were PU-polyols (PUP). Afterwards, PUP materials (20g PUP/100g polymer) were blended with starch and water at 90 ºC and 100 rpm for 20 min. As a result, the hydrophobicity of modified starches was enhanced, while the toughness and thermal stability of the material increased. In general, PUP synthesized with high branched polyols can improve the compatibility with TPS.

Brandelero *et al*. (2010, 2011) studied TPS/PBAT blended by blown extrusion by analysing the effect of the process steps on the film properties. On the one hand, they produced pellets of TPS (starch and glycerol) which were then extruded again with PBAT; and on the other hand, they extruded native starch, glycerol and PBAT using only one step. The second method permits an increase in the polymer contact area, resulting in similar characteristics for the different film formulations with high or low starch content. Likewise, this method reduces the processing cost.

Other works focused on PBSA; this is one of the promising aliphatic polyesters with desirable properties, such as biodegradability, melt processability, good mechanical properties and both chemical and thermal resistance. Jbilou *et al*. (2013) prepared blends of corn flour/PBSA, with glycerol as plasticizer, using extrusion and injection moulding. They found that the increase of PBSA in the blends promoted a rise in TS, EM and E and a decrease in WVP.

The addition of PVOH to starch nanocomposites produced a highly ordered intercalated structure (Dean *et al.*, 2008; Ali *et al*., 2011). Katerinopoulou *et al*., 2014 characterized acetylated corn starch (ACS)/PVOH/clay nanocomposite films. Replacing glycerol by PVOH in ACS-Na-MMT systems improved the mechanical strength due to the creation of hydrogen bonds between ACS and PVOH. The addition of 30g PVOH/100g starch, replacing the total amount of glycerol by

PVOH, caused an increase in the EM (from 82 MPa to 3464 MPa), and the TS (from 3.09 to 37.69) but a decrease in E (from 30.5 to 2.25). Another promising biodegradable polymer is PEG, which is biocompatible, non-toxic and water soluble (Dhawan *et al*., 2005). Yu *et al*. (2013) prepared TPS/(PEG) blends by extrusion, using different concentrations of PEG. They observed that the thermal stability of TPS is improved when PEG is added. However, the mechanical properties did not exhibit a clear trend.

I.1.3.4. Blends with non-biodegradable plastics

Starch can be destructured and blended with different synthetic polymers to satisfy a broad range of attributes. Typical synthetic polymers combined with TPS are LDPE (Prachayawarakorn *et al*., 2010; Pushpadass *et al*., 2010; Sabetzadeh *et al*., 2012; Prachayawarakorn & Pomdage, 2014), high density polyethylene (HDPE) (Taguet *et al*., 2009, 2014), PP (Ferreira *et al*., 2014) and polyamides (PA) (Landreau *et al*., 2009; Teyssandier *et al*., 2011). For this purpose, the use of a compatibilizer was necessary in most cases.

The main reasons for blending TPS with synthetic polymers are the promotion of the moisture barrier properties and the improvement of the strength and flexibility of the TPS. These combinations also lead to a decrease in the cost and an increase in the degradability of the material. Pushpadass *et al*. (2010) studied TPS/LDPE blends processed by extrusion. Composites with a starch:LDPE ratio of 95:5 had a WVP value of 2.18 x 10^{-4} g·day^{-1}·Pa^{-1}·m^{-1} and, when the LDPE ratio increased (a ratio of 85:15), the WVP decreased by 14.2%. Scanning Electron Microscope (SEM) micrographs of the films showed that there was no miscibility between the two polymers; for this purpose, the use of a compatibilizer was necessary. Sabetzadeh *et al*. (2012) and Prachayawarakorn & Pomdage (2014) used PE-g-MA as compatibilizer in these kinds of blends. Sabetzadeh *et al*. (2012) blended

TPS/LDPE, at different ratios, and added 3g PE-g-MA/100g polymer. Blends of TPS/LDPE (40/60), with compatibilizer, led to a decrease in EM (~44%), TS (~46%) and E (~73%) as compared to the reference TPS. So, the addition of other additives is necessary to enhance the mechanical properties. Prachayawarakorn & Pomdage (2014) studied the effect of carrageenan on properties of TPS/LDPE composite blends reinforced by cotton fibres and processed by compounding and injection moulding. They used 2.5g PE-g-MA/100g polymer and a TPS:LDPE weight ratio of 1:1. A significant improvement in the mechanical properties of the composites was obtained through the addition of carrageenan and fibres. The best mechanical properties were found for the composites modified by both carrageenan and cotton fibres. An increase in the stress at break and Young's modulus of 27.5% and 320%, respectively, was obtained.

Taguet *et al*. (2009) studied the interface/morphology relationship in HDPE/TPS blends prepared by extrusion by using different concentrations of glycerol and PE-g-MA. When there was a high content of glycerol (>24%) in the TPS, a 20% TPS-based binary blend with HDPE reached an elongation at break value of as much as 200%. When the appropriate level of PE-g-MA copolymer was added, this elongation further increased to 600%. The added PE-g-MA initially reacts with the glycerol-rich outer layer, but if the amount of compatibilizer is high enough, it reacts with the starch-rich phase. An optimal combination of both added PE-g-MA and an interfacial glycerol-rich phase promoted the best possible mechanical properties. Likewise, Taguet *et al*. (2014) studied the mechanical behaviour of blends HDPE/TPS (80/20) compatibilized with HDPE-g-MA. The authors studied the effect of different concentrations of glycerol and compatibilizer. The compatibilization of HDPE/TPS blends increases the surface area of TPS particles by decreasing their size. The addition of HDPE-g-MA promotes a reaction between maleic anhydride and the -OH of the glycerol leading to a reduction in the glycerol

content in the TPS phase. This phenomenon increases the stiffness of the TPS phase, thus leading to a significant decrease in toughness and deformation of the material.

PP is another material blended with TPS, although it has not been extensively studied. Ferreira *et al*. (2014) observed the effect of organoclays on TPS/PP (70/30) blends. The plasticizers were the glycerol (25% with respect to starch dry mass) and acetyl tributyl citrate (ATBC) (15% with respect to the PP mass). The compatibilizer used was Polybond® 3200. Organoclay was added at different concentrations, from 1 to 5% with respect to the total mass of polymer. The use of ATBC avoids the exudation of glycerol from the material. However, the compatibilizer was ineffective probably because of its low degree of MA substitution. Organoclay layers acted as a barrier against the diffusion of humidity within the starch matrix, preventing its retrogradation.

Finally, Landreau *et al*. (2009) and Teyssandier *et al*. (2011) studied blends of TPS with polyamide 11 (PA11) and polyamide 12 (PA12). In the first work, the morphologies and properties of TPS/PA11 blends were determined. These materials were compatibilized by means of carboxymethyl cellulose (CMC) addition (1g CMC /100g dry polymer). CMC interacts with PA11 through its sodium neutralized anionic groups, probably by the metal complexation and hydrogen bonding of the amide groups. The blends exhibited good mechanical properties (high TS and high E), even when TPS was the major component. Teyssandier *et al*. (2011) studied the compatibilization of TPS/PA12 blends through the addition of bisphenol A diglycidyl ether (DGEBA) and poly(ethylene-co-butyl acrylate-co-maleic anhydride) terpolymer (Lotader 3410). The PA12 crystallization in TPS/PA12 blends was found to be heavily dependent on the DGEBA content, while the introduction of Lotader 3410 had no influence. The addition of the first one promotes an increase in E as a consequence of the better

adhesion between the polymeric matrix and the dispersed phase, although a decrease in EM may be observed.

I.1.3.5. Compatibilizers, plasticisers and other additives in food packaging

The FDA's food additive regulations, found in Title 21, Parts 170–197 of the Code of Federal Regulations (CFR), cover both direct and indirect additives. The term ''indirect food additive'' refers to substances that are not intended to, but nevertheless become, components of food as a result of use in articles that are in contact with food (i.e., substances used in packaging materials) (Yam *et al*., 2009). The formulations designed for food packaging should contain only direct and indirect food additives. In the European Union the plastic materials and articles intended to come into contact with food are regulated by the Union Guidelines on Regulation (EU) No 10/2011.

In most cases, polymers in multiple-phase blends are immiscible and require a compatibilizer for blending. Usually, immiscible TPS/polymer blends are improved through the addition of MA, (Wu, 2003; Taguet *et al*., 2009, Prachayawarakorn *et al*., 2010; Sabetzadeh *et al*., 2012; Prachayawarakorn & Pomdage, 2014) diethyl maleate (DEM) or glycidyl methacrylate (GMA) grafted polymers (Figure I.6). PCL-g-DEM and PCL-g-GMA contributed to efficiently combine TPS/PCL in blends (Sugih *et al.*, 2009).

Other compatibilizers, such as CMC, have been used in the compatibilization of TPS/PA11 (Landreau *et al*., 2009); DGEBA and Lotader 3410 improved TPS/PA12 combinations (Teyssandier *et al*., 2011); glycidyl methacrylate grafted poly(ethylene octane) (GPOE) enhanced the properties of TPS/PLA blends (Shi *et al*., 2011) and VTMS was used in the compatibilization of TPS/LDPE blends (Prachayawarakorn *et al*., 2010).

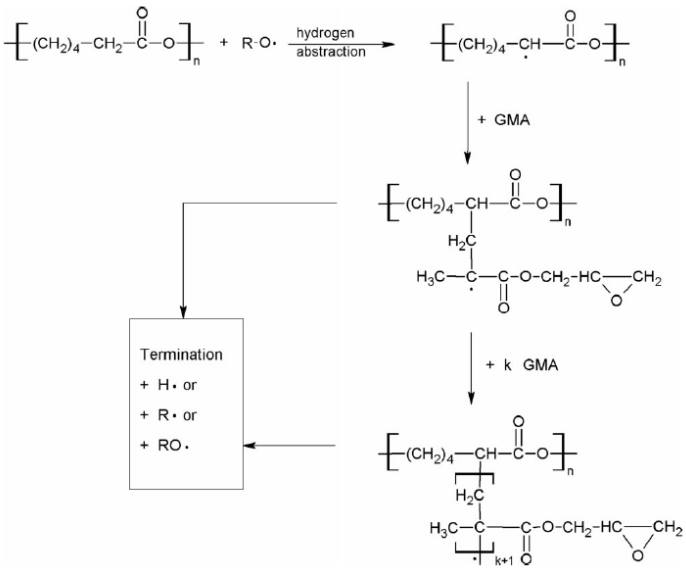

Figure I.6.-Simplified reaction mechanism for the grafting reaction between PCL and GMA according to Sugih *et al.* (2009).

Wu (2003) studied the physical and biodegradable properties of PCL/starch composites as compared to PCL-g-MA/starch binary blends. The mass ratios of starch to PCL were set at 10:90, 20:80, 30:70, 40:60, and 50:50. Plasticizer was not added to the polymer matrix. The great compatibility of PCL-g-MA with starch led to a much better dispersion and homogeneity of starch in the PCL-g-MA matrix and, consequently, to noticeably better properties. In the same way, the PCL-g-MA /starch blend is more easily processed, at lower melt temperatures, than PCL/starch blends. Other authors (Sugih *et al.*, 2009) studied the synthesis and properties of reactive interfacial agents (PCL-g-GMA and PCL-g-DEM) for starch/PCL blends. Interfacial agents were used as compatibilizers of starch/PCL blends at different ratios. At a fixed starch amount (20 wt.%) PCL-g-DEM showed a better compatibilization effect than PCL-g-GMA. The compatibilized blends exhibited significantly higher values of EM than the non-compatibilized ones.

Another extensively documented polymer is PLA. Shi *et al.* (2011) studied the physical properties of PLA/TPS and PLA/TPS blends with GPOE as compatibilizer. The content of TPS ranged from 0 to 50 wt.% and the content of GPOE from 0 to 20 wt.% with respect to the total weight. Glycerol at 20% with respect to dry starch was used as plasticizer. The elongation at break and impact strength of the ternary blends significantly increased when the addition of GPOE was added. The morphology of ternary blends with GPOE indicated that the starch granules melted and a good compatibility between PLA and TPS was reached in the matrix.

Another interesting compound that can act as an appropriate compatibilizer is CA because it has cross-linking capability through the reaction of its carboxyl groups (Ghanbarzadeh *et al*., 2010). The three carboxyl groups in CA molecules can interact with the hydroxyl groups of the starch molecules through the formation of ester groups (Figure I.7). This reaction can improve the water vapour barrier properties of the starch matrix due to the reduction of available hydroxyl groups, while decreasing the crystallization and retrogradation phenomena of the starch polymers (Shi *et al*., 2007). CA can also act as a compatibilizer, plasticizer and depolymerization agent simultaneously, depending on the processing conditions (Chabrat *et al*., 2012).

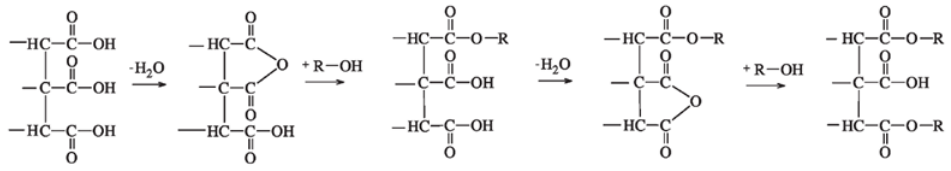

Figure I.7.-Conventional mechanism of dry cross-linking of polymers with hydroxyl groups, such as starch and cellulose, by citric acid, according to Reddy & Yang, 2010).

Olivato *et al*. (2012a) carried out a comparative study regarding the effect of different organic acids on the performance of TPS/polyester blow films. The influence of CA, malic acid (MaA) and tartaric acid (TA) in TPS/PBAT (55:45) films was evaluated. 1.5 (wt.%) of TA and CA produced films with an improved tensile strength (6.8 and 6.7 MPa, respectively), reduced the WVP and gave rise to a more homogeneous structure. The incorporation of the acids produced esterification reactions and/or starch hydrolysis. In the same way, Olivato *et al*. (2012b) compared the effect of citric acid and anhydride maleic on TPS/PBAT (55:45) films obtained by blown extrusion, containing glycerol in different concentrations. Although MA is a more reactive compound, it was a less efficient crosslinking agent (lower tensile strength) than CA, at similar concentrations. The WVP values were improved by high levels of CA (1.5 wt.%) and intermediate levels of glycerol (9.25 wt.%). Other authors (Garcia *et al*., 2014) evaluated TPS/PBAT (60:40) blend films plasticized with glycerol (different proportions) containing CA, with and without sodium hypophosphite (SHP), produced by blown extrusion. The TS of the films with CA and CA/SHP increased by 47% and 104%, respectively, as compared with the control film, while the elongation of the films with compatibilizer and catalyst (CA/SHP) increased by 125.7%. Films with CA and CA/SHP had a much greater EM than that of the control, while a significant reduction in the WVP values was observed.

Abdillahi *et al*. (2013) studied the effects of CA on TPS/PLA (75:25) blends prepared by injection moulding by using glycerol (15 wt.%) as plasticizer. CA was used in different ratios up to 20 parts (wt.) with respect to the polymer. The values of barrier properties proved that CA acted as compatibilizer for ratios of between 0 and 10 parts. The presence of CA significantly reduced the WVP and O_2P by up to 80% and 90%, respectively. When the addition exceeds 10 parts, CA acted as a

plasticizer and/or promoted the hydrolysis of the starch glycosidic bonds, leading to the plasticization of TPS/PLA blends and to a decrease in the WVP.

I.1.4. Final Remarks

It has become necessary to use biodegradable materials from renewable sources for food packaging in order to reduce the current environmental problems caused by conventional plastics while improving the sustainability of industrial processes. However, in terms of properties and cost, the competitiveness of bioplastics needs to be improved. Petroleum-derived plastics exhibit good mechanical properties and low water vapour sensitivity and permeability, which represent a significant advantage for food packaging, although in some cases they have poor oxygen barrier properties. Table A.I.6 (see Appendix A) shows the values of mechanical and barrier properties of some conventional plastics commonly used in food packaging. Their tensile strength, elongation, water vapour uptake capacity and water vapour permeability are more closely aligned with the food packaging requirements than that exhibited by bioplastic materials, particularly by starch-based films. Figure I.8 shows the locus of food packaging necessities in terms of water vapour and oxygen barrier properties (according to Schmid *et al.*, 2012), where the close fit of some of the plastics to the food necessities can be seen.

The location of starch materials on the map of barrier properties is very good in terms of their oxygen permeability but it is far from water barrier requirements and, what is worse, the high water uptake capacity of starch materials leads to an increase in water vapour permeability (and also in oxygen permeability) in line with the moisture gain and polymer matrix plasticization. Likewise, the mechanical properties of starch-based materials are also very sensitive to moisture content and ageing due to the starch retrogradation processes, which are promoted by molecular mobility associated with moisturizing. So, despite their low oxygen permeability,

the high water sensitivity of starch materials limits their industrial food packaging applications. Therefore, it is crucial to modify these materials in order to increase their hydrophobicity and facilitate their optimal use, taking advantage of the ready availability and low cost of starch.

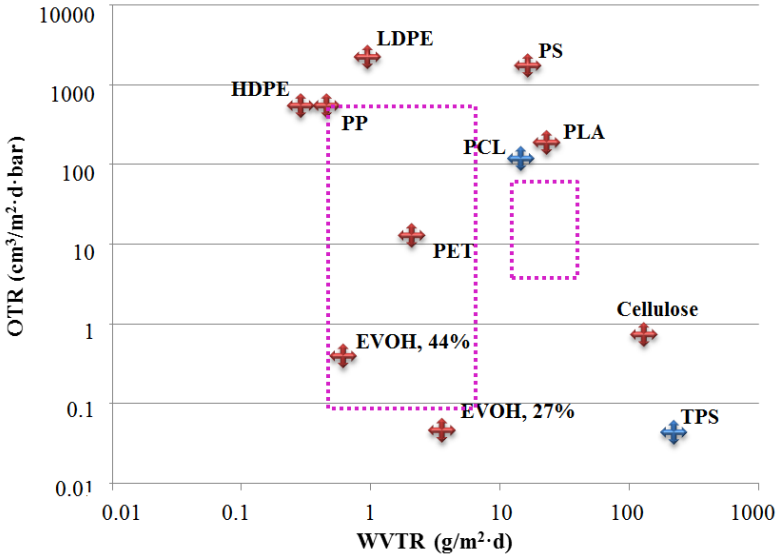

Figure I.8.-Comparison between barrier requirements of some foods (dotted lines) and barrier properties of some plastics used in food packaging. WTR and O_2TR values of materials are normalized at 100µm of thickness.

The present thesis studies different alternative means of improving physical properties of starch-based films, particularly their hydrophilic character. To this end, the blending of starch with more hydrophobic polymers and other compounds is examined.

I.1.5. APPENDIX A: see Tables A.I.1, A.I.2, A.I.3, A.I.4, A.I.5 and A.I.6

Table A.I.1.-Mechanical properties of starch-based films taking into account the preparation techniques and the strategies for improvement.

Method	Starch	Formulations	Strategy to improve	Plasticizer and Eq. RH	Thickness (µm)	EM (MPa)	TS (MPa)	E (%)	Reference
Extrusion	Corn starch	TPS/PCL (20/80)	Organic filler. Radiation.	Gly: 30% Eq. RH: 65%	1000	62 ± 2	1.7 ± 0.2	13.1 ±0.9	Campos *et al.*, 2012
		TPS/PCL (20/80) + sisal (20%)				103 ± 7	3.8 ± 0.5	8.9 ±1.3	
		TPS/PCL (20/80) + radiation				63 ± 2	1.8 ± 0.2	23 ± 3	
		TPS + PCL (20/80) + sisal(20%) + radiation				63 ± 3	4.9 ± 0.4	6.2 ±0.5	
	Wheat starch	TPS	Compatibilizer.	Gly: 33% Eq. RH: 50%	N.R.	N.R.	2	113	Landreau *et al.*, 2009
		TPS/PA11 (70/30) + CMC (1%)					20 ± 2	150 ± 12	
		TPS/PA11 (50/50) + CMC (1%)					16 ± 2	180 ± 26	
		TPS/PA11 (40/60) + CMC (1%)					20.0 ± 1.2	160 ± 22	
		TPS/PLA/PCL (50/45/5)	Blends with synthetic biodegradable polymer.	Gly: 24% Eq. RH: N.R.	N.R.	700	N.R.	13	Sarazin *et al.*, 2008
		TPS/PLA/PCL (50/45/5)		Gly: 36% Eq. RH: N.R.		600		38	
	Potato starch	TPS	Starch modification: high amylose.	Gly: 45% Eq. RH: 50 and 70%	N.R.	45 ± 4	3	47 ± 2	Thuwall *et al.*, 2006
		MTPS				36 ± 7	4.9 ± 0.3	80 ± 11	

Table A.I.1. (Continued)

		MTPS + 5% dextrin				68 ± 16	5.0 ± 0.3	67 ± 8	
Blown extrusion	Corn starch	MTPS (12.5%) + TPS (87.5%) (12.5/87.5)	Starch modification: acetylated starch.	Gly: 20% Eq. RH: 65%	80 ± 8	N.R.	27 ± 3	4.7 ±0.2	López *et al.*, 2013
		MTPS/TPS (94/6)		Gly: 15% Eq. RH: 65%	76 ± 14		16.2 ± 0.4	2.6 ±0.5	
		MTPS/TPS (17.5/82.5)		Gly: 15% Eq. RH: 65%	129 ± 14		24 ± 3	6.1 ±0.2	
		MTPS/TPS (54.5/45.5)		Gly: 17.5% Eq. RH: 65%	122 ± 14		17 ± 2	3.9 ±0.2	
Injection moulding	Corn starch	TPS	Organic filler.	Gly: 36% Eq. RH: 50%	N.R.	40	7	48	Müller *et al.*, 2014
		TPS/WF (98/2)				240	25	2	
		TPS/WF (96/4)				400	30	1	
		TPS	Organic filler.	Gly: 30% Eq. RH: 50%	1200	90 ± 20	4.0 ± 0.6	82 ± 20	Salaberria *et al.*, 2014
		TPS/CHNC (90/10)				290 ± 20	7.5 ± 0.9	22 ± 10	
		TPS/CHNC (80/20)				380 ± 50	11 ± 2	12.0 ±0.8	
		TPS/CHNF (90/10)				380 ± 60	11 ± 3	19 ± 2	
		TPS/CHNF (80/20)				510 ± 110	14 ± 4	9 ± 2	
	Corn flour	TPS/PBSA (70/30)	Blends with synthetic biodegradable polymer.	Gly: 25% Eq. RH: 50%	2000	189 ± 15	3.9 ± 0.6	16 ± 2	Jbilou *et al.*, 2013
		TPS/PBSA (70/30)				279 ± 10	11.9 ± 0.6	64 ± 36	
	Wheat starch	TPS/HDPE (20/80) + HDPE-g-MA (4%)	Blends with non-biodegradable plastic. Compatibilizer.	Gly: 24% Eq. RH: 50%	3050	N.R.	N.R.	30	Taguet *et al.*, 2009
		TPS/HDPE (20/80) + HDPE-g-MA (13%)						50	
		TPS/HDPE (20/80) + HDPE-g-MA (4%)		Gly: 32%				280	

Table A.I.1. (Continued)

		TPS/HDPE (20/80) + HDPE-g-MA (13%)		Eq. RH: 50%				600	
		TPS	Plasticiser.	Gly: 25% Eq. RH: 50%	2800	587 ± 41	12.3 ± 0.4	45 ± 3	Yu *et al*., 2013
		TPS/PEG (90/10)				557 ± 23	11.3 ± 0.2	15 ± 2	
		TPS/PEG (75/25)				719 ± 26	11.2 ± 0.6	3.5 ±0.2	
		TPS/PEG (60/40)				700 ± 16	11.6 ± 0.3	4.1 ±0.3	
		TPS/PEG (50/50)				597 ± 30	8.6 ± 0.6	134 ± 17	
		TPS/HDPE (80/20)	Blends with non-biodegradable plastic. Compatibilizer.	Gly: 24% Eq. RH: 50%	3050	1510 ± 190	17	46 ± 20	Taguet *et al*., 2014
		TPS/HDPE (80/20) + HDPE-g-MA (6%)				1470 ± 230	21	18 ± 10	
		TPS/HDPE (80/20) + HDPE-g-MA (9%)		Gly: 28% Eq. RH: 50%		1100 ± 120	19	310 ± 90	
		TPS/HDPE (80/20) + HDPE-g-MA 9%)		Gly: 36% Eq. RH: 50%		1040 ± 90	18	310 ± 70	
		TPS/HDPE (80/20) + HDPE-g-MA (13%)		Gly: 40% Eq. RH: 50%		1110 ± 200	17	210 ± 60	
	Cassava starch	TPS/LDPE (50/50) + PE-g-MA (2.5%)	Blends with non-biodegradable plastics. Compatibilizer. Organic filler. Gelling agent.	Gly: 30% Eq. RH: 60%	N.R.	50	8.5	260	Prachayawarakorn & Pomdage, 2014
		TPS/LDPE (50/50) + PE-g-MA (2.5%) + CF (5%)				170	11	160	
		TPS/LDPE (50/50) + PE-g-MA (2.5%) + CG (10%)				140	9.5	95	
		TPS/LDPE (50/50) + PE-g-MA (2.5%) + CF (5%) + CG (10%)				210	11	90	
	Native starch	TPS/PCL (20/80)	Blends with synthetic biodegradable polymer.	Gly: 38% Eq. RH: 50%	3000	134 ± 5	14.4 ± 0.6	> 1000	Li & Favis, 2010
		TPS/PCL (50/50)				73.1 ± 1.0	7.0 ± 0.4	> 1000	

Table A.I.1. (Continued)

		TPS/PCL (80/20)				15 ± 2	2.2 ± 0.7	455 ± 90	
	Aesculus Hippocastanum starch (A.H)	TPS (30% Gly)	Plasticizer. New sources of starch.	Gly and MalA Eq. RH: N.R.	N.R.	3.0 ± 0.3	1.5 ± 0.2	1.0 ±0.2	Castaño *et al.*, 2014
		TPS (15% Gly) + 15% MalA				N.R.	1.5 ± 0.2	0.3 ±0.2	
	Araucaria Araucana starch (A.A.)	TPS (30% Gly)				4.0 ± 0.5	2.4 ± 0.2	1.1 ±0.2	
		TPS (15% Gly) + 15% MalA				N.R.	2.0 ± 0.3	0.8 ±0.2	
Compression moulding	Corn starch	TPS	Blends with natural biopolymer.	Gly: 30% Eq. RH: 60%	110 ± 2	1049 ± 38	10.7 ± 0.2	2.4 ±0.3	Lopez *et al.*, 2014
		TPS/CH (86/14)			139 ± 2	1188 ± 68	12.5 ± 0.8	1.6 ±0.2	
		TPS/CHT (86/14)			121 ± 3	1081 ± 58	12.6 ± 0.6	1.9 ±0.4	
		TPS	Blends with non-biodegradable plastic. Compatibilizer.	Gly: 35% Eq. RH: N.R.	2000	250	12	300	Sabetzadeh *et al.*, 2012
		TPS/LDPE (20/80) + PE-g-MA (3%)				231	9	140	
		TPS/LDPE (40/60) + PE-g-MA (3%)				140	6.5	80	
		TPS/PCL (20/80)	Blends with synthetic biodegradable polymer. Compatibilizer.	Without plasticizer Eq. RH: N.R.	2000	337	10.5	425	Sugih *et al.*, 2009
		TPS/PCL (20/80) + PCL-g-DEM				342	11	385	
		TPS/PCL (20/80) + PCL-g-GMA				380	10	343	
		TPS/ESO (99/1) + Et3N (0.2%) : MTPS	Starch modification: Et3N and ESO.	Gly: 28% Eq. RH: 40%	2000	150	2.5	83	Belhassen *et al.*, 2014
		TPS/ESO (97/3) + + Et3N (0.2%) : MTPS				235	4	59	
		TPS	Blends with natural biopolymer. Compatibilizer. Plasticiser.	Gly: 30% Eq. RH: 53%	268 ± 28	278 ± 75	10 ± 2	28 ± 10	Ortega-Toro *et al.*, 2014
		TPS/HPMC (83.3/16.7)			204 ± 28	262 ± 70	10.0 ± 1.1	21 ± 7	
		TPS/HPMC (83.3/16.7) + CA (1%)			158 ± 13	380 ± 90	9.1 ± 0.5	12 ± 7	

Table A.I.1. (Continued)

		TPS	Inorganic filler.	Gly: 30% Eq. RH: 60%	N.R.	23 ± 2	1.19 ± 0.04	62 ± 4	López *et al*., 2015
		TPS/TN (97/3)				25 ± 2	1.80 ± 0.13	59.1 ±1.5	
		TPS/TN (95/5)				38 ± 3	2.34 ± 0.04	59.0 ±1.1	
		TPS-GlyPh/PLA (20/80)	Organic filler. Other additives: flame retardant, surface treating agent	Gly and GlyPh: 25% Eq. RH: N.R.	4000	1600	33	2.6 ±0.2	Bocz *et al*., 2014
		TPS-GlyPh/PLA (20/80) + Flax-Psil (35%)				1500	26	1.9 ±0.2	
		TPS-GlyPh/PLA (20/80) + Flax-Psil (40%) + APP (16%)				1700	21	1.3 ±0.2	
	Wheat starch	TPS + PA12 (30/70)	Blends with synthetic biodegradable polymer. Compatibilizer.	Gly: 20% Eq. RH: 50%	1000	850	32	30	Teyssandier *et al.* 2011
		TPS + PA12 (30/70) + DGEBA (1%)				980	42	250	
		TPS + PA12 (30/70) + Lotader 3410 (5%)				740	30	230	
	Cassava starch	TPS	Organic filler.	Gly: 30% Eq. RH: 60%	200 ± 7	39 ± 4	1.7 ± 0.4	11 ± 3	Versino *et al*., 2015
		TPS + cassava bagasse (98.5/1.5)			192 ± 12	83 ± 5	4.3 ± 0.5	15.7 ±1.4	
		TPS + cassava root peel (98.5/1.5)			193 ± 9	64 ± 6	3.0 ± 0.4	12 ± 3	
		MTPS/PLA (20/80)	Starch modification: MA	Gly: 25% Eq. RH: N.R.	500	188 ± 20	17.3 ± 0.6	556 ± 12	Wootthikanokkhan *et al*., 2012
		MTPS/PLA (30/70)				141 ± 18	13.0 ± 0.7	79 ± 20	
		MTPS/PLA (40/60)				151 ± 8	15.5 ± 0.9	56 ± 4	
		TPS/PLA (70/30)	Blends with synthetic biodegradable polymer. Coating with natural	Gly: 30% Eq. RH: N.R.	900-1200	60 ± 9	1.7 ± 0.2	19 ± 2	Soares *et al*., 2013
		TPS/PLA (70/30) + CH (spray)				422 ± 23	3.7 ± 0.5	2.6 ±0.5	

Table A.I.1. (Continued)

		TPS/PLA (70/30) + CH (immersion)	biopolymer.			214 ± 56	2.8 ± 0.4	5.5 ±1.4	
		TPS/PLA (70/30)	Blends with synthetic biodegradable polymer. Coating with natural biopolymer.	Gly: 30% Eq. RH: N.R.	N.R.	60 ± 9	1.7 ± 0.2	19 ± 2	Soares *et al*., 2014
		TPS/PLA (70/30) + CH (C.S.)				382 ± 126	6 ± 2	1.9 ±0.4	
		TPS/PLA (70/30) + CH (C.F.)				422 ± 23	3.7 ± 0.5	2.6 ±0.5	
	Cassava starch	TPS/PLA (80/20) + CA (2%) + SA (2%)	Organic Filler. Compatibilizer. Plasticisers.	Gly: 30% Eq. RH: 53%	N.R.	1182 ± 165	16.5 ± 1.3	14.5 ±0.7	Teixeira *et al*., 2012
	Cassava bagasse (b)	TPSb/PLA (80/20) + CA (2%) + SA (2%)				1664 ± 126	19.9 ± 0.9	2.0 ±0.3	
	Potato starch	TPS	Blends with synthetic biodegradable polymer. Inorganic filler.	Gly: 30% Eq. RH: N.R.	N.R.	146 ± 6	1.8 ± 0.2	3.6 ±0.9	B *et al*., 2014
		TPS/PLA (60/40)				305 ± 14	5.6 ± 0.3	4.3 ±0.9	
		TPS/PLA (60/40) + Na-MMT (1%)				329 ± 14	7.9 ± 0.3	6.0 ±1.2	

Table A.I.2.-Water vapour permeability of starch-based films taking into account the preparation techniques and the strategies for improvement.

Method	Starch	Formulations	Strategy to improve	Plasticizer	Δ Relative Humidity	WVP (g day^{-1}Pa^{-1}m^{-1})	Thickness (μm)	Reference
Extrusion and Extrusion-coated	Corn starch	TPS + LDPE (95/5)	Blends with non-biodegradable plastic.	Gly: 30%	100-50%	2.2 (x10^{-4})	400-500	Pushpa-dass *et al.*, 2010
		TPS + LDPE (90/10)				1.7 (x10^{-4})	400-500	
		TPS + LDPE (85/15)				1.9 (x10^{-4})	400-500	
	Potato starch	GP + 1 layer SBC (1.2 g/m^2)	Inorganic filler. Starch modification: Hydroxypropylated and oxidized. SBC: starch + PEG + 33% Na-MMT based on dry starch: total solid content 20.3%).	PEG 400: 30%	100-50%	5.1 (x10^{-10})	N.R.	Olsson *et al.*, 2014
		GP + 2 layers SBC (3 g/m^2)				4.2 (x10^{-10})		
		LPB + 1 layer SBC (3.8 g/m^2)				47.4 (x10^{-10})		
		LPB + 2 layers SBC (7.1 g/m^2)				13.7 (x10^{-10})		
		LPB + 2 layers SBC (9.1 g/m^2)				6.2 (x10^{-10})		
Blow extrusion	Corn starch	MTPS/TPS (12.5/87.5)	Starch modification: acetylated starch.	Gly: 20%	75-0%	1.4 ± 0.3 (x10^{-10})	80 ± 8	López *et al.*, 2013
		MTPS/TPS (94/6)		Gly: 15%		0.88 ± 0.05 (x10^{-10})	76 ± 14	
		MTPS/TPS (17.5/82.5)		Gly: 20%		1.3 ± 0.2 (x10^{-10})	123 ± 12	
		MTPS/TPS (54.5/45.5)		Gly: 15%		1.2 ± 0.2 (x10^{-10})	129 ± 14	
	Cassava starch	TPS	Plasticizer. Method of production.	Gly: 30%	90-64%	20 ± 4 (x10^{-7})	N.R.	Brandelero *et al.*, 2011
		TPS/PBAT (80/20)				3.94 ± 0.03 (x10^{-7})		
		TPS/PBAT (50/50)				2.4 ± 0.2 (x10^{-7})		
		TPS/PBAT(55/45)	Blends with synthetic biodegradable polymer. Compatibilizer. Plasticizer.	Gly: 18%	75-33%	3.11 ± 0.02 (x10^{-5})	100-150	Olivato *et al.*, 2012b
		TPS/PBAT (55/45) + CA (1.5%)				1.69 ± 0.02 (x10^{-5})	100-150	
		TPS/PBAT (55/45) + MA (1.5%)				3.3 ± 0.7 (x10^{-5})	100-150	
		TPS/PBAT (55/45) + CA (0.75%) + MA (0.75%)				4.0 ± 0.3 (x10^{-5})	100-150	

Table A.I.2. (Continued)

		TPS/PBAT (55/45) + CA (0.375%)	Blends with synthetic biodegradable polymer. Compatibilizer. Plasticizer.	Gly: 18%	75-33%	1.5 ± 0.2 (x10^{-5})	100-150	Olivato *et al*., 2012a
		TPS/PBAT (55/45) + MaA (0.375%)				1.6 ± 0.2 (x10^{-5})	100-150	
		TPS/PBAT (55/45) + TA (0.375%)				1.6 ± 0.2 (x10^{-5})	100-150	
		TPS/PBAT (60/40)	Blends with synthetic biodegradable polymer. Compatibilizer. Plasticizer.	Gly: 11%	75-33%	5.8 ± 0.6 (x10^{-6})	100-150	García *et al*., 2014
		TPS/PBAT (60/40) + CA (0.8%)		Gly: 10.2%		3.50 ± 0.13 (x10^{-5})	100-150	
		TPS/PBAT (60/40) + CA (0.8%) + SHP (0.38%)		Gly: 10.2%		3.8 ± 0.4 (x10^{-5})	100-150	
		TPS/PBAT (33/67)	Blends with synthetic biodegradable polymer. Additives.	Gly: 30%	33-0%	0.57 ± 0.02 (x10^{-7})	147 ± 58	Brandelero *et al*. 2010
					90-64%	2.4 ± 0.2 (x10^{-7})	147 ± 58	
		TPS/PBAT (33/67) + Tween 80 (2%)			33-0%	5.3 ± 0.3 (x10^{-7})	1206 ± 200	
					90-64%	22 ± 6 (x10^{-7})	1206 ± 200	
		TPS/PBAT (60/40) + CA (0.01%) + MS (0.5%)	Blends with synthetic biodegradable polymer. Compatibilizer. Plasticizer.	Gly: 32%	64-33%	7.2 ± 0.2 (x10^{-6})	103 ± 9	Shirai *et al*., 2013
		TPS/PBAT/PLA (50/40/10) + CA (0.01%) + MS (0.5%)				6.3 ± 0.3 (x10^{-6})	131 ± 10	
		TPS/PBAT/PLA (40/40/20) + CA (0.01%) + MS (0.5%)				5.0 ± 0.7 (x10^{-6})	405 ± 59	
Injection moulding	Wheat flour	TPS/PLA (75/25)	Blends with synthetic biodegradable polymer. Compatibilizer. Plasticizer.	Gly: 15%	60-0%	1.4 ± 0.2 (x10^{-5})	1000 ± 100	Abdillahi *et al*., 2013
		TPS/PLA (75/25) + CA (2%)				0.24 ± 0.02 (x10^{-5})	1100 ± 20	
		TPS/PLA (75/25) + CA (10%)				0.29 ± 0.06 (x10^{-5})	1000 ± 100	
		TPS/PLA (75/25) + CA (20%)				1.26 ± 0.14 (x10^{-5})	1000 ± 100	
Compression moulding	Corn starch	TPS	Blends with natural biopolymer. Compatibilizer. Plasticizer.	Gly: 30%	100-53%	1.16 ± 0.06 (x10^{-4})	268 ± 28	Ortega-Toro *et al*., 2014
		TPS/HPMC (83.3/16.7)				0.58 ± 0.05 (x10^{-4})	204 ± 28	
		TPS/HPMC (83.3/16.7) + CA (1%)				0.34 ± 0.04 (x10^{-4})	158 ± 13	
		TPS	Blends with natural biopolymer.	Gly: 30%	100-50%	1.15 ± 0.08 (x10^{-4})	110 ± 2	Lopez *et al*., 2014
		TPS/CH (86/14)				0.75 ± 0.03 (x10^{-4})	138 ± 2	

Table A.I.2. (Continued)

		TPS/CHT (86/14)				0.51 ± 0.02 ($x10^{-4}$)	121 ± 3	
		TPS	Inorganic filler.	Gly: 30%	50-0%	1.11 ± 0.09 ($x10^{-4}$)	N.R.	López *et al.*, 2015
		TPS/TN (97/3)				0.80 ± 0.05 ($x10^{-4}$)		
		TPS/TN (95/5)				0.830 ± 0.009 ($x10^{-4}$)		
	Cassava starch	TPS/PLA (70/30)	Blends with synthetic biodegradable polymer. Coating with natural biopolymer.	Gly: 30%	75-0%	4.3 $\pm$ 0.5 ($x10^{-7}$)	900-1200	Soares *et al.*, 2013
		TPS/PLA (70/30) + CH (spray)				3.1 $\pm$ 0.2 ($x10^{-7}$)		
		TPS/PLA (70/30) + CH (immersion)				3.3 $\pm$ 0.2 ($x10^{-7}$)		
		TPS/PLA (70/30)	Blends with synthetic biodegradable polymer. Coating with natural biopolymer.	Gly: 30%	75-0%	4.3 $\pm$ 0.5 ($x10^{-7}$)	N.R.	Soares *et al.*, 2014
		TPS/PLA (70/30) + CH (C.S.)				1.75 $\pm$ 0.05 ($x10^{-7}$)		
		TPS/PLA (70/30) + CH (C.F.)				3.1 $\pm$ 0.2 ($x10^{-7}$)		
		TPS	Inorganic filler.	Gly: 25%	75-0%	1.9 ± 0.2 ($x10^{-5}$)	394 ± 28	Müller *et al.*, 2012
		TPS/MMT (96/4)				0.7 ± 0.2 ($x10^{-5}$)	485 ± 37	
		TPS/MMT(94/6)				0.7 ± 0.2 ($x10^{-5}$)	515 ± 37	
		TPS	Organic filler.	Gly: 30%	50-0%	1.30 ($x10^{-5}$)	200 ± 7	Versino *et al.*, 2015
		TPS + cassava bagasse (98.5/1.5)				1.30 ($x10^{-5}$)	192 ± 12	
		TPS + cassava root peel (98.5/1.5)				1.34 ($x10^{-5}$)	193 ± 9	

Table A.I.3.-Oxygen permeability (O_2P) of starch-based films taking into account the preparation techniques and the strategies for improvement.

Method	Starch	Formulations	Strategy to improve	Plasticizer and Eq. RH	O_2P ($cm^3/m\ s\ Pa$)	Thickness (μm)	Reference
Blown extrusion	Corn starch	MTPS/TPS (12.5/87.5)	Starch modification: acetylated starch.	Gly: 20%; Eq. RH: 65%	$4.13 \pm 0.11\ (x10^{-10})$	80 ± 8	López *et al*., 2013
		MTPS/TPS (94/6)		Gly: 15%; Eq. RH: 65%	$2.08 \pm 0.08\ (x10^{-10})$	76 ± 14	
		MTPS/TPS (17.5/82.5)		Gly: 20%; Eq. RH: 65%	$3.31 \pm 0.08\ (x10^{-10})$	123 ± 12	
		MTPS/TPS (54.5/45.5)		Gly: 15%; Eq. RH: 65%	$2.98 \pm 0.08\ (x10^{-10})$	129 ± 14	
Injection moulding	Corn starch	TPS/Lotader 3210 (80/20)	Filler. Compatibilizer.	Gly: 35% Eq. RH: N.R.	$7.8\ (x10^{-12})$	400	Privas *et al*., 2013
		TPS/Lotader 3210 (80/20) + LS (2%)			$6.0\ (x10^{-12})$	400	
		TPS/Lotader 3210 (80/20) + LS (4%)			$6.1\ (x10^{-12})$	400	
	Wheat flour	TPS/PLA (75/25)	Blends with synthetic biodegradable polymer. Compatibilizer. Plasticizer.	Gly: 15% Eq. RH: 50%	$5.44 \pm 0.02\ (x10^{-13})$	1000 ± 100	Abdillahi *et al*., 2013
		TPS/PLA (75/25) + CA (2%)			$0.35 \pm 0.02\ (x10^{-13})$	1100 ± 20	
		TPS/PLA (75/25) + CA (10%)			$1.60 \pm 0.03\ (x10^{-13})$	1000 ± 100	
		TPS/PLA (75/25) + CA (20%)			$1.40 \pm 0.2\ (x10^{-13})$	1000 ± 100	
Compression moulding	Corn starch	TPS/HPMC (83.3/16.7)	Blends with natural biopolymer. Compatibilizer. Plasticizer.	Gly: 30% Eq. RH: 53%	$1.3 \pm 0.5\ (x10^{-13})$	268 ± 28	Ortega-Toro *et al*., 2014
		TPS/HPMC (83.3/16.7) + CA (1%)			$4.0 \pm 1.0\ (x10^{-13})$	204 ± 28	
		TPS/HPMC (83.3/16.7)			$5.0 \pm 1.0\ (x10^{-13})$	158 ± 13	
		TPS	Inorganic filler	Gly: 30% Eq. RH: 75%	$6.0 \pm 0.5\ (x10^{-11})$	N.R.	López *et al*., 2015
		TPS/TN (97/3)			$4.6 \pm 0.3\ (x10^{-11})$		
		TPS/TN (95/5)			$4.4 \pm 0.2\ (x10^{-11})$		

Table A.I.4.-Gas permeability of starch-based films taking into account the preparation techniques and the strategies for improvement.

Method	Starch	Formulations	Strategy to improve	Plasticizer and Eq. RH	Gas	Permeability	Thickness (µm)	Reference
Extrusion-coated	Potato starch	GP + 1 layer SBC (1.2 g/m^2)	Inorganic filler. Starch modification: Hydroxypropylated and oxidized. SBC: starch + PEG + 33% Na-MMT based on dry starch: total solid content 20.3%).	PEG 400 (30%) Eq. RH: 50%	Air (nm/ Pa . s)	0	N.R.	Olsson *et al*. 2014
		GP + 2 layers SBC (3 g/m^2)				0		
		LPB + 1 layer SBC (3.8 g/m^2)				> 65		
		LPB + 2 layers SBC (7.1 g/m^2)				1.9		
		LPB + 2 layers SBC (9.1 g/m^2)				0.3		
Blown extrusion	Corn starch	MTPS/TPS (12.5/87.5)	Starch modification: acetylated starch.	Gly: 20% Eq. RH: 65%	CO_2 (cm^3/m s Pa)	5.0 ± 0.3 (x10^{-9})	80 ± 8	López *et al*., 2013
		MTPS/TPS (94/6)		Gly: 15% Eq. RH: 65%		2.7 ± 0.2 (x10^{-9})	76 ± 14	
		MTPS/TPS (17.5/82.5)		Gly: 20% Eq. RH: 65%		4.13 ± 0.14 (x10^{-9})	123 ± 12	
		MTPS/TPS (54.5/45.5)		Gly: 15% Eq. RH: 65%		3.85 ± 0.04 (x10^{-9})	129 ± 14	

Table A.I.5.-Thermal properties of starch-based films taking into account the preparation techniques and the strategies for improvement.

Method	Starch	Formulations	Strategy to improve	Plasticizer and Eq. RH	Thermal properties (ºC)	Reference
Extru-sion	Corn starch	TPS	Starch modification: MA	Gly: 25% Eq. RH: N.R.	TGA Onset: 302	Hablot *et al*., 2013
		TPS/PBAT (40/60)			TGA Onset: 321	
		TPS/PBAT (40/60) + MA (2%)			TGA Onset: 295	
Injection moulding	Corn starch	TPS	Organic filler	Gly: 30% Eq. RH: 50%	$T_{g\beta}$: -48 $T_{g\alpha}$: 67 TGA Onset: 252	Salaberria *et al*. 2014
		TPS/CHNC (90/10)			$T_{g\beta}$: -47 $T_{g\alpha}$: 75 TGA Onset: 230	
		TPS/CHNC (80/20)			$T_{g\beta}$: -47 $T_{g\alpha}$: 76 TGA Onset: 222	
		TPS/CHNF(90/10)			$T_{g\beta}$: -46 $T_{g\alpha}$: 74 TGA Onset: 259	
	Aesculus Hippocastanum starch (A.H) and	TPS (30% Gly)	Plasticizer. New sources of starch	Gly and MalA Eq. RH: N.R.	TGA T_{max}: 302	Castaño *et al*., 2014
		TPS (15% Gly) + 15% MalA			TGA T_{max}: 302	
	Araucaria Araucana starch (A.A.)	TPS (30% Gly)			TGA T_{max}: 307	
		TPS (15% Gly) + 15% MalA			TGA T_{max}: 307	
Compression moulding	Corn starch	TPS	Blends with natural biopolymers. Compatibilizer. Plasticizer.	Gly: 30% Eq. RH: 0%	T_g: 125 ± 4	Ortega-Toro *et al*., 2014
		TPS/HPMC (83.3/16.7)			T_g: 112 ± 3	
		TPS/HPMC (83.3/16.7) + CA (1%)			T_g: 105 ± 9	
		TPS	Blends with natural biopolymer.	Gly: 30% Eq. RH: 60%	T_m: 155 ± 12	Lopez *et al*., 2014
		TPS/CH (86/14)			T_m: 152 ± 14	
		TPS/CHT (86/14)			T_m: 147 ± 12	
		TPS	Blends with synthetic biodegradable polymer. Compatibilizer	Gly: 20% Eq. RH: N.R.	TGA Onset: 270	Shi *et al*., 2011
		TPS/PLA (20/80)			TGA Onset: 280	
		TPS/PLA (20/80) + GPOE (15%)			TGA Onset: 290	

Table A.I.5. (Continued)

		TPS	Blends with synthetic biodegradable polymer.	Gly: 30% Eq. RH: N.R.	TGA Onset: 290		Cai *et al.*, 2014
		TPS/PCL (40/60)			TGA Onset: 288		
		TPS/PCL (60/40)			TGA Onset: 278		
		TPS/PU2(80/20)	Blends with synthetic biodegradable polymer.	Without Eq. RH: 60%	TGA T_{max}: 337		Zhang *et al.*, 2012
		TPS/PU3 (80/20)			TGA T_{max}: 340		
		TPS/PU4 (80/20			TGA T_{max}: 343		
		TPS	Blends with non-biodegradable plastics. Compatibilizer. Plasticizer. Inorganic filler.	Glycerol (25% based on starch) and ATBC 15% based on PP) Eq. RH: 80%	TGA T_{max}: 305		Ferreira *et al.*, 2014
		TPS/PP-ATBC (70/30)			TGA T_{max}: 309		
		TPS/PP-ATBC (70/30) + MMT (1%)			TGA T_{max}: 308		
	Cassava starch	TPS	Organic filler.	Gly: 30% Eq. HR: 60%	$T_{g\beta}$: -45 ± 4 $T_{g\alpha}$: 27 ± 8	T_m: 155 ± 10	Versino *et al.*, 2015
		TPS + cassava bagasse (98.5/1.5)			$T_{g\beta}$: -45 ± 5 $T_{g\alpha}$: 46 ± 8	T_m: 219.1 ± 0.9	
		TPS + cassava root peel (98.5/1.5)			$T_{g\beta}$: -48 ± 5 $T_{g\alpha}$: 77 ± 8	T_m: 187 ± 3	
		TPS	Organic filler.	Gly: 30% Eq. RH: N.R.	TGA Onset: 296	TGA T_{max}: 319	Lomelí-Ramírez *et al.*, 2014
		TPS/Coconut fibre (80/20)			TGA Onset: 311	TGA T_{max}: 311	
		TPS/Coconut fibre (70/30)			TGA Onset: 306	TGA T_{max}: 306	
	Potato starch	TPS	Blends with synthetic biodegradable polymers. Inorganic filler.	Gly: 30% Eq. RH: N.R.	TGA Onset: 290	TGA T_{max}: 300	B *et al.*, 2014
		TPS/PLA (60/40)			TGA Onset: 310	TGA T_{max}: 340	
		TPS/PLA (60/40) + Na-MMT (1%)			TGA Onset: 310	TGA T_{max}: 341	
	Rice starch	TPS	Blends with non-biodegradable plastics Organic filler. Compatibilizer.	Gly: 50% Eq. RH: 50%	TGA Onset: 301		Prachayawarakorn *et al.*, 2010
		TPS/CF (90/10)			TGA Onset: 303		
		TPS/LDPE (70/30)			TGA Onset: 301		

Table A.I.6.-Mechanical, thermal and barrier properties and degradation in soil of conventional polymers and typical biodegradable polymers

Polymer	Properties					
	Mechanical	**Thermal (ºC)**	**WVP (g /(day·Pa·m)**	**O_2P (cm^3/m·s·Pa)**	**CO_2P (cm^3/m·s·Pa)**	**Soil degradation**
HDPE	TM: 862 MPa TS: 21-52 MPa E: 10-500% (Harper, 2004)	T_m: 205-280 (Harper, 2004)	(1.16-2.52) x 10^{-9} (90% RH, 25µm) (Harper, 2004)	(0.13-1.12) x 10^{-11} (0% RH, 25µm) (Harper, 2004)	(1.12-2.90) x 10^{-11} (0% RH, 25µm) (Harper, 2004)	0% Mass loss in 2 years (Bastioli, 2005)
LDPE	TM: 138-278MPa TS: 8.3-17.2 MPa E: 225-600% (Harper, 2004)	T_m: 180-280 (Harper, 2004) T_g: -30 (Bastioli, 2005)	4.66 x 10^{-9} (90% RH, 25µm) (Harper, 2004)	(1.12-3.78) x 10^{-11} (0% RH, 25µm) (Harper, 2004)	(2.25-22.5) x 10^{-11} (0% RH, 25µm) (Harper, 2004)	Molecular weight decrease after 32-37 years (Ohtake *et al.*, 1998)
LLDPE	TM: 172 MPa TS: 24-55 MPa E: 400-800% (Harper, 2004)	T_m: 160-280 (Harper, 2004) T_g: -122 to -20.5 (Yam, 2009)	4.66 x 10^{-9} (90% RH, 25µm) (Harper, 2004)	(1.12-3.78) x 10^{-11} (0% RH, 25µm) (Harper, 2004)	(2.25-22.5) x 10^{-11} (0% RH, 25µm) (Harper, 2004)	
PP	TS: 81.4 MPa TM: 2760 MPa (Harper, 2004) E: 35-475% (Yam, 2009)	T_m: 220-225 (Harper, 2004) T_g: -14 to 5 (Yam, 2009)	Oriented: 1.50 x 10^{-9} (25µm, 90 % RH) (Harper, 2004) Non-oriented: 3.76 x 10^{-9} (25µm, 90 % RH) (Harper, 2004)	Oriented: 0.72 x 10^{-11} (25µm, 90 % RH) (Harper, 2004) Non-oriented: 1.07 x 10^{-11} (25µm, 90 % RH) (Harper, 2004)	Oriented: (1.35 – 2.43 x 10^{-11} Non-oriented: (2.25-3.6) x 10^{-11} (25 ºC) (Yam, 2009)	3% CO_2 in 12 weeks (Bastioli, 2005)
PS	EM: 2.800 MPa TS: 45 MPa TM: 3100 MPa (Harper, 2004)	T_g: 83-94 (Yam, 2009)	3.34 x 10^{-6} (25µm) (Harper, 2004)	(1.12-18) x 10^{-8} (Yam, 2009)	(3.14-6.7) x 10^{-8} (Yam, 2009)	No degradation after 32 years (Albertsson & Karlsson, 1988)

Table A.I.6. (Continued)

PET	TS: 159 MPa TM: 9960 MPa UE: 30-300% (Harper, 2004)	T_m: 212-265 ªC (Harper, 2004)	6.9 x 10^{-9} (Yam, 2009)	(1.32-1.77) x 10^{-9} (Yam, 2009)	8.67 x 10^{-13} (oriented polymer) (Yam, 2009)	~15% CO_2 in 2 years (ISO 14851, 1999)
Nylon 6	TS: 52 MPa TM: 2300 MPa E: 50-200% (Harper, 2004)	T_m: 230-280 (Harper, 2004)	4.14 x 10^{-8} (Yam, 2009)	(8.96-13.4) x 10^{-11} (Yam, 2009)	(44.8-53.7) x 10^{-11} (Yam, 2009)	
EVOH	TS: 71.6 MPa EM: 2647 MPa E: 230% (Ethylene content: 32mol% (Yam, 2009)	T_m: 156-196 (24-48 mol % ethylene content) (Yam, 2009)	5.5 x 10^{-9} (40ºC, 90% RH, 44 mol% ethylene) 14.7 x 10^{-9} (40ºC, 90% RH, 32 mol% ethylene) (Yam, 2009)	4.48 x 10^{-15} (23 ºC, aw: 0) 134 x 10^{-15} (23 ºC, aw: 0.95) (Bastioli, 2005)	Oriented: 4.5 x 10^{-15} (25µm, 70 % RH, 32 mol% ethylene) Oriented: 4.5 x 10^{-14} (25µm, 90 % RH, 44 mol% ethylene) (Harper, 2004)	
PVOH	TS: 36 MPa (Extruded, 25 ºC) E: 225% (Extruded, 25 ºC) (Mark, 1999)	T_m: 200 ºC (Mark, 1999)	4.5 x 10^{-13} 38 ºC, 90% RH) (Yam, 2009)	2.65 x 10^{-11} (24ºC) (Yam, 2009)	2.7 x 10^{-15} (Dry conditions) (Yam, 2009)	8% mass loss in 2 years (Bastioli, 2005)
PLA	TM: 3834 MPa FM: 3689 E: 4% (Bastioli, 2005) EM: 8.6MPa (Yam, 2009)	T_m: 184 T_g: 60 (Bastioli, 2005)	1.51 ± 0.04 x 10^{-6} (25 ºC) (Yam, 2009)	1.7 ± 0.09 x 10^{-12} (25 ºC) (Yam, 2009)	3.88 ± 0.07 x 10^{-12} (25 ºC) (Yam, 2009)	14% CO_2 in 45 days (McCarthy *et al*., 1999)
PCL	EM: 304 ± 11 TSy: 18 ± 1 MPa E: > 1000% Ey: 13 ± 4% (Ortega-Toro, et al., 2015)	T_m: 63.5 ± 0.6 T_c: 12.6 ± 0.6 (Ortega-Toro, et al., 2015)	2.88 ± 0.9 x 10^{-6} (25 ºC, 53% RH) (Ortega-Toro, et al., 2015)			95% mass loss in 1 year PCL/starch blend: 48% mass loss in 40 days (Bastioli, 2005)

Table A.I.6. (Continued)

PHB	TS: 40 MPa FM: 3500 MPa E: 8% (Bastioli, 2005)	T_m: 180 T_g: 4 (Bastioli, 2005)	1.9×10^{-13} (23 ºC, 50% RH) (Petersen *et al*., 2001)	5.12×10^{-12} (23 ºC, 50% RH) (Petersen *et al*., 2001)		~97% mass loss in 2 years (Calmon *et al*., 1999)
Mater-Bi: corn starch A	TS: 9 ± 1MPa TeS: 480 ± 123 MPa E: 23 ± 7% (thickness: 20µm) (Petersen *et al*., 2001)		3.7×10^{-9} (23 °C and 50% RH) (Petersen *et al*., 2001)	9.9×10^{-12} (23 ºC, 0% RH oxygen and 75% RH nitrogen) (Petersen *et al*., 2001)	1.35×10^{-10} (23 ºC, 0% RH oxygen and 75% RH nitrogen) (Petersen *et al*., 2001)	
Mater-Bi: corn starch B	TS: 18 ± 2 MPa TeS: 145 ± 42 MPa E: 6 ± 0 % (thickness: 20µm) (Petersen *et al*., 2001)			6.9×10^{-12} (23 ºC, 0% RH oxygen and 75% RH nitrogen) (Petersen *et al*., 2001)	0.84×10^{-10} (23 ºC, 0% RH oxygen and 75% RH nitrogen) (Petersen *et al*., 2001)	

E: Elongation at Break Point; **EM**: Elastic Modulus; **Ey**: Elongation at yield Point; **FM**: Flexural Modulus; $\mathbf{T_c}$: crystallization temperature; **TeS**: Tear Strenght; $\mathbf{T_g}$: glass transition temperature; **TM**: Tensile Modulus; $\mathbf{T_m}$: melting temperature; **TS**: Tensile Strenght; **TSy**: Tensile Strengh at yield point; **UE**: Ultimate Elongation.

I.2. REFERENCES

Ali, S. S., Tang, X., & Faubion, J. (2011). Structure and physical properties ofstarch/poly vinyl alcohol/sodium montmorillonite nanocomposite films. Journalof Agricultural and Food Chemistry, 59, 12384–12395.

Abbès, B., Ayad, R., Prudhomme, J. C., & Onteniente, J. P. (1998). Numerical simulation of thermoplastic wheat starch injection molding process. Polymer Engineering and Science, 38, 2029-2038.

Abdillahi, H., Chabrat, E., Rouilly, A. & Rigal, L. (2013). Influence of citric acid on thermoplastic wheat flour/poly(lactic acid)blends. II. Barrier properties and water vapor sorption isotherms. Industrial Crops and Products, 50, 104– 111.

Albertsson, A-C., & Karlsson, S. (1988). The three stages in degradation of polymers-polyethylene as a model substance. Journal of Applied Polymer Science, 35, 5, 1289-1302.

Alves, J. S., dos Reis, K. C., Menezes, E. G. T., Pereira, F. V., & Pereira, J. (2015). Effect of cellulose nanocrystals and gelatin in corn starch plasticized films. Carbohydrate Polymers, 115, 215–222.

Avérous, L. & Boquillón, N. (2004). Biocomposites based on plasticized starch: Thermal and mechanical behaviours. Carbohydrate Polymers, 56(2), 111–122.

B, A., Suin, S., & Khatua, B. B. (2014). Highly exfoliated eco-friendly thermoplastic starch (TPS)/poly (lacticacid)(PLA)/clay nanocomposites using unmodified nanoclay. Carbohydrate Polymers, 110, 430–439.

Bastioli, C. (2005). Handbook of biodegradable polymer. (1st ed.). Shawbury, Shrewsbury, Shropshire, Rapra technology limited.

Belhassen, R., Vilaseca, F., Mutjé, P., & Boufi, S. (2014). Thermoplasticized starch modified by reactive blending with epoxidized soybean oil. Industrial Crops and Products, 53, 261– 267.

Bocz, K., Szolnoki, B., Marosi, A., Tábi, T., Wladyka-Przybylak, M., & Marosi, G. (2014). Flax fibre reinforced PLA/TPS biocomposites flame retarded with multifunctional additive system. Polymer Degradation and Stability 106, 63-73.

Bonilla, J., Talón, E., Atarés, L., Vargas, M., & Chiralt, A. (2013). Effect of the incorporation of antioxidants on physicochemical and antioxidant properties of wheat starch–chitosan films. Journal of Food Engineering, 118, 271–278.

Brandelero, R. P. H., Grossmann, M. V. G & Yamashita, F. (2011). Effect of the method of production of the blends on mechanical and structural properties of biodegradable starch films produced by blown extrusion. Carbohydrate Polymers, 86, 1344– 1350.

Brandelero, R. P. H., Yamashita, F., & Grossmann, M. V. G. (2010). The effect of surfactant Tween 80 on the hydrophilicity, water vapor permeation, and the mechanical

properties of cassava starch and poly(butylene adipate-co-terephthalate) (PBAT) blend films. Carbohydrate Polymers, 82, 1102–1109.

Brown, W. H., & Poon, T. (2005). Introduction to organic chemistry. (3rd ed.). New York: Wiley.

Cai, J., Xiong, Z., Zhou, M., Tan, J., Zeng, F., MeihuMa, Lin, S., & Xiong, H. (2014). Thermal properties and crystallization behavior of thermoplasticstarch/poly(ε-caprolactone) composites. Carbohydrate Polymers, 102, 746– 754.

Calmon, A., Guillaume, S., Bellon-Maurel, V., Feuilloley, P., & Silvestre, F. (1999). Evaluation of material biodegradability in real conditions–development of a burial test and an analysis methodology based on numerical vision. Journal of environmental polymer degradation, 7(3), 157-166.

Campos, A., Marconcini, J. M., Martins-Franchetti, S. M., & Mattoso, L. H. C. (2012). The influence of UV-C irradiation on the properties of thermoplastic starch and polycaprolactone biocomposite with sisal bleached fibers. Polymer Degradation and Stability, 97, 1948-1955.

Cano, A., Jiménez, A., Cháfer, M., Gónzalez, C., & Chiralt, A. (2014). Effect of amylose:amylopectin ratio and rice bran addition on starch films properties. Carbohydrate Polymers, 111, 543–555.

Carvalho, A. J. F. (2008). Starch: major sources, properties and applications as thermoplastic materials. In M. N. Belgacem & A. Gandini (Eds.), Monomers, polymers and composites from renewable resources. Amsterdam: Elsevier.

Castaño, J., Rodríguez-Llamazares, S., Contreras, K., Carrasco, C., Pozo, C., Bouza, R., Franco, C. M. L., & Giraldo, D. (2014). Horse chestnut (Aesculus hippocastanum L.) starch: Basicphysico-chemical characteristics and use as thermoplastic material. Carbohydrate Polymers, 112, 677–685.

Castillo, L., López, O., López, C., Zaritzky, N., García, M. A., Barbosa, S., & Villar, M. (2013). Thermoplastic starch films reinforced with talc nanoparticles. Carbohydrate Polymers, 95, 664– 674.

Chabrat, E., Abdillahi, H., Rouilly, A., & Rigal, L. (2012). Influence of citric acid and water on thermoplastic wheat flour/poly(lactic acid) blends. I: Thermal, mechanical and morphological properties. Industrial Crops and Products, 37(1), 238–246.

Chaudhary, A. L., Miler, M., Torley, P. J., Sopade, P. A., & Halley, P. J. (2008). Amylose content and chemical modification effects on the extrusion of thermoplastic starch from maize. Carbohydrate Polymers, 74, 907–913.

Cheetham, N. W. H., & Tao, L. (1998). Variation in crystalline type with amylose content in maize starch granules: an X-ray powder diffraction study. Carbohydrate Polymers, 36(4), 277–284.

Curvelo, A. A. S., Carvalho, A. J. F., & Agnelli, J. A. M. (2001). Thermoplastic starch-cellulosic fibers composites: preliminary results. Carbohydrate Polymers, 45: 183-188.

Cyras, V. P., Manfredi, L. B., Ton-That, M. T., & Vazquez, A. (2008). Physical and mechanical properties of thermoplastic starch/montmorillonite nanocomposite films. Carbohydrate Polymers, 73, 55–63.

Dean, K. M., Do, M. D., Petinakis, E., & Yu, L. (2008). Key interactions in biodegrad-able thermoplastic starch/poly(vinyl alcohol)/montmorillonite micro- and nanocomposites. Composites Science and Technology, 68, 1453–1462.

Della Valle, G., Boche, Y., Colonna, P., & Vergnes, B. (1995). The extrusion behaviour of potato starch. Carbohydrate Polymers, 28, 255–264.

Dhawan, S., Dhawan, K., Varma, M., & Sinha, V. R. (2005). Applications of poly(ethylene oxide) in drug delivery systems. Part II. Pharmaceutical technology, 29(9), 82–96.

Djordjevic. D. (2001). Coextrusion. Shawbury, Shrewsbury, Shropshire, Rapra technology limited.

Doane, W. M. (1992). USDA research on starch-based biodegradable plastics. Starch, 44, 293–295.

Durrani, C. M., & Donald, A. M. (1995). Physical characterization of amylopectin gels. Polymer Gels and Networks, 3(1), 1–27.

European Bioplastics Association. (2013). The behavior of bioplastic films in mechanical recycling streams. Meta study. URL: http://en.european-bioplastics.org/wp-content/uploads/2014/publications/Bioplastic_films_in_mechanical_recycling_streams (accessed on January 2015).

European Bioplastics Association. (2014). URL: http://en.european-bioplastics.org/technologymaterials/ (accessed on January 2015).

Fabra, M. J., Talens, P., & Chiralt, A. (2008). Tensile properties and water vapor permeability of sodium caseinate films containing oleic acid–beeswax mixtures. Journal of Food Engineering, 85(3), 393–400.

Fakhouri, F. M., Costa, D., Yamashita, F., Martelli, S. M., Jesus, R. C., Alganer, K., Collares-Queiroz, F. P., & Innocentini-Mei, L. H. (2013). Comparative study of processing methods for starch/gelatin films. Carbohydrate Polymers, 95, 681– 689.

Ferreira, W. H., Khalili, R. R., Junior, M. J. M., & Andrade, C. T. (2014). Effect of organoclay on blends of individually plasticizedthermoplastic starch and polypropylene. Industrial Crops and Products, 52, 38– 45.

Fishman, M. L., Coffin, D. R., Onwulata, C. I., & Willet, J. L. (2006). Two stage extrusion of plasticized pectin/poly(vinyl alcohol) blends. Carbohydrate Polymers, 65(4), 421–429.

Funke, U., Bergthaller, W., & Lindhauer, M. G. (1998). Processing and characterization of biodegradable products based on starch. Polymer Degradation and Stability, 59, 293-296.

García, M. A., Martino, M. N., & Zaritzky, N. E. (2000). Lipid addition to improve barrier properties of edible starch-based films and coatings. Journal of Food Science, 65(6), 941-944.

Garcia, P. S., Grossmann, M. V. E., Shirai, M. A., Lazaretti, M. M., Yamashita, F., Muller, C. M. O., & Mali, S. (2014). Improving action of citric acid as compatibiliser in starch/polyesterblown films. Industrial Crops and Products, 52, 305– 312.

Ghanbarzadeh, B., Almasi, H., & Entezami, A. A. (2010). Physical properties of edible modified starch/carboxymethyl cellulose films. Innovative Food Science & Emerging Technologies, 11(4), 697-702.

Hablot, E., Dewasthale, S., Zhao, Y., Zhiguan, Y., Shi, X., Graiver, D., & Narayan, R. (2013). Reactive extrusion of glycerylated starch and starch–polyester graft copolymers. European Polymer Journal, 49, 873–881.

Harper, C. A. (2004). Handbook of Plastics, elastomers & Composites. (4th ed.). Sydney, Mc Graw-Hill.

Halley, P., Rutgers, R., Coombs, S., Kettels, J., Gralton, J., & Christie, G. (2001). Developing biodegradable mulch films from starch-based polymers. Starch/Stärke, 53(8), 362–367.

Hoover, R. (2001). Composition, molecular structure, and physicochemical properties of tuber and root starches: a review. Carbohydrate Polymers, 45, 253–267.

Hulleman, S. H. D., Kalisvaart, M. G., Janssen, F. H. P., Feila, H., & Vliegenthart, J. F. G. (1999). Origins of B-type crystallinity in glycerol-plasticised, compression moulded potato starches. Carbohydrate Polymers, 39, 351–360.

Huneault, M. A., & Li, H. (2007). Morphology and properties of compatibilized polylactide/thermoplastic starch blends. Polymer, 48, 270-280.

International Standardisation, ISO 14851. Determination of the Ultimate Aerobic Biodegradability of Plastic Materials in an Aqueous Medium – Method by Measuring the Oxygen demand in a Closed Respirometer; 1999.

Jana, T., & Maiti, S. (1999). A biodegradable film, 1. Pilot plant investigation for production of the biodegradable film**.** Die angewandte makromolekulare Chemie, 267(1), 16–19.

Jbilou, F., Joly, C., Galland, S., Belard, L., Desjardin, V., Bayard, R., Dole, P., & Degraeve, P. (2013). Biodegradation study of plasticised corn flour/poly(butylene succinate-co-butylene adipate) blends. Polymer Testing, 32, 1565–1575.

Jenkins, P. J., Cameron, R. E., & Donald, A. M. (1993). A universal feature in the structure of starch granules from different botanical sources. Starch/Stärke, 45(12), 417–420.

Jiménez, A., Fabra, M. J., Talens, P., & Chiralt, A. (2012). Edible and Biodegradable Starch Films: A Review. Food Bioprocess Technology, 5, 2058–2076.

Jiménez, A., Fabra, M. J., Talens, P., & Chiralt, A. (2013a). Physical properties and antioxidant capacity of starch-sodium caseinate films containing lipids. Journal of Food Engineering, 116 (3), 695-702.

Jiménez, A., Fabra, M. J., Talens, P., & Chiralt, A. (2013b). Phase transitions in starch based films containing fatty acids. Effect on water sorption and mechanical behaviour. Food Hydrocolloids, 30(1), 408-418.

Katerinopoulou, K., Giannakas, A., Grigoriadi, K., Barkoula, N. M., & Ladavos, A. (2014). Preparation and characterization of acetylated cornstarch–(PVOH)/clay nanocomposite films. Carbohydrate Polymers, 102, 216– 222.

Kim, M. S., Lee, W. I., Han, W. S., & Vautrin, A. (2011). Optimisation of location and dimension of SMC precharge in compression moulding process. Computers and Structures, 89, 1523-1534.

Krishna, M., Nindo, C. I., & Min, S. C. (2012). Development of fish gelatin edible films using extrusion and compression molding. Journal of Food Engineering, 108, 337–344.

Landreau, E., Tighzert, L., Bliard, C., Berzin, F., & Lacoste, C. (2009). Morphologies and properties of plasticized starch/polyamide compatibilized blends. European Polymer Journal, 45, 2609–2618.

Li, G., & Favis, B. D. (2010). Morphology development and interfacial interactions in polycaprolactone/thermoplastic-starch blends. Macromolecular Chemestry and Physics, 211, 321–333.

Liu, H., Xie, F., Yu, L., Chen, L., & Li, L. (2009). Thermal processing of starch-based polymers. Progress in Polymer Science, 34, 1348–1368.

Liu, Z. (2005). Edible films and coatings from starch. In J. H. Han (Ed.), Innovations in food packaging. London: Elsevier Academic Press.

Lomelí-Ramírez, M. G., Kestur, S. G., Manríquez-González, R., Iwakiri, S., Bolzon de Muniz, G., & Flores-Sahagun, T. S. (2014). Bio-composites of cassava starch-green coconut fiber: Part II—structure and properties. Carbohydrate Polymers, 102, 576– 583.

Lopez, O. V., Garcia, M. A., Villar, M. A., Gentili, A., Rodriguez, M. S., & Albertengo, L. (2014). Thermo-compression of biodegradable thermoplastic corn starch films containing chitin and chitosan. LWT - Food Science and Technology, 57, 106-115.

López, O. V., Castillo, L. A., García, M. A., Villar, M. A., & Barbosa, S. E. (2015). Food packaging bags based on thermoplastic corn starch reinforced with talc nanoparticles. Food Hydrocolloids, 43, 18-24

López, O. V., Zaritzky, N. E., Grossmann, M. V. E., & García, M. A. (2013). Acetylated and native corn starch blend films produced by blown extrusion. Journal of Food Engineering, 116, 286–297.

Ma, X., Chang, P., Yu, J., & Stumborg, M. (2009). Properties of biodegradable citric acid-modified granular starch/thermoplastic pea starch composites. Carbohydrate Polymers, 75, 1–8.

Maningat, C. C., Seib, P. A., Bassi, S. D., Woo, K. S., & Lasater, G. D. (2009). Wheat starch: production, properties, modification and uses. In J. BeMiller, & R. Whistler (Eds.), Starch: Chemistry and Technology. AP: Elsevier.

Mark, J., E. (1999). Polymer Data Handbook. (2nd ed.). New York: Oxford University Press, Inc.

Martin, O., & Avérous, L. (2001). Poly(lactic acid): plasticization and properties of biodegradable multiphase systems. Polymer, 42, 6209-6219.

Martin, O., Schwach, E., Avérous, L., & Couturier, Y. (2001). Properties of biodegradable multilayer films based on plasticized wheat starch. Starch–Stärke, 53(8), 372–380.

Martin, O & Avérous, L. (2002). Comprehensive experimental study of a starch/polyesteramide coextrusion. Journal of Applied Polymer Science, 86(10), 2586–2600.

Matzinos, P., Tserki, V., Gianikouris, C., Pavlidou, E., & Panayiotou, C. (2002). Processing and characterization of LDPE/starch/PCL blends. European Polymer Journal, 38, 1713–1720.

McCarthy, S. P., Ranganthan A. & Ma, W. (1999). Advances in properties and biodegradability of co-continuous, immicisible, biodegradable, polymer blends Macromolecular Symposia, 144, 63-72.

McGlashan, S. A., & Halley, P. (2003). Preparation and characterisation of biodegradable starch-based nanocomposite materials. Polymer International, 52, 1767–1773.

Memon, A. & Nakai, A. (2013). Fabrication and Mechanical Properties of Jute Spun Yarn/PLA Unidirection Composite by Compression Molding. Energy Procedia, 34, 830-838.

Moad, G. (2011). Chemical modification of starch by reactive extrusion. Progress in Polymer Science, 36, 218–237.

Mościcki, L., Mitrus, M., Wójtowicz, A., Oniszczuk, T., Rejak, A., & Janssen, L. (2012). Application of extrusion-cooking for processing of thermoplastic starch (TPS). Food Research International, 47(2), 291-299.

Müller, C. M. O., Laurindo, J. B., & Yamashita, F. (2012). Composites of thermoplastic starch and nanoclays produced by extrusion and thermopressing. Carbohydrate Polymers, 89, 504–510.

Müller, P., Renner, K., Móczó, J., Fekete, E., & Pukánszky, B. (2014). Thermoplastic starch/wood composites: Interfacial interactions andfunctional properties. Carbohydrate Polymers, 102, 821–829.

Ohtake, Y., Kobayashi, T., Asabe, H., Murakami, N., & Ono K., (1998). Oxidative degradation and molecular weight change of LDPE buried under bioactive soil for 32–37 years. Journal of Applied Polymer Science, 70(9), 1643-1648.

Olivato, J. B., Grossmann, M. V. E., Bilck, A. P., & Yamashita, F. (2012a). Effect of organic acids as additives on the performance of thermoplastic starch/polyester blown films. Carbohydrate Polymers, 90, 159–164.

Olivato, J. B., Grossmann, M. V. E., Yamashita, F., Eiras, D., & Pessan, L. A. (2012b). Citric acid and maleic anhydride as compatibilizers in starch/poly(butylene adipate-co-terephthalate) blends by one-step reactive extrusion. Carbohydrate Polymers, 87, 2614–2618.

Olsson, E., Johansson, C., Larsson, J., & Järnström, L. (2014). Montmorillonite for starch-based barrier dispersion coating-Part 2: Pilot trials and PE-lamination. Applied Clay Science, 97-98, 167–173.

Ortega-Toro, R., Jiménez, A., Talens, P., & Chiralt, A. (2014). Properties of starch–hydroxypropyl methylcellulose based films obtained by compression molding. Carbohydrate Polymers, 109, 155–165.

Ortega-Toro, R., Collazo-Bigliardi, S., A., Talens, P., & Chiralt, A. (2015). Influence of citric acid on the properties and stability of starch-polycaprolactone based films. Journal of Applied Polymer Science, DOI: 10.1002/app.42220.

Otey, F. H., Mark, A. M., Mehltretter, C. L., & Russell, C. R. (1974). Starch-based film for degradable agricultural mulch. Industrial & Engineering Chemistry Product Research and Development, 13, 90–92.

Otey, F. H., Westhoff, R. P., & Doane, W. M. (1980). Starch-based blown films. Industrial and Engineering Chemistry Product Research and Development, 19, 592–595.

Petersen, K., Nielsen, P. V., & Olsen, M. B. (2001). Physical and Mechanical Properties of Biobased Materials-Starch, Polylactate and Polyhydroxybutyrate. Starch/Stärke, 53, 356–361.

Pinto, C., Carbajal, G., Wypych, A., Ramos, L., & Satyanarayana, K. (2009). Studies of the effect of molding pressure and incorporation of sugarcane bagasse fibers on the structure and properties of polyhydroxybutyrate. Composites Part A Applied Science and Manufacturing, 40(5), 573–582.

Prachayawarakorn, J., & Pomdage, W. (2014). Effect of carrageenan on properties of biodegradable thermoplastic cassava starch/low-density polyethylene composites reinforced by cotton fibers. Materials and Design, 61, 264–269.

Prachayawarakorn, J., Sangnitidej, P. & Boonpasith, P. (2010). Properties of thermoplastic rice starch composites reinforced by cotton fiber or low-density polyethylene. Carbohydrate Polymers, 81, 425–433.

Privas, E., Leroux, F., & Navard, P. (2013). Preparation and properties of blends composed of lignosulfonated layered double hydroxide/plasticized starch and thermoplastics. Carbohydrate Polymers, 96, 91–100.

Pushpadass, H. A., Bhandari, P., & Hanna, M. A. (2010). Effects of LDPE and glycerol contents and compounding on the microstructure and properties of starch composite films. Carbohydrate Polymers, 82, 1082–1089.

Raquez, J. M., Nabar, Y., Srinivasan, M., Shin, B. Y., Narayan, R., & Dubois, P. (2008a). Maleated thermoplastic starch by reactive extrusión. Carbohydrate Polymers, 74, 159–169.

Raquez, J. M., Nabar, Y., Narayan, R., & Dubois, P. (2008b). In situ compatibilization of maleated thermoplastic starch/polyester melt-blends by reactive extrusion. Polymer Engineering & Science, 48(9), 1747-1754.

Reddy, N., & Yang, Y. (2010). Citric acid cross-linking of starch films. Food Chemistry 118, 702–711.

Rodríguez-Castellanos, W., Martínez-Bustos, F., Jiménez-Arévalo, O., González-Núñez, R., & Galicia-García, T. (2013). Functional properties of extruded and tubular films of sorghum starch-based glycerol and Yucca Schidigera extract. Industrial Crops and Products, 44, 405–412.

Rodriguez-Gonzalez, F. J., Ramsay B. A., & Favis, B. D. (2004). Rheological and thermal properties of thermoplastic starch with high glycerol content. Carbohydrate Polymers, 58, 139–147.

Sabetzadeh, M., Bagheri, R., & Masoomi, M. (2012). Effect of corn starch content in thermoplastic starch/low-density polyethylene blends on their mechanical and flow properties. Journal of Applied Polymer Science, 126, E63–E69.

Salaberria, A. M., Labidi, J., & Fernandes, S. C. M. (2014). Chitin nanocrystals and nanofibers as nano-sized fillers into thermoplastic starch-based biocomposites processed by melt-mixing. Chemical Engineering Journal, 256, 356–364.

Salgado, P. R., López-Caballero, M. E., Gómez-Guillén, M. C., Mauri, A. N., & Montero, M. P. (2013). Sunflower protein films incorporated with clove essential oil have potential application for the preservation of fish patties. Food Hydrocolloids, 33(1), 74-84.

Sarazin, P., Li, G., Orts, W. J., & Favis, B. D. (2008). Binary and ternary blends of polylactide, polycaprolactone and thermoplastic starch. Polymer 49, 599-609.

Schmid, M., Dallmann, K., Bugnicourt, E., Cordoni, D., Wild, F., Lazzeri, A., & Noller, K. 2012. Properties of whey-protein-coated films and laminates as novel recyclable food packaging materials with excellent barrier properties. International Journal of Polymer Science, 8, 1-7.

Shen, L., Haufe, J., & Patel, M. K. (2009). Product overview and market projection of emerging bio-based plastics. PRO-BIP. Ultrecht: European Polysaccharide network of excellence (EPNOE) and European Bioplastics.

Shi, Q., Chen, C., Gao, L., Jiao, L., Xu, H., & Guo, W. (2011). Physical and degradation properties of binary or ternary blends composed of poly (lactic acid), thermoplastic starch and GMA grafted POE. Polymer Degradation and Stability, 96, 175-182.

Shi, R., Zhang, Z., Liu, Q., Han, Y., Zhang, L., Chen, D., & Tian, W. (2007). Characterization of citric acid/glycerol co-plasticized thermoplastic starch prepared by melt blending. Carbohydrate Polymers, 69(4), 748-755.

Shin, B. Y., Jang, S. H., & Kim, B. S. (2011). Thermal, morphological, and mechanical properties of biobased and biodegradable blends of poly(lactic acid) and chemically modified thermoplastic starch. Polymer engineering and science, 51(5), 826-834.

Shirai, M. A., Olivato, J. B., Garcia, P. S., Müller, C. M. O., Grossmann, M. V. E., & Yamashita, F. (2013). Thermoplastic starch/polyester films: Effects of extrusion process and poly (lactic acid) addition. Materials Science and Engineering C, 33, 4112–4117.

Shogren, R. L. (1992). Effect of moisture content on the melting and subsequent physical aging of corn starch. Carbohydrate Polymers, 19(2), 83–90.

Shogren, R. L., & Jasberg, B. K. (1994). Aging properties of extruded high amylose starch. Journal of Environmental Polymer Degradation, 2(2), 99–109.

Smith, A. M. (2001). The biosynthesis of starch granules. Biomacromolecules, 2(2), 335–341.

Soares, F. C., Yamashita, F., Müller, C. M. O., & Pires, A. T. N. (2013). Thermoplastic starch/poly(lactic acid) sheets coated with cross-linked chitosan. Polymer Testing, 32, 94–98.

Soares, F. C., Yamashita, F., Müller, C. M. O., & Pires, A. T. N. (2014). Effect of cooling and coating on thermoplastic starch/ poly(lactic acid) blend sheets. Polymer Testing, 33, 34–39.

Sugih, A. K., Drijfhout, J. P., Picchioni, F., Janssen, L. P. B M., & Heeres, H. J. (2009). Synthesis and properties of reactive interfacial agents for polycaprolactone-starch blends. Journal of Applied Polymer Science, 114, 2315–2326.

Taghizadeh, A., & Favis, B. D. (2013). Carbon nanotubes in blends of polycaprolactone/thermoplastic starch. Carbohydrate Polymers, 98, 189–198.

Taguet, A., Bureau, M. N., Huneault, M. A., & Favis, B. D. (2014). Toughening mechanisms in interfacially modifiedHDPE/thermoplastic starch blends. Carbohydrate Polymers, 114, 222–229.

Taguet, A., Huneault, M. A., & Favis, B. D. (2009). Interface/morphology relationships in polymer blends with thermoplastic starch. Polymer, 50, 5733–5743.

Teixeira, E., Da Róz, A., Carvalho, A., & Curvelo, A. (2007). The effect of glycerol/sugar/water and sugar/water mixtures on the plasticization of thermoplastic cassava starch. Carbohydrate Polymers, 69, 619–624.

Teixeira, E., Curvelo, A. A. S., Corrêa, A. C., Marconcini, J. M., Glenn, G. M., & Mattoso, L. H. C. (2012). Properties of thermoplastic starch from cassava bagasse and cassava starch and their blends with poly (lactic acid). Industrial Crops and Products, 37, 61– 68.

Teyssandier, F., Cassagnau, P., Gérard, J. F., & Mignard, N. (2011). Reactive compatibilization of PA12/plasticized starch blends: Towards improved mechanical properties. European Polymer Journal, 47, 2361–2371.

Thunwall, M., Kuthanová, V., Boldizar, A., & Rigdahl, M. (2008). Film blowing of thermoplastic starch. Carbohydrate Polymers, 71, 583–590.

Thunwall, M., Kuthanova´, V., Boldizar, A., & Rigdahl, M. (2006b). On the stress–strain behaviour of thermoplastic starch melts. International Journal of Polymer Analysis and Characterisation, 11(6), 419–428.

Thuwall, M., Boldizar, A., & Rigdahl, M. (2006a). Extrusion processing of high amylose potato starch materials. Carbohydrate Polymers, 65, 441–446.

Todd, R. H., Allen, D. K.,& Alting, L. (1993). Manufacturing Processes Reference Guide. New York: Industrial P, Incorporated.

Van Soest, J. J. G., & Essers, P. (1997). Influence of amylose-amylopectin ratio on properties of extruded starch plastic sheets. Journal of Macromolecular Science–Pure Applied Chemistry. A, 34(9), 1665–1689.

Versino, F., López, O. V., & García, M. A. (2015). Sustainable use of cassava (Manihot esculenta) roots as raw material for biocomposites development. Industrial Crops and Products, 65, 79–89.

Wang, Y., & Xie, W. (2010). Synthesis of cationic starch with a high degree of substitution in an ionic liquid. Carbohydrate Polymers, 80, 1172–1177.

Whistler, R. L., BeMiller, J. N., & Paschall, B. F. (1984). Starch: chemistry and technology (2nd ed.). New York: Academic

Wilhelm, H., Sierakowski, M., Souza, G.,& Wypych, F. (2003). Starch films reinforced with mineral clay. Carbohydrate Polymers, 52, 101–110.

Willet, J. L., Jasberg, B. K., & Swanson, C. L. (1995). Rheology of thermoplastic starch: effects of temperature, moisture content, and additives on melt viscosity. Polymer Engineering and Science, 35(2), 202–210.

Wootthikanokkhan, J., Wongta, N., Sombatsompop, N., Kositchaiyong, A., Wong-On, J., na Ayutthaya, S. I., & Kaabbuathong, J. (2012). Effect of blending conditions on mechanical, thermal, and rheological properties of plasticized poly(lactic acid)/ maleated thermoplastic starch blends. Journal of Applied Polymer Science, 124, 1012–1019.

Wu, C. S. (2003). Physical properties and biodegradability of maleated polycaprolactone/starch composite. Polymer Degradation and Stability, 80, 127–134.

Xie, F., Yu, L., Liu, H., & Chen, L. (2006). Starch Modification Using Reactive Extrusion. Starch/Stärke, 58, 131–139.

Yam., K. L. (2009). Encyclopedia of packaging technology. (3rd ed.). New Brunswick, New Jersey: Wiley. A Jhon Wiley and Sons, Inc, Publication.

Yu, F., Prashantha, K., Soulestin, J., Lacramp, M.-F., & Krawczak, P. (2013). Plasticized-starch/poly(ethylene oxide) blends prepared by extrusion. Carbohydrate Polymers, 91, 253– 261.

Yu, L. (2009). Biodegradable polymer blends and composites from renewable resources. Hoboken, New Jersey: John Wiley & Sons, Inc.

Zema, L., Loreti, G., Melocchi, A., Maroni, A., & Gazzaniga, A. (2012). Injection Molding and its application to drug delivery. Journal of Controlled Release, 159, 324–331.

Zhai, J., Chen, H., Colla, E., & Wu, T. (2003). Direct current field adjustable ferroelectric behaviour in (Pb, Nb)(Zr, Sn, Ti)O_3 antiferroelectric thin films. Journal of Physics Condensed Matter, 15(6), 963.

Zhang, Y., Leng, Y., Zhu, M., Fan, B., Yan, R., & Wu, Q. (2012). Starches modified with polyurethane microparticles: Effects of hydroxyl numbers of polyols in polyurethane. Carbohydrate Polymers, 88: 1208-1213.

Zhong, F., Li, Y., Ibanz, A. M., Oh, M. H., Mckenzie, K. S., & Shoemaker, C. (2009). The effect of rice variety and starch isolation method on the pasting and rheological properties of rice starch pastes. Food Hydrocolloids, 23, 406–414.

Zullo, R., & Iannace, S. (2009). The effects of different starch sources and plasticizers on film blowing of thermoplastic starch: Correlation among process, elongational properties and macromolecular structure. Carbohydrate Polymers, 77: 376–383.

II. OBJECTIVES

II.1. DISSERTATION OBJECTIVES

II.1.1. General Objective

The general objective of the present Doctoral Thesis is to enhance physical properties of starch-based films by blending with different hydrophobic compounds, using different strategies, such as the addition of compatibilizers or bilayer formation, and processing methods (casting, melt blending, extrusion and compression moulding).

II.1.2. Specific Objectives

The specific objectives are:

- ✓ To study the effect of the addition of sorbitan esters of different fatty acids on the physical properties of film-forming dispersions and films of corn starch-glycerol based blends.

- ✓ To study the effect of citric acid addition on the structural and physical properties of corn starch films obtained by melt blending and compression moulding, combined with different ratios of HPMC.

- ✓ To characterize the structural and physical properties and thermal behaviour of corn starch-PCL blend films, with a wide range of polymer ratios, obtained by melt blending and compression moulding.

✓ To analyse the influence of citric acid addition on the structural, thermal and physical properties of starch-PCL blend films obtained by melt blending and compression moulding.

✓ To analyse the influence of adding polyethylene glycol on the structural, thermal and physicochemical properties of compression moulded starch films containing a low ratio (less than 10%) of PCL.

✓ To analyse the influence of PCL grafted with maleic anhydride and glycidyl methacrylate on the physical and structural properties of starch-PCL blend films obtained by extrusion and compression moulding.

✓ To analyse the physical and structural properties of starch-PCL bilayer films obtained by compression moulding by incorporating commonly used food antimicrobials and antioxidants (potassium sorbate and ascorbic acid) at the layers' interface.

III. CHAPTERS

CHAPTER 1

EFFECT OF THE INCORPORATION OF SURFACTANTS ON THE PHYSICAL PROPERTIES OF CORN STARCH FILMS

Rodrigo Ortega-Toro, Alberto Jiménez, Pau Talens & Amparo Chiralt

Food Hydrocolloids, *38*, 66-75 (2014)

The effect of surfactant addition on structural, mechanical, optical and barrier properties of corn starch-glycerol based films was studied. Sorbitan monopalmitate, monostearate or monooleate were incorporated into starch-glycerol (1:0.25) at a surfactant:starch ratio of 0.15:1. The film forming dispersions (FFD) were characterized as to rheology, ζ-potential, particle size distribution and contact angle. Film characterization was carried out at 1 and 5 storage weeks (at 25ºC and 53% relative humidity). Surfactants led to different particle size distribution, zeta potential and viscosity in FFD, and film extensibility, depending on their hydrophobicity and melting properties. Their incorporation to the corn starch-glycerol films produced a coarser film microstructure due to the appearance of free surfactant aggregates or V-amylose inclusion complexes which produce discontinuities in the amorphous continuous matrix. The size of these crystalline complexes was smaller for the surfactant with the lowest hydrophobicity with saturated fatty acid (span 40). This contributed to decrease the WVP values with respect to surfactant-free film. Films containing surfactants were less hard, resistant and extensible, and more permeable to oxygen, than surfactant-free films, but they did not notably affect the film gloss and transparency. Saturated fatty acid compounds with higher melting temperature are recommended to ensure a finer microstructure in the final film which favours water barrier efficiency.

VNIVERSITAT POLITECNICA
VALENCIA
EX TECHNICA
PROGRESSIO

1.1. INTRODUCTION

The environmental conservation policies, the integral use of natural resources and the reduction of hydrocarbon reserves have generated particular interest in developing alternatives to petroleum synthetic polymers for different industrial uses, particularly for foodstuffs. Several studies focused on the development of biodegradable materials to replace, at least partially, conventional plastics. The materials obtained from natural biopolymers, such as polysaccharides, are an interesting alternative, of which, starch is one of the most promising materials for the manufacture of biodegradable plastics (Ma *et al*., 2009). This polymer is a renewable, low cost resource, readily available and has thermoplastic characteristics which permit it to be processed easily by using conventional synthetic polymer methods (Shah *et al*., 1995). However, starch presents worse physical characteristics than synthetic polymers. Its main weaknesses are its highly hydrophilic nature, which makes it a poor water vapour barrier, and the fact that it undergoes retrogradation processes, which implies that its mechanical properties vary over time. Nevertheless, their properties can be modified by adding small quantities of chemical compounds (García *et al*., 2000, Ma *et al*., 2009).

Plasticizers act by increasing the molecular mobility in the polymeric network, thus improving mechanical properties, but reducing the water vapour barrier properties (Rosen, 1993). Glycerol can be added as a plasticizer to improve the mechanical properties of the film, increasing the flexibility and tensile strength by lowering the glass transition temperature (Vieira *et al*., 2011).

Other components with potential capacity to improve some properties of the starch-based films are surfactants. Some studies have found that surfactants may enhance the wettability and stability of the dispersions (Ghebremeskel *et al*., 2007; Chen *et al*., 2009), reduce the starch retrogradation (Jovanovich & Añón, 1999) and improve the water vapour barrier properties (Villalobos *et al*., 2006). Vieira *et al*.,

2011 have observed that if the surfactant was added without glycerol, it had a significant effect on mechanical properties but did not significantly modify the water vapour barrier properties. Nevertheless, if the surfactant was added with glycerol, it provoked a reduction in the tensile strength and an increase in both elongation and water vapour permeability. Surfactants have been added to different polysaccharide matrices, such as tapioca starch/decolorized hsian-tsao leaf gum films (Chen *et al*., 2009). When concentration and HLB of surfactant increased, there was an observed improvement in the water vapour barrier properties, although films showed a loss of mechanical resistance. Nevertheless, in matrices of corn starch reinforced with microfibres of cellulose, the mechanical properties were improved with the addition of glyceryl monostearate by the formation of complexes which increase the V-type crystallinity (Mondragón *et al*., 2008).

Working on films of potato starch and glycerol, Rodríguez *et al*. (2006) observed that the presence of surfactants increased the wettability of film forming dispersions, with a synergistic effect between glycerol and surfactants. Similarly, in chitosan films, surfactants showed a synergistic effect with the glycerol on the water vapour permeability (Ziani *et al*., 2008). Zhong & Li (2011) also observed that the addition of surfactants and citric acid diminished the surface tension in the film forming dispersions and the formation of crystalline forms in kudzu starch films.

Despite several works have report the effect of different surfactants on biopolymer films, no previous studies have been published in corn starch films containing this kind of compounds, except that reported by Jimenez *et al.* 2012 where the effect of different fatty acids, with very low (between 1-2) hydrophilic-lipophilic balance (HLB), was analysed. A low HLB value indicates the predominant lipophilic balance in the molecular structure which can contribute to limit the water vapour permeability of the films, although slightly higher values could improve the better

integration of these compounds in the hydrophilic matrix. Likewise, the presence of saturated and unsaturated hydrocarbon chains could also play a relevant role in the component interactions in the matrix. In this sense, the study of the effect a family of surfactants with intermediate HLB values containing saturated or unsaturated chains could give interesting information about the different effects on the properties of the film forming dispersions and films, which are relevant for both coating applications on a determined product and film formation for packaging ends. Surfactants incorporated to film aqueous forming dispersions can act as carrier vehicles of non-polar bioactive compounds (such as antimicrobials or antioxidants), making their dispersion easy in the non-polar core of the formed micellar structures.

The aim of this work was to study the effect of addition of sorbitan esters of different fatty acids (saturated and unsaturated), with low-intermediate HLB values (sorbitan monopalmitate: 6.7, sorbitan monostearate: 4.7 and sorbitan monooleate: 4.3) on physical properties of film forming dispersions (particle size distribution, ζ-potential, contact angle) and films (mechanical, optical, structural and barrier properties) of corn starch-glycerol based blends. The effect of storage time on film properties was also analyzed.

1.2. MATERIAL AND METHODS

1.2.1. Materials

Corn starch was obtained from Roquette (Roquette Laisa España, Benifaió, Spain). The glycerol and surfactants (sorbitan monopalmitate: span 40, sorbitan monostearate: Span 60 and sorbitan monooleate: Span 80) were provided by Panreac Química, S.A. (Castellar del Vallès, Barcelona, Spain).

1.2.2. Preparation of film-forming dispersions (FFD)

Four different dispersions based on corn starch, glycerol and surfactant were prepared by using starch:glycerol:surfactant ratios of 1:0.25:0.15. The starch:surfactant ratio was chosen on the basis of previous studies (Jimenez *et al*., 2012). Corn starch (1% w/w in distilled water) was gelatinized in a thermostat-controlled bath at 95 °C for 30 min. Then, the glycerol and the surfactants (previously melted) were added and the mixtures were homogenized. The homogenization was carried out under vacuum, to avoid bubble formation, by using a venturi vacuum pump connected to the homogenization chamber. This step was performed at 95 ºC using a rotor-stator homogenizer (Ultraturrax T25, Janke and Kunkel, Germany) for 1 min at 13,500 rpm and for 3 min at 20,500 rpm. Melting temperature of surfactants are 46-47, 54-57 and 0.98 ºC, respectively for Span 40, Span 60 and Span 80. Therefore, they remain in liquid state during the homogenization step, thus making their dispersion easy. Prior to the characterization, FFD were cooled to 25 °C. Sample control (FFD-C) was considered as a dispersion containing only starch and glycerol. FFD with surfactants span 40, span 60 and span 80 were designated FFD-S40, FFD -S60 and FFD-S80, respectively.

1.2.3. Characterization of the film-forming dispersions

1.2.3.1. Rheological behaviour

The rheological behaviour of FFD was analyzed in triplicate at 25 °C by means of a rotational rheometer (Haake Rheostress1, Thermo Electric Corporation, Germany), by using a coaxial cylinder sensor system (Z34DIN Ti). Rheological curves were obtained after a sample resting time in the sensor of 5 min at 25 °C.

The shear stress (σ) was measured as a function of shear rate ($\dot{\gamma}$) from 0 to 512 s^{-1}, obtaining the up and down curves taking 5 min for each one.

1.2.3.2. Particle size, ζ-potential and surface tension measurements

The droplet size distribution, volume-length mean diameter ($D_{4.3}$) and volume-surface mean diameter ($D_{3.2}$) were determined in FFD, in triplicate, with a laser light scattering instrument (Malvern Mastersizer, Malvern Instruments, Worcestershire, U.K.). To obtain ζ-potential values, all FFD were diluted to a droplet concentration of 0.02% using deionised water. ζ-Potential was determined at 25 °C by mean of Zetasizer nano-Z (Malvern Instruments, Worcestershire, UK). The Smoluchowsky mathematical model was used to convert the electrophoretic mobility into ζ-potential values.

The surface tension was determined at 25 °C by means of the ring method using a ring tensiometer (Mobil-K9 Tensiometer, Kruss GmbH, Hamburg, Germany) and a platinum-iridium ring of 19.09 mm in diameter. Measurements were performed in triplicate in each FFD.

1.2.3.3. Contact angle

Due to the potential application in multilayer packaging of these dispersions with synthetic polymers, contact angle (θ) was measured on the surface of polyethylene terephthalate (PET) (Cubil S. L. Barcelona, Spain) polypropylene (PP) (Cubil S. L. Barcelona, Spain) and polystyrene (PS) (Cubil S. L. Barcelona, Spain). The shape of a sessile drop (0.01 ml) was studied after 10 s by means of a Video-Based Contact Angle Meter model OCA 20 (DataPhysics Instruments GmbH, Filderstadt,

Germany). Image analyses were carried out using SCA20 software. Ten replicates were made per formulation.

1.2.4. Preparation and characterization of films

Films were obtained by casting method. The mass of the FFD containing 1 g of total solids was spread evenly over a teflon casting plate of 15 cm diameter resting on a level surface. Films were formed by drying for approximately 48h at 45% RH and 20 °C. Dry films could be peeled intact from the casting surface and they were conditioned for 1 and 5 weeks at 53% RH and 25°C depending on the analysis. RH in the storage chamber was controlled by using an oversaturated solution of Magnesium nitrate-6-hydrat (Panreac Quimica, S.A.). Films without surfactant (control) are denominated F-C and films containing Span 40, Span 60 and Span 80, FS-40, FS-60 and F-S80, respectively. Film thickness was measured with a Palmer digital micrometer to the nearest 0.0025 mm at 4-6 random position, depending on the analysis.

1.2.4.1. Scanning electron microscopy (SEM)

Microstructural analysis of the films was carried out by SEM using a scanning electron microscope JEOL JSM-5410 (Japan). Film samples were maintained in a desiccator with P_2O_5 (Panreac Quimica, S.A.) for two weeks to ensure that water was not present in the sample (theoretical relative humidity in desiccator 0). Afterwards, films were frozen in liquid nitrogen and cryofractured to observe the cross-section and surface of the samples. Films were fixed on copper stubs, gold coated, and observed using an accelerating voltage of 10 kV.

1.2.4.2. X-ray diffraction

X-ray diffraction patterns were recorded using an X-ray diffractometor (XRD, Bruker AXS/D8 Advance). All the aged samples (equilibrated for five weeks at 25 °C and 53% RH) were analyzed between 2θ: 5º and 50º, using Kα Cu radiation (λ: 1.542 Å), 40 kV and 40 mA with a step size of 0.05º. For this analysis, samples were cut into 4 cm squares, prior to storage, in order to avoid breakage during handling. Span 40 and Span 60 reagents were also analyzed in order to identify their characteristic

1.2.4.3. Atomic force microscopy (AFM)

The surface morphology of dried aged films (equilibrated in a desiccator with P_2O_5 for 1 week) was analyzed using an atomic force microscope (Multimode 8, Bruker AXS, Santa Barbara, USA) with a NanoScope® V controller electronics. Measurements were taken from several areas of the film surface (50 x 50 µm and 5 x 5 µm) using the Tapping mode. According to method ASME B46.1 (ASME, 1995), the following statistical parameters related with sample surface roughness were calculated: average roughness (Ra: average of the absolute value of the height deviations from a mean surface), root-mean-square roughness (Rq: root-mean-square average of height deviations taken from the mean data plane), and factor of roughness (r: ratio between the three-dimensional surface and two-dimensional area projected onto the threshold plane). Three replicates were considered to obtain these parameters.

Phase Imaging mode derived from Tapping Mode, that goes beyond topographical data, was also applied. Phase imaging is the mapping of the phase lag between the periodic signal that drives the cantilever and the oscillations of the cantilever. Changes in the phase lag indicate changes in the properties of the sample surface in

composition, adhesion, friction, viscoelasticity, and other properties, including electric and magnetic.

1.2.4.4. Optical properties

The film transparency was determined by applying the Kubelka-Munk theory for multiple scattering to the reflection spectra (Hutchings, 1999). The surface reflectance spectra of the films were determined from 400 to 700 nm with a spectrocolorimeter CM-3600d (Minolta Co., Tokyo, Japan) on both a white and a black background. As the light passes through the film, it is partially absorbed and scattered, which is quantified by the absorption (K) and the scattering (S) coefficients. Internal transmittance (Ti) of the films was quantified using eq. (1.1). In this equation R_0 is the reflectance of the film on an ideal black background. Parameters *a* and *b* were calculated by eqs. (1.2) and (1.3), where R is the reflectance of the sample layer backed by a known reflectance R_g. Measurements were taken in triplicate for each sample on the free film surface. Wavelength of 450 nm was considered for analysis.

$$T_i = \sqrt{(a - R_0)^2 - b^2} \tag{1.1}$$

$$a = \frac{1}{2}\left(R + \frac{R_0 - R + R_g}{R_0 R_g}\right) \tag{1.2}$$

$$b = \sqrt{a^2 - 1} \tag{1.3}$$

The gloss was measured on the free film surface, at 60° incidence angle, according to the ASTM standard D523 method (ASTM, 1999), by means of a flat surface gloss meter (Multi Gloss 268, Minolta, Germany). Measurements were taken in triplicate for each sample and three films of each formulation were considered. All results were expressed as gloss units, relative to a highly polished surface of black glass standard with a value near to 100. Transparency and gloss measurements were carried out with films conditioned for 1 week (initial time) and 5 weeks (final time) in hermetic desiccators at 25 °C and 53% RH.

1.2.4.5. Moisture content

Films previously conditioned at 53% RH were dried for 24h at 60 °C in a natural convection stove and subsequently placed in a desiccator with P_2O_5 at 25 °C for 2 weeks. The reported results represent the mean values of at least three samples.

1.2.4.6. Water vapour permeability (WVP)

WVP measurements were carried out with films conditioned for 1 and 5 weeks in hermetic desiccators at 25 °C and 53% RH. WVP of films was determined by using the ASTM E96-95 (ASTM, 1995) gravimetric method, taking into account the modification proposed by McHugh et al., 1993. Films were selected for WVP tests based on the lack of physical defects. Distilled water was placed in Payne permeability cups (3.5 cm diameter, Elcometer SPRL, Hermelle/s Argenteau, Belgium) to expose the film to 100% RH on one side. Once the films were secured, each cup was placed in a relative humidity equilibrated cabinet at 25 °C, with a fan placed on the top of the cup in order to reduce resistance to water vapour transport, thus avoiding the stagnant layer effect in this exposed side of the film. RH of the cabinets (53%) was held constant using oversaturated solutions of magnesium

nitrate-6-hydrate. The free film surface during film formation was exposed to the lowest relative humidity to simulate the actual application of the films in high water activity products when stored at intermediate relative humidity. The cups were weighed periodically (0.0001 g) and water vapour transmission (WVTR) was determined from the slope obtained from the regression analysis of weight loss data versus time, once the steady state had been reached, divided by the film area. From WVTR data, the vapour pressure on the film's inner surface (p2) was obtained with eq. (1.4), proposed by McHugh *et al.* (1993), to correct the effect of concentration gradients established in the stagnant air gap inside the cup.

$$WVTR = \frac{PDL_n\left[\frac{P - p_2}{P - p_1}\right]}{RT\Delta z} \tag{1.4}$$

where P, total pressure (atm); D, diffusivity of water through air at 25 °C (m2 /s); R, gas law constant (82.057 x 10^{-3} m^3 atm $kmol^{-1}$ K^{-1}); T, absolute temperature (K); Δz, mean stagnant air gap height (m), considering the initial and final z value; p_1, water vapour pressure on the solution surface (atm); and p_2, corrected water vapour pressure on the film's inner surface (atm). Water vapour permeance was calculated using eq. (1.5) as a function of p_2 and p_3 (pressure on the film's outer surface in the cabinet).

$$permeance = \frac{WVTR}{p_2 - p_3} \tag{1.5}$$

Permeability was obtained by multiplying the permeance by the average film thickness.

1.2.4.7. Oxygen permeability (O_2P)

The oxygen permeation rate of the corn starch films was determined at 53% RH and 25 °C using an OX-TRAN Model 2/21 ML Mocon (Lippke, Neuwied, Germany). Film samples were previously conditioned for 1 or 5 weeks at 25 ºC and 53% RH by using magnesium nitrate-6-hydrate saturated solutions. Two samples were placed in the equipment for analysis and they were conditioned in the cells for 6 h, then the transmission values were determined every 20 min until the equilibrium was reached. The exposure area during the tests was 50 cm^2 for each formulation. In order to obtain the oxygen permeability, film thickness was considered in all cases. Measurements were carried out in triplicate.

1.2.4.8. Tensile properties

The mechanical behaviour of films was tested by using conditioned samples (1 or 5 weeks at 25 ºC and 53% RH). A universal test Machine (TA.XTplus model, Stable Micro Systems, Haslemere, England) was used to determine the tensile strength (TS), elastic modulus (EM), and elongation (E) of the films, according to ASTM standard method D882 (ASTM, 2001) EM, TS, and E were determined from the stress-strain curves, estimated from force-distance data obtained for the different films (2.5 cm wide and 10 cm long). Equilibrated samples were mounted in the film-extension grips of the testing machine and stretched at 50 mm min^{-1} until breaking. The relative humidity of the environment was held at nearly 53% during the tests, which were performed at 25 °C. At least seven replicates were obtained from each sample.

1.2.5. Statistical analysis

Statgraphics Plus for Windows 5.1 (Manugistics Corp., Rockville, MD) was used to carry out statistical analyses of data through analysis of variance (ANOVA). Fisher's least significant difference (LSD) was used at the 95% confidence level.

1.3. RESULTS AND DISCUSSION

1.3.1. Properties of film forming dispersions

Figure 1.1 shows the particle size distribution for the film forming dispersions containing corn starch and surfactants (Span 40, Span 60 and Span 80). The values of mean diameters $D_{3,2}$ and $D_{4.3}$ are shown in Table 1.1. A similar distribution is observed in all cases. Most of the volume fraction of the dispersed particles is under 1 µm in size, although there are large particles (over 10 µm) in all cases that greatly contribute to the average size. $D_{4.3}$ values indicate that the particle size of FFD-S80 was significantly smaller ($p < 0.05$) than those of FFD-S40 and FFD-S60 whereas no significant differences ($p < 0.05$) were observed between the particle sizes of these last FFD.

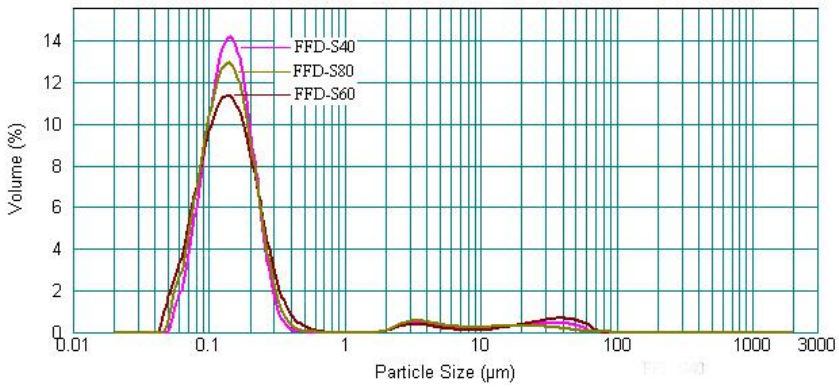

Figure 1.1.-Particle size distribution of film forming dispersions containing corn starch and surfactants (Span 40, Span 60 and Span 80).

Surfactants, as polar lipids, form different kind of molecular association (association colloids) in aqueous systems, where the hydrocarbon chains are oriented to minimize the contact with water molecules. These aggregates (micellar structures) have different size and shape depending on their relative water affinity (HLB) and the overall balance of molecular interactions which minimize the total free energy of the system (Dickinson, 1992). Usually, the lower the water affinity (HLB) the greater the aggregation number and so, the greater the particle size. In this sense, it is remarkable that S80, with the lowest HLB, forms the smallest particles which could be related with the double bond in the oleic acid chain, which make the packing of molecules more difficult. This is also related with the liquid state of this compound under room conditions, whereas S40 and S60 are solids under the same conditions. There are a greater proportion of large particles in FFD-S60 and FFD-S40, which may be associated with the formation of big aggregates of the surfactant molecules (Villalobos *et al*., 2005) or even combined aggregates of surfactants and starch polymer chains. Associations of helical amylose which give rise to gel zones in the FFD could also be detected as particles in the measurements. Surfactant molecules can also participate in these associations through the formation of complexes with helical conformation of amylose (Wokadala *et al*., 2012).

Table 1.1 shows the rheological behaviour, ζ-potential, surface tension and contact angle with different polymer films (PET: Polyethylene terephthalate, PP: polypropylene, PS: polystyrene) of FFDs containing corn starch and surfactants. All film-forming dispersions showed similar rheological behaviour. At low shear rates, Newtonian behaviour was observed, but from a determined shear rate, FFDs exhibited shear thickening behaviour. No differences were observed between up and down which means that no tixotropic effects occur during the fluid flow.

Table 1.1 shows the Newtonian viscosity values in the first step and the shear rate values where the change in behaviour occurs, which range between 130 and 173s^{-1}. The shear thickening behaviour from a determined shear rate can be explained by the induced orthokinetic flocculation of particles. Particle aggregates retain a part of the continuous phase and this, together with the greater flow resistance of the bigger aggregates, defines the higher shear stress-shear rate relationship or flow resistance (Peker & Helvaci, 2007). Non-Newtonian behaviour has previously been observed by other authors in starch dispersions and pastes (Zhong *et al*, 2009) where the viscosity varied according to the shear rate applied. Table 1.1 shows that the presence of surfactants caused a significant increase ($p < 0.05$) in the Newtonian viscosity in all cases; the FFD-S40 dispersion exhibiting the highest values. No significant differences were observed between the FFD-S60 and FFD-S80 formulations despite their different particle sizes. This viscosity increase provoked by the addition of surfactants is explained by the greater concentration of dispersed/dissolved species in the aqueous media.

All dispersions had negative ζ-potential values with significant differences ($p < 0.05$) among formulations (Table 1.1). All FFDs containing surfactants showed higher values of ζ-potential than that containing only starch. This can be due to the promotion of the adsorption of negative ions on the polar heads of the surfactant associations. Some authors (Ho & Ahmad, 1999; Hsu & Nacu, 2003) have reported that at pH near 7, non-ionic surfactants attract OH^- ions of the aqueous medium, thus increasing the surface charge of the lipid associations while a pH decrease is promoted. In Table 1.1, the lower pH of FFD-S60 and FFD-S80 can be observed, while these FFDs also showed the highest surface charge. Variations in ζ-potential could also be due to the different degree of hydrolysis in sorbitan esters, giving rise to free fatty acids with ionisable groups.

Table 1.1.-Mean particle size, rheological behaviour, ζ-potential, pH, surface tension and contact angle of the film forming dispersions. . Mean values and standard deviation.

Films	Particle Size		Rheological behaviour		ζ-potential (mV)	pH	Surface tension (mN/m)	Contact angle		
	$D_{4.3}$ (µm)	$D_{3.2}$ (µm)	Viscosity (Pa.s) $\cdot 10^3$	Shear rate (s^{-1})*				PET	PP	PS
FFD-C	-	-	1.83 ± 0.02^{a}	131 ± 2^{a}	-3.6 ± 0.8^{a}	6.42 ± 0.02^{a}	69.2 ± 0.8^{a}	52 ± 2^{a1}	82 ± 3^{a2}	65 ± 2^{a3}
FFD-S40	2.0 ± 0.8^{a}	0.14 ± 0.02^{b}	2.70 ± 0.02^{b}	173 ± 2^{b}	-15 ± 2^{b}	6.44 ± 0.02^{a}	43.8 ± 0.5^{b}	64 ± 3^{b1}	85 ± 2^{b2}	66 ± 2^{b3}
FFD-S60	2.1 ± 0.6^{a}	0.139 ± 0.008^{ab}	2.16 ± 0.02^{c}	150.2 ± 0.2^{c}	-26.9 ± 1.5^{c}	6.20 ± 0.02^{ab}	48.0 ± 1.0^{c}	63 ± 4^{b1}	88 ± 4^{c2}	67 ± 2^{c3}
FFD-S80	1.2 ± 0.6^{b}	0.137 ± 0.006^{a}	2.18 ± 0.07^{c}	151.4 ± 2.3^{c}	-29.3 ± 1.4^{d}	6.06 ± 0.02^{b}	41.9 ± 0.5^{d}	57 ± 4^{c1}	81 ± 2^{a2}	67 ± 2^{c3}

Different superscript letters within the same column indicate significant differences among formulations ($p < 0.05$). Different superscript numbers within the same row indicate significant differences due to different polymer films ($p < 0.05$). (*) Limit of shear rate from which shear thickening behaviour was observed.

The ζ-potential is defined as the electrostatic potential in the layer of the particle electrophoretic mobility and greatly affects the stability of the colloidal systems by electrostatic forces (Ravina & Moramarco, 1993). Accordingly, the most stable FFD would be FFD-S80 and FFD-S60 because the contribution of repulsive forces between particles to the stability would be greater. However, it should be noted that colloidal stabilization is the result of the interaction of numerous factors. In the case of FFD, the particle charge may not be enough to ensure stability of the dispersion because it is a complex system in which the hydrocolloid interactions (amylose and amylopectin) also play an important role. In particular, the viscosity of the continuous phase, which depends on the molecular interactions, greatly affects the system stability. So, as FFD-S80 and FFD-S60 are less viscous, destabilization phenomena during film drying could take place more easily, promoting coalescence and creaming, despite their greater surface charge. Other factors, such as the physical state of the lipid, may affect the coalescence phenomena, this being inhibited in solid lipids.

Surface tension values showed significant differences ($p < 0.05$) among formulations. The control dispersion (FFD-C) exhibited similar values to pure water (72 mN/m at 25 °C), but, as expected, the presence of surfactants reduced the surface tension of the dispersions to values below 47.6 mN/m at 25 °C. The surface tension reduction in the FFDs is interesting from the point of view of their application on a determined surface as coatings, since this favours their extensibility during the product coating (Fernandez *et al.,* 2006) and the possible formation of multi-layer materials with other polymers (Chen *et. al.,* 2010)

The contact angle values of FFD on the surface of different polymer films (PET: Polyethylene terephthalate, PP: polypropylene, PS: polystyrene) are shown in Table 1.1. Values lower than 90º indicate surface wettability and therefore greater extensibility of the dispersion on the polymer. The polymer which was least

wettable with the studied dispersions was PP, since the greatest contact angles were obtained in this case ($p < 0.05$). PET had the lowest contact angles and therefore it offers the best possibilities to be coated with the studied FFDs, for instance as vehicles of active compounds, thus obtaining multi-layer films. Nevertheless, the obtained values were dependent on the composition of the FFDs and it was remarkable that the formulations without surfactant were those which showed the greatest extensibility despite their higher surface tension.

1.3.2. Microstructure of the films

Films obtained had 50 ± 5 μm in thickness, regardless of the FFD composition. The final structure of the film depends on both the interactions of film components and the drying conditions of the film-forming dispersion and has a great impact on the different film properties (Villalobos *et al*., 2005). The microstructural analysis of the films gives relevant information about the arrangement of the components, which, in turn, allows us to explain the differences in the barrier, mechanical or optical properties of the films.

Figure 1.2 shows the SEM micrographs of the surface (left) and the cross-section (right) of starch based films with and without surfactants, conditioned for one week. Control films (F-C) showed an homogeneous structure, coherent with the formation of a compact arrangement of polymer chains. The addition of surfactants resulted in less homogeneous films whose differences can be observed in the cross-section images. Films with surfactants showed a coarser cross section than the control films, which suggests that polymer chain packaging was interrupted by other structural elements present in the matrix. These elements may be free surfactant particles, resulting from the micellar structure in the aqueous FFD and surfactat particles of V-amylose inclusion complexes which produce discontinuities of different magnitude in the amorphous continuous matrix, thus contributing to

weaken the bond strength between the polymer chains in the amorphous matrix. Interactions of polar lipids with V-amylose leads to complex formation, where the helical conformation of amylose traps the hydrocarbon chains of lipids, as has been previously described by other authors (Singh *et al*., 2002). V-amylose forms small particles with size in the nano or micro scale, depending on medium conditions (Lesmes *et al*., 2009). In F-S80, micro-droplets of span 80 (liquid at room temperature) can be seen in the matrix, whereas no droplets can be observed for F-S40 and F-S60, but finer no spherical formations. Lipid droplets also appear on the F-S80 film surface, even larger than in the cross-section due to the coalescence and creaming phenomena occurring in the drying step. Similar phenomena were observed by other authors (Zhong & Li, 2011) in kudzu starch films. The presence of droplets in F-S80 films is related with the liquid state of span 80 at room temperature and reveals the no total integration of the lipid in the starch matrix, and its separation in a dispersed liquid phase. Span 40 and span 60 seem also separated (discontinuities in the matrix) but their solid state at room temperature did not allow droplets formation, but crystalline or amorphous solid particles.

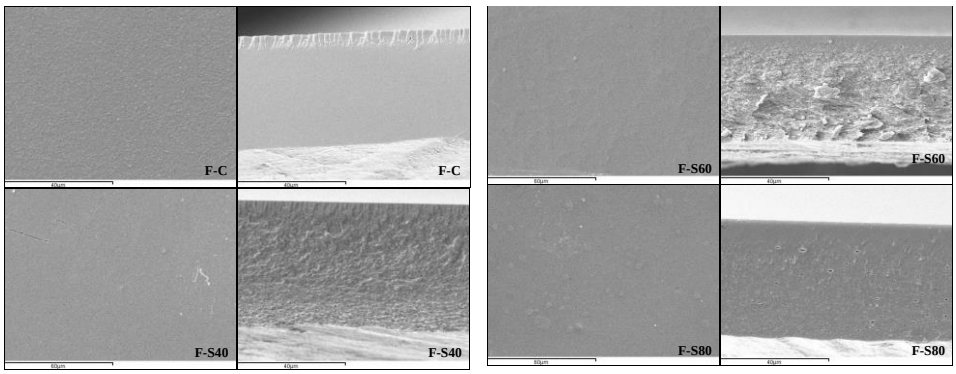

Figure 1.2.-SEM micrographs of surface and cross section of corn starch films with and without surfactants (Span 40, Span 60 and Span 80).

Figure 1.3 shows the phase imaging analysis obtained from the Tapping Mode AFM for films conditioned for five weeks. The phase image is providing material property contrast on the film surface since this technique is sensitive to variations in composition, adhesion, friction, viscoelasticity, and other surface properties (Baker *et al*., 2001). In control film (F-C), the image reveals the presence of lighter zones which can be attributed to crystalline aggregates of helical amylose (Baker *et al.*, 2001).

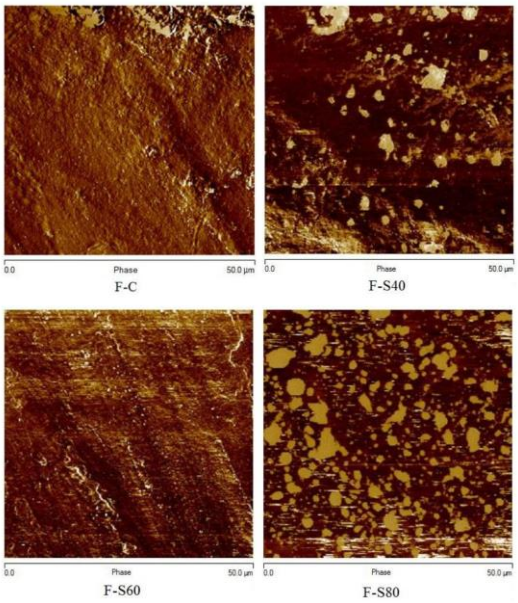

Figure 1.3. -AFM phase imaging of corn starch films with and without surfactants (Span 40, Span 60 and Span 80).

In films containing span 40 the presence of lighter spots reveals the presence of lipid particles on the film surface due to lipid coalescence and creaming during film drying and subsequent solidification. The excess of lipid contributed to its separation in the matrix and its migration to the film surface where solidifies,

according to its high melting temperature (46-47 ºC). In the case of span 60, no big lipid formations were observed on the film surface probably due to its higher melting temperature (54-57ºC), which contribute to inhibit coalescence phenomena during the film drying step, which also limits creaming, due to the restrictions in the particle size growth. For the film containing span 80 (liquid at room temperature, melting point: 0.98 ºC) a great proportion of lipid formations can be observed on the film surface, coherent with a high progress of the coalescence and creaming phenomena during the film drying. The irregular shape of lipid droplets reveals that they are droplet aggregates, whose surface is covered by a thin polymer layer, which entraps them.

The melting properties and molecular characteristics of the surfactant had an impact on the film structure and surface morphology which will affect the film properties, mainly its mechanical and optical parameters.

Figure 1.4a shows X-ray diffraction (XRD) spectra of corn starch films with and without surfactants, equilibrated at 25°C and 53% RH for 5 weeks. Generally, the native starch crystallinity is types A and B, type C being an intermediate form (Jiménez *et al.*, 2013); crystalline V type could also be observed, corresponding to the amylose helical associations, which are the result of the amylose complexation with other substances, such as lipids (Jiménez *et al.*, 2013). The addition of surfactants affected the crystallization pattern of the films. Control film showed the typical peaks of amylose V-type, with a peak of maximum intensity at 2θ 17º and other peaks at 2θ about 15º, 20º and 22 º (Lesmes *et al.*, 2009). When surfactants were added, two main peaks are shown at 2θ about 13° and 20°, as has been observed for V-type amylose hosting complexes with long chain fatty acids (Lesmes *et al.*, 2009). So, the XRD spectra reveal that surfactants in the film induce the formation of complexes with amylose, as observed for other lipids. Wokadala *et al.*, (2012) reported peaks at 2θ 7.5º, 13º and 20º, attributable to V-

type crystallinity as a result of the presence of amylose-lipid complexes in hydrolyzed maize starch in the presence of stearic acid.

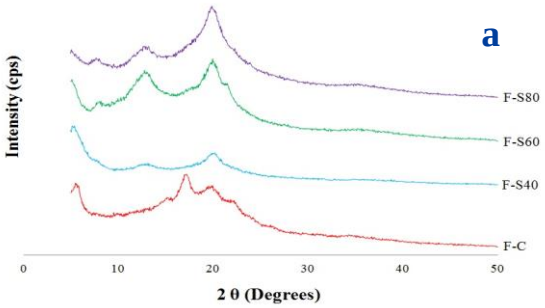

2θ (º)	Intensity (cps·10^{-2}) F-C	F-S40	F-S60	F-S80
6				
7.5			25	25
12.6		16	42	31
14.8	31			
17	43		33	
20	37	21	48	53
22	29		35	

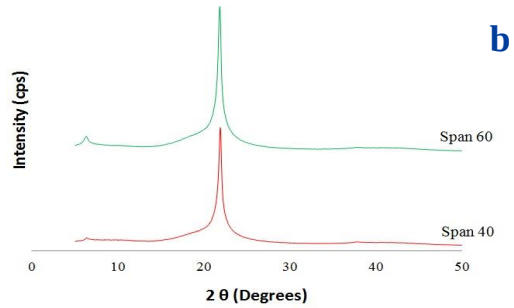

2θ (º)	Intensity (cps·10^{-2}) Span40	Span60
6	41	82
7.5		
12.6		
14.8		
17		
20		
22	631	779

Figure 1.4.-XRD spectra and angles (2θ degrees) and intensity (cps·10^{-2}) of crystalline peaks of (a) corn starch films with and without surfactants and (b) pure surfactants (Span 40 and Span 60).

By considering the XRD pattern of the pure surfactants (Figure 1.4b), where a very sharp peak appears at 2θ 22º, in both cases, the non-crystalline forms of the non-complexed (free) lipid in the films must be deduced, since at this angle no sharp peak was observed in the film XRD diffraction spectra.

These results indicate that in the structure of surfactant-starch films, V-type amylose complexes are formed with surfactant molecules giving rise to crystalline aggregates, whereas the excess of lipid is not crystallized. These crystalline

aggregates interrupt the starch matrix producing discontinuities in the same way as the free surfactant molecules. In the case of span 80, free lipids are clearly observable in the SEM micrographs as liquid droplets dispersed in the starch matrix, with a high degree of lipid creaming on the film surface. Film F-S40 showed the lowest peak intensity in the XRD spectra, which suggests that V-type crystalline forms were the smallest in size, which could have a positive effect on the film properties.

1.3.3. Physical properties of films

Table 1.2 shows the optical properties (gloss at incidence angle of 60° and internal transmittance at 450 nm) of corn starch films with and without surfactants, conditioned for one and five weeks. The gloss values obtained were less than 35 units and, therefore, films can be considered of low gloss (Villalobos *et al*., 2005). The addition of surfactants did not have a significant effect ($p > 0.05$) on the gloss values as compared with the control formulation. In the case of F-S80, the gloss significantly increased during the storage time, which did not occur in the other cases. This increase can be attributed to a progressive migration of the liquid droplets to the film surface, in line with the progressive chain aggregations and the reduction of the matrix volume. The fluid lipid acted as a filler of the micro-pores in the surface, thus reducing the apparent roughness and increasing the gloss. Table 1.2 shows the values of roughness parameters (R_a, R_b and r) analyzed through AFM in films stored for five weeks. No significant differences in the film roughness were detected, except for F-S40 where higher values were obtained. Nevertheless, this difference was not coherent with the gloss values, unlike that reported by other authors (Villalobos *et al.,* 2005). This can be due to the liquid state of span 80 which interferes with the cantilever signal in terms of the height of peaks on the surface.

All films were highly transparent, as deduced by the values of the internal transmittance (Ti) in Table 1.2. This is associated with a greater homogeneity in the film structure. The addition of surfactants resulted in a slight decrease of the transparency with respect to the control film, in line with a more anisotropic structure due to the formation of crystalline forms and the presence of dispersed surfactants aggregates, with a different refractive index, which enhance light scattering, as observed by Jimenez *et al.* (2012) in corn starch films containing fatty acids.

Table 1.2.-Surface roughness parameters and optical properties (gloss and transparency) of corn starch films with and without surfactants (Span 40, Span-60 and Span 80). Mean values and standard deviation.

Films	Surface roughness			Gloss 60°		T_i (450 nm)	
	Ra (nm)	Rq (nm)	r (%)	Initial	Final	Initial	Final
F-C	271 ± 18^{a}	363 ±20^{a}	2.0 ± 0.5^{a}	23 ± 5^{ab1}	18 ± 4^{a1}	85.6 ± 0.2^{a1}	83.1 ± 0.2^{a2}
F-S40	571 ± 176^{b}	775 ± 194^{b}	3.6 ± 0.2^{b}	21 ± 2^{ab1}	20 ± 6^{a1}	84.9 ± 0.2^{b1}	84.9 ± 0.2^{b1}
F-S60	322 ± 58^{a}	394 ± 70^{a}	2.1 ± 0.7^{a}	29 ± 8^{b1}	22 ± 5^{a1}	83.62 ± 0.14^{c1}	84.69 ± 0.12^{b2}
F-S80	390 ± 11^{a}	488 ± 20^{c}	3.1 ±0.9^{ab}	17 ± 5^{a1}	35 ± 6^{b2}	82.53 ± 0.12^{d1}	82.52 ± 0.06^{c1}

Different superscript letters within the same column indicate significant differences among formulations ($p < 0.05$). Different superscript numbers within the same row indicate significant differences due to storage time ($p < 0.05$).

The F-S80 films showed a significantly ($p < 0.05$) lower Ti, which can be attributed to the liquid droplet dispersion observed in the film microstructure. During film storage, no notable changes in Ti could be observed, although control films showed a slight decrease which could be attributed to the greater progress of amylose crystallization, thus inducing a greater degree of anisotropy (Jimenez *et al.*, 2012).

Table 1.3 shows the moisture content, water vapour permeability (WVP), oxygen permeability (O_2P) and mechanical properties of corn starch films, with and without surfactants. The incorporation of surfactants greatly decreased the equilibrium water content of the films, even if this is considered in the lipid free basis (4.3, 4.9 and 5.4, respectively for the films with span 40, span 60 and span 80). This agrees with the changes in the packing of a part of the polymer chains involved in the V-type crystalline forms complexing the lipids, which reduces the water binding capacity of these chains.

The WVP was measured at a gradient of 53-100% RH. At one week of storage, the addition of span 40 implied a significant ($p < 0.05$) reduction of WVP, although this was not observed for films containing span 60 (without significant differences with respect to the control) and span 80, where a significant increase was observed, more markedly at 5 weeks' storage. The improvement of the water vapour barrier properties due to the addition of surfactants has been observed in different matrices, such as tapioca starch with sucrose esters (Chen *et al.*, 2009), hydroxypropyl methylcellulose with span 60 and sucrose esters (Villalobos *et al*., 2006) and kudzu starch and ascorbic acid based films with Tween 20 (Zhong & Li, 2011). The scarce effect of surfactants on WVP observed in these films, regardless of their hydrophobicity, could be explained by the formation of crystalline structures in all cases (even in control films) which could be a strong limitation factor for transfer of water molecules.

In terms of WVP, the different behaviour induced by each of the three studied surfactants must be related with the structural differences reached in the matrix for each case. F-S40 showed the smallest V-type crystalline forms, as deduced from RX spectra, which could imply a great increase in the tortuosity factor for mass transfer in the matrix, thus reducing WVP.

Table 1.3.- Moisture content (Xw: g water/g dry film**)** , water vapour permeability, oxygen permeability and mechanical properties of corn starch films with and without surfactants (Span 40, Span 60, and Span 80). Mean values and standard deviation.

Films	Xw	WVP ($g \cdot mm \cdot KPa^{-1} \cdot h^{-1} \cdot m^{-2}$)		$O_2P \cdot 10^{13}$ ($cm^3 \cdot m^{-1} \cdot s^{-1} \cdot Pa^{-1}$)		EM (MPa)		TS (MPa)		E (%)	
		Initial	Final	Initial	Final	Initial	Final	Initial	Final	Initial	Final
F-C	0.070 ± 0.005^{a}	4.4 ± 0.6^{b1}	5.37 ± 0.07^{b1}	0.65 ± 0.02^{a1}	0.46 ± 0.02^{a2}	2115 ± 236^{c1}	2494 ± 148^{b2}	24.3 ± 4.6^{c1}	28.3 ± 2.9^{b1}	2.5 ± 0.5^{b1}	2.3 ± 0.7^{b1}
F-S40	0.038 ± 0.002^{b}	3.1 ± 0.5^{a1}	3.5 ± 0.3^{a1}	1.59 ± 0.02^{b1}	1.55 ± 0.02^{c1}	991 ± 145^{a1}	1454 ± 231^{a2}	10.5 ± 1.8^{ab1}	10.2 ± 2.3^{a1}	2.2 ± 0.7^{b1}	0.8 ± 0.2^{a2}
F-S60	0.044 ± 0.003^{bc}	4.0 ± 0.3^{b1}	3.7 ± 0.2^{a1}	1.4 ± 0.2^{b1}	1.39 ± 0.14^{bc1}	963 ± 244^{a1}	1347 ± 151^{a2}	8.4 ± 1.2^{a1}	9.8 ± 1.8^{a1}	1.3 ± 0.5^{a1}	0.9 ± 0.2^{a2}
F-S80	0.048 ± 0.002^{c}	5.4 ± 0.2^{c1}	6.17 ± 0.15^{c2}	1.09 ± 0.14^{ab1}	1.29 ± 0.03^{b1}	1388 ± 235^{b1}	1447 ± 104^{a1}	11.5 ± 1.9^{b1}	11.8 ± 1.3^{a1}	1.2 ± 0.3^{a1}	1.0 ± 0.2^{a1}

Different superscript letters within the same column indicate significant differences among formulations ($p < 0.05$). Different superscript numbers within the same row indicate significant differences due to storage time ($p < 0.05$)

On the contrary, the increase in WVP provoked by the addition of span 80 could be related with the greater size of crystalline complexes. Lesmes *et al.* (2009) demonstrated that increased fatty acid unsaturation affects the microscopic and nanoscopic arrangement of V-amylose, and fatty acid unsaturation leads to bigger and more disperse populations. This can suppose a more open structure where water molecules could diffuse more easily. No significant differences ($p < 0.05$) between WVP of the films stored for one and five weeks were observed, except for F-S80 where WVP increased over time. This could be explained by the above mentioned migration of the free liquid droplets of span 80 to the film surface, leaving fewer hydrophobic areas or void nanopores in the matrix, which facilitate transfer of water molecules.

Oxygen permeability values (Table 1.3) significantly ($p < 0.05$) increased when surfactants were incorporated into the films, as usually happens when hydrophobic components are added, since these substances are more permeable to gases due to their greater chemical affinity and solubility (Miller & Krochta, 1997). The oxygen permeability did not vary with the storage time, except in the control film, where it decreased significantly ($p < 0.05$). This can be explained by the progressive increase in the film crystallinity, as observed in previous works (Donhowe & Fennema, 1993; Jimenez *et al.* 2012).

Table 1.3 shows the values of the parameters used to describe the mechanical properties of starch based films at 25 °C and 53% RH: elastic modulus (EM), tensile strength (TS) and elongation at break (E). In general, the addition of surfactants caused the decrease of EM, TS and E, in agreement with the formation of a more anisotropic structure with reduced cohesion forces. Similar results were observed by Jimenez *et al*. (2012) in corn starch films when fatty acids were added. Rodriguez, *et al*. (2006) also observed that the addition of surfactants in the presence of glycerol causes a significant reduction in tensile strength and

elongation at break with respect to the control formulation. TS and EM initial values for F-S80 were significantly higher ($p < 0.05$) than for the other films with surfactants, which showed very similar values. This indicates that bonding forces in the matrix were more intense in the F-S80 films. Nevertheless, all films were very short, especially F-S60 and F-S80, which showed the lowest deformation at break, thus indicating the low capacity of the structural elements to slippage during tensile test without structural failure. This can be attributed, in part, to the formation of crystalline zones with low deformability.

1.4. CONCLUSIONS

Incorporation of span 40, 60 or 80 into the corn starch-glycerol film forming dispersions led to different particle size distribution, zeta potential, viscosity and extensibility on other films, depending on their hydrophobicity and melting properties (related with the unsaturation in the fatty acid chain). These aspects affected the final film microstructure and its surface morphology, since the growing of the surfactant molecule aggregates during the film drying (loss of water availability) occurred to a different extent, depending on the dispersion stability. When the surfactant melting temperature was the highest (span 60), creaming of surfactants in the film surface was not observed and the size of the final lipid aggregates in the film were lower. Likewise, the size of the type-V crystalline amylose complexes was smaller for the surfactant with the highest HLB value with saturated fatty acid (span 40). This contributed to decrease the WVP values with respect to surfactant-free film. Nevertheless, films containing surfactants were less hard, resistant and extensible than surfactant-free films, but they did not notably affect the film gloss and transparency. The use of surfactants in film formulation can be useful to incorporate non-polar bioactive compounds in the aqueous film forming dispersions. In this sense, the obtained results allow us to recommend

saturated fatty acid compounds with higher melting temperature to ensure a finer microstructure in the final film which favour water barrier efficiency.

1.5. REFERENCES

American Society for Testing and Materials, ASTM E96-95. Standard test methods for water vapor transmission of materials. In annual book of ASTM. Philadelphia; 1995.

American Society for Testing and Materials, ASTM D523. Standard test method for specular gloss. In annual book of ASTM. Philadelphia; 1999.

American Society for Testing and Materials, ASTM D882. Standard test method for tensile properties of thin plastic sheeting. In annual book of ASTM. Philadelphia; 2001.

American Society of Mechanical Engineers, ASME B46.1. Surface texture: Surface roughness, waviness and lay. New York; 1995.

Baker, A. A., Miles, M. J., & Helbert, W. (2001). Internal structure of the starch granule revealed by AFM. Carbohydrate Research, 330, 249–256.

Chen, C. H., Kuo, W. S., & Lai, L. S. (2009). Effect of surfactants on water barrier and physical properties of tapioca starch/decolorized hsian-tsao leaf gum films. Food Hydrocolloids, 23, 714–721.

Chen, C. H., Kuo, W. S., & Lai, L. S. (2010). Water barrier and physical properties of starch/decolorized hsian-tsao leaf gum films: Impact of surfactant lamination. Food Hydrocolloids, 24, 200–207.

Dickinson, E. (1992). An introduction to Food Colloids. Oxford: Oxford Univesity Press.

Donhowe, L. G. & Fennema, O. (1993). The effects of solutton composition and drying temperature on crystallinity, permeability and mechamcal properties of methylcellulose films. Journal of Food Processing and Preservation, 17(4), 231-246.

Fernández, L., Díaz de Apodaca, E., Cebrián, M., Villarán, M. C. & Maté, J. I (2006). Effect of the unsaturation degree and concentration of fatty acids on the properties of WPI-based edible films. European Food Research and Technology, 224(4), 415-420.

García M., Martino, M., & Zaritzky, N. (2000). Lipid addition to improve barrier properties of edible starch-based films and coatings. Food Chemistry and Toxicology, 65(6), 941-946.

Ghebremeskel, A. N., Vemavarapu, C., & Lodaya, M. (2007). Use of surfactants as plasticizers in preparing solid dispersions of poorly soluble API: Selection of polymer–surfactant combinations using solubility parameters and testing the processability. International Journal of Pharmaceutics, 328, 119–129.

Ho, C. C., & Ahmad, K. (1999). Electrokinetic Behavior of Palm Oil Emulsions in Dilute Electrolyte Solutions. Journal of Colloid and Interface Science, 216, 25–33.

Hsu, J. P., & Nacu, A. (2003). Behavior of soybean oil-in-water emulsion stabilized by nonionic surfactant. Journal of Colloid and Interface Science, 259, 374–381.

Hutchings, J. B. (1999). Food color and appearance. (2nd ed.). Gaithersburg, Maryland, USA: Aspen Publishers, Inc.

Jiménez, A., Fabra, M. J., Talens, P., & Chiralt, A. (2012). Effect of re-crystallization on tensile, optical and water vapour barrier properties of corn starch films containing fatty acids. Food Hydrocolloids, 26, 302-310.

Jiménez, A., Fabra, M. J., Talens, P., & Chiralt, A. (2013). Phase transitions in starch based films containing fatty acids. Effect on wáter sorption and mechanical behaviour. Food Hydrocolloids, 30, 408-418.

Jovanovich, G., & Añón, M. (1999). Amylose–lipid complex dissociation. A study of the kinetic parameters. Biopolymers, 49(1), 81–89.

Lesmes, U., Cohen, S. H., Shener, Y., & Shimoni, E. (2009). Effects of long chain fatty acid unsaturation on the structure and controlled release properties of amylose complexes. Food Hydrocolloids, 23, 667–675.

Ma, X., Chang, P., Yu, J., & Stumborg, M. (2009). Properties of biodegradable citric acid-modified granular starch/thermoplastic pea starch composites. Carbohydrate Polymers, 75(1), 1–8.

McHugh, T. H., Avena-Bustillos, R., & Krochta, J. M. (1993). Hydrophobic edible films: modified procedure for water vapour permeability and explanation of thickness effects. Journal of Food Science, 58(4), 899–903.

Miller, K. S., & Krochta, J. M. (1997). Oxygen and aroma barrier properties of edible films: A review. Trends in Food Science and Technology, 81, 228-237.

Mondragón, M., Arroyo, K., & Romero-García, J. (2008). Biocomposites of thermoplastic starch with surfactant. Carbohydrate Polymers, 74, 201–208.

Peker, S. M., & Helvaci, S. S. (2007). Solid-liquid two phase flow. In Concentrated Suspensions. Elsevier.

Ravina, L., & Moramarco, N. (1993). Everything you want to know about coagulation & flocculation. Zeta-meter, Inc., Virginia.

Rodríguez, M., Osés, J., Ziani, K., & Maté, J. I. (2006). Combined effect of plasticizers and surfactants on the physical properties of starch based edible films. Food Research International, 39, 840–846.

Rosen, S. L. (1993). Fundamental principles of polymeric materials. (2nd ed.). New York: Wiley Interscience.

Shah, P., Bandopadhyay, S., & Bellare, J. (1995). Environmentally degradable starch filled low density polyethylene. Polymer Degradation and Stability, 47(2), 165–173.

Singh, J., Singh, N., & Saxena, S. K. (2002). Effect of fatty acids on the rheological properties of corn and potato starch. Journal of Food Engineering, 52(1), 9-16.

Vieira, M., Altenhofen, M., Oliveira L., & Masumi, M. (2011). Natural-based plasticizers and biopolymer films: A review. European Polymer Journal, 47, 254–263.

Villalobos, R., Chanona, J., Hernández, P., Gutiérrez, G., & Chiralt, A. (2005). Gloss and transparency of hydroxypropyl methylcellulose films containing surfactants as affected by their microstructure. Food Hydrocolloids, 19, 53–61.

Villalobos, R., Hernández-Muñoz, P., & Chiralt, A. (2006). Effect of surfactants on water sorption and barrier properties of hydroxypropyl methylcellulose films. Food Hydrocolloids, 20, 502–509.

Wokadala, O. C., Ray, S. S. & Emmambux, M. N. (2012). Occurrence of amylose–lipid complexes in teff and maize starch biphasic pastes. Carbohydrate Polymers, 90, 616–622.

Zhong, F., Li, Y., Ibañes, A. M., Oh, M. H., McKenzie, K. S., & Shoemaker, C. (2009). The effect of rice variety and starch isolation method on the pasting and rheological properties of rice starch pastes. Food Hydrocolloids, 23, 406–414.

Zhong, Y., & Li, Y. (2011). Effects of surfactants on the functional and structural properties of kudzu (*Pueraria lobata*) starch/ascorbic acid films. Carbohydrate Polymers, 85, 622–628.

Ziani, K., Osés, J., Coma, V., & Maté, J. I. (2008). Effect of the presence of glycerol and Tween 20 on the chemical and physical properties of films based on chitosan with different degree of deacetylation. LWT - Food Science and Technology, 41, 2159-2165.

CHAPTER 2

PROPERTIES OF STARCH-HYDROXYPROPYL METHYLCELLULOSE BASED FILMS OBTAINED BY COMPRESSION MOULDING

Rodrigo Ortega-Toro, Alberto Jiménez, Pau Talens, & Amparo Chiralt

Carbohydrate Polymers, 109, 155–165 (2014)

Corn starch-glycerol (1:0.3) films, containing or not citric acid (1g/100 g starch) and HPMC (10 and 20 g/100g starch), are obtained by compression moulding. The microstructure of the films, the thermal behaviour, the X-Ray diffraction spectra and the physical properties (mechanical, barrier and optical) were analysed after 1 and 5 storage weeks at 25ºC and 53% relative humidity. The bonded citric acid and film solubility were also determined. Starch-HPMC blend films showed a dispersed phase of HPMC in a continuous, starch-rich phase with lower glass transition than HPMC-free films. The addition of citric acid also provoked a decrease in glass transition in line with the partial hydrolysis of starch chains. Both components implied a decrease in the water vapour permeability while the oxygen permeability slightly increased. Although citric acid only provoked a small hardening effect in the films, it greatly decreased their extensibility (weak cross-linking effect), which seems to increase during film storage. Starch crystallization during storage was inhibited by both citric acid and HPMC.

VNIVERSITAT POLITECNICA
VALENCIA
EX TECHNICA
PROGRESSIO

2.1. INTRODUCTION

Society's awareness of the importance of both environmental conservation and green technologies, and the growing environmental contamination caused by synthetic polymers based on petroleum, have led to an increased interest in developing environmentally friendly materials, such as biodegradable polymers based on polysaccharides. In the development of biodegradable materials, starch is the most promising of the polysaccharide polymers, due to its low cost, great processability, and abundance (Yoon *et al*., 2006; Ghanbarzadeh *et al*., 2011). Starch films exhibit some good properties, such as high barrier to oxygen, carbon dioxide and lipids. However, poor water vapour permeability and mechanical properties, and the recrystallization during storage, are limitations of this material (Kester & Fennema, 1986; Arık Kibar & Us, 2013).

The deficiencies in the properties of starch films can be improved by different methods. The phenomenon of the recrystallization of starch films could be solved by combining starch with other polymers, as has been proven by other authors (Funami *et al.*, 2005; Jiménez *et al.*, 2012a). Hydroxypropyl methylcellulose (HPMC) is a cellulose-derived polymer commonly used for obtaining edible, biodegradable films (Albert & Mittal, 2002; Villalobos *et al.*, 2006; Sánchez-González, *et al.*, 2009) with good availability and processability (Fahs *et al.*, 2010; Jiménez *et al*., 2012a) which have excellent film-forming properties (Villalobos *et al*., 2006). Compared to other polymers, HPMC films have great mechanical strength, (Jiménez *et al.*, 2010; 2012a) but limited barrier properties. In this sense, Jiménez *et al.* (2012a) observed that the oxygen permeability of HPMC films obtained by casting was approximately 100 times higher than cornstarch films, while the water barrier properties are similar for films made from both polymers.

Nevertheless, the thermal stability of HPMC films means that they can be thermally processed using industrial equipment, and previous studies (Jiménez *et*

al., 2012a) revealed inhibition of starch crystallization when blend films were obtained by casting the aqueous dispersions, the films showing a more amorphous character. So, HPMC-starch blends could be used to obtain thermally processed films with interesting properties, although phase separation in corn starch-HPMC films obtained by casting has been observed by scanning electron microscopy (Jiménez *et al*., 2012a), with the films exhibiting a starch-rich phase and a HPMC-rich phase in what is practically a bi-layer film.

The poor compatibility of these polymers can be limited by the incorporation of compatibilizer compounds, which promotes the esterification of the starch -OH groups. For this purpose, cross-linking agents, such as phosphorus oxychloride, sodium trimetaphosphate, sodium tripolyphosphate, epichlorohydrin, and 1,2,3,4-diepoxybutane, were used (Seker & Hanna, 2006; Reddy & Yang, 2010). These substances are relatively toxic and expensive (Reddy & Yang, 2010), so their use in food packaging is not recommendable. However, using polycarboxylic acids as cross-linking agents is a good alternative. This is especially so in the case of citric acid, a low cost organic acid widely used in the food industry, that acts as a cross-linking agent due to the presence of several carboxyl groups in its molecular structure (Ghanbarzadeh *et al.,* 2010). These groups can react with the hydroxyl groups of starch molecules through the formation of esters. According to Reddy & Yang (2010), the esterification reaction using polycarboxylic acids occur with the polymer hydroxyl groups, at high temperatures (about 160 ºC), through the formation of anhydride groups (Yang *et al.,* 1997). This interaction can decrease the retrogradation and recrystallization of starch during storage time (Ghanbarzadeh *et al*., 2011). The compatibilizer effect of the citric acid in the starch-polymer blends, as well as an improvement in the properties of starch films, have been reported in several studies (Yu *et al.,* 2005; Shi *et al.,* 2008; Ma *et al.,* 2009; Reddy & Yang, 2010; Ghanbarzadeh *et al*., 2010; 2011). The most

promising results derived from the addition of citric acid to the polymeric matrix are the increase in thermal stability and the improvement in the barrier properties (Yu *et al*., 2005; Reddy & Yang, 2010).

The aim of this work was to study the effect of citric acid addition on the structural and physical properties of corn starch films obtained by compression moulding, combined with different ratios of HPMC, using glycerol as plasticizer. The effect of storage time on the film properties was also analyzed.

2.2. MATERIALS AND METHODS

2.2.1. Materials

Corn starch was obtained from Roquette (Roquette Laisa Spain, Benifaió, Spain). Its moisture content was 10% w/w and amylose percentage was 14%. Glycerol was purchased from Panreac Química, S.A. (Castellar del Vallès, Barcelona, Spain). Hydroxypropyl methylcellulose (HPMC) and citric acid (CA) were provided by Fluka (Sigma–Aldrich Chemie, Steinheim, Germany).

2.2.2. Film preparation

Native starch and glycerol, as plasticizer, were dispersed in water. HPMC was hydrated in cold water (5% w/w) under continuous stirring. The HPMC dispersion and the aqueous mixture of starch and glycerol were mixed in different ratios to obtain two blends with 1:0.1 and 1:0.2 starch:HPMC ratios. The polymer:glycerol ratio was 1:0.3. CA was mixed to obtain four blends with and without CA; a constant starch:CA ratio of 1:0.01 was used in every case. Blends of starch-glycerol and starch-glycerol-citric acid, in the previously described ratios, were

studied as control formulations. The abbreviations used for the studied formulations were: SG: starch-glycerol; CA: citric acid; H10: 10g HPMC/100 g starch; H20: 20g HPMC/100 g starch.

The formulations were hot-mixed on a two-roll mill (Model LRM-M-100, Labtech Engineering, Thailand) at 160 °C and 8 rpm for 20 minutes. A visual good miscibility of HPMC, CA and starch was obtained. A trowel was used during mixing to smoothly spread the material on the rolls. The paste sheet formed was removed from the mill and conditioned at 25 °C and 53% Relative Humidity (RH), using a $Mg(NO_3)_2$ saturated solutions (Panreac Quimica, SA, Castellar del Valles, Barcelona, Spain), for 48 hours.

Afterwards, films were obtained by compression moulding (Model LP20, Labtech Engineering, Thailand). Four grams of the pre-conditioned paste were put onto steel sheets and pre-heated on the heating unit for about 5 min. Compression moulding was performed at 160°C for 2 minutes at a pressure of 30 bars, followed by 6 minutes at 130 bars; thereafter, the cooling cycle was applied for 3 minutes. The films were conditioned at 25°C and 53% RH for 1 week for the initial time characterization and for 5 weeks for the final time characterization.

2.2.3. Film characterization

2.2.3.1. Film thickness

A Palmer digital micrometer was used to measure film thickness to the nearest 0.0025 mm at six random positions around the film.

2.2.3.2. Scanning electron microscopy (SEM)

The microstructural analysis of the cross-sections and surface of the films was carried out by means of a scanning electron microscope (JEOL JSM-5410, Japan). The film samples were maintained in desiccators with P_2O_5 for two weeks to guarantee that water was not present in the sample and observations were taken in duplicate for each film sample and in two films per formulation.

Film pieces, 0.5 cm^2 in size, were cryofractured from films and fixed on copper stubs, gold coated, and observed using an accelerating voltage of 10 kV.

2.2.3.3. X-ray diffraction

A diffractometer (XRD, Bruker AXS/D8 Advance) was used to record the X-ray diffraction patterns. All the samples (equilibrated for one and five weeks at 25 °C and at 53% RH) were analyzed at 25 °C and 53% RH, between 2θ = 5° and 2θ = 30° using Kα Cu radiation (λ: 1.542 Å), 40 kV and 40 mA with a step size of 0.05°. For this analysis, samples were cut into 4 cm squares. Pure citric acid was also analyzed, so as to identify its characteristic peaks.

2.2.3.4. Atomic force microscopy (AFM)

Samples equilibrated for five weeks at 25 °C and 0% RH, using P_2O_5 saturated solutions (Panreac Quimica, SA, Castellar del Valles, Barcelona, Spain), were used. The surface morphology of the films was analyzed using an atomic force microscope (Multimode 8, Bruker AXS, Santa Barbara, USA) with NanoScope® V controller electronics. Measurements were taken from several areas of the film surface (20 μm^2) using the PeakForce QNM mode. Method ASME B46.1 (ASME, 1995) was used to calculate the following statistical parameters related with sample

roughness: average roughness (Ra: average of the absolute value of the height deviations from a mean surface), root-mean-square roughness (Rq: root-mean-square average of height deviations taken from the mean data plane), and factor of roughness (r: ratio between the three-dimensional surface and two-dimensional area projected onto the threshold plane). The DMT modulus, derived from the Peak Force QNM Mode, was also applied to obtain the surface maps showing the heterogeneities present in the surface properties. Three replicates were considered for each sample.

2.2.3.5. Optical properties

The Kubelka-Munk theory for multiple scattering was applied to the reflection spectra to determine the film's transparency (Hutchings, 1999). The surface reflectance spectra were determined from 400 to 700 nm using a spectro-colorimeter CM- 3600d (Minolta Co., Tokyo, Japan) on both a white and a black background. As the light passes through the film, it is partially absorbed and scattered, which is quantified by the absorption (K) and the scattering (S) coefficients. The internal transmittance (Ti) of the films was determined using eq. (1). In this equation, R_0 is the reflectance of the film on an ideal black background. Parameters *a* and *b* were calculated by means of eqs. (2) and (3), where R is the reflectance of the sample layer backed by a known reflectance, Rg. Three replicates were used for each sample on the free film surface. For the purposes of the analysis, a wavelength of 450 nm was considered.

$$T_i = \sqrt{(a - R_0)^2 - b^2} \qquad (2.1)$$

$$a = \frac{1}{2}\left(R + \frac{R_0 - R + R_g}{R_0 R_g}\right) \quad (2.2)$$

$$b = \sqrt{a^2 - 1} \quad (2.3)$$

The gloss was determined on the free film surface, at a 60° incidence angle by means of a flat surface gloss meter (Multi Gloss 268, Minolta, Germany), following the ASTM standard D523 method (ASTM, 1999). The measurements of each sample were taken in triplicate and three films were measured from each formulation. The results were expressed as gloss units (GU), relative to a highly polished surface of black glass standard with a value near to 100 GU.

2.2.3.6. Moisture content

The films that had been previously conditioned at 53% RH were dried for 24h at 60 °C (J.P. Selecta, S.A. Barcelona, Spain) and placed in a desiccator with P_2O_5 (Panreac Quimica, S.A. Castellar Vallés, Barcelona) adjusting them to 0% RH and 25 °C for 2 weeks. The reported results represent the average of three samples.

2.2.3.7. Water vapour permeability (WVP)

The WVP of films was determined by means of the ASTM E96-95 (ASTM, 1995) gravimetric method, taking the modification proposed by McHugh *et al.* (1993) into account. Distilled water was placed in Payne permeability cups (3.5 cm diameter, Elcometer SPRL, Hermelle/s Argenteau, Belgium) to expose the film to 100% RH on one side. Once the films were secured, each cup was placed in a relative humidity equilibrated cabinet at 25 °C, with a fan placed on the top of the

cup in order to reduce resistance to water vapour transport, thus avoiding the stagnant layer effect in this exposed side of the film. The RH of the cabinets (53%) was held constant using oversaturated solutions of magnesium nitrate-6-hydrate. The cups were weighed periodically (0.0001 g) and water vapour transmission (WVTR) was determined from the slope obtained from the regression analysis of weight loss data versus time, once the steady state had been reached, divided by the film area. From WVTR data, the vapour pressure on the film's inner surface (p2) was obtained using eq. (4), proposed by McHugh *et al*. (1993), to correct the effect of concentration gradients.

$$WVTR = \frac{P \cdot D \cdot L_n \left[P - p_2 \backslash P - p_1\right]}{R \cdot T \cdot \Delta z} \qquad (2.4)$$

where P, total pressure (atm); D, diffusivity of water through air at 25 °C (m2 /s); R, gas law constant (82.057 x 10^{-3} m^3 atm $kmol^{-1}$ K^{-1}); T, absolute temperature (K); Δz, mean stagnant air gap height (m), considering the initial and final z value; p_1, water vapour pressure on the solution surface (atm); and p_2, corrected water vapour pressure on the film's inner surface (atm). Water vapour permeance was calculated using eq. (5) as a function of p_2 and p_3 (pressure on the film's outer surface in the cabinet).

$$permeance = \frac{WVTR}{p_2 - p_3} \qquad (2.5)$$

Permeability was calculated by multiplying the permeance by film thickness.

2.2.3.8. Oxygen permeability (O_2P)

The oxygen permeation rate of the films was determined at 53% RH and 25 °C using an OX-TRAN (Model 2/21 ML Mocon Lippke, Neuwied, Germany). The samples were conditioned at the relative humidity level of the test in a desiccator using magnesium nitrate-6-hydrate saturated solutions. Three samples were placed in the equipment for analysis, and the transmission values were determined every 20 min until equilibrium was reached. The exposure area during the tests was 50 cm^2 for each sample. To obtain the oxygen permeability, the film thickness was considered in every case.

2.2.3.9. Tensile properties

A universal test Machine (TA.XTplus model, Stable Micro Systems, Haslemere, England) was used to determine the tensile strength (TS), elastic modulus (EM), and elongation (E) of the films, following ASTM standard method D882 (ASTM, 2001). EM, TS, and E were determined from the stress-strain curves, estimated from force-distance data obtained for the different films (2.5 cm wide and 5 cm long). Equilibrated samples were mounted in the film-extension grips of the testing machine and stretched at 50 mm min^{-1} until breaking. The relative humidity of the environment was held constant, at approximately 53% during the tests, which were performed at 25 °C. At least ten replicates were obtained from each sample.

2.2.3.10. Film solubility and bonded citric acid

Film solubility was determined by keeping the sample in bidistilled water at a film: water ratio of 1:10, for 48h. Three replicates were made for each formulation. After 48h, the film samples were transferred to a convection oven (J.P. Selecta, S.A., Barcelona, Spain) for 24 h at 60 °C to remove the free water and afterwards

transferred to a desiccator with P_2O_5 at 25 ºC for 2 weeks to complete film drying. Film water solubility was estimated from its initial and final weights. The water solution was used to determine the bonded citric acid in the film. Free citric acid was assumed to dissolve in the aqueous phase and was determined by titration of an aliquot of the solution with NaOH (0.1 N), using phenolphthalein as indicator. Three replicates were considered for each formulation.

2.2.3.11. Thermal properties

A Differential Scanning Calorimeter (DSC 1 Star^e System, Mettler-Toledo Inc., Switzerland) was used to analyze the thermal properties. Weighted amounts of samples were placed into aluminum pans and sealed and drilled to promote the bonded moisture loss during heating. The curves were obtained using a double scan. First, a scan from 0 °C to 160 °C at 50 °C/min was used where the bonded water in the film was eliminated. Then the temperature was lowered to 0 °C at the same speed, and finally heated to 160 °C at 20 °C / min (in this scan, starch glass transition was analyzed). The initial and final weights of the pans were registered to assess water loss during the first heating.

2.2.3.12. Statistical analysis

Statgraphics Plus for Windows 5.1 (Manugistics Corp., Rockville, MD) was used to carry out statistical analyses of data through an analysis of variance (ANOVA). Fisher's least significant difference (LSD) was used at the 95% confidence level.

2.3. RESULTS

2.3.1. Film thickness, water solubility and bonded citric acid.

Constant compression moulding conditions were maintained during processing in order to submit all the formulations to a similar thermomechanical treatment. In agreement with the different composition, the differing response of the samples to the same treatment can be estimated by the film thickness. The values of this parameter obtained for every formulation are shown in Table 2.1.

Table 2.1.-Thickness, film solubility (g solubilised film/g initial dried film) and bonded citric acid (ratio with respect to the amount in the film) of the films equilibrated at 53% relative humidity and 25 ºC and the glass transition temperature (onset: T_{go} and midpoint: T_{gm}) of dried films.

Films	Thickness (µm)	Film solubility (**) (g/g)	Bonded citric acid (*)	T_{go} (°C)	T_{gm} (°C)
HPMCG	---	---	---	102 ± 2^{c}	113 ± 2^{c}
SG	268 ± 28^{a}	0.19 ± 0.07^{a}	---	111 ± 2^{b}	125 ± 4^{b}
SG-CA	217 ± 22^{cd}	0.35 ± 0.03^{b}	0.80 ± 0.03^{a}	106 ± 2^{c}	119 ± 2^{bc}
SG-H10	257 ± 19^{b}	0.15 ± 0.02^{a}	---	105 ± 2^{c}	114 ± 7^{cd}
SG-H10-CA	229 ± 13^{c}	0.32 ± 0.06^{b}	0.83 ± 0.04^{a}	85 ± 5^{e}	100 ± 3^{e}
SG-H20	204 ± 18^{d}	0.18 ± 0.02^{a}	---	94 ± 2^{d}	112 ± 3^{d}
SG-H20-CA	158 ± 13^{e}	0.31 ± 0.05^{b}	0.89 ± 0.09^{a}	85 ± 2^{e}	105 ± 9^{e}

(*) At 5 storage weeks; (**) At initial time, without significant differences with respect to the final time. Different superscript letters within the same column indicate significant differences among formulations ($p < 0.05$).

As can be observed, the film thickness decreases when HPMC was incorporated into the film (from 268 µm to 204 µm). This phenomenon is related with the increase in the blend flowability when HPMC is present in the blend, which is

probably related with the decrease in the glass transition of the blend commented on below. The addition of citric acid also contributed to the decrease in the film thickness, thus indicating the promotion of the blend's flowability. Due to its cross-linking effect, citric acid has not only been reported to be a compatibilizer of biopolymers (Reddy & Yang, 2010; Olivatto *et al.*, 2012; Menzel *et al.*, 2013) but also a plasticizer in its free form (Ghanbarzadeh *et al*., 2011). Thus, this organic acid can have a relevant impact on the rheological behaviour of blends during compression, which affects the final film thickness.

Table 2.1 also shows the solubility of the studied films in water at initial time. Values at final time (5 weeks) were not included due to the fact that no significant differences were found with respect to the initial values. The results show that the addition of citric acid is a key factor in terms of the integrity of films submitted to water action. Films containing citric acid showed higher solubility (0.31-0.35g/g) than citric acid-free films (0.15-0.19g/g). These results seem contradictory since the cross-linking activity of citric acid is related with an increase in the hydrophobicity as a result of the formation of ester groups. Nevertheless, the addition of citric acid is also related with a decrease in the pH values, which may give rise to a partial hydrolysis of glucosidic linkage (Olsson *et al.*, 2013). In this way, the values of bonded citric acid in films at 5 weeks of storage time (Table 2.1) are relevant since an important amount of citric acid remains free to contribute to the pH decrease. The contents of bonded citric acid ranged from 80 % (SG-CA) to 89% (SG-H20-CA) with respect to the total amount present in the film, there being no significant differences ($p > 0.05$) between samples. This indicates that this component partially reacts with the –OH groups of the polymer chains, although about 15% of the added amount is free in the matrix and could act as plasticizer.

2.3.2. Film microstructure

Figures 2.1a and b show SEM micrographs of the cross sections of films, containing (Figure 2.1b) or not (Figure 2.1a) citric acid, conditioned at 25 ºC and 53% RH for 1 (initial time) or 5 weeks (final time). At the initial time, the control formulations (SGi and SG-CAi) exhibited a homogeneous structure with some cracks which are related with the more brittle nature of this formulation under the observation conditions. The low water content and the electron beam in the microscopy chamber provoked the formation of these microcracks, as observed previously for other starch films (Jiménez *et al.,* 2012b).

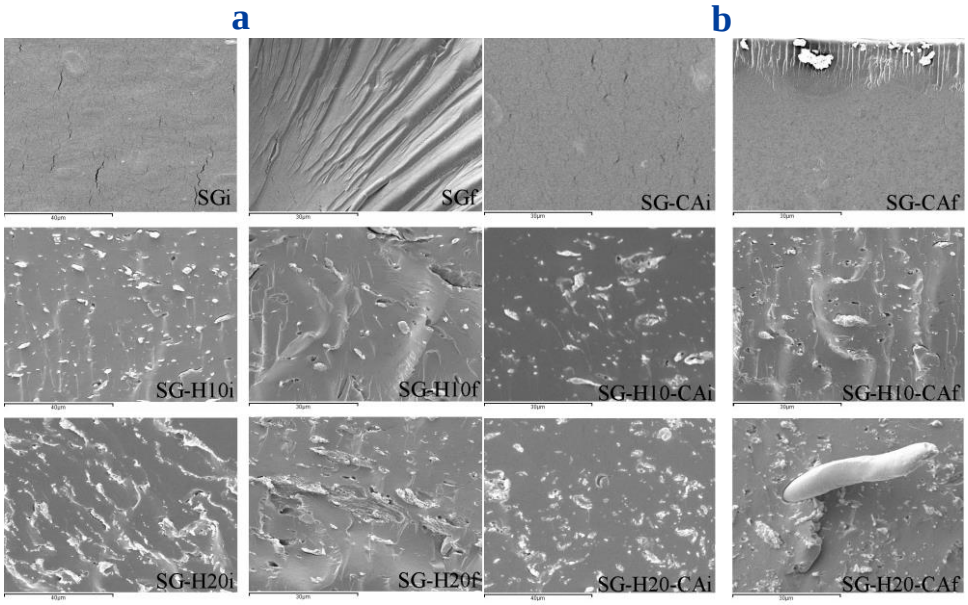

Figure 2.1.-SEM micrographs of the cross sections of films without (a) and with (b) citric acid after 1 (i: Initial time) and 5 (f: Final time) weeks of storage at 53% relative humidity and 25 ºC.

The addition of HPMC gave rise to a two-phase structure in which this polysaccharide constitutes the dispersed phase embedded in a starch continuous phase, which can be observed both at initial and final storage times. The

incompatibility of HPMC and starch has previously been observed in films obtained by casting (Jiménez *et al*., 2012a). Phase separation has also been reported in other polysaccharide blends such as potato maltodextrin in admixture with locust bean gum, gum arabic and carboxymethyl cellulose, and starch–chitosan blend films (Annable *et al.*, 1994; Mathew & Abraham, 2008). The different behaviour of continuous and dispersed phases in response to cryofracture is remarkable. Whereas a very hard, rigid matrix can be deduced for the starch continuous phase, HPMC particles can be inferred to be more rubbery and soft in nature, and, in some cases, they appeared greatly deformable (sample SG-H20-CAf).

Citric acid addition did not contribute to avoid the formation of microcracks as can be observed in Figure 2.1b (SG-CAi), despite its plasticizing effect on the matrix (Yu *et al.*, 2005) as deduced from the film thickness values. In HPMC-containing films, citric acid addition did not significantly affect their microstructural appearance in comparison with acid-free films and the HPMC dispersed phase was also observed in films. Nevertheless, a small increase in the polymer miscibility could be promoted, without notably affecting the visible film microstructure.

The effect of storage time on the film microstructure is also shown in Figure 2.1. Starch-glycerol films, containing or not citric acid (SGf, SG-CAf), show the extensive formation of crystalline zones, as revealed by the irregular, layered fracture surface, which point to the growth of the crystalline regions. This was especially notable for CA- free starch films whereas wider amorphous regions are still observable for starch films containing CA. In this case, the advance of the crystalline front from the film surface to the inner part of the film can be observed, probably due to the easier water uptake from the environment and the subsequent increase in the molecular mobility. The greater advance of these crystalline structures in citric acid-free films suggests that, despite its apparent plasticizing

effect, this organic acid contributes to partially inhibit starch recrystallization as mentioned by other authors (Shi *et al.*, 2007). The possible starch depolymerization provoked by acid hydrolysis could also affect the crystallization advance.

In HPMC-containing films, crystalline regions are not observed to the same extent as in starch films and, although HPMC appears in a dispersed phase, its partial miscibility in starch matrix may also contribute to inhibit starch crystallization as observed by Jiménez *et al*. (2012a) for HPMC-corn starch films obtained by casting.

The peak force quantitative nano-mechanical mapping AFM-based method is a good tool with which to analyse the nanostructure of biopolymer based films. This tool allows us to measure the Young modulus of the film at each point on its surface. Figure 2.2 shows the results obtained for studied films stored for 1 week and 5 weeks under controlled conditions. Raw data were converted into 2D images and their scale is expressed as DMT modulus.

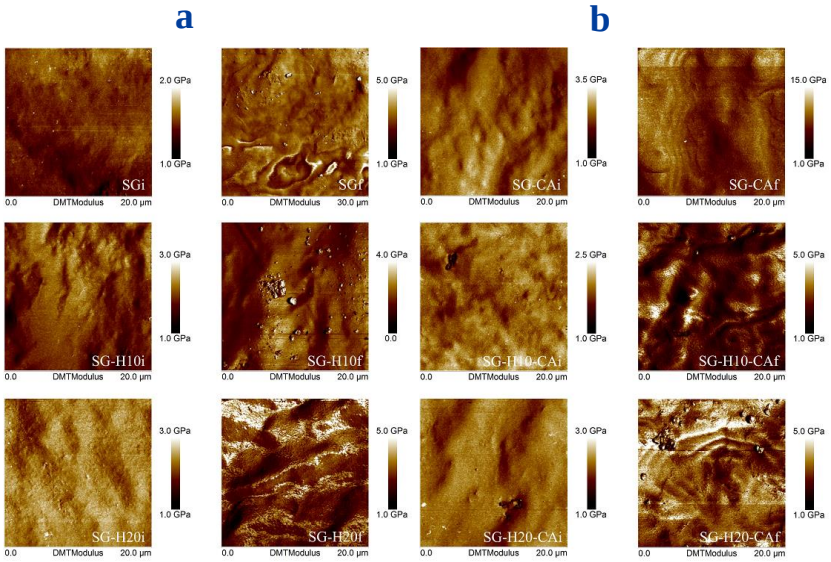

Figure 2.2.-AFM images (force mode) of films without (a) and with (b) citric acid after 1 (i: Initial time) and 5 weeks (f: Final time) of storage at 53% relative humidity and 25 ºC.

At initial time, films show a more homogeneous Young's modulus (up to 3.5 GPa), since no drastic changes are observed in the surface maps. Citric acid addition implied an increase in the surface modulus in agreement with the cross-linking effect, which is less marked in films containing HPMC. Likewise, the modulus values significantly increased with storage time (up to 15 GPa in HPMC-free films with citric acid), in part due to the progress of recrystallization phenomena. In HPMC-free samples, a greater increase was observed in line with a greater ratio of crystallinity, as observed by SEM. This increase was especially marked when these samples contained citric acid (SG-CAf), probably due to the combined effect of the cross-linking, which could progress throughout time. In samples with HPMC, more heterogeneous values of surface modulus were obtained, probably due to the fact that crystal growth was inhibited in areas near to HPMC zones.

2.3.3. X-ray diffraction

X-ray diffraction patterns obtained for both films stored for 1 week and those aged for 5 weeks are presented in Figure 2.3. Obtained patterns correspond with the formation of V-type structures, resulting from the formation of complexes of helical amylose forms with substances such as aliphatic fatty acids, surfactants, emulsifiers, alcohols, glycerol or dimethyl sulfoxide (Famá *et al.*, 2005). This type of conformation may be formed when endogenous lipids form complexes within the amylose helices (Gelders *et al.*, 2004). These patterns have previously been observed by other authors for starch or amylose with peaks at 2θ ~7, 14 and 20º (Famá *et al*., 2005; Chen *et al.*, 2009; Lesmes *et al.*, 2009). Nevertheless, the addition of citric acid or HPMC to the starch films promoted the formation of polymorphs since the intensity of peaks at 2θ 7º and 21º is enhanced, whereas the intensity at 2θ 20º decreased in most of the samples stored for 1 week. In general, the intensity of the peaks increased for stored samples thus indicating the growth in

the crystal size, which was especially marked for control film (SG), as observed by SEM (Figure 2.1). Nevertheless, most of the crystalline regions for the rest of the films seem to be formed during the compression and cooling, when the molecular mobility is still high (Rindlav-Westling *et al.*, 1998; Standing *et al.*, 2001).

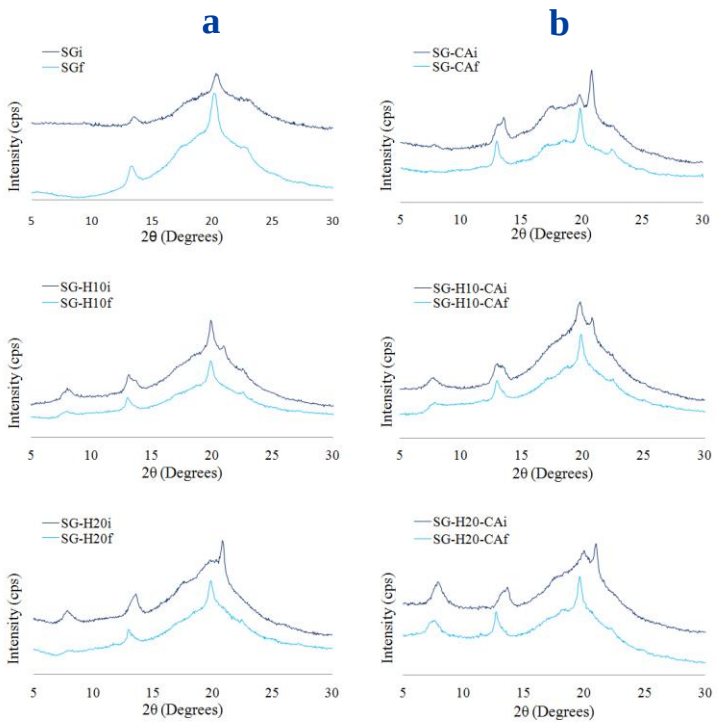

Figure 2.3.-X-Ray diffraction patterns of films without (a) and with (b) citric acid after 1 (i: Initial time) and 5 weeks (f: Final time) of storage at 53% relative humidity and 25 ºC.

When citric acid was added, the surface modulus obtained by peak force quantitative nano-mechanical mapping significantly increased, as mentioned above. Nevertheless, this change is not only attributable to a greater increase in crystallinity, as deduced from X-R diffraction patterns at initial and final storage times. So, the cross-linking progress or rearrangement of crystals and components

throughout storage can be inferred for this sample. In this sense, Reddy & Yang (2010) suggested that some of the amorphous regions of citric-acid cross-linked starch films may be better oriented after cross-linking, thus affecting the film mechanical behaviour. In this sense, SG-CA film presented a sharp peak at 2θ 21º at initial time whose intensity decreased with storage, whereas the intensity of the 2θ 20º peaks increased. This confirms the reorganization of components and the final formation of other polymorph crystals.

Regarding the effect of HPMC addition, it seems that this component is able to limit the starch recrystallization, since no significant changes in intensity are observed in XRD spectra after 5 storage weeks. Nevertheless, as observed for SG-CA film, the relative intensity of some peaks increased or decreased due to the molecular rearrangement and the formation of other polymorphic structures closer to that of starch films. Although HPMC is a totally amorphous polymer (Cai *et al.*, 2011; Jiménez *et al*., 2012a), starch films containing HPMC were semicrystalline, as observed in Figure 2.3. Jiménez *et al*. (2012a) obtained starch-HPMC films and analysed, by wide angle X-ray diffraction, their crystallinity. This was lower as the HPMC content increased, the films being almost totally amorphous when the HPMC content was 50%.

Figure 2.4 shows the X-ray diffraction pattern of pure citric acid in which the main peaks are at 2θ 14º, 17º, 19º, 24º, 26º and 29º. These are not found in the obtained films, which indicates that no crystalline citric acid is formed during film drying, even when it is non-bonded to the polymers. Similar results are obtained by (Shi *et al*., 2007), which point to its dispersion in the polymeric matrix at molecular level.

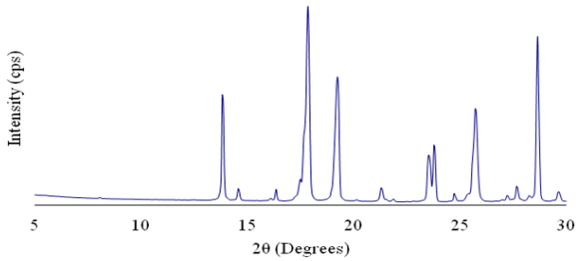

Figure 2.4.-XRD patterns of pure citric acid.

2.3.4. Glass transition of films

DSC analysis of the films allows us to know the possible changes in the glass transition of components due to their interactions in the matrix. In principle, two glass transitions are expected according to the two phases (continuous-starch and dispersed-HPMC phases) observed by SEM. Different authors have also reported the presence of two different glass transitions due to the phase separation of plasticizer at high water activity, where water-polymer interactions predominate over plasticizer-polymer ones (Debeaufort & Voilley, 1997; Jiménez *et al.*, 2013). Glass transition values of dry films are shown in Table 2.1, together with the value of HPMC with the same ratio of glycerol as that present in the films. Figure 2.5 shows the obtained thermograms for the different samples in the range of glass transitions. The value for HPMC-glycerol blends was slightly lower than that obtained for starch-glycerol films (113 compared to 125 ºC at the midpoint). In the blend films, only one glass transition was clearly observed, which was attributed to the starch phase which represents the greatest proportion of the film. The relatively low ratio of HPMC in the film makes the observation of its glass transition difficult. Nevertheless, the T_g value of the starch phase changed when citric acid or HPMC were added to the film. Citric acid incorporation supposed a decrease of about 5 ºC in T_g, which can be attributed to the plasticizing effect of the free citric

acid in the matrix and/or to the degree of starch depolymerization provoked by citric acid, as deduced from the film solubility values, which reduces the overall molecular weight of the polymers.

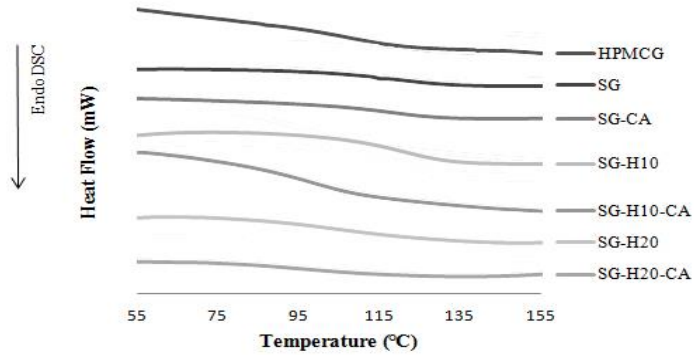

Figure 2.5.-Thermograms of dry films and HPMC-glycerol sample, showing glass transition (midpoint marked with arrow).

Different authors (Menzel *et al.*, 2013) report this effect of citric acid in starch systems when it was added as a cross-linking agent. Although an anti-plasticizing effect could be expected from cross-linking due to the associated decrease in the molecular mobility (Yu *et al.*, 2005), the overlapped hydrolysis effect masks it.

When HPMC was incorporated in the film without citric acid, a decrease in the T_g of about 10 ºC was also observed, which indicates that a partial miscibility of both polymers occurs in the blend with a T_g value nearer to that of HPMC. When both, citric acid and HPMC, are present in the film, T_g value ranged between 100-105 ºC, reflecting both the plasticizing effect of citric acid and the mixing effect of HPMC. So, phase separation between starch and HPMC was not total as deduced from these results and the continuous phase is a starch-rich phase containing glycerol, free citric acid and HPMC molecules. Both free citric acid and glycerol could also

be present in the HPMC dispersed phase since their chemical structures are compatible.

The decrease in the T_g provoked by both components explains the higher flowability of the blends shown during compression-moulding, commented on above.

2.3.5. Mechanical properties

Figure 2.6 shows the stress-Hencky strain curves obtained for the films studied, conditioned at 25 ºC and 53% RH for 1 week. The SG film was the most resistant and flexible, while the addition of HPMC brought about a slight reduction to the film resistance to break and to the elongation at break: the higher the HPMC content, the less resistant the film. This can be attributed to the presence of a dispersed phase in the starch matrix (as observed in Figure 2.1) which leads to a loss in the cohesion forces in the film. In this sense, a greater dispersed phase ratio lowers the cohesion forces and then the film resistance to break. The addition of citric acid had a great impact on the film stretchability, since elongation at break was reduced by up to 60% (from 28% to 11%). The shortening of the films caused by the citric acid is coherent with the cross-linking effect, since the slippage of polymer chains during the tensile test is limited by their strong inter-chain bonds. Nevertheless, the elastic modulus only slightly increases after the addition of citric acid, this increase only being significant in the sample with 20% HPMC. Similar behaviour was observed for the tensile strength at break. These results seem to indicate that inter-chain bonding did not progress enough, as observed by other authors for higher contents of citric acid (Reddy & Yang, 2010), and that HPMC chains seem to participate in the cross-linking reactions, probably through the hydroxy-propyl group which can be more readily available for reaction.

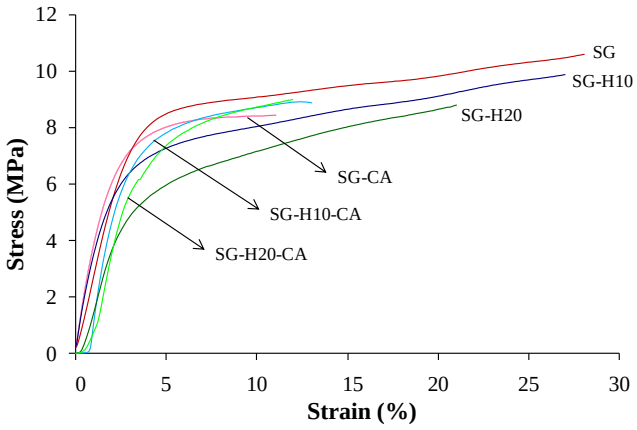

Figure 6.-Typical stress-strain curves of the different films after 1 week of storage.

Figure 2.7 also shows the values of the mechanical parameters of the films after 5 storage weeks. For every formulation, the elongation at break significantly decreases while the elastic modulus and the tensile strength increase. There are different mechanisms responsible for this behaviour. On the one hand, starch tends to recrystallize over time, as commented on above, which explains the observed behaviour of the formulation without HPMC or citric acid (Mali *et al.*, 2006). Apart from crystallization, the progressive aggregation of polymer chains throughout time has been observed for starch films and starch dispersions (Rindlav-Westling *et al*., 1998; Funami *et al*., 2005; Jiménez *et al*., 2012a) which provokes an increase in the matrix compactness and the subsequent changes in the tensile response.

The cross linking effect of citric acid could also be extended throughout time, thus contributing to the changes in the mechanical properties. In this sense, the sample with the highest elastic modulus and lowest stretchability after 5 storage weeks is the one that contains the highest ratio of HPMC and citric acid, which also points to the fact that HPMC chains participate in the citric acid cross-linking action. This

phenomenon would be associated with the non-bonded citric acid (11-20%, according to Table 2.1) that remains free after film formation and which is able to react with the hydroxyl groups of polymers during storage

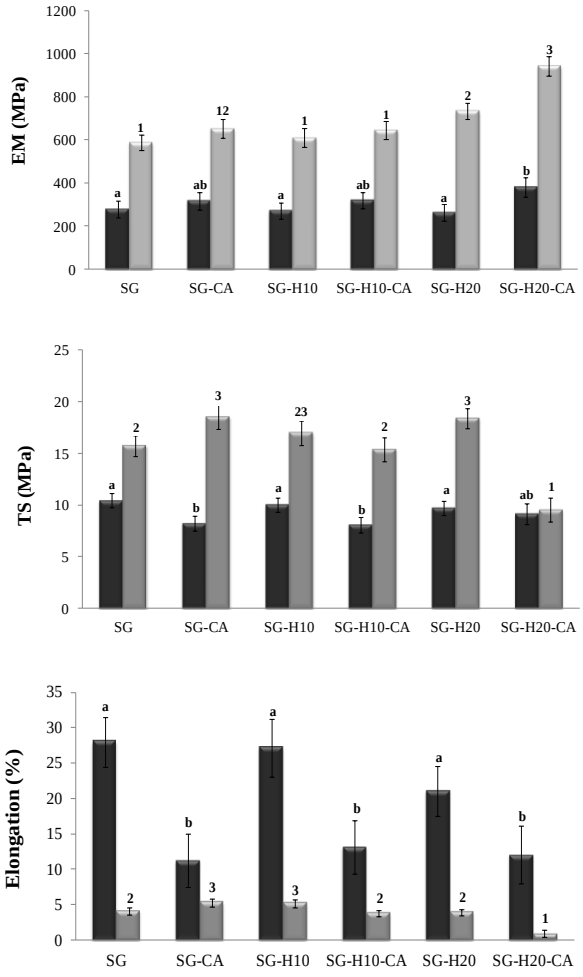

Figure 2.7.-Mean values of elastic modulus and stress and strain at break for the different films stored for 1 (black bars) and 5 (grey bars) weeks at 53% relative humidity and 25 ºC. LSD intervals (95% confidence level) for each mean value are shown.

2.3.6. Barrier properties

One of the main features to take into account when biodegradable polymers are used for packaging application is their ability to avoid mass transfer mechanisms. In this way, a good barrier against aroma, water vapour and gases is generally desired. Table 2.2 shows the values of water vapour, oxygen permeability and water content for films conditioned for 1 week and those aged for 5 weeks.

Table 2.2.-Mean values and standard deviation of water content (Xw: g water/g dry film), water vapour and oxygen permeabilities of the different films after 1 (Initial time) and 5 (Final time) weeks of storage at 53% relative humidity and 25 ºC.

Films	Xw		WVP ($g \cdot mm \cdot KPa^{-1} \cdot h^{-1} \cdot m^{-2}$)		$O_2P \cdot 10^{13}$ ($cm^3 \cdot m^{-1} \cdot s^{-1} \cdot Pa^{-1}$)	
	Initial	Final	Initial	Final	Initial	Final
SG	0.062 ± 0.002^{a1}	0.079 ± 0.004^{a2}	18.1 ± 1.4^{a1}	16 ± 2^{a1}	< D.L.	1.3 ± 0.5^{a}
SG-CA	0.059 ± 0.002^{ab1}	0.076 ± 0.002^{ab2}	12 ± 2^{b1}	15.6 ± 1.2^{a1}	2.6 ± 0.5^{a1}	2.81 ± 0.04^{b1}
SG-H10	0.056 ± 0.004^{b1}	0.075 ± 0.002^{ab2}	13 ± 2^{b1}	14 ± 2^{a1}	1.4 ± 0.3^{a1}	2.5 ± 0.5^{ab1}
SG-H10-CA	0.054 ± 0.003^{b1}	0.073 ± 0.002^{ab2}	11 ± 2^{b1}	11 ± 2^{b1}	2.2 ± 0.2^{a1}	4.0 ± 1.0^{c2}
SG-H20	0.055 ± 0.002^{b1}	0.071 ± 0.003^{b2}	12.0 ± 1.1^{b1}	11.0 ± 1.2^{b1}	4.1 ± 1.0^{b1}	5.1 ± 0.9^{cd1}
SG-H20-CA	0.054 ± 0.003^{b1}	0.070 ± 0.007^{b1}	9.1 ± 1.1^{c1}	10.1 ± 0.4^{b1}	5.0 ± 1.2^{b1}	6.0 ± 0.9^{d1}

D.L.: 0.1 $cm^3/(m^2.day)$. Different superscript letters within the same column indicate significant differences among formulations ($p < 0.05$). Different superscript numbers within the same row indicate significant differences due to storage time ($p < 0.05$).

At initial time, the water vapour permeability values were significantly reduced by HPMC and the addition of citric acid, exhibiting the lowest value when both citric acid and the highest HPMC ratio were present in the film. Ghanbarzadeh *et al*. (2011) also found that the addition of citric acid reduced WVP when the concentrations ranged between 5 and 20%. They explained this effect in terms of

the substitution of hydroxyl groups (-OH) by hydrophobic esters and by the fact that citric acid introduced a tortuous path for water molecules to pass through the films due to the cross linking effect. These authors also found that another cellulose derivative (carboxymethylcellulose) was effective at reducing the WVP and related this phenomenon with the fact that carboxymethylcellulose is less hydrophilic than starch (Ma *et al.*, 2008). Nevertheless, HPMC has been reported to produce worse water vapour barriers (Jiménez *et al*., 2010; 2012a). Thus, the positive effect of HPMC on the water vapour barrier of the studied films may be due to its cooperative effect on the cross-linking effect, as previously commented on.

Storing the films for 5 weeks had no effect on the WVP values, regardless of the film composition, despite the fact that a significant increase ($p < 0.05$) in the film moisture content occurred during storage. A similar result was reported by Jiménez *et al*. (2012c) for starch-glycerol films. They found a significant increase in the film's moisture content after 5 storage weeks, at the same time as they became more brittle, as observed in the present work. In this sense, it is remarkable that the formation of crystalline regions implies a gain in water content, since a great amount of water molecules are bonded to the crystalline conformations (Rindlav *et al.*, 1997). So, the water gain of the films could be associated with the water bonded to the crystalline regions which did not contribute to the plasticization of the amorphous matrix and therefore, did not affect the barrier properties.

As regards oxygen permeability, SG was the least permeable film, mainly at initial time when the equipment was not able to take measurements due to the very low quantity of oxygen molecules that passed through the film. Different studies have pointed out the very good oxygen barrier properties of starch compared with other polymers (Miller & Krochta, 1997; Jiménez *et al*., 2012ab). The addition of HPMC significantly increased ($p < 0.05$) the oxygen permeability as previously observed by Jiménez *et al*., 2012a, which coincides with the higher oxygen permeability of

this polymer. Storage time did not affect the oxygen barrier properties, unlike what occurred with the water vapour barrier.

2.3.7. Optical properties

Optical properties are relevant when a polymeric matrix is tested as a packaging material. Ghanbarzadeh *et al*. (2010) commented that film colour can be an important factor in terms of the consumer acceptance of both edible and inedible films. In the same sense, Hutchings (1999) explained that the most outstanding optical properties with which to evaluate the impact on the appearance and colour of coated products are opacity and gloss. Table 2.3 shows the gloss values (measured at 60º) and internal transmittance values (at 450 nm) for films stored for 1 or 5 weeks at 25 ºC and 53% RH. The gloss values were very low for every formulation (between 10.2 GU to 12 GU), regardless of the film composition and the storage time. Higher gloss values have been found for both pure HPMC (Jiménez *et al*., 2010) and starch-glycerol films (Jiménez *et al*., 2012c) obtained by casting. Nevertheless, for starch films blended with other polymers, such as chitosan (Bonilla *et al.*, 2013) or HPMC (Jiménez *et al*., 2012a), similar gloss values are reported. Film gloss is directly related with the surface topography, which can be determined by atomic force microscopy. The corresponding surface roughness parameters for the obtained films are shown in Table 2.3, where neither a different composition nor a varying storage time led to there being any significant differences in the parameters.

Table 2.3 also includes the values of internal transmittance (Ti) for films after 1 and 5 storage weeks. High values of internal transmittance are associated with highly transparent films. On the contrary, more opaque films correspond with low values of internal transmittance. The Ti values ranged from 74 to 81 and were

dependent on the formulation, but were not significantly affected by the storage time.

Table 2.3.-Mean values and standard deviation of surface roughness parameters and optical properties of the different films after 1 (Initial time) and 5 (Final time) weeks of storage at 53% relative humidity and 25 ºC.

Formulation	Surface roughness				Gloss 60° (GU)		T_i (450 nm)	
	Rq (nm) initial	Rq (nm) final	r (%) initial	r (%) final	Initial	Final	Initial	Final
SG	263 ± 63^{ab1}	356 ± 64^{ab1}	6.0 ± 1.0^{a1}	2 ± 0.5^{a2}	12.0 ± 0.5^{a1}	11.5 ± 0.4^{ab2}	77.0 ± 1.1^{ab1}	76.9 ± 0.5^{a1}
SG-CA	206 ± 72^{ab1}	302 ± 70^{b1}	2.5 ± 0.2^{ab1}	2 ± 0.5^{a1}	11.0 ± 0.5^{b1}	12.0 ± 1.0^{c2}	80.9 ± 0.5^{c1}	82.0 ± 1.1^{c1}
SG-H10	319 ± 147^{a1}	272 ± 76^{ab1}	2.1 ± 0.4^{ab1}	2.0 ± 0.8^{a1}	11.1 ± 1.2^{b1}	11.0 ± 1.1^{a1}	75 ± 0.5^{d1}	75.4 ± 0.5^{b1}
SG-H10-CA	233 ± 35^{ab1}	214 ± 83^{a1}	2.2 ± 0.8^{b1}	1.3 ± 0.3^{a1}	10.2 ± 0.3^{c1}	12.1 ± 1.0^{bc2}	78.2 ± 0.2^{a1}	79.0 ± 0.3^{d1}
SG-H20	169 ± 43^{b1}	214 ± 20^{a1}	1.2 ± 0.2^{b1}	2.1 ± 1.0^{a1}	10.9 ± 0.9^{bc1}	11.5 ± 0.5^{ab2}	74.0 ± 0.9^{d1}	74.1 ± 0.9^{b1}
SG-H20-CA	232 ± 42^{ab1}	228 ± 23^{a1}	2.1 ± 0.9^{ab1}	2.0 ± 0.9^{a1}	10.6 ± 0.5^{bc1}	11.1 ± 1.2^{a1}	76.0 ± 1.1^{b1}	77.0 ± 1.1^{a1}

Different superscript letters within the same column indicate significant differences among formulations ($p < 0.05$). Different superscript numbers within the same row indicate significant differences due to storage time ($p < 0.05$).

Considering these results, all of the films can be considered quite transparent. It is remarkable that, whereas the incorporation of citric acid promotes a slight increase in transparency, HPMC slightly increases film opacity, in agreement with the appearance of a dispersed phase which enhances light scattering. The effect of citric acid is opposite to that observed by Olivatto *et al.*, (2012) for starch-PBAT films obtained by reactive extrusion with citric acid, where a significant increase in opacity is observed. These authors related the cross-linking activity of the acid with a higher polymeric chain compaction, which modifies the refractive index and hinders the passage of the light through the matrix. The relatively low ratio of citric acid (1% with respect to starch) in the films and the commented depolymerisation

effect, which gives rise to a less compact matrix, can explain the different behaviour

2.4. CONCLUSIONS

Corn starch films containing HPMC (10 and 20%, with respect to starch) obtained by compression moulding showed a dispersed phase of HPMC in a continuous starch-rich phase with a lower glass transition than HPMC-free films. The addition of citric acid as a compatibilizer also provoked a decrease in glass transition in line with a depolymerisation effect brought about by acid hydrolysis. Both components implied a decrease in the water vapour permeability but a slight increase in oxygen permeability. Although citric acid provoked a mild hardening effect in the films, it greatly decreased extensibility pointing to a weak cross-linking effect, which seems to increase during film storage to a greater extent in films with the highest ratio of HPMC. Starch crystallization was slightly modified by both components which induce the formation of other polymorphs mainly at initial time (1 storage week). Starch crystallization during storage was inhibited by both citric acid and HPMC. A greater ratio of citric acid could be interesting as a means of promoting both a more significant cross-linking effect and greater HPMC compatibility with starch.

2.5. REFERENCES

Albert, S., & Mittal, G. S. (2002). Comparative evaluation of edible coatings to reduce fat uptake in a deep-fried cereal product. Food Research International, 35(2), 445–458.

Annable, P., Fitton, M. G., Harris, B., Philips, G. O., & Williams, P. A. (1994). Phase behaviour and rheology of mixed polymer systems containing starch. Food Hydrocolloids, 8(4), 351–359.

Arık Kibar, E. A., & Us, F. (2013). Thermal, mechanical and water adsorption properties of corn starch–carboxymethylcellulose/methylcellulose biodegradable films. Journal of Food Engineering, 114(1), 123–131.

American Society for Testing and Materials, ASTM E96-95. Standard test methods for water vapor transmission of materials. In annual book of ASTM. Philadelphia; 1995.

American Society for Testing and Materials, ASTM D523. Standard test method for specular gloss. In annual book of ASTM. Philadelphia; 1999.

American Society for Testing and Materials, ASTM D882. Standard test method for tensile properties of thin plastic sheeting. In annual book of ASTM. Philadelphia; 2001.

American Society of Mechanical Engineers, ASME B46.1. Surface texture: Surface roughness, waviness and lay. New York; 1995.

Bonilla, J., Talón, E., Atarés, L., Vargas, M., & Chiralt, A. (2013). Effect of the incorporation of antioxidants on physicochemical and antioxidant properties of wheat starch-chitosan films. Journal of Food Engineering, 118(3), 271-278.

Chen, C., Kuo, W., & Lai, L. (2009). Rheological and physical characterization of film-forming solutions and edible films from tapioca starch/decolorized hsian-tsao leaf gum. Food Hydrocolloids, 23(8), 2132-2140.

Debeaufort, F., & Voilley, A. (1997). Methylcellulose-based edible films and coatings: 2. Mechanical and thermal properties as a function of plasticizer content. Journal of Agricultural and Food Chemistry, 45, 685-689.

Famá, L., Rojas, A., Goyanes, S., & Gerschenson, L. (2005). Mechanical properties of tapioca-starch edible films containing sorbates. LWT-Food Science and Technology, 38(6), 631-639.

Fahs, A., Brogly, M., Bistac, S., & Schmitt, M. (2010). Hydroxypropyl methylcellulose (HPMC) formulated films: Relevance to adhesion and friction surface properties. Carbohydrate Polymers, 80(1), 105–114.

Funami, T., Kataoka, Y., Omoto, T., Goto, Y., Asai, I., & Nishinari, K. (2005). Effects of non-ionic polysaccharides on the gelatinization and retrogradation behavior of wheat starch. Food Hydrocolloids, 19(1), 1–13.

Gelders, G. G., Vanderstukken, T. C., Goesaert, H., & Delcour, J. A. (2004). Amylose-lipid complexation: a new fractionation method. Carbohydrate Polymers, 56(4), 447-458.

Ghanbarzadeh, B,. Almasi, H., & Entezami, A. A. (2010). Physical properties of edible modified starch/carboxymethyl cellulose films. Innovative Food Science & Emerging Technologies, 11(4), 697-702.

Ghanbarzadeh, B,. Almasi, H., & Entezami, A. A. (2011). Improving the barrier and mechanical properties of corn starch-based edible films: Effect of citric acid and carboxymethyl cellulose. Industrial Crops and Products, 33(1), 229-235.

Hutchings, J. B. (1999). Food color and appearance. (2nd ed.). Gaithersburg, Maryland, USA: Aspen Publishers, Inc.

Jiménez, A., Fabra, M,J., Talens, P., & Chiralt, A. (2010). Effect of lipid self-association on the microstructure and physical properties of hydroxypropyl-methylcellulose edible films containing fatty acids. Carbohydrate Polymers, 82(3), 585-593.

Jiménez, A., Fabra, M. J., Talens, P., & Chiralt, A. (2012a). Influence of hydroxypropylmethylcellulose addition and homogenization conditions on properties and ageing of corn starch based films. Carbohydrate Polymers, 89(2), 676– 686.

Jiménez, A., Fabra, M. J., Talens, P., & Chiralt, A. (2012b). Effect of sodium caseinate on properties and ageing behaviour of corn starch based films. Food Hydrocolloids, 29(2), 265-271.

Jiménez, A., Fabra, M. J., Talens, P., & Chiralt, A. (2012c). Effect of re-crystallization on tensile, optical and water vapour barrier properties of corn starch films containing fatty acids. Food Hydrocolloids, 26(1), 302-310.

Jiménez, A., Fabra, M. J., Talens, P., & Chiralt, A. (2013). Phase transitions in starch based films containing fatty acids. Effect on water sorption and mechanical behaviour. Food Hydrocolloids, 30 (1), 408-418.

Kester, J., & Fennema, O. (1986). Edible films and coatings: A review. Food Technology, 40, 47–59.

Kou, W., Cai, C., Xu, S., Wang, H., Liu, J., Yang, D., & Zhang, T. (2011). In vitro and in vivo evaluation of novel immediate release carbamazepine tablets: Complexation with hydroxypropyl-β-cyclodextrin in the presence of HPMC. International Journal of Pharmaceutics, 409(1–2), 75–80.

Lesmes, U., Cohen, S. H., Shener, Y., & Shimoni, E. (2009). Effects of long chain fatty acid unsaturation on the structure and controlled release properties of amylose complexes. Food Hydrocolloids, 23(3), 667-675.

Ma, X., Chang, P. R., & Yu, J. (2008). Properties of biodegradable thermoplastic pea starch/carboxymethyl cellulose and pea starch/microcrystalline cellulose composites. Carbolydrate Polymers, 72(3), 369-375.

Ma, X., Chang, P. R., Yu, J., & Stumborg, M. (2009). Properties of biodegradable citric acid-modified granular starch/thermoplastic pea starch composites. Carbohydrate Polymers, 75(1), 1-8.

Mathew, S., & Abraham, T. E. (2008). Characterisation of ferulic acid incorporated starch-chitosan blend films. Food Hydrocolloids, 22(5), 826–835.

McHugh, T. H., Avena-Bustillos, R., & Krochta, J. M. (1993). Hydrophobic edible films: Modified procedure for water vapour permeability and explanation of thickness effects. Journal of Food Science, 58(4), 899–903.

Menzel, C., Olsson, E., Plivelic, T. S., Andersson, R., Johansson, C., Kuktaite, R., Järnström, L., & Koch, K. (2013). Molecular structure of citric acid cross-linked starch films. Carbohydrate Polymers, 96(1), 270-276.

Miller, K. S., & Krochta, J. M. (1997). Oxygen and aroma barrier properties of edible films: A review. Trends in Food Science & Technology, 8(7), 228-237.

Olivato, J. B., Grossmann, M. V. E., Yamashita, F., Eiras, D., & Pessan, L. A. (2012). Citric acid and maleic anhydre as compatibilizers in starch/poly(butylene adipate-co-terephthalate) blends by one-step reactive extrusion. Carbohydrate Polymers, 87(4), 2614-2618.

Olsson, E., Menzel, C., Johansson, C., Andersson, R., Koch, K., & Järnström, L. (2013). The effect on pH on hydrolysis, cross-linking and barrier properties of starch barriers containing citric acid. Carbohydrate Polymers, 98(2), 1505-1513.

Reddy, N., & Yang, Y. (2010). Citric acid cross-linking of starch films. Food Chemistry, 118(3), 702-711.

Rindlav, A., Hulleman, S. H. D., & Gatenholm, P. (1997). Formation of starch films with varying crystallinity. Carbohydrate Polymers, 34(1–2), 25–30.

Rindlav-Westling, A., Stading, M., Hermansson, A. M., & Gatenholm, P. (1998). Structure, mechanical and barrier properties of amylose and amylopectin films. Carbohydrate Polymers, 36(2–3), 217–224.

Sánchez-González, L., Vargas, M., González-Martínez, C., Chiralt, A., & Cháfer, M. (2009). Characterization of edible films based on hydroxypropylmethylcellulose and tea tree essential oil. Food Hydrocolloids, 23(8), 2102–2109.

Seker, M., & Hanna, M. A. (2006)**.** Sodium hydroxide and trimetaphosphate levels affect properties of starch extrudates. Industrial Crops and Products, 23(3)**,** 249–255.

Shi, R., Zhang, Z., Liu, Q., Han, Y., Zhang, L., Chen, D., & Tian, W. (2007). Characterization of citric acid/glycerol co-plasticized thermoplastic starch prepared by melt blending. Carbohydrate Polymers, 69(4), 748-755.

Shi, R., Bi, J., Zhang, Z., Zhu, A., Chen, D., Zhou, X., Zhang, L., & Tian, W. (2008). The effect of citric acid on the structural properties and cytotoxicity of the polyvinyl alcohol/starch films when molding at high temperature. Carbohydrate Polymers, 74(4), 763–770.

Stading, M., Rindlav-Westling, A., & Gatenholm, P. (2001). Humidity-induced structural transitions in amylose and amylopectin films. Carbohydrate Polymers, 45 (3), 209–217.

Villalobos, R., Hernández-Muñoz, P., & Chiralt, A. (2006). Effect of surfactants on water sorption and barrier properties of hydroxypropyl methylcellulose films. Food Hydrocolloids, 20(4), 502–509.

Yang, C. Q., Wang, X., & Kang I. (1997). Ester cross-linking of cotton fabric by polymeric carboxylic acids and citric acid. Textile Research Journal, 67(5): 334–342.

Yoon, S.-D., Chough, S.-H., & Park, H.-R. (2006). Properties of starch-based blend films using citric acid as additive. II. Journal of Applied Polymer Science, 100(3), 2554–2560.

Yu, J., Wang, N., & Ma, X. (2005). The effects of citric acid on the properties of thermoplastic starch plascitized by glycerol. Starch–Stärke, 57(10), 494-504.

CHAPTER 3

PHYSICAL AND STRUCTURAL PROPERTIES AND THERMAL BEHAVIOUR OF STARCH-POLY(ε–CAPROLACTONE) BLEND FILMS FOR FOOD PACKAGING

Rodrigo Ortega-Toro, Jessica Contreras, Pau Talens, & Amparo Chiralt

Food Packaging and Shelf Life, doi:10.1016/j.fpsl.2015.04.001

Structural and physical properties (barrier, mechanical, and optical properties) and thermal behaviour of corn starch-PCL blend films, containing glycerol as plasticizer, obtained by compression moulding, at 160ºC and 130 bars, were studied. The stability on the films' properties was also evaluated. Blend films showed phase separation of the polymers in a heterogeneous matrix with starch rich regions and PCL rich regions. Nevertheless, a small miscibility of PCL in the starch phase was detected trough the shift in the glass transition temperature of the starch phase, which leads to a partial inhibition of amylose crystallization during film formation and storage. The lack of interfacial adhesion of PCL and starch phases promoted films' fragility and reduced stretchability, although elastic modulus of the films with small PCL ratios increased. Water barrier properties of starch films were improved as the PCL increased in the blend, but oxygen permeability increased. Due to the food compatibility of this polymer blends (without any toxic compound) these could be an interesting alternative for food packaging, where some drawbacks of starch films has been overcome.

VNIVERSITAT POLITECNICA
VALENCIA
EX TECHNICA PROGRESSIO

3.1. INTRODUCTION

In the last decade, there has been growing interest in the development of biodegradable materials for applications in packaging technology, medicine or agriculture in order to mitigate the problems caused by non-biodegradable petroleum-derived plastics (Hubackova *et al*., 2013). In this sense, starch is a promising polymer because it is abundant, cheap and renewable (Lourdin, Valle, & Colonna, 1995). Although starch shows a high capacity to form homogeneous films with excellent oxygen barrier properties, they exhibit some drawbacks, such as poor mechanical properties, and high water vapour sensitivity which leads to high water vapour permeability (Averous & Boquillon, 2004; Ghanbarzadeh *et al.,* 2011), and retrogradation. This consists of a slow recoiling of gelatinized amylose and amylopectin molecules which back into their native helical arrangements or into a new single helix conformation. The retrogradation is undesirable as it increases crystallinity and reduces film elongation over time. In order to improve the starch film properties, blends with other components, such as plasticizers, cross-linking agents or other polymers have been studied. Glycerol can be added as a plasticizer to enhance the mechanical properties of the film, increasing the flexibility (Vieira *et al*., 2011).

The addition of other thermoplastic polymers to form blend starch films can modulate the films' properties in order to improve their functionality. Of the commercially available biodegradable polymeric materials, blends based on thermoplastic starch (TPS) and hydrophobic synthetic polymers, such as aliphatic polyesters, could offer adequate solutions (Di Franco *et al.*, 2004).

PCL is aliphatic polyester obtained by chemical synthesis from crude oil. PCL-based films have good water resistance. It is a thermoplastic, biodegradable, biocompatible and semi-crystalline polymer that has a very low glass transition temperature (~-60ºC) (Cao *et al.,* 2008). It also has a low melting point (58–60 °C),

low viscosity, and is easily processable (Flieger *et al.,* 2003). PCL can be blended with other polymers to improve stress crack resistance, dyeability and adhesion and has been used in combination with polymers such as cellulose propionate, cellulose acetate butyrate, polylactic acid and polylactic acid-co-glycolic acid (Woodruff & Hutmacher, 2010; Takala *et al*., 2013).

Properties of PCL-starch blends have been analysed by several authors for different applications. Averous *et al.* (2000), studied the mechanical properties, the thermal and thermo-mechanical behaviour and the hydrophobicity of wheat TPS-PCL materials blended by extrusion and injection moulded, containing different ratios of TPS and PCL (up to 40 wt.%). They found a phase separation of polymers due to their incompatibility, although thermal transitions of each polymer suffered minor shifts in the characteristic temperatures. The hydrophobicity of the blends considerably increased as compared with TPS. Rosa *et al*. (2004) also analysed the properties of PCL blends with different ratios of gelatinized and non-gelatinized corn starch. They observed that the melt flow index increased when the PCL ratio increased in the blend, while PCL reduced the water sorption capacity of the materials. A decrease in the crystallinity of PCL in the blends was also observed.

On the basis of previous studies, and despite the polymer incompatibility, PCL-starch blends could offer properties that are of interest for the development of biodegradable packaging materials for food products where some drawbacks of starch films, such as their highly hydrophilic nature, poor water barrier properties and retrogradation phenomena could be overcome, while no potentially toxic compounds are present in the film formulation, which is crucial for food packaging applications (Duquesne *et al*., 2001). Likewise, biodegradability of starch-PCL blends has been reported by Sawada (1994) and Yang & Wu (1999). These authors found a reduction of the PCL degradation time when it is blended with starch.

The aim of this work was to characterize the structural and physical properties (barrier, mechanical, and optical properties) and thermal behaviour of corn starch-PCL blend films, with a wide range of polymers' ratios, obtained by compression moulding. The stability during storage time on the films' properties was also evaluated.

3.2. MATERIALS AND METHODS

3.2.1. Materials

Corn starch was purchased from Roquette (Roquette Laisa Spain, Benifaió, Spain). Glycerol was obtained from Panreac Química, S.A. (Castellar del Vallès, Barcelona, Spain). Polycaprolactone (pellets ~3 mm, average M_n 80.000 Da, impurities <1.0% water) was provided by Fluka (Sigma–Aldrich Chemie, Steinheim, Germany). P_2O_5 and $Mg(NO_3)_2$ were obtained from Panreac Química, S.A. (Castellar Vallés, Barcelona).

3.2.2. Film processing

Native starch and glycerol were dispersed in water. The starch:glycerol ratio (w/w) was 1:0.3, which was established on the basis of previous studies (Ortega-Toro *et al.*, 2014) PCL was dispersed in the aqueous slurry of starch and glycerol containing 0.5 g water/g starch at different ratios to obtain four blends with 80:20, 60:40, 40:60, 20:80 starch:PCL ratios (w/w). Mass fraction of every formulation is shown in Table 3.1. The blends were named S80, S60, S40 and S20, respectively. Starch-glycerol (S) and pure PCL films were used as controls.

The formulations were gradually mixed on a two-roll mill (Model LRM-M-100, Labtech Engineering, Thailand) at 160 °C and 8 rpm for 30 minutes until a homogeneous paste sheet was obtained. The obtained paste sheets were conditioned at 25 °C and 53% relative humidity (RH) for 48 hours before compression moulding.

The films were obtained by compression moulding (Model LP20, Labtech Engineering, Thailand). Four grams of the paste were put onto steel sheets and preheated on the heating unit for 5 min. Films were obtained by compressing at 160 °C for 2 minutes at 30 bars, followed by 6 minutes at 130 bars; thereafter a cooling cycle was applied for 3 minutes. The obtained films were conditioned at 25 °C and 53% RH for 1 and 5 weeks for their characterization.

3.2.3. Film characterization

3.2.3.1. Film thickness, moisture content and solubility in water

The film thickness was measured with a Palmer digital micrometer at six random positions around the film. Regarding moisture content, the films were conditioned at 53% RH and dried for 24 h at 60 °C using a convection oven (J.P. Selecta, S.A. Barcelona, Spain) and placed in a desiccator at 25 °C with P_2O_5 for 2 weeks. This assay was performed in triplicate.

The solubility in water was determined holding the sample in bi-distilled water for 48 h, considering a film:water ratio of 1:10. Afterwards, the samples were transferred to a convection oven (J.P. Selecta, S.A., Barcelona, Spain) for 24 h at 60 °C to remove free water and then were transferred to a desiccator with P_2O_5 at 25 ºC for 2 weeks till constant weight. Solubility in water was obtained from the

initial and final weights of the films. Three samples were used for each formulation.

3.2.3.2. Water Vapour Permeability (WVP) y Oxygen Permeability (O_2P)

The ASTM E96-95 (ASTM, 1995) gravimetric method was used for determining the WVP of the films. The modification proposed by McHugh, Avena-Bustillos, & Krochta (1993) was considered. Distilled water was placed in Payne permeability cups (3.5 cm diameter, Elcometer SPRL, Hermelle/s Argenteau, Belgium) to expose the film to 100% RH on one side. Each cup was placed in a cabinet equilibrated at 25 °C and 53% RH, with a fan placed on the top of the cup in order to reduce the resistance to water vapour transport, thus avoiding the stagnant layer effect in this exposed side of the film. The relative humidity of the cabinet (53%) was held constant using $Mg(NO_3)_2$ oversaturated solutions. The cups were weighed periodically (0.0001 g) and the water vapour transmission (WVTR) was determined from the slope obtained from the regression analysis of weight loss data versus time. From this data, WVP was obtained according to Jiménez *et al*. (2012).

The oxygen permeation rate of the films was determined using an OX-TRAN Model 2/21 ML (Mocon Lippke, Neuwied, Germany) in samples conditioned at 53% RH and 25 °C. The transmission values were determined every 20 min until to reach the equilibrium. The exposure area during the tests was 50 cm^2. Three samples were studied for each formulation.

3.2.3.3. Tensile properties

A universal test machine (TA.XTplus model, Stable Micro Systems, Haslemere, England) was used to determine the tensile properties of films. The tensile strength (TS), the elastic modulus (EM), and the elongation (E) of the films were

determined from the stress-strain curves, estimated from force-distance data obtained for different films (2.5 cm wide and 5 cm long), according to the ASTM standard method D882 (ASTM, 2001). Equilibrated samples were mounted in the film-extension grips of the testing machine and stretched at 50 mm min^{-1} until breaking. Tests were carried out at 25 ºC and 53% RH. Ten replicates were considered for each formulation.

3.2.3.4. Optical properties

The Kubelka-Munk theory for multiple scattering was applied to the reflection spectra to determinate the film's transparency (Hutchings, 1999). The surface reflectance spectrum was determined from 400 to 700 nm with a spectro-colorimeter CM- 3600d (Minolta Co., Tokyo, Japan) on both a white and a black background. Internal transmittance (Ti) was obtained according to Jiménez *et al*. (2012).

The gloss was determined at an incidence angle of 85°, according to the ASTM standard D523 method (ASTM, 1999) using a flat surface gloss meter (Multi.Gloss 268, Minolta, Germany). Three films of each formulation were considered, taking three measurements in each sample. All results are expressed as gloss units (GU), relative to a highly polished surface of black glass standard with a value near to 100 GU.

3.2.3.5. Thermal properties

A Differential Scanning Calorimeter DSC 1 Star^{e} System (Mettler-Toledo Inc., Switzerland) was used to analyse the phase transitions in the polymer matrices. 10-15 mg of film samples were placed into aluminium pans, sealed and perforated to favour possible moisture loss during the heating run. Three scans were performed

for the sample analyses. First, sample was heated from -80 °C to 160 °C at a heating rate of 20 °C/min, from which PCL melting properties (ΔH_m,T_m) were obtained and in which the bonded water in the film was eliminated. In the second scan, the temperature was lowered to -80 °C at the same rate and the PCL crystallization properties (ΔH_c, T_c) were obtained. Finally, samples were heated to 160 °C at a 20 °C/min to obtain the starch glass transition temperature and melting properties of PCL. The initial and final weights of the pans were registered to assess water loss during the first heating step.

3.2.3.6. X-ray diffraction (XRD)

A diffractometer (XRD, Bruker AXS/D8 Advance) was used to obtain X-ray diffraction patterns. All samples (equilibrated for 1 and 5 weeks) were analyzed at 25 °C and 53% RH, between 2θ: 5° and 30° using Kα Cu radiation (λ: 1.542 Å), 40 kV and 40 mA with a step size of 0.05°. For this analysis, 4 cm^2 samples were used.

3.2.3.7. Scanning Electron Microscopy (SEM)

The microstructural analysis of cross-sections of films was carried out by using a Scanning Electron Microscope (JEOL JSM-5410, Japan). Film samples were maintained in desiccators with P_2O_5 for two weeks at 25 °C and observations were carried out in at least two samples per formulation. Pieces of about 0.5 cm^2 were immersed in liquid nitrogen and then cryo-fractured to observe the revealed surface. They were mounted on copper stubs and gold-coated for observation, using an accelerating voltage of 10 kV.

3.2.3.8. Atomic Force Microscopy (AFM)

Samples conditioned for 5 weeks at 25 °C and 53% RH using P_2O_5 were observed by AFM to analyze their surface morphology using an Atomic Force Microscope (Multimode 8, Bruker AXS, Santa Barbara, USA) with a NanoScope® V controller electronics. Measurements were taken from several areas of film surface (20 μm^2) using PeakForce QNM® mode (Quantitative Nanomechanical Mapping). The DMT Modulus mode derived from PeakForce QNM was plotted in the 2-D plane of the sample. Three samples were analyzed for each formulation.

3.2.3.9. Statistical analysis

Statgraphics Plus for Windows 5.1 (Manugistics Corp., Rockville, MD) was used to carry out statistical analyses of data through analysis of variance (ANOVA). Fisher's least significant difference (LSD) was used at the 95% confidence level.

3.3. RESULTS

3.3.1. Physical properties of films

3.3.1.1. Thickness, extensibility, water solubility and moisture content.

Table 3.1 shows the thickness and the extensibility (film surface per mass unit during the compression moulding) of the starch-PCL based films equilibrated at 25 °C and 53% RH for 1 week. A significant decrease in thickness and an increase in extensibility ($p < 0.05$) were observed when the content of PCL rose in the films, indicating greater flowability. Films without PCL were the thickest as a result of the greater resistance to flow of the material during compression.

Table 3.1.-Mass fraction (Xi, g compound/g wet formulation) of the different components (starch: S, PCL, glycerol: Gly and water) in wet formulation before melt blending and mean values and standard deviation of thickness, extensibility, solubility in water (g solubilised film/g initial dried film) and moisture content (g water/g dried film) of the starch:PCL films conditioned at 53% RH and 25 ºC for 1 week (initial) and 5 weeks (final).

Films	X_s	X_{PCL}	X_{Gly}	X_{water}	Thickness (µm)	Extensibility (cm^2/g)	Solubility in water		Xw	
							Initial	Final	Initial	Final
S	0.556	0.000	0.167	0.277	268 ± 28^{a}	24 ± 2^{a}	0.19 ± 0.07^{a1}	0.24 ± 0.05^{a1}	0.0613 ± 0.0006^{a1}	0.079 ± 0.004^{a2}
S80	0.488	0.122	0.146	0.244	221 ± 9^{b}	32 ± 2^{b}	0.132 ± 0.003^{b1}	0.137 ± 0.013^{b1}	0.0535 ± 0.0008^{b1}	0.061 ± 0.002^{b2}
S60	0.405	0.270	0.122	0.203	168 ± 13^{cd}	45 ± 6^{c}	0.13 ± 0.03^{b1}	0.13 ± 0.02^{b1}	0.0409 ± 0.0006^{c1}	0.046 ± 0.002^{c2}
S40	0.303	0.454	0.091	0.152	173 ± 13^{c}	45 ± 3^{c}	0.091 ± 0.011^{b1}	0.101 ± 0.009^{b1}	0.027 ± 0.002^{d1}	0.031 ± 0.004^{d1}
S20	0.172	0.690	0.052	0.086	185 ± 19^{c}	47 ± 8^{c}	0.014 ± 0.003^{c1}	0.017 ± 0.004^{c1}	0.0122 ± 0.0010^{e1}	0.0136 ± 0.0013^{e1}
PCL	0.000	1.000	0.000	0.000	149 ± 17^{d}	57 ± 9^{d}	0.00022 ± 0.00011^{c1}	0.0004 ± 0.0002^{c1}	0.003 ± 0.002^{f1}	0.0021 ± 0.0005^{f1}

Different superscript letters within the same column indicate significant differences between formulations ($p < 0.05$). Different superscript numbers within the same row indicate significant differences due to storage time ($p < 0.05$).

These results show the promotion of the flowability of polymer blends by the addition of PCL, as observed by Rosa *et al*. (2004), thus favouring their thermo-processing.

Table 3.1 also shows the solubility in water and the moisture content of the films. The moisture content showed significant changes ($p < 0.05$) with the storage time for formulations S, S80 and S60. As expected, the higher the starch content in the films, the greater the water sorption capacity (Averous *et al*., 2000; López *et al*., 2013). The hydrophobic character of PCL reduces the water adsorption capacity of the blend films and their equilibrium moisture content. Likewise, when the ratio of PCL in the films increased, their water solubility decreased, as shown in Table 3.1, without significant ($p < 0.05$) changes during storage. The results confirm the expected changes in the water affinity of the films when the ratio of PCL increased, which supposes an advantage with respect to starch materials.

3.3.1.2. Barrier properties

Table 3.2 shows the values of Water Vapour Permeability (WVP) at a RH gradient of 53-100% and at 25 ºC, after 1 and 5 storage weeks. The WVP values fell significantly ($p < 0.05$) when the PCL ratio increased in the films, without significant changes during storage. Nevertheless, the obtained values for starch-PCL blends were not in the established range of WVTR for food systems' requirements (Schmid *et al*. 2012) and additional reduction would be necessary. In this sense the bilayer films composed by a PCL layer and starch-PCL blend layer could be and alternative since perpendicular resistance of both layers to water vapour transfer would be much more effective. The WVP values of the PCL layer are in the range of the WVTR requirements for meat and MAP products (Schmid *et al*. 2012).

Table 3.2.-Mean values and standard deviation of barrier properties of the starch:PCL films conditioned at 53% RH and 25 ºC for 1 week (initial time) and 5 weeks (final time).

Films	WVP (g-mm/KPa·h·m^2)		$O_2P \cdot 10^{15}$ (cm^3·m^{-1}·s^{-1}·Pa^{-1})	
	Initial	Final	Initial	Final
S	18.1 ± 1.4^{a1}	16 ± 2^{a1}	< D.L.	< D.L.
S80	11 ± 2^{b1}	9.3 ± 0.6^{b1}	6.5 ± 0.3^{a1}	6 ± 3^{a1}
S60	8 ± 2^{c1}	5.4 ± 0.4^{c1}	33 ± 12^{b1}	26 ± 3^{b1}
S40	3.7 ± 0.4^{d1}	3.3 ± 0.3^{d1}	>D.L.	>D.L.
S20	2.7 ± 0.2^{d1}	2.3 ± 0.3^{d1}	>D.L.	>D.L.
PCL	0.120 ± 0.004^{e1}	0.117 ± 0.011^{e1}	>D.L.	>D.L.

D.L.: 0.1-200 cm^3/(m^2.day). Different superscript letters within the same column indicate significant differences between formulations ($p < 0.05$). Different superscript numbers within the same row indicate significant differences due to storage time ($p < 0.05$).

Table 3.2 also shows the Oxygen Permeability (O_2P) values of the films. The control film (S) had such low oxygen permeability that this value could not be measured with the equipment used. The very low O_2P of starch films has been reported by other authors (López *et al.*, 2013). However, PCL films and those containing a high ratio of this component (S40, S20) exhibited such high O_2P values that they were beyond the measurement range of the equipment. Samples S80 and S60 showed a significant increase ($p < 0.05$) in the O_2P values with respect to the pure starch films as a result of the PCL addition. No significant changes in the O_2P of the films occurred during the storage. The hydrophobic character of PCL promoted the increase in the oxygen permeability due to their chemical affinity which favours the gas solubility in the polymer matrix (Park *et al.*, 1996). So, the incorporation of PCL into starch matrices modifies their barrier properties, improving the water vapour barrier properties, but reducing the barrier to oxygen.

Oxygen barrier properties of net starch films cover the whole range of food packaging requirements, but when the PCL ratio increased in the blend films, different food products fall outside of their O_2TR range (Schmid *et al*. 2012). As

commented on above, and according with the barrier properties of each film, the formation of PCL-starch bilayer films would be an adequate option to obtain materials appropriate for food packaging, particularly meat and MAP products or nuts and snacks.

3.3.1.3. Tensile properties

Figure 3.1 shows the typical stress-strain curves of the starch:PCL films stored at 53% RH for 1 week. The pure PCL films showed a high plastic deformation after the yield point as shown in Figure 3.1a.

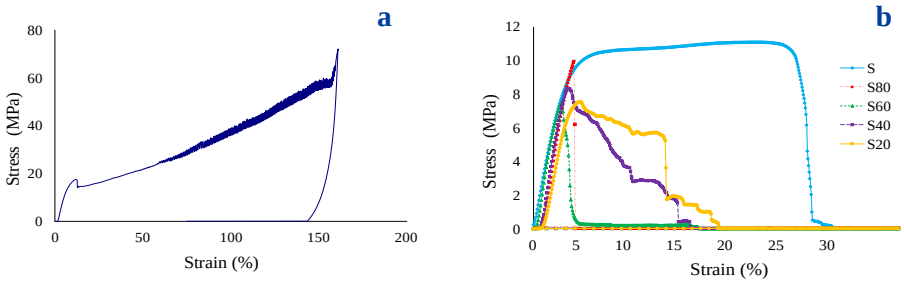

Figure 3.1.-Typical stress-strain curves of the starch:PCL films stored at 53% RH for 1 week: a) PCL film; b) Starch (S) and blend films: S80, S60, S40 and S20.

Values of the strength and deformation in the yield point were 18.17 ± 1.06 MPa and 13 ± 4%, respectively. PCL is a ductile polymer which can be deformed until 1100% in agreement with Ishiaku *et al*. (2002). Films containing low ratio of starch (S20 and S40 samples) exhibited an initial rupture followed by subsequent partial breaks (Figure 3.1b), while blends with less PCL content exhibited only one clear break point (Figure 3.1b). This indicates that PCL tend to be the continuous phase as its ratio increase in the matrix, but the interruptions provoked by the starch

phase promote the film failure, thus losing the ductile properties of PCL, as reported by Averous *et al*. (2000).

Table 3.3 shows the tensile properties of the films conditioned at 53% RH and 25 ºC for 1 and 5 weeks of storage. Significant changes ($p < 0.05$) were observed in all tensile parameters when PCL was added to starch films. Despite the fact that the elastic modulus of pure PCL and pure S films did not show significant differences, their blends exhibited higher values. Nevertheless, the resistance to break (TS) and extensibility (E) of the films significantly ($p < 0.05$) decreased when PCL was incorporated. No significant differences in any tensile parameter were observed for the different blends. The obtained results were similar to those reported by Corradini *et al*. (2004) for blends of PCL and zein, and by Ishiaku *et al*. (2002) for PCL and sago starch blends. In both cases, the incompatibility of polymers was observed.

The effect of storage time on the mechanical properties of the blend films reveals different behaviour depending on the PCL ratio. Films with higher ratios of starch (up to 60%) exhibit a marked increase (nearly two times) in the elastic modulus over the storage time, whereas no significant changes were observed for films whose starch content was under 40%. This suggests that retrogradation phenomena occurred in the continuous starch matrix, giving rise to recrystallization and chain aggregation which makes the cohesion forces in the polymer network more intense (Mali *et al.,* 2006). This effect was not observed for films with the greatest proportions of PCL, where EM did not change during storage time. Blend films did not show changes in the resistance at break (TS values), although this increased in pure starch films in line with the retrogradation effects. Deformation at break decreased in all the films over storage time, except for the one that contained the greatest ratio of PCL. This reduction is especially marked in pure starch films.

The incorporation of PCL into starch matrices seems to reduce the changes in the mechanical properties of starch films throughout time, but the polymer incompatibility makes its efficiency limited due to the phase separation of polymers and the increase in the interface area where adhesion forces are not intense enough.

Table 3.3. -Mean values and standard deviation of mechanical properties of the starch:PCL films conditioned at 53% RH and 25 ºC for 1 week (initial) and 5 weeks (final).

Films	EM (MPa)		TS (MPa)		E (%)	
	Initial	Final	Initial	Final	Initial	Final
S	278 ± 75^{a1}	587 ± 65^{b2}	10 ± 2^{a1}	15.7 ± 1.2^{a2}	28 ± 10^{a1}	4.1 ± 0.4^{a2}
S80	405 ± 82^{bc1}	719 ± 72^{c2}	9 ± 3^{b1}	9.9 ± 0.9^{b1}	3.5 ± 1.2^{b1}	1.7 ± 0.5^{c2}
S60	390 ± 56^{bc1}	662 ± 67^{c2}	7.2 ± 0.9^{b1}	7.1 ± 0.6^{d1}	2.7 ± 0.6^{b1}	2.0 ± 0.5^{c2}
S40	430 ± 47^{c1}	391 ± 105^{a1}	7.5 ± 0.7^{b1}	6.2 ± 1.2^{d1}	2.7 ± 0.5^{b1}	1.9 ± 0.3^{c2}
S20	372 ± 22^{b1}	337 ± 71^{a1}	7.5 ± 0.8^{b1}	8.2 ± 1.2^{c1}	3.2 ± 0.5^{b1}	3.2 ± 1.1^{b1}
PCL	304 ± 11^{a1}	314 ± 51^{a1}	---	---	---	---

Different superscript letters within the same column indicate significant differences between formulations ($p < 0.05$). Different superscript numbers within the same row indicate significant differences due to storage time ($p < 0.05$).

3.3.1.4. Thermal properties

Table 3.4 shows the thermal properties of the studied films obtained from DSC analysis. The T_g value of starch (obtained from the second heating scan) was about 126 ºC, similar to that reported by other authors (Ortega-Toro *et al*., 2014). In S20 formulation, the T_g value of starch was not observed because of the very weak signal associated with the low starch ratio in the sample.

Table 3.4.-Mean values and standard deviation of thermal properties of the starch:PCL films.

Films	Glass transition		Fusion on the first scan				Crystallization		Fusion on the second scan	
			Initial time		Final time					
	T_g midpoint	ΔCp	T_m peak	ΔH_m (J/g PCL)	T_m peak	ΔH_m (J/g PCL)	T_c peak	ΔH_c (J/g PCL)	T_m peak	ΔH_m (J/g PCL)
S	126.0 ± 0.3^{a}	0.112 ± 0.002^{a}	---	---	---	---	---	---	---	---
S80	114.31 ± 0.05^{b}	0.128 ±0.002^{b}	62.9 ± 0.6^{a1}	72.3 ± 1.3^{a1}	63.29 ± 0.11^{a1}	82.3 ± 0.7^{a2}	12.5 ± 0.6^{a}	52.3 ± 0.3^{a}	55.4 ± 0.3^{a}	51.2 ± 1.3^{a}
S60	114.8 ± 0.2^{b}	0.126 ± 0.004^{b}	63.0 ± 0.2^{a1}	72.5 ± 0.6^{a1}	63.3 ± 0.2^{a1}	81.9 ± 1.0^{a2}	12.33 ± 0.07^{a}	52.2 ± 0.8^{a}	55.13 ± 0.04^{a}	51.0 ± 1.3^{a}
S40	114.509 ± 0.09^{b}	0.123 ± 0.005^{b}	63.10 ± 0.15^{a1}	72.7 ± 0.8^{a1}	63.02 ± 0.15^{a1}	82.8 ± 0.4^{a2}	12.2 ± 0.6^{a}	51.1 ± 0.8^{a}	55.1 ± 0.2^{a}	51.1 ± 1.1^{a}
S20	---	---	63.5 ± 0.5^{a1}	73.1 ± 0.5^{a1}	63.6 ± 0.4^{a1}	82.4 ± 0.4^{a2}	12.3 ± 0.4^{a}	51.6 ± 0.3^{a}	55.5 ± 0.4^{a}	51.1 ± 1.0^{a}
PCL	---	---	63.5 ± 0.6^{a1}	72.8 ± 1.4^{a1}	63.7 ± 0.6^{a1}	82.2 ± 1.5^{a2}	12.6 ± 0.6^{a}	52.4 ± 0.3^{a}	55.4 ± 0.4^{a}	51.0 ± 1.2^{a}

Different superscript letters within the same column indicate significant differences between formulations ($p < 0.05$). Different superscript numbers within the same row indicate significant differences due to storage time ($p < 0.05$).

The T_g value of PCL was not detected due to the operation temperature range of the equipment, although its value (-60 °C) was reported by other authors (Averous *et al*., 2000). When PCL was incorporated, the T_g of starch decreased significantly (ΔT_g~12ºC), regardless of the ratio of PCL. This suggests a partial miscibility of PCL in the starch phase. The decrease in T_g, as well as the higher values of ΔCp, is coherent with the lower molecular weight of PCL, which reduced the mean molecular weight of the starch-rich phase. This favours the plasticization of the starch phase, thus increasing its flowability during thermo-processing, as previously commented on, while favouring its thermo-processing.

The melting behaviour of PCL, characterized in the first heating scan, was similar for every film, regardless of the PCL ratio, even for 100% PCL films. The T_m value for films stored for 1 week was 63°C and the ΔH_m was 72 J/g of PCL, similar to those reported by other authors (Averous *et al*., 2000; Matzinos, Tserki *et al.*, 2002; Kweo *et al.*, 2003). For samples stored for 5 weeks, although the same T_m values were obtained, ΔH_m slightly increased (about 82 J/g of PCL) which indicates that the degree of crystallinity of PCL in the films increased throughout storage in both pure and blend films. No effect of starch on the PCL crystallinity was observed in the films.

The crystallization behaviour of PCL during the cooling step was also constant for all the samples, regardless of the film composition. The T_c value (peak) was about 12 °C and the ΔH_c was close to 52 J/g of PCL. As compared with melting constants, the values of T_c and ΔH_c were lower, revealing the supercooling effect during the cooling step after the previous melting. As expected, the ΔH_m values of the second heating step reproduced those obtained for ΔH_c, since all crystallized PCL melts during heating.

The results reveal that, for the obtained films, starch did not affect the melting behaviour of PCL, which, in turn, suggests a very low, or null, miscibility of starch

in the PCL-rich phase. Likewise, the crystallization of the PCL progress during storage time and supercooling occurred in fast cooling processes, as given by the DSC analysis. This is in contrast to that described by other authors (Averous *et al*., 2000; Matzinos *et al*., 2002; Wang *et al*., 2005) who report a small inhibition of PCL crystallization in PCL-starch blend films obtained by different techniques.

3.3.1.5. Optical properties

Table 3.5 shows the gloss at an 85° incidence angle and the internal transmittance at 650 nm of the films conditioned for 1 and 5 weeks. Films of pure components (PCL and S) presented the highest gloss values, while blend films were less glossy with no marked differences. The decrease in the gloss of blends can be attributed to changes in the surface roughness caused by the immiscibility of the polymers, which gives rise to the formation of a heterogeneous matrix with greater surface roughness (Jiménez *et al*., 2012). No formulation exhibited significant changes in the film gloss over storage time.

Table 3.5.-Mean values and standard deviation of optical properties of the starch:PCL films coditioned at 53% relative humidity and 25 ºC for 1 week (initial) and 5 weeks (final).

Films	Gloss (85°)		Ti (650nm)	
	Initial	Final	Initial	Final
S	40 ± 5^{b1}	37.2 ± 1.5^{bc1}	85.1 ± 0.3^{a1}	84.2 ± 0.2^{a1}
S80	29 ± 9^{c1}	31 ± 9^{ab1}	82.4 ± 0.6^{b1}	82.5 ± 1.1^{ab1}
S60	38 ± 6^{bc1}	37 ± 4^{abc1}	81.2 ± 1.3^{bc1}	81.6 ± 0.7^{bc1}
S40	29 ± 10^{c1}	30 ± 5^{a1}	79.4 ± 0.9^{cd1}	79.93 ± 0.12^{cd1}
S20	38 ± 10^{bc1}	42 ± 9^{c1}	78.6 ± 0.4^{d1}	78.7 ± 1.1^{d1}
PCL	59 ± 16^{a1}	57 ± 9^{d1}	78 ± 2^{d1}	78 ± 2^{d1}

Different superscript letters within the same column indicate significant differences between formulations ($p < 0.05$). Different superscript numbers within the same row indicate significant differences due to storage time ($p < 0.05$).

The internal transmittance values decreased when the ratio of PCL in the matrix rose, in line with the greater opacity of this polymer. The PCL formulation had the lowest transmittance and in no case did any significant changes in internal transmittance occur during the storage time.

3.3.2. Nano and microstructure of the films

Figure 3.2 shows the micrographs of the cross sections of films obtained by SEM.

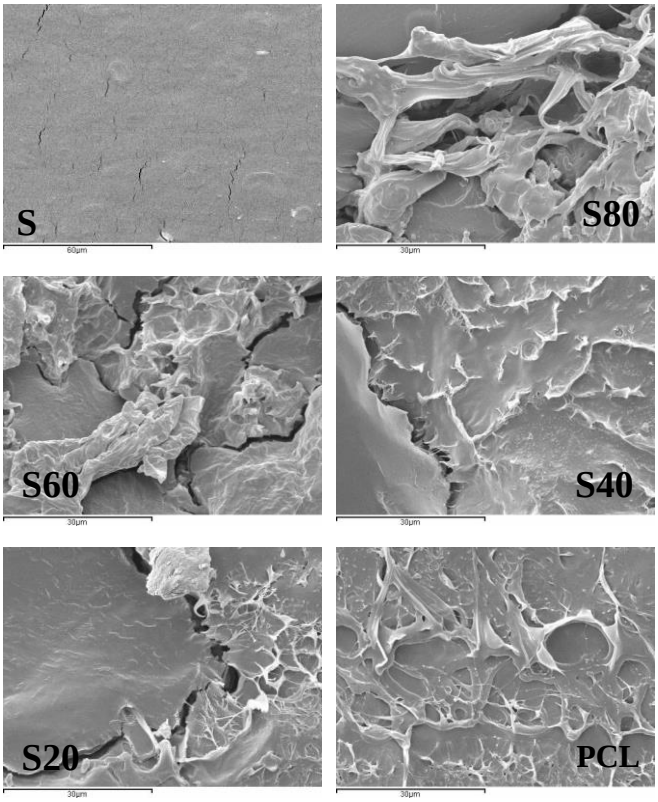

Figure 3.2.-SEM micrographs of the starch:PCL films stored at 53% RH and 25 ºC for 1 week.

The heterogeneity of the blends was observed, evidencing the lack of miscibility of both polymers while the S and PCL films presented a homogeneous structure. No granules of native starch were observed in any case, which indicates that starch was effectively melted in the process used, giving rise to thermoplastic starch. Random-order conglomerates of starch and PCL were observed in the blend films. Likewise, blends exhibited poor interfacial adhesion, due to the different polymer polarities (Rosa *et al.*, 2003; Corradini *et al*., 2004). The PCL phase can be clearly distinguished due to its ductile behaviour, which defines a particular cryofracture pattern, promoting stretched filamentous formations. The spontaneous detachment of both phases caused a loss in cohesion of the blend matrix and the lack of stretchability of the blend films (Ishiaku *et al*., 2002; Corradini *et al*., 2004).

Figure 3.3 shows the DMT modulus maps of the films obtained from the PeakForce QNM AFM analyses.

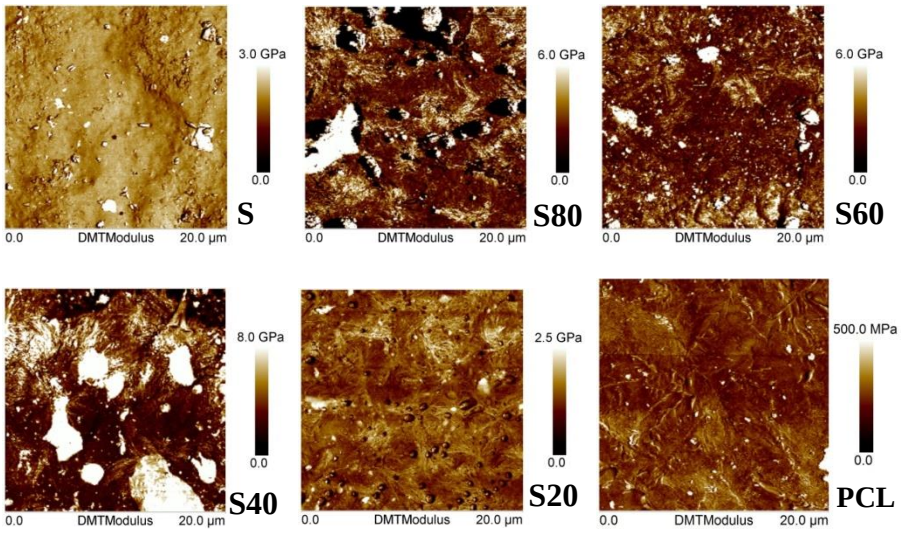

Figure 3.3.-AFM images of the starch:PCL films stored at 53% RH and 25 ºC for 5 weeks.

The polymer matrices with pure components (S or PCL) show quite a homogeneous structure in terms of the surface mechanical response in line with the homogeneity of the material. The S surface was harder than the PCL, in agreement with the higher value of the elastic modulus of starch films after 5 storage weeks. Blend films had a more heterogeneous surface modulus, exhibiting light and dark areas, according to the distribution of harder (starch phase) and softer (PCL) regions at surface level. The film with formulation S20 shows the structure which bears the most similarity to pure PCL films, due to the small ratio of starch which interrupts the continuity of the PCL matrix.

The X-ray diffraction patterns of the films stored for 1 and 5 weeks are shown in Figure 3.4. The diffraction spectra of S films showed peaks at 13.5° 20º and 24º 2θ angle, characteristic of the helical amylose-lipid complexes in the V-type crystallization form (Matzinos *et al*., 2002; Gelders *et al.*,2004). The intensity of the peaks increased in films stored for 5 weeks, which indicates the progress of amylose crystallization during storage.

PCL films show the characteristics peaks of the crystalline polymer at 21º, 22º and 24º 2θ angle. No notable changes in diffraction pattern were observed for these films during storage. For the blend films with the highest ratio of PCL, S20 and S40, the diffraction spectra were similar to those of the PCL film, which indicates that starch crystalline forms were not present after 1 or 5 storage weeks. Nevertheless, samples with higher ratios of starch, S60 and, especially S80, showed the starch typical peak at 13.5º and an overlapping of the characteristic peaks of PCL and some of the starch in the 2θ angle range of 20-24º. In these films, the relative intensity of the starch peaks is lower than in pure starch films. This suggests that starch crystallization is partially inhibited by blending with PCL, mainly when the PCL ratio increased in the blend.

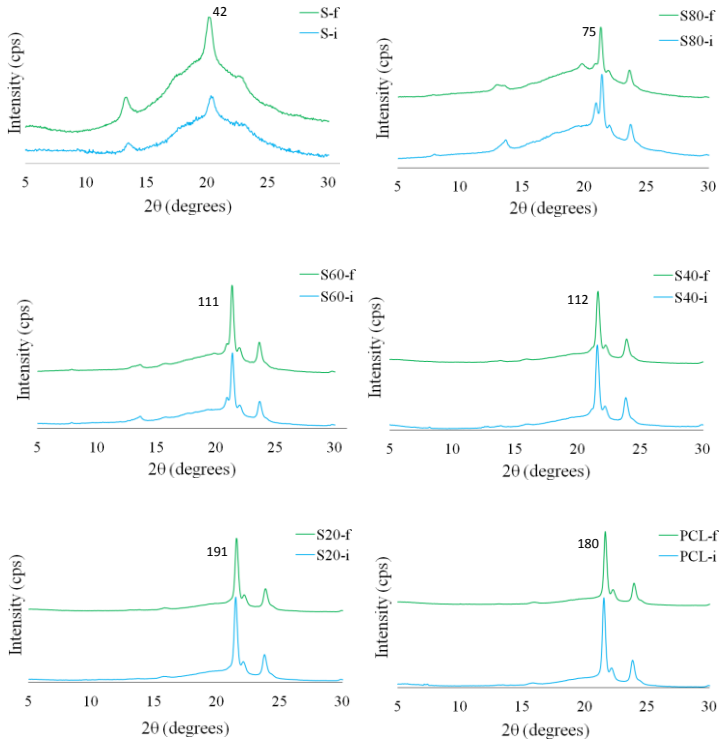

Figure 3.4.-XRD patterns of the starch:PCL films conditioned at 53% RH and 25 ºC for 1(i: initial time) and 5 (f: final time) weeks.

3.4. CONCLUSIONS

Corn starch and PCL blend films, containing 30% glycerol with respect to starch, could be obtained by compression moulding at 160ºC and 130 bars. The films showed phase separation of the polymers, exhibiting a heterogeneous blend matrix where starch-rich regions and PCL-rich regions could be observed. Nevertheless, a small degree of PCL miscibility in the starch phase was detected through the shift in the glass transition temperature of the starch phase, which leads to the partial

inhibition of amylose retrogradation during film formation and storage. The lack of interfacial adhesion of the PCL and starch phases promoted the films' fragility and reduced their elongation, although small PCL ratios increased the elastic modulus of the films, indicating its adequate properties as reinforcing filler in starch matrices. Water barrier properties of starch films were improved as the PCL increased in the blend but worsening of the oxygen barrier properties was obtained. Bilayer films with both PCL and starch blend layers could meet the requirements for packaging of some foods such as meat and MAP products. Nevertheless, the overall migration in different food simulants must be assessed, according to migration limits established by regulation for plastic materials in contact with food.

3.5. REFERENCES

American Society for Testing and Materials, ASTM E96-95. Standard test methods for water vapor transmission of materials. In annual book of ASTM. Philadelphia, 1995.

American Society for Testing and Materials, ASTM D523. Standard test method for specular gloss. In annual book of ASTM. Philadelphia; 1999.

American Society for Testing and Materials, ASTM D882. Standard test method for tensile properties of thin plastic sheeting. In annual book of ASTM. Philadelphia; 2001.

Averous, L., & Boquillon, N. (2004). Biocomposites based on plasticized starch: thermal and mechanical behaviours. Carbohydrate Polymers, 56(2), 111–122.

Averous, L., Moro, L., Dole P., & Fringant, C. (2000). Properties of thermoplastic blends: starch–polycaprolactone. Polymer, 41(11), 4157–4167.

Cao, X., Chang, P. R., & Huneault, M. A. (2008). Preparation and properties of plasticized starch modified with poly (ε-caprolactone) based waterborne polyurethane. Carbohydrate Polymers, 71(1), 119-125.

Corradini, E., Mattoso, L. H. C., Guedes, C. G. F., & Rosa, D. S. (2004). Mechanical, thermal and morphological properties of poly(ε-caprolactone)/zein blends. Polymers for Advanced Technologies, 15(6), 340–345.

Di Franco, C. R., Cyras V. P., Busalmen, J. P., Ruseckaite, R. A., & Vázquez, A. (2004). Degradation of polycaprolactone/starch blends and composites with sisal fibre. Polymer Degradation and Stability, 86(1), 95-103.

Duquesne E., Rutot D., Degee P., & Dubois P. (2001). Synthesis and characterization of compatibilized poly(ε-caprolactone)/granular starch composites. Macromolecular Symposia, 175(1), 33–43.

Flieger, M., Kantorová, M., Prell, A., Řezanka, T., & Votruba, J. (2003). Biodegradable Plastics from Renewable Sources. Folia Microbiologica, 48(1), 27–44.

Gelders, G. G., Vanderstukken, T. C., Goesaert, H., & Delcour, J. A. (2004). Amylose-lipid complexation: a new fractionation method. Carbohydrate Polymers, 56(4), 447-458.

Ghanbarzadeh, B,. Almasi, H., & Entezami, A. A. (2011). Improving the barrier and mechanical properties of corn starch-based edible films: Effect of citric acid and carboxymethyl cellulose. Industrial Crops and Products, 33(1), 229-235.

Hubackova, J., Dvorackova, M., Svoboda, P., Mokrejs, P., Kupec, J., Pozarova, I., Alexy, P., Bugaj, P., Machovsky, M., & Koutny, M. (2013). Influence of various starch types on PCL/starch blends anaerobic biodegradation. Polymer Testing, 32(6), 1011–1019.

Hutchings, J. B. (1999). Food color and appearance. (2nd ed.). Gaithersburg, Maryland, USA: Aspen Publishers, Inc.

Ishiaku, U. S., Pang, K. W., Lee, W. S., & Mohd Ishak, Z. A. (2002). Mechanical properties and enzymic degradation of thermoplastic and granular sago starch filled poly (ε-caprolactone). European Polymer Journal, 38(2), 393-401.

Jiménez, A., Fabra, M. J., Talens, P., & Chiralt, A. (2012). Effect of re-crystallization on tensile, optical and water vapour barrier properties of corn starch films containing fatty acids. Food Hydrocolloids, 26(1), 302-310.

Kweon, D. K., Kawasaki, N., Nakayama, A., & Aiba, S. (2003). Preparation and characterization of starch/polycaprolactone blend. Journal of Applied Polymer Science, 92(3), 1716–1723.

López, O. V., Zaritzky, N. E., Grossmann, M. V. E., & García, M. A. (2013). Acetylated and native corn starch blend films produced by blown extrusión. Journal of Food Engineering, 116(2), 286-297.

Lourdin, D., Valle, G. D., & Colonna, P. (1995). Influence of amylose content on starch films and foams. Carbohydrate Polymers, 27(4), 261-270.

Mali, S., Grossmann, M. V. E., García, M. A., Martino, M. N., & Zaritzky, N. E. (2006). Effects of controlled storage on thermal, mechanical and barrier properties of plasticized films from different starch sources. Journal of Food Engineering, 75(4), 453-460.

Matzinos, P., Tserki, V., Kontoyiannis, A., & Panayiotou, C. (2002). Processing and characterization of starch/polycaprolactone products. Polymer Degradation and Stability, 77(1), 17–24.

McHugh, T. H., Avena-Bustillos, R., & Krochta, J. M. (1993). Hydrophobic edible films: Modified procedure for water vapour permeability and explanation of thickness effects. Journal of Food Science, 58(4), 899–903.

Ortega-Toro, R., Jiménez, A., Talens, P., & Chiralt, A. (2014). Properties of starch-hydroxypropyl methylcellulose based films obtained by compression molding. Influence of citric acid as cross-linking agent**.** Carbohydrate Polymers, 109, 155–165.

Park, J. W., Testin, R. F., Vergano, P. J., Park, H. J., & Weller, C. L. (1996). Fatty acid distriburion and its effect on oxygen permeability in laminated edible films. Journal of Food Science, 61(2), 401-406.

Rosa, D. S., Guedes, C. G. F., Pedroso, A. G., & Calil, M. R. (2004). The influence of starch gelatinization on the rheological, thermal, and morphological properties of poly(ε-caprolactone) with corn starch blends. Materials Science and Engineering C, 24(5), 663–670.

Rosa, D. S., Rodrigues T. C., Guedes C. G. F., & Calil, M. R. (2003). Effect of thermal aging on the biodegradation of PCL, PHB-V, and their blends with starch in soil compost. Journal of Applied Polymer Science, 89(13), 3539-3546.

Sawada, H. (1994). In Y. Doi and K. Fukuda (Eds.), Biodegradable Plastics and Polymers. Amsterdam: Elsevier Science.

Schmid, M., Dallmann, K., Bugnicourt, E., Cordoni, D., Wild, F., Lazzeri, A., & Noller, K. (2012). Properties of whey-protein-coated films and laminates as novel recyclable food packaging materials with excellent barrier properties. International Journal of Polymer Science, 8, 1-7.

Takala, P. N., Salmieri, S., Boumail, A., Khan, R. A., Vu, K. D., Chauve, G., Bouchard, J., & Lacroix, M. (2013). Antimicrobial effect and physicochemical properties of bioactive trilayer polycaprolactone/methylcellulose-based films on the growth of foodborne pathogens and total microbiota in fresh broccoli. Journal of Food Engineering, 116(3), 648–655.

Vieira, M., Altenhofen, M., Oliveira, L., & Masumi, M. (2011). Natural-based plasticizers and biopolymer films: a review. European Polymer Journal, 47, 254-263.

Wang, Y., Rodriguez-Perez, M. A., Reis, R. L., & Mano, J. F. (2005). Thermal and thermomechanical behaviour of polycaprolactone and starch/polycaprolactone blends for biomedical applications. Macromolecular Materials and Engineering, 290(8), 792–801.

Woodruff, M. A., & Hutmacher, D. W. 2010. The return of a forgotten polymer-Polycaprolactone in the 21st century. Progress in Polymer Science, 35(10), 1217–1256.

Yang, S-R. & Wu, C. H. (1999). Degradable plastic films for agricultural applications in Taiwan Macromolecular Symposia, 144, 101-112.

CHAPTER 4

INFLUENCE OF CITRIC ACID ON THE PROPERTIES AND STABILITY OF STARCH-POLYCAPROLACTONE BASED FILMS

Rodrigo Ortega-Toro, Sofía Collazo-Bigliardi, Pau Talens, & Amparo Chiralt

Journal of Applied Polymer Science, DOI: 10.1002/app.42220

The influence of citric acid on structural and physicochemical properties of blend films based on corn starch and polycaprolactone (PCL) was studied. Films were obtained by melt blending of starch and PCL and compression moulding. Phase separation of polymers observed by SEM and AFM was reduced by citric acid incorporation. Citric acid affected both starch and PCL crystallization as deduced from the X-ray diffraction patterns and values of melting enthalpy. Glass transition of starch was reduced by PCL incorporation, while this occurred to a greater extent in films containing CA. Obtained results point to enhanced interactions between PCL and starch chains in films with citric acid, although this only quantitatively benefits the film properties at a low PCL ratio. Compounding starch with small amounts of PCL, using glycerol and citric acid, can supply films with better functional properties than net starch films.

VNIVERSITAT POLITECNICA
VALENCIA
EX TECHNICA PROGRESSIO

4.1. INTRODUCTION

Packaging films, made of synthetic polymers, cause serious ecological problems due to their non-biodegradability. Increased social awareness about environmental protection has made it necessary to intensify research for the purposes of developing biodegradable packaging materials (Flieger *et al*., 2003). These materials must be competitive in price and should have similar properties to the petroleum-derived plastics (García *et al*., 2004). In the last few years there has been a significant increase in the number of studies about biodegradable packaging materials from economically viable sources. Of these materials, starch is remarkable for its low cost, renewability and processability by means of traditional thermoplastic techniques (Yoon *et al.*, 2006; Ghanbarzadeh *et al*., 2011)

Starch represents more than 60% of the cereal grains produced worldwide and it is relatively easy to extract (Lourdin *et al*., 1995). Of the so-called bioplastics, starch is of great importance because of its low cost, availability and technical characteristics. Starch-based films are continuous, homogeneous, odourless and colourless while exhibiting very low oxygen permeability (Dole *et al*., 2004; Liu, 2005; Ortega-Toro *et al*., 2014a). However, they have some disadvantages such as high hydrophilicity (water sensitivity) and poor mechanical properties as compared to conventional synthetic polymers (Averous & Boquillon, 2004). Furthermore, depending on temperature and relative humidity (RH), the starch film structure undergoes changes during storage, e.g. in crystallinity and chain aggregations, which greatly affect the films' physical properties (Rindlav *et al*., 1997; Bergo *et al*., 2010). To improve and maintain their properties it is necessary to add plasticizers, fillers or cross-linking agents. The most common plasticizer used in starch-based films is glycerol. This polyol reduces the intermolecular attractive forces in the native starch and increases its flexibility or stretchability (Mali *et al*., 2005).

On the other hand, polycaprolactone (PCL) is one of the most commercially available biodegradable polymers. It is synthetic and thermoplastic, with interesting properties such as its low water solubility and permeability and high degree of extensibility (Flieger *et al*., 2003; Averous *et al*., 2000). Several authors have shown that blends of PCL and starch are readily biodegradable and thermoprocessable by conventional methods (Matzinos *et al*., 2002; Rosa *et al*., 2005; Calil *et al*., 2007; Campos *et al*., 2012). However, starch and PCL (chemical structures shown in Figure I.2 and I.5) are chemically incompatible and their blends show phase separation (Averous *et al*., 2000), which implies that the obtained materials are heterogeneous with insufficiently improved properties, as occurs with other starch blends with more hydrophobic polymers of different polarity (Annable *et al*., 1994; Mathew & Abraham, 2008). This is the main limit of the starch/PCL blends, represented by the lacking of adhesion between the polysaccharide and the synthetic polymer matrices owing to their different polarity giving consequently poor final properties. In fact, starch and hydrophobic polymers (as PCL) are immiscible and simple mixing produce blends with separate phase. To improve the compatibility and the adhesion between the phases of the two immiscible polymers, different strategies, such as the incorporation of compatibilizers to the starch blends, have been analysed. Avella *et al*. (2000) introduced a reactive functional group (pyromellitic anhydride) on a PCL phase to increase the polar nature of the matrix and so to improve the adhesion between the components of materials.

Citric acid (CA) can be an appropriate compatibilizer because it is a cheap organic acid widely used in the food industry with cross-linking capability through the reaction of its carboxyl groups (Ghanbarzadeh *et al*., 2010; Ortega-Toro *et al*., 2014b). The three carboxyl groups in CA molecules can interact with the hydroxyl groups of the starch molecules through the formation of esters, which contributes

to the decrease in the hydrophilic nature of the starch. According to other authors, esterification using polycarboxylic acids takes place with the polymer's hydroxyl groups at high temperatures (about 160 °C), through the formation of anhydride groups (Reddy & Yang, 2010). This reaction can contribute to improve the water vapour barrier properties of the starch matrix due to the reduction of available hydroxyl groups (Thiebaud *et al*., 1997) while decreasing the crystallization and retrogradation phenomena of the starch polymers (Shi *et al*., 2007). CA can also act as compatibilizer, plasticizer and depolymerization agent with different polymers depending on the processing conditions (Chabrat *et al*., 2012). Likewise, citric acid can act as a catalyst for e-CL polymerization and transesterification reactions in PCL (Labet & Thielemans, 2009). The incorporation of CA to starch-PCL blends could improve the polymers' compatibility due to the enhancement of the starch hydrophobicity through the process of esterification, thus giving rise to films with more adequate properties for food packaging: with less water and time sensitivity and better mechanical response. CA has been used as compatibilizer in starch/poly(butylene adipate-co-terephthalate) films obtained by one-step reactive extrusion, notably improving of the film properties (Olivato *et al*., 2012). Likewise, properties of starch/ poly(lactic acid) blend films were also improved by adding CA (Chabrat *et al*., 2012; Wang *et al*., 2007). No previous studies have been found about the effect of citric acid on starch-PCL blend films.

The aim of this work was to analyze the influence of citric acid addition on the structural, thermal and physical properties of starch-polycaprolactone blend films obtained by compression moulding, and their stability throughout the storage time.

4.2. MATERIALS AND METHODS

4.2.1. Materials

Corn starch was purchased from Roquette (Roquette Laisa Spain, Benifaió, Spain). Glycerol was obtained from Panreac Química, S.A. (Castellar del Vallès, Barcelona, Spain). Polycaprolactone (pellets ~3 mm, average Mn 80.000 Daltons, impurities <1.0% water) was provided by Fluka (Sigma–Aldrich Chemie, Steinheim, Germany). Citric acid was provided by Fisher (Scientific Afora, Valencia, Spain). Phosphorus pentoxide (P_2O_5), Magnesium nitrate-6-hydrate ($Mg(NO_3)_2$), sodium hydroxide (NaOH) and phenolphthalein were obtained from Panreac Química, S.A. (Castellar Vallés, Barcelona).

4.2.2. Film preparation

Eleven formulations based on starch and PCL, with and without CA, were prepared. Starch:PCL ratios (w/w) were 100:0, 90:10, 80:20, 70:30, 60:40 and 0:100 while a starch:CA ratio of 1:0.01 (w/w) was used. 30% (wt.) of glycerol with respect to the starch content was added as plasticizer. Native starch and glycerol were dispersed in distilled water (2 g of starch / g water) and, afterwards, PCL was added to the aqueous mixture. The blends were identified by the percentage of starch (S) and the presence of citric acid (CA): S90, S90-CA, S80, S80-CA, S70, S70-CA, S60, S60-CA. Films with 100% starch (S), with and without CA, and PCL (PCL) were also analyzed for comparisons.

Aqueous blends were progressively melt-blended using a two-roll mill (Model LRM-M-100, Labtech Engineering, Thailand) at 160 °C and 8 rpm for 30 min until a homogeneous paste sheet was obtained. The CA was added to the blends in the last 5 min of the homogenization. The paste sheet formed was conditioned at 25 °C

and 53% RH using $Mg(NO_3)_2$ oversaturated solutions for 48 h before compression moulding.

The films were obtained by compression moulding (Model LP20, Labtech Engineering, Thailand). Four grams of the paste were put onto steel sheets and preheated on the heating unit for 5 min. The films were performed at 160 °C for 2 min at 30 bars, followed by 6 min at 130 bars; thereafter, a cooling cycle (40ºC/min) was applied for 3 min. The films obtained were conditioned at 25 °C and 53% RH for 1 (initial time) and 5 (final time) weeks before their characterization.

4.2.3. Film characterization

4.2.3.1. Film thickness and extensibility

The film thickness was measured with a Palmer digital micrometer (Palmer–Comecta, Spain, +/- 0.001 mm) at six random positions around the film. The extensibility during the thermo-compression step was estimated by the relationship between the surface and the weight of films with known dimensions. This parameter was expressed in cm^2/g of the film.

4.2.3.2. Structural properties

The surface morphology of the samples, conditioned for 5 weeks at 25 °C and 53% relative humidity (RH), was analyzed using an Atomic Force Microscope (AFM) (Multimode 8, Bruker AXS, Santa Barbara, USA) with a NanoScope® V controller electronics. Measurements were taken using the PeakForce QNM® mode (Quantitative Nanomechanical Mapping). The statistical parameters: root-mean-

square roughness (Rq: root-mean-square average of height deviations taken from the mean data plane), and roughness factor (r: ratio between the three-dimensional surface and two-dimensional area projected onto the threshold plane), were calculated according to the method ASME B46.1 (1995) The DMT Modulus map, derived from PeakForce QNM, was obtained. Three replicates for each formulation were taken to obtain these parameters.

The microstructural analysis of the cross-sections of the films was carried out by using a Scanning Electron Microscope (SEM) (JEOL JSM-5410, Japan). The film samples were maintained in desiccators with P_2O_5 for 2 weeks at 25 °C and the observations were made in duplicate for each formulation. Pieces of about 0.5 cm^2 were cut from films and mounted on copper stubs perpendicularly to their surface. Samples were gold coated and observed, using an accelerating voltage of 10 kV.

A diffractometer (XRD, Bruker AXS/D8 Advance) was used to obtain the X-ray diffraction spectra. All samples (equilibrated for 1 and 5 weeks) were analyzed at 25 °C and 53% RH, between 2θ: 5° and 30° using Kα Cu radiation (λ: 1.542 Å), 40 kV and 40 mA with a step size of 0.05°. For this analysis, the samples were cut into 4 cm^2. The crystallinity degree (CD) of starch matrices was calculated as the ratio between the absorption peaks and the total diffractogram area, expressed as percentage, by using OriginPro 8.5 software. Moreover, basal spacing for starch crystallites was calculated applying the Bragg equation.

4.2.3.3. Thermal behaviour

A Differential Scanning Calorimeter DSC 1 Star^e System (Mettler-Toledo Inc., Switzerland) was used to analyze phase transitions (PCL crystallization and starch glass transition) of the films. Weighed amounts of samples were placed into aluminium pans, sealed and drilled to favour moisture loss during the heating step.

The thermograms were obtained using three scans. First, a scan from -80 °C to 160 °C at a rate of 50 °C/min was used to obtain the PCL melting properties, while the bonded water in the film was released. The initial and final weights of the pans were registered to assess water loss during the first heating step. Then, the temperature was lowered to -80 °C at a rate of 50 °C/min. In this cooling step, the PCL crystallization temperature (T_c) and enthalpy (ΔH_c) were obtained. Finally, samples were heated to 160 °C at a rate of 20 °C/min in order to analyze the starch glass transition and the melting properties of PCL.

4.2.3.4. Physicochemical properties

The film water content was determined in samples conditioned at 53% RH and 25ºC. Samples were dried for 24 h at 60 °C using a convection oven (J.P. Selecta, S.A. Barcelona, Spain). Afterwards, the samples were placed in a desiccator at 25 °C with P_2O_5 for 2 weeks. This was carried out in triplicate.

The film solubility in water was determined by holding the sample in bi-distilled water (film:water ratio of 1:10) for 48 h. Afterwards, these samples were transferred to a convection oven (J.P. Selecta, S.A., Barcelona, Spain) for 24 h at 60 °C to remove free water and then transferred to a desiccator with P_2O_5 at 25 ºC for 2 weeks to remove the residual water. Their initial and final weights were taken to calculate the amount of the film solubilized in water. These analyses were carried out in triplicate for each formulation. The bonded citric acid in the film was also determined in this test, by titration of the water solution. Free CA was assumed to dissolve in the aqueous phase and was determined by titration of an aliquot of the solution with NaOH (0.1 N), using phenolphthalein as indicator. Analyses were carried out in triplicate for each formulation.

A universal test machine (TA.XT plus model, Stable Micro Systems, Haslemere, England) was used to determine the elastic modulus (EM) and the tensile strength (TS), and the elongation (E) at break of the films, according to the ASTM D882 (2001) 2.5-cm-wide and 5-cm-long equilibrated samples were mounted in the film-extension grips of the testing machine and stretched at 50 mm min^{-1} until breaking. Ten replicates were performed for each formulation.

The ASTM E96-95 gravimetric method was used to determine the Water Vapour Permeability (WVP) of the films, considering the modification proposed by McHugh *et al*. (1993). Distilled water was placed in Payne permeability cups (3.5 cm diameter, Elcometer SPRL, Hermelle/s Argenteau, Belgium) to expose the film to 100% RH on one side. Each cup was placed in a cabinet equilibrated at 25 °C and 53% RH, with a fan placed on the top of the cup in order to reduce the resistance to water vapour transport, thus avoiding the stagnant layer effect in this exposed side of the film. The relative humidity of the cabinet (53%) was held constant using $Mg(NO_3)_2$ oversaturated solutions. The cups were weighed periodically (0.0001 g) and the water vapour transmission (WVTR) was determined from the slope obtained from the regression analysis of weight loss data versus time. From WVTR data, the vapour pressure on the film's inner surface (p_2) was obtained with eq. (4.1), proposed by McHugh *et al*. (1993) to correct the effect of the concentration gradients.

$$WVTR = \frac{PDL_n\left[\frac{P - p_2}{P - p_1}\right]}{RT\Delta z} \qquad (4.1)$$

where P, total pressure (atm); D, diffusivity of water through air at 25 °C (m^2 /s); R, gas law constant (82.057 x 10^{-3} m^3 atm $kmol^{-1}$ K^{-1}); T, absolute temperature (K); Δz, mean stagnant air gap height (m), considering the initial and final z value; p_1, water vapour pressure on the solution surface (atm); and p_2, corrected water vapour pressure on the film's inner surface (atm). Water vapour permeance was calculated using eq. (4.2) as a function of p2 and p3 (pressure on the film's outer surface in the cabinet).

$$permeance = \frac{WVTR}{p_2 - p_3} \tag{4.2}$$

The permeability was calculated by multiplying the permeance by film thickness. This analysis was carried out in triplicate.

The Oxygen Permeability (O_2P) of the films was determined using an OX-TRAN Model 2/21 ML (Mocon Lippke, Neuwied, Germany) according to the ASTM D3985–05 (2010). Three samples conditioned at 53% RH and 25 °C for each formulation were analysed. The transmission values were determined every 20 min until equilibrium was reached. The film area used in the tests was 50 cm^2. The film thickness was considered in all cases to obtain the O_2P values.

The transparency of the films was determined using the Kubelka-Munk theory for multiple scattering (Hutchings, 1999), as was the gloss, at 85° incidence angle, according to the ASTM D523 (1999) The surface reflectance spectrum was determined from 400 to 700 nm with a spectro-colorimeter CM- 3600d (Minolta Co., Tokyo, Japan) on both a white and a black background. As light passes through the film, it is partially absorbed and scattered, which is quantified by the

absorption (K) and the scattering (S) coefficients. Internal transmittance (Ti) of films was determined using eq. (4.3).

$$T_i = \sqrt{(a - R_0)^2 - b^2} \tag{4.3}$$

where R_0 is the reflectance of the film on an ideal black background. The parameters a and b were calculated by eqs. (4.4) and (4.5).

$$a = \frac{1}{2}(R + \frac{R_0 - R + R_g}{R_0 R_g}) \tag{4.4}$$

$$b = \sqrt{a^2 - 1} \tag{4.5}$$

where R is the reflectance of the sample layer backed by a known reflectance Rg. Three replicates were used for each formulation. Internal transmittance (Ti) at 650 nm was used to compare samples.

The gloss was determined using a flat surface gloss meter (Multi.Gloss 268, Minolta, Germany). Three films of each formulation were analyzed, taking three measurements in each sample film. All results are expressed as gloss units (GU), relative to a highly polished surface of black glass standard with a value near to 100 GU.

4.2.3.5. Statistical analysis

Statgraphics Plus for Windows 5.1 (Manugistics Corp., Rockville, MD) was used to carry out statistical analyses of data through analysis of variance (ANOVA). Fisher's least significant difference (LSD) was used at the 95% confidence level.

4.3. RESULTS

4.3.1. Thickness and extensibility

Table 4.1 shows the mass fraction (Xi) of the different components in dried films, thickness of the obtained films and their extension during the compression moulding step, expressed as the area per mass unit of the material. The PCL films were thinner than the other formulations due to their greater flowability and extensibility. In contrast, the film thickness tended to increase when the amount of starch in the matrix rose, due to the starch's reduced ability to flow. Incorporation of citric acid in the formulations led to an increase in the extensibility with net starch films, but had an opposite effect on starch-PCL blends with the lowest PCL ratio, and had no significant effect on films with over 30% PCL, when the influence of the greater amount of PCL in the film flowability was more notable. Chabrat *et al.* (2012) report for blend films of wheat flour and PLA, processed at high temperature, that citric acid in the blends acts as compatibilizer (esterification, hydrogen bonds), as starch plasticizer and/or as depolymerization agent for both starch and PLA. Similar effects could be expected for CA in the studied S-PCL blends as concerns the starch-CA interactions. In fact, plasticization and/or depolymerization effects can be deduced from the increase in the flowability of the starch when citric acid was added. Its opposite effect at low PCL ratios in the film

could point to the promotion of the inter chain forces between both polymers promoted by CA.

Table 4.1.-Mass fraction (Xi) of the different components in dried films and mean values and standard deviation of film thickness and extensibility during the thermo-compression step.

Films	X_S	X_{PCL}	X_{Gly}	X_{CA}	Thickness (µm)	Extensibility (cm^2/g)
S	0.7692	-	0.2308	-	268 ± 22^{e}	24 ± 2^{a}
S-CA	0.7634	-	0.2290	0.0076	217 ± 22^{c}	32 ± 4^{bc}
S90	0.7087	0.0787	0.2126	-	232 ± 17^{cd}	28 ± 2^{abc}
S90-CA	0.7037	0.0782	0.2111	0.0070	293 ± 27^{f}	24 ± 2^{a}
S80	0.6452	0.1613	0.1935	-	221 ± 9^{cd}	32 ± 2^{c}
S80-CA	0.6410	0.1603	0.1923	0.0064	239 ± 17^{d}	27 ± 2^{ab}
S70	0.5785	0.2479	0.1736	-	224 ± 9^{cd}	31 ± 2^{bc}
S70-CA	0.5752	0.2465	0.1726	0.0058	227 ± 11^{cd}	29.8 ± 0.6^{bc}
S60	0.5085	0.3390	0.1525	-	168 ± 13^{b}	45 ± 6^{d}
S60-CA	0.5059	0.3373	0.1518	0.0051	172 ± 14^{b}	41 ± 2^{d}
PCL	-	1.0000	-	-	149 ± 17^{a}	57 ± 9^{e}

Different superscript letters within the same column indicate significant differences among formulations ($p < 0.05$).

4.3.2. Structural analysis

Atomic Force Microscopy PeakForce QNM mode was used to acquire the images shown in Figure 4.1, where the DMT modulus maps for the samples' surfaces are plotted. The control formulations (S and PCL) showed more homogenous values of the surface modulus than the blend films, although a great difference in their values can be observed for both control films. Net starch films had a much harder surface than net PCL films. The addition of CA to starch films did not introduce notable changes in the surface homogeneity, but in some areas, higher values of the modulus were registered, which could be due to the CA crosslinking effect. When

the PCL was added to the starch matrix, the heterogeneity of the material greatly increased while the modulus reached values near to those obtained for starch films, with very soft zones, corresponding to the non-crystallized domains. In samples containing 90% starch, the incorporation of CA seemed to reduce the modulus heterogeneity level and they were harder (the surface area percentage with values of the modulus lower than 1.5 GPa was 1.2% and 67.9% respectively for films with and without CA). This suggests that CA could be responsible for cross-linking in the starch phase (Ortega-Toro *et al.*, 2014b) at the same time as it contributes to enhance the polymer compatibility to some extent. This effect was not observed, or was masked, when the content of PCL was higher.

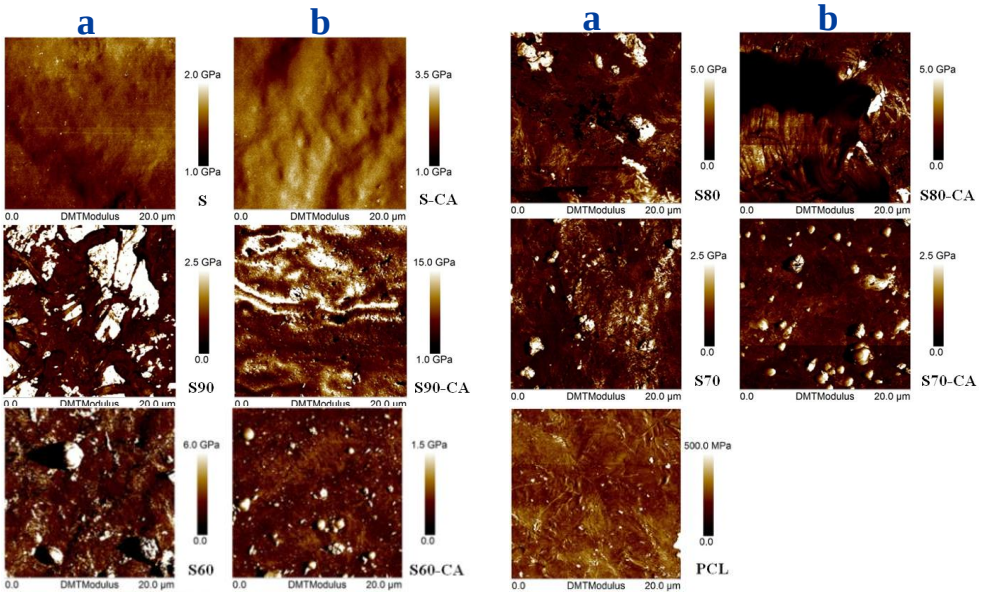

Figure 4.1.–DMT Modulus maps obtained by AFM of starch:PCL films without (a) and with (b) citric acid.

Figure 4.2 shows SEM micrographs of the cross-section of the studied films, with or without citric acid, conditioned at 25 ºC and 53% RH for one week. S and PCL

samples have a continuous and homogeneous structure. The PCL sample showed its typical cryo-fracture behaviour in liquid nitrogen, where elongation of the amorphous zones (very ductile, T_g= -67 ºC-Avella *et al*., 2000) can be observed despite the low temperature. When PCL was added to the starch matrix, the films were heterogeneous, in agreement with the non-compatibility of the polymers. In the formulations with low PCL ratio (S90), an effective distribution of PCL in the starch matrix can be observed. Nevertheless, when the proportion of PCL increased (S70 and S60) large domains of interpenetrated PCL-rich and starch-rich phases were observed.

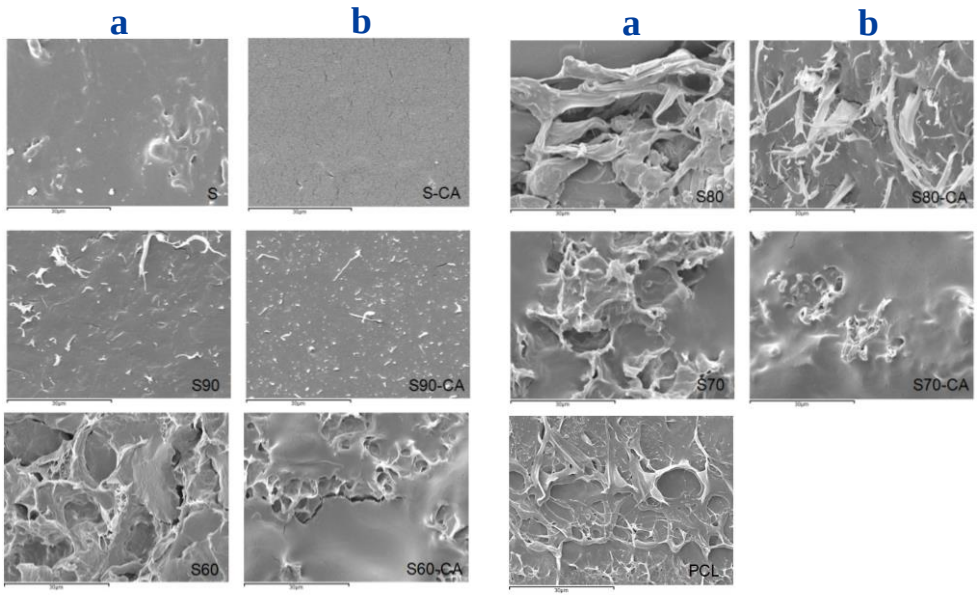

Figure 4.2.-SEM micrographs of starch:PCL films without (a) and with (b) citric acid.

The addition of citric acid caused changes in the films' microstructure. The S-CA films showed a continuous matrix with some cracks, which suggests the formation of a more brittle matrix. Likewise, S-CA films were more homogeneous than the S

films, which indicates that citric acid contributes to the fragmentation and dissolution of the native starch granules (acid gelatinization), as observed by other authors (Yu *et al*., 2005; Ma *et al*., 2009). Likewise, in the formulations with less PCL (S80-CA and S90-CA), the CA promotes changes in the dispersion of PCL in the starch matrix; PCL particles are finer and better dispersed in the starch continuous phase. Similar results were reported by Chabrat *et al*. (2012) for blend films of wheat flour-PLA-glycerol (75:25:15) with different ratios of citric acid. In the formulations S70-CA and S60-CA, the changes were not evident probably due to the fact that the ratio of PCL is too high to be compatible with the starch. The increase in polymer compatibility of PCL may be due to the partial esterification of starch hydroxyl groups with CA, and its depolymerisation effects on both polymers which can induce a greater affinity between them (Reddy & Yang, 2010; Chabrat *et al*., 2012).

Figure 4.3 shows the X-ray diffraction patterns and crystallinity degree (CD) of the films stored for 1 and 5 weeks under controlled conditions. Spectrum of S films presented low intensity, broad diffraction peaks and a large amorphous scattering halo. These characteristics correspond to a semi-crystalline polymer with low crystallinity. In all formulations containing starch, the typical crystalline forms of amylose were V type, with peaks at 2θ of about 13 and 20º. This V-type crystalline structure is formed by crystallization of amylose in single helices involving glycerol or lipids. Nevertheless, this V-type crystalline structure can be divided into two subtypes, namely V_a (anhydrous) with peaks at 13.2º and 20.6º and V_h (hydrated) with peaks at 12.6º and 19.4º (Castillo *et al*., 2013). These two subtypes could be observed in the different films, depending on their composition and storage time.

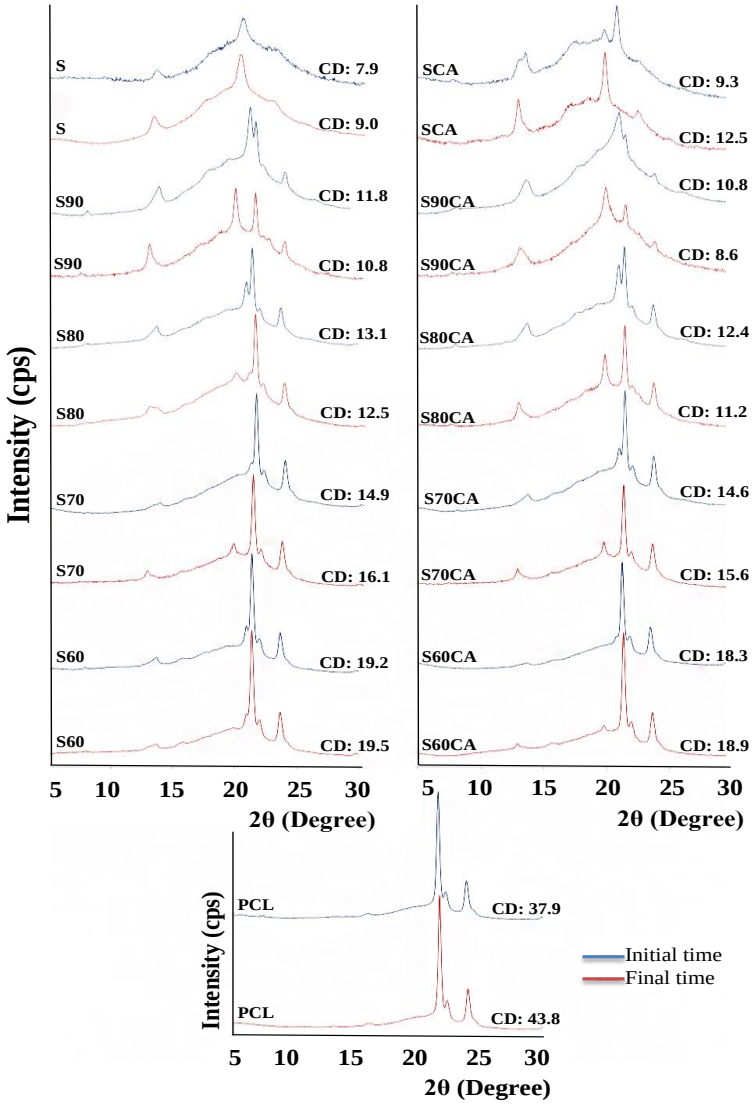

Figure 4.3.-X-Ray diffraction patterns of starch:PCL films without (a) and with (b) citric acid at initial and final time of storage at 53% relative humidity and 25 ºC.

Starch-glycerol films showed V_a subtype at both storage times, whereas when they contained citric acid, both V_a and V_h subtypes were initially formed and predominantly developed into the V_a subtype during storage. So, CA addition

promoted the simultaneous formation of V_a and V_h crystalline subtypes, while the crystallinity degree increased at both 1 and 5 storage weeks. This could be due to the hydrolysis effect which, upon reducing the mean molecular weight, promotes molecular mobility, thus favouring the crystalline arrangement. At five storage weeks, there were no differences between the observed peaks for S and S-CA samples, although the increase in the crystallinity degree was higher in S-CA.

Some authors (Xie *et al*., 2006) reported that the citrate substituent altered chain packing and generated more amorphous structures in starch. Nevertheless, probably due to the hydrolysis effect, CA promoted starch crystallization under the conditions used for film preparation.

In PCL starch blends, the characteristic peaks of crystalline PCL appeared, but starch peaks can also be distinguished, since overlapping only occurs at 2θ near 21º. In all these blends, starch showed the V_a subtype crystallization at initial time but it became the V_h subtype after the 5 storage weeks, regardless of the presence of CA. This tendency was only observed when PCL was present in the film, which suggests that PCL induced the formation of this crystalline subtype. The interplanar basal spacing deduced from 2θ values was greater for the V_h form than for V_a, these being 6.7 and 4.3 Å and 7.0 and 4.6 Å, respectively for V_a and V_h.

When the amount of PCL increased, sharper and more intense peaks were observed in the diffractograms, due to the PCL crystallinity, with the main peaks at 2θ: 22º and 24º, as reported by Mark (1999). According to the theory of kinematical scattering, peak sharpening is caused by either greater crystal size or the absence of lattice defects. The crystallinity degree in the films increased when the PCL ratio rose, due to the predominantly crystalline structure of this polymer. In general, CA addition to starch PCL blends gave rise to a slightly lower ratio of crystallinity in the films at both 1 and 5 storage weeks, contrary to what was observed for net starch films. No clear effect of storage time could be observed in blend films, since

small increases or decreases in the percentage of crystallinity could be observed, depending on the formulation.

Therefore, CA or PCL slightly modified the starch crystallization pattern. CA promoted the crystalline forms in glycerol plasticized starch films, whereas it reduced the total crystallinity degree in the films when they contain PCL, which could indicate that CA affected the PCL crystallinity degree. In general, a slight progress of crystallization occurred during storage time, but this was not appreciable for blend films with a lower ratio of PCL. CA promoted the formation of V_h subtype crystalline forms in starch films, as well as PCL at long storage times.

4.3.3. Thermal analysis

Table 4.2 shows the thermal properties of the studied films conditioned for 1 and 5 weeks. Two heating scans and one cooling scan were performed. In the first heating scan, the melting temperature (T_m) of PCL was determined as the peak temperature of the endotherm as well as the melting enthalpy (ΔH_m). This has been analyzed for samples stored for different times (1 and 5 weeks, initial and final) in order to detect changes in the PCL crystalline structure, as could be deduced from X ray diffraction patterns. During the cooling step, the crystallization temperature (T_c peak) and enthalpy (ΔH_c) of PCL were obtained from the crystallization exotherm. Finally, during the second heating scan, the melting temperature and enthalpy of the newly crystallized PCL (during the cooling step) and the glass transition temperature (T_g) of starch (midpoint) were determined.

The T_g of the starch phase significantly decreased ($p < 0.05$) when PCL was incorporated into the starch matrix. This decrease was constant (about 12 ºC), regardless of the PCL ratio in the blend.

Table 4.2.-Mean values and standard deviation of thermal properties of the starch:PCL films stored for 1 week (Initial) and 5 weeks (final).

Films	Glass transition (T_g)	Crystallization		Fusion in the first heating scan				Fusion in the second heating scan	
				Initial		Final			
		T_c peak	ΔH_c (J/g PCL)	T_m peak	ΔH_m (J/g PCL)	T_m peak	ΔH_m (J/g PCL)	T_m peak	ΔH_m (J/g PCL)
S	126.0 ± 0.3^{d}	---	---	---	---	---	---	---	---
S-CA	113.0 ± 0.7^{b}	---	---	---	---	---	---	---	---
S90	114.5 ± 0.7^{c}	12.0 ± 0.2^{a}	51.4 ± 0.9^{bc}	62.4 ± 0.7^{bc}	72.4 ± 0.4^{a}	63.9 ± 0.6^{b}	81.9 ± 1.0^{ab}	55.18 ± 0.05^{bcd}	51.8 ± 1.3^{a}
S90-CA	101.6 ± 0.2^{a}	12.10 ± 0.14^{a}	$49.2 \pm 0.9a$	61.1 ± 0.9^{a}	72.1 ± 0.5^{a}	63.84 ± 0.08^{b}	79.7 ± 0.5^{a}	54.0 ± 0.2^{a}	50 ± 2^{a}
S80	114.31 ± 0.05^{c}	12.5 ± 0.6^{ab}	52.3 ± 0.3^{c}	62.9 ± 0.6^{c}	72.3 ± 1.3^{a}	63.29 ± 0.11^{ab}	82.3 ± 0.7^{b}	55.4 ± 0.3^{d}	51.2 ± 1.3^{a}
S80-CA	101.2 ± 0.2^{a}	12.6 ± 0.4^{ab}	49.3 ± 0.9^{a}	60.97 ± 0.12^{a}	72.2 ± 0.4^{a}	63.92 ± 0.11^{b}	81.0 ± 1.5^{ab}	54.11 ± 0.05^{a}	50.5 ± 0.9^{a}
S70	114.35 ± 0.13^{c}	12.3 ± 0.3^{ab}	52.0 ± 0.6^{c}	62.32 ± 0.62^{bc}	72.1 ± 0.3^{a}	63.32 ± 0.04^{ab}	81.7 ± 0.9^{ab}	54.9 ± 0.2^{bc}	51.4 ± 1.4^{a}
S70-CA	101.53 ± 0.13^{a}	12.95 ± 0.07^{b}	50.7 ± 1.1^{abc}	61.55 ± 0.03^{ab}	72.4 ± 0.4^{a}	63.39 ± 0.11^{ab}	79.9 ± 0.6^{a}	54.8 ± 0.4^{b}	49.9 ± 1.1^{a}
S60	114.8 ± 0.2^{c}	12.33 ± 0.07^{ab}	52.2 ± 0.8^{c}	63.0 ± 0.2^{c}	72.5 ± 0.6^{a}	63.3 ± 0.2^{ab}	81.9 ± 1.0^{ab}	55.13 ± 0.04^{bcd}	51.0 ± 1.3^{a}
S60-CA	100.9 ± 0.5^{a}	12.3 ± 0.3^{ab}	50.3 ± 0.2^{ab}	61.51 ± 0.02^{ab}	72.2 ± 0.4^{a}	63.07 ± 0.04^{a}	79.8 ± 0.4^{a}	54.88 ± 0.14^{b}	49.7 ± 1.0^{a}
PCL	---	12.6 ± 0.6^{ab}	52.4 ± 0.3^{c}	63.5 ± 0.6^{a}	72.8 ± 1.4^{a}	63.7 ± 0.6^{a}	82.2 ± 1.5^{b}	55.4 ± 0.4^{cd}	51.0 ± 1.2^{a}

Different superscript letters within the same column indicate significant differences among formulations ($p < 0.05$).

This indicates that PCL partially solubilizes in the starch phase, thus decreasing the mean molecular weight of the amorphous blend and the molecular mobility, which reduces the T_g value. The amount of PCL that the starch phase can incorporate at a molecular level was less than 10%, since this sample also shows two phases, as revealed by the microstructural analyses.

The incorporation of citric acid also led to a decrease in the T_g values of starch (ΔT about 13 ºC) and this effect was maintained for starch-PCL blend films. This decrease in the T_g can be attributed to a depolymerisation effect in starch, which implies a reduction in the polymer molecular weight leading to an increase in the molecular mobility, but also to a better solubilisation of PCL in the starch phase with a similar impact in the mean molecular weight of this amorphous phase or to a combination of these two phenomena, as reported by Chabrat *et al*. (2012) for wheat flour-PLA blend films.

The T_c values of the PCL in the different films were 12 ºC and there were no significant differences between the different formulations or net PCL films. The crystallization enthalpy (ΔH_c) was about 52 J/g PCL for samples without CA and slightly decreased (49-50 J/g PCL) when CA was present in the film, the difference being statistically significant. This suggests that changes in the ability of PCL to crystallize were induced by citric acid, in agreement with that deduced from the X-ray diffraction data.

The melting behaviour of PCL in the first heating scan, where no fusion was previously provoked, gave T_m values from 61 to 63.5 °C and ΔH_m values of about 72 J/g of PCL for samples stored for 1 week, regardless of the film formulation; this indicates that, at this storage time, PCL is crystallized to the same extent in every case. Similar results have been reported by other authors for films of wheat thermoplastic starch/PCL blends (Averous *et al*., 2000) LDPE/starch/PCL blends14 or chlorinated starch- PCL blends (Kweon *et al*., 2003). Nevertheless, after 5

storage weeks, a slight increase was observed in the melting peak, T_m, and ΔH_m, which indicates that the crystallization of PCL progresses slightly during storage. This occurred to a slightly lesser extent when CA was incorporated to the formulation (lower values of ΔH_m).

Likewise, the T_m and ΔH_m obtained in the second scan were lower than the values obtained in the first scan, as observed by other authors for pure PCL (Koenig & Huang, 1995). The ΔH_m values of the second scan were very close to the ΔH_c values, in line with the melting of the crystallized polymer during the thermal scanning (Campos *et al*., 2012). From the melting parameters obtained in the first and second scans, supercooling effects during the cooling step in DSC analyses can be deduced, while citric acid slightly reduces the ability of PCL to crystallize. This suggests that there are molecular changes in the polymer either brought about by depolymerisation or by the occurrence of stronger interactions with the starch chains promoted by citric acid.

4.3.4. Physicochemical properties

Figure 4.4 shows typical tensile curves of the different films stored for 1 week under controlled conditions. The incorporation of CA to the net starch film provoked a decrease in the film stretchability, while the resistance to break and elastic modulus were hardly affected. This has previously been reported and attributed to the crosslinking of starch chains, which reduced their possibilities of slipping during the tensile test (Ortega-Toro *et al*., 2014b). Nevertheless, in blend films with a low ratio of PCL (S90 and S80), citric acid greatly increased the film stretchability, although the elastic modulus and resistance to break were reduced. This suggests that the polymer compatibility increased and that the films gain extension ability associated with the presence of a very stretchable polymer, such as PCL. This is particularly effective in films containing the lowest PCL ratio.

Blend films with a higher ratio of PCL, both with and without citric acid, exhibited a very low deformation capacity and break at low deformation levels probably due to the low adhesion forces between the phases in the matrix, where both polymers are arranged in large domains of separated phases with scarce union forces between them.

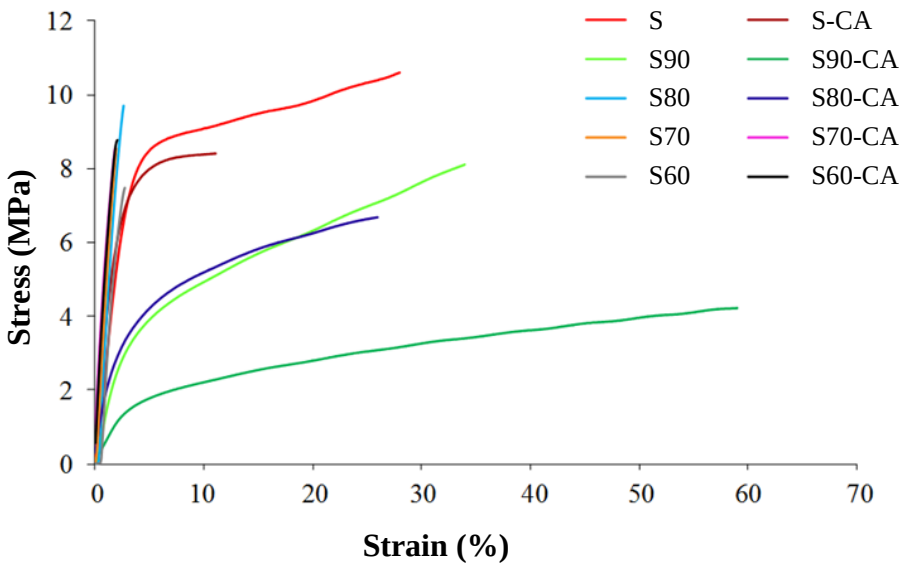

Figure 4.4.-Typical stress-strain curves of the different films after 1 week of storage.

Figure 4.5 shows the tensile parameter values at 1 and 5 storage weeks for the different formulations. When the starch is blended with PCL, EM was greater than in the control formulations (S and PCL), except for sample S90 where EM was significantly lower ($p < 0.05$). Likewise, EM values significantly increased during storage in almost every case, which indicates that starch chain aggregations progressively increased in the continuous phase, thus hardening the matrix. The increase in EM for PCL concentrations over 20% suggests that the conformation of

the starch chains in the starch domains changed in the presence of the hydrophobic PCL chains in the matrix, thus promoting stronger intermolecular bonds, while the forces in the union zones are weak. The latter was reflected in the significant decrease in the film's resistance to break and stretchability when the PCL ratio increased in the matrix. Only the S90 sample gains extensibility, as compared to the S control, especially when it contains CA (S90-CA), although it loses resistance to break. These results indicate that, at this PCL ratio, a better integration of both polymers occurred, as deduced from thermal behaviour and microstructural analyses. This integration was enhanced when CA was added to the film, which led to a significant gain in the film stretchability, probably through the role of PCL chains in the matrix. Net PCL films exhibited very ductile behaviour with yield point (not break) at 18.17 ± 1.06 MPa and 13 ± 4 percentage deformation. Other authors reported that the PCL films' break occurs at 1100% (Ishiaku *et al*., 2002). The incorporation of CA to the films caused a reduction in the EM and the resistance (TS) at break of the blend films, except for the S60 sample where both parameters slightly increased. As concerns elongation, CA greatly promotes the extensibility of S90 and S80 samples, whereas it did not affect the very low values of the S70 and S80 samples.

These results are coherent with a combined effect of CA, previously reported by other authors for starch blend films: cross linking between starch chains, or even with the end hydroxyl groups of PCL (loss of stretchability), partial hydrolysis of the starch and PCL chains and plasticizing effect of the non-bonded citric acid molecules (decrease in the elastic modulus and resistance to break) (Ghanbarzadeh *et al*., 2011; Chabrat *et al*., 2012; Ortega-Toro *et al*., 2014b). The differentiated behaviour of S90 and S80 samples with a relatively low ratio of PCL indicates that the interactions between starch and PCL chains promoted by citric acid

predominate over the overall behaviour of non-well-adhered separate phases of PCL and starch in blend films.

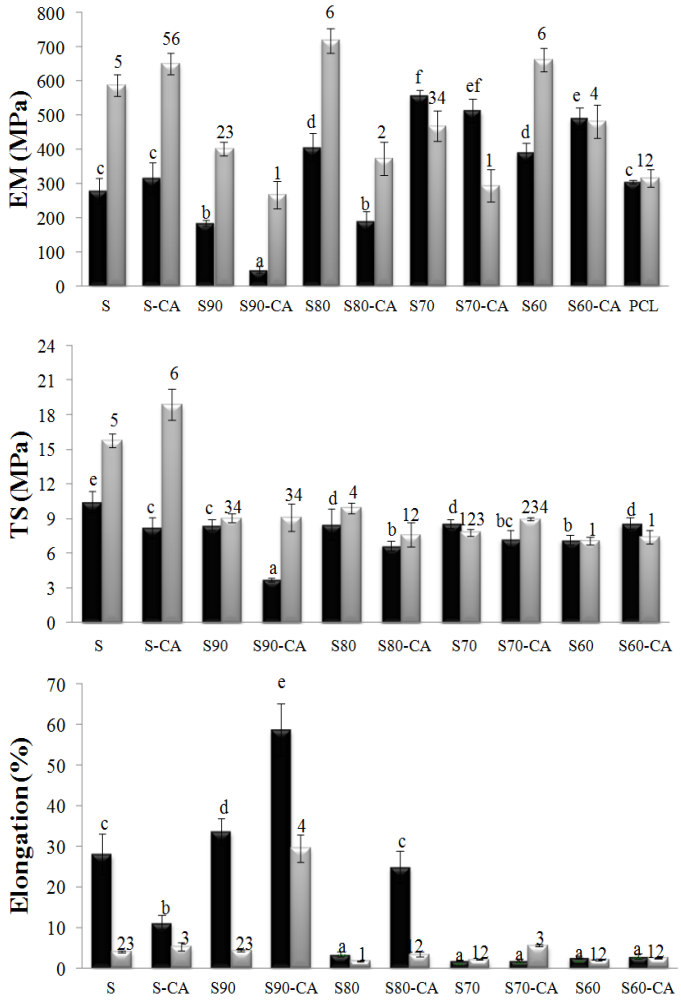

Figure 4.5.- Mean values of EM, TS and elongation for the different films stored for 1 (black bars) and 5 (grey bars) weeks. LSD intervals (95% confidence level) are shown. Different letters or numbers on the columns indicate significant differences among formulations after 1 or 5 storage weeks, respectively.

As concerns the development of the mechanical behaviour of the films during storage time, two trends were observed. When the proportion of PCL was low (S90 and S80 samples with and without CA), the EM and TS parameters increased and the elongation decreased. The changes were not marked when the amount of PCL was high (S70, S70-CA, S60 and S60-CA). As previously commented on, this suggests that starch chain aggregation progressed during storage (retrogradation phenomenon), even when CA or PCL was added, this being more notable when the starch dominated in the matrix. Nevertheless, films with 10% PCL and CA maintained a good mechanical response after 5 weeks' storage time.

Table 4.3 shows the values and standard deviation of the equilibrium water content, water solubility and bonded citric acid of the studied films at the initial and final storage times. The water content (Xw) decreased when the amount of PCL rose in the blend due to its hydrophobic character. In general, at 1 week of storage, formulations with citric acid exhibited a significantly lower ($p < 0.05$) water content than the CA-free films. This indicates that a certain extent of esterification of the starch hydroxyl groups could occur during the film's thermo-processing (blend in roll mills and compression moulding) at the high temperature used (160 °C) and in the absence of water, since these are adequate conditions for citric acid esterification reactions with chain hydroxyls (Reddy &Yang, 2010). The fall in the number of hydroxyls will reduce the water affinity of the polymer, while cross-linking between different starch chains will reinforce the intermolecular binding, by introducing covalent bonds thus improving the water uptake resistance (Krumova *et al*., 2000; Yu *et al*., 2005; Ghanbarzadeh *et al*., 2011). Nevertheless, a significant increase ($p < 0.05$) in the films' water content during the storage time was observed in every case, except in the pure PCL film, thus indicating that the equilibrium was not reached at 1 week of storage. At this time, the effect of citric

acid on the films' moisture content was not significant, which suggests that there was no notable reduction of active points for water adsorption.

Table 4.3.-Mean values and standard deviation of water content (Xw), film solubility (g solubilised film/g initial dried film) and bonded citric acid (ratio with respect to the amount in the film) of the different films stored at 53% relative humidity and 25 ºC.

Films	Xw (g water/g dried film)		Film solubility		Bonded citric acid
	Initial	Final	Initial	Final	
S	0.0613 ± 0.0006^{h1}	0.079 ± 0.004^{g2}	0.19 ± 0.07^{d1}	0.24 ± 0.05^{d1}	---
S-CA	0.059 ± 0.002^{gh1}	0.076 ± 0.002^{fg2}	0.35 ± 0.03^{f1}	0.371 ± 0.012^{f1}	0.80 ± 0.03^{a}
S90	0.0664 ± 0.0004^{i1}	0.074 ± 0.003^{ef2}	0.120 ± 0.009^{bc1}	0.138 ± 0.002^{b2}	---
S90-CA	0.0543 ± 0.0007^{ef1}	0.0713 ± 0.0005^{e2}	0.328 ± 0.005^{f1}	0.331 ± 0.005^{e1}	0.84 ± 0.03^{a}
S80	0.0535 ± 0.0008^{e1}	0.061 ± 0.002^{d2}	0.132 ± 0.003^{bc1}	0.137 ± 0.013^{b1}	---
S80-CA	0.056 ± 0.003^{ef1}	0.061 ± 0.015^{d2}	0.362 ± 0.013^{f1}	0.32 ± 0.02^{e2}	0.86 ± 0.03^{a}
S70	0.057 ± 0.003^{fg1}	0.063 ± 0.004^{d1}	0.099 ± 0.003^{b1}	0.106 ± 0.006^{b1}	---
S70-CA	0.047 ± 0.003^{d1}	0.0578 ± 0.005^{c2}	0.24 ± 0.02^{e1}	0.30 ± 0.02^{e2}	0.81 ± 0.04^{a}
S60	0.0409 ± 0.0006^{c1}	0.046 ± 0.002^{b2}	0.13 ± 0.03^{bc1}	0.13 ± 0.02^{b1}	---
S60-CA	0.03331 ± 0.00014^{b1}	0.0458 ± 0.0014^{b2}	0.16 ± 0.02^{cd1}	0.19 ± 0.02^{c1}	0.83 ± 0.04^{a}
PCL	0.003 ± 0.002^{a1}	0.0021 ± 0.0005^{a1}	0.00022 ± 0.00011^{a1}	0.0004 ± 0.0002^{a1}	---

Different superscript letters within the same column indicate significant differences among formulations ($p < 0.05$). Different superscript numbers within the same row indicate significant differences due to storage time ($p < 0.05$).

As concerns the water solubility of films, the values were lower than the glycerol mass fraction in the films except in the case of those films containing citric acid (Table 4.1), which indicates that in no case is this component completely released to the water medium. Compared to the S formulation, films without citric acid experienced a significant ($p < 0.05$) decrease in water solubility when PCL was present in the film, regardless of its ratio; this is coherent with their increased hydrophobic character and the subsequent inhibition of the mass transport rate of polar water soluble compounds.

On the other hand, the film solubility increased when CA was added, although this was slightly reduced for higher PCL ratios. The increase in this parameter suggests the partial hydrolysis of macromolecules caused by citric acid, resulting in a greater quantity of linear, smaller fragments of starch which are more water soluble (Olivato *et al*., 2012; Carvalho *et al*., 2005). Yoon et al. (2006) reported an increase in the solubility of starch-polyvinyl alcohol (PVA) blend films when the CA concentration increased. Likewise, a similar effect was reported for modified starch-polyvinyl alcohol blends (Lee *et al*., 2007; Yun *et al*., 2008). Shi *et al*. (2007) reported a decrease in the polymer molecular weight when citric acid was added to thermoplastic corn starch as co-plasticizer with glycerol. The lower values of the citric acid induced water solubility, when PCL ratio increased in the blends, suggest that no notable hydrolysis of this polymer occurred.

The values of the ratio of bonded CA with respect to the amounts added to the films did not differ significantly from formulation to formulation. This suggests that CA reacts with starch chains or with glycerol, taking into account that the CA-glycerol-starch ratios were constant in every formulation and that the CA-PCL ratio decreased as PCL rose in the blend. So, neither are there any notable CA-PCL reactions (such as possible transesterification) nor does the PCL presence affect the starch or glycerol reactions with CA. Esterification reactions of CA with glycerol

have previously been described in starch-glycerol-citric acid films (Holser, 2008). Nevertheless, this reaction could not be confirmed from the obtained data, since for films with CA solubility values were always greater than the mass fraction of glycerol in the films, even when the PCL ratio was at its highest and the solubility value at its lowest.

Table 4.4 shows the water vapour permeability (WVP) and oxygen permeability (O_2P) of the studied films after 1 and 5 storage weeks. The addition of PCL promoted a significant decrease ($p < 0.05$) in the WVP of the studied films; the higher the PCL content, the greater the reduction for films stored for both 1 and 5 weeks. The hydrophobic phase in the starch matrix can explain this behaviour, since the material presents a greater tortuosity factor for the transport of water molecules. The incorporation of CA to the starch matrix did not imply a significant reduction in WVP values in films equilibrated for 5 weeks, when they gained moisture content. It is likely that the crosslinking and hydrolysis phenomena effects on mass transport properties of the material were balanced. In blend films, CA did not improve water vapour barrier properties.

The O_2P values for S and PCL formulations were not shown because their values were outside the sensitivity range of the equipment used: those of the S formulation were too low and those of the net PCL films too high. The O_2P values of blend films significantly ($p < 0.05$) increased in line with the PCL ratio in the film, while the addition of CA did not present a notable effect. No notable changes in the O_2P values of the films were observed after 5 storage weeks. So, the barrier properties of starch films were positively affected by PCL blending for water vapour but negatively affected for oxygen, in agreement with the different chemical affinity of PCL with both molecules. Even in samples with 10% PCL, where citric acid acts as a compatibilizer, there was no observed impact of this compound on film barrier properties.

Table 4.4.-Mean values and standard deviation of water vapour permeability (WVP) and oxygen permeability (O_2P) of the different films after 1 (Initial) and 5 (Final) weeks of storage at 53% relative humidity and 25 ºC.

Films	WVP (g·mm·KPa^{-1}·h^{-1}·m^{-2})		$O_2P \cdot 10^{15}$ (cm^3·m^{-1}·s^{-1}·Pa^{-1})	
	Initial	Final	Initial	Final
S	18.1 ± 1.4^{h1}	16 ± 2^{e1}	< D.L.	< D.L.
S-CA	12 ± 2^{de1}	15.6 ± 1.2^{e1}	0.26 ± 0.05^{a1}	0.281 ± 0.004^{a1}
S90	14.5 ± 0.7^{f1}	15.8 ± 1.2^{e1}	0.22 ± 0.09^{a1}	0.23 ± 0.15^{a1}
S90-CA	13.0 ± 1.4^{ef1}	15 ± 2^{e1}	0.4 ± 0.2^{a1}	0.54 ± 0.06^{a1}
S80	11 ± 2^{de1}	9.3 ± 0.6^{cd1}	6.5 ± 0.3^{ab1}	6 ± 3^{b1}
S80-CA	10.0 ± 0.6^{d1}	10.8 ± 1.0^{d1}	2.4 ± 0.3^{a1}	3.9 ± 0.2^{ab2}
S70	7.5 ± 0.7^{c1}	10.4 ± 0.7^{cd2}	17.1 ± 0.9^{cd1}	14.6 ± 1.1^{c1}
S70-CA	6.3 ± 0.7^{c1}	8.5 ± 0.3^{c1}	11.6 ± 1.2^{bc1}	12 ± 2^{c1}
S60	8 ± 2^{c1}	5.4 ± 0.4^{b1}	33 ± 2^{e1}	26 ± 3^{d1}
S60-CA	2.9 ± 0.8^{b1}	3.55 ± 0.11^{b1}	24 ± 2^{d1}	27.1 ± 0.8^{d1}
PCL	0.120 ± 0.04^{a1}	0.117 ± 0.011^{a1}	> D.L.	> D.L.

D.L.: 0.1-200 cm^3/(m^2.day). Different superscript letters within the same column indicate significant differences among formulations ($p < 0.05$). Different superscript numbers within the same row indicate significant differences due to storage time ($p < 0.05$).

Table 4.5 presents the values and standard deviation of roughness parameters, internal transmittance at 650 nm, and gloss at 85º of the studied films conditioned under controlled conditions for 1 and 5 weeks. In general, the roughness parameters did not show marked differences while they did exhibit a slight tendency to decrease when the PCL ratio increased, the net PCL films were not as rough as net starch films. Likewise, the roughness tended to decrease after the addition of CA in line with the promotion of the fragmentation and gelatinization of starch granules caused by the acid (Yu *et al*., 2005; Wang *et al*., 2009; Chabrat *et al*., 2012). In the analysis of this parameter, it is necessary to take into account that the compression moulding could affect the surface roughness and mask the effect caused by the components of the polymeric matrix.

Table 4.5.-Mean values and standard deviation of surface roughness parameters and optical properties of the different films after 1 (Initial time) and 5 (Final time) weeks of storage at 53% relative humidity and 25 ºC.

Films	Roughness parameters		Gloss (85°)		Ti (650nm)	
	r (%)	Rq (nm)	Initial	Final	Initial	Final
S	6.1 ± 0.9^{abc}	263 ± 63^{a}	40 ± 5^{c1}	37.2 ± 1.5^{bcd1}	85.1 ± 0.3^{h1}	84.2 ± 0.2^{fg2}
S-CA	2.5 ± 0.2^{a}	206 ± 72^{a}	39 ± 5^{c1}	32 ± 2^{b1}	85.5 ± 0.6^{h1}	85.9 ± 0.8^{g1}
S90	13 ± 5^{d}	247 ± 65^{a}	37 ± 9^{bc1}	35 ± 6^{bc1}	77.3 ± 0.6^{bc1}	79.8 ± 0.6^{cd2}
S90-CA	3.2 ± 1.2^{a}	200 ± 38^{a}	52 ± 3^{d1}	43 ± 17^{de2}	79.4 ± 0.3^{def1}	81.1 ± 0.4^{de2}
S80	8 ± 3^{bc}	255 ± 26^{a}	29 ± 9^{c1}	31 ± 9^{b1}	82.4 ± 0.6^{g1}	82.5 ± 1.1^{ef1}
S80-CA	14 ± 4^{d}	497 ± 35^{b}	20 ± 13^{a1}	14 ± 2^{a1}	73.6 ± 0.6^{a1}	76.0 ± 0.7^{a1}
S70	8 ± 3^{bc}	271 ± 68^{a}	34 ± 10^{bc1}	46 ± 4^{e2}	80.90 ± 0.14^{efg1}	80.9 ± 0.4^{de1}
S70-CA	11 ± 3^{cd}	265 ± 72^{a}	31 ± 9^{bc1}	35 ± 10^{bcd1}	76.2 ± 0.7^{b1}	77.1 ± 0.6^{ab1}
S60	5.6 ± 1.4^{ab}	210 ± 79^{a}	38 ± 6^{c1}	37 ± 4^{bcd1}	81.2 ± 1.3^{fg1}	81.6 ± 0.7^{de1}
S60-CA	9.2 ± 1.3^{bcd}	214 ± 26^{a}	50 ± 7^{d1}	41 ± 10^{cde2}	78.8 ± 0.8^{cde1}	79.4 ± 0.8^{cd1}
PCL	6.0 ± 0.9^{ab}	195 ± 25^{a}	59 ± 16^{e1}	57 ± 9^{f1}	78 ± 2^{cd1}	78 ± 2^{bc1}

Different superscript letters within the same column indicate significant differences among formulations ($p < 0.05$). Different superscript numbers within the same row indicate significant differences due to storage time ($p < 0.05$).

The gloss of the films was related with their surface roughness (Sánchez-González *et al*., 2012) and, therefore, the process by which it is obtained can also affect it. In general, the films showed low gloss, their values ranging between 20 and 59 GU, with high variability, and without clear tendencies as a function of their composition. The net PCL films exhibited the highest gloss values according to their lowest roughness parameters obtained by AFM.

The internal transmittance (Ti), as a measure of film transparency, tended to decrease in line with the PCL ratio, according to the greater heterogeneity of the matrix with two non-miscible phases and a different refractive index. The incorporation of CA improved the film transparency of the S90 sample, but increased the film's opacity in the other blend films. No notable changes in this parameter occurred while the film was stored for 5 weeks. The different effect of

CA in the S90 films is coherent with the improvement in the polymer compatibility deduced from the thermal and mechanical behaviour of these films.

4.4. CONCLUSIONS

Citric acid improves the properties of corn starch-PCL blend films with a low PCL ratio (S:PCL ratio of 90:10), while it was not effective at compabilizing blends with higher amounts of PCL. This was observed in the microstructural analyses and deduced from the film's physicochemical properties. The incorporation of CA in the films affected both starch and PCL crystallization as deduced from the X-ray diffraction patterns of starch and PCL melting enthalpy values. The glass transition of starch was reduced by the incorporation of PCL in line with its partial solubilization in the starch phase, but lower than 10% with respect to starch. This decrease was greater in the presence of citric acid. So, citric acid promoted stronger interactions between PCL and starch chains, although this only quantitatively benefited the film properties at a low PCL ratio. In fact, blend films with a 90:10 starch:PCL ratio with citric acid exhibited the highest stretchability, with good mechanical resistance. The water solubility of the films increased when they contained citric acid, due to the acid hydrolysis of starch, although the water transfer rate was limited in blend films. Citric acid did not affect the barrier properties of the blend films which showed intermediate values, between those of net starch and PCL films, according to their ratio in the film. So, compounding starch with small amounts of PCL, using glycerol and citric acid, can supply films with better functional properties than net starch films.

4.5. REFERENCES

Annable, P., Fitton, M.G., Harris, B., Philips, G. O., & Williams, P. A. (1994). Phase behavior and rheology of mixed polymer systems containing starch. Food Hydrocolloids, 8(4), 351-359.

American Society for Testing and Materials, ASTM E96-95. Standard test methods for water vapor transmission of materials. In annual book of ASTM. Philadelphia; 1995.

American Society for Testing and Materials, ASTM D523. Standard test method for specular gloss. In annual book of ASTM. Philadelphia; 1999.

American Society for Testing and Materials, ASTM D882. Standard test method for tensile properties of thin plastic sheeting. In annual book of ASTM. Philadelphia; 2001.

American Society for Testing and Materials, ASTM 3985-05. Standard test method for oxygen gas transmission rate through plastic film and sheeting using a coulometric sensor; 2010.

American Society of Mechanical Engineers, ASME B46.1. Surface texture: Surface roughness, waviness and lay. New York; 1995.

Avella, M., Errico, M. E., Laurienzo, P., Martuscelli, E., Raimo, M., & Rimedio, R. (2000). Preparation and characterisation of compatibilised polycaprolactone/starch composites. Polymer, 41(10), 3875-3881.

Averous, L., & Boquillon, N. (2004). Biocomposites based on plasticized starch: thermal and mechanical behavior. Carbohydrate Polymers, 63(1), 61-71.

Averous, L., & Moro, L., Dole, P., Fringant, C. (2000). Properties of thermoplastic blends: starch polycaprolactone. Polymer, 41, 4157-4167.

Bergo, P., Sobral, P. J. A., & Prison, J. M. (2010). Effect of glycerol on physical properties of cassava starch films. Journal of Food Processing and Preservation, 34(2), 401–410.

Calil, M. R., Gaboardi, F., Bardi, M. G. A., Rezende, M. L., & Rosa, D. S. (2007). Enzymatic degradation of poly (e-caprolactone) and cellulose acetate blends by lipase and a-amylase. Polymer Testing, 26(2), 257–261.

Campos, A., Marconcini, J. M., Martins-Franchetti, S. M., & Mattoso, L. H. C. (2012). The influence of UV-C irradiation on the properties of thermoplastic starch and polycaprolactone biocomposite with sisal bleached fibers. Polymer Degradation and Stability, 97(10), 1948-1955.

Carvalho, A. J. F., Zambon, M. D., da Silva Curvelo, A. A., & Gandini, A. (2005). Thermoplastic starch modification during melt processing: Hydrolysis catalyzed by carboxylic acids. Carbohydrate Polymers, 62(4), 387–390.

Castillo, L., López, O., López, C., Zaritzky, N., García, M. A., Barbosa, S., & Villar, M. (2013). Thermoplastic starch films reinforced with talc nanoparticles. Carbohydrate Polymers, 95, 664– 674.

Chabrat, E., Abdillahi, H., Rouilly, A., & Rigal, L. (2012). Influence of citric acid and water on thermoplastic wheat flour/poly(lactic acid) blends. I: Thermal, mechanical and morphological properties. Industrial Crops and Products, 37 (1), 238– 246.

Dole, P., Joly, C., Espuche, E., Alric, I., & Gontard, N. (2004). Gas transport properties of starch based films. Carbohydrate Polymers, 58(3), 335–343.

Flieger, M., Kantorová, M., Prell, A., Rezanka, T., & Votruba, J. (2003). Biodegradable plastics from renewable sources. Folia Microbiol, 48(1), 27-44.

García, M. A., Pinotti, A., Martino, M. N., & Zaritzky, M. E. (2004). Characterization of composite hydrocolloid films. Carbohydrate Polymers, 56(3), 339–345.

Ghanbarzadeh, B., Almasi, H., & Entezami, A. A. (2010). Physical properties of edible modified starch/carboxymethyl cellulose films. Innovative Food Science & Emerging Technologies, 11(4), 697-702.

Ghanbarzadeh, B., Almasi, H., & Entezami, A. A. (2011). Improving the barrier and mechanical properties of corn starch-based edible films: Effect of citric acid and carboxymethyl cellulose. Industrial Crops and Products, 33, 229–235.

Holser, R. A., 2008. Thermal analysis of glycerol citrate/starch blends. Journal Applied Polymer Science, 110, 1498–1501.

Hutchings, J. B. (1999). Food color and appearance. (2nd ed.). Gaithersburg, Maryland, USA: Aspen Publishers, Inc.

Ishiaku, U. S., Pang, K. W., Lee, W. S., & Mohd Ishak, Z. A. (2002). Mechanical properties and enzymic degradation of thermoplastic and granular sago starch filled poly (ε-caprolactone). European Polymer Journal, 38(2), 393-401.

Krumova, M., Lopez, D., Benavente, R., Mijangos, C., & Perena, J. M., (2000). Effect of crosslinking on the mechanical and thermal properties of poly(vinyl alcohol). Polymer, 41(26), 9265–9271.

Koenig, M. F., & Huang, S. J. (1995). Biodegradable blends and composites of polycaprolactone and starch derivatives. Polymer, 36(9), 1877-1882.

Kweon, D. K., Kawasaki, N., Nakayama, A., & Aiba, S. (2003). Preparation and characterization of starch/polycaprolactone blend. Journal of Applied Polymer Science, 92(3), 1716–1723.

Labet, M., & Thielemans, W. (2009). Synthesis of polycaprolactone: a review. Chemical Society Reviews, 38, 3484–3504.

Lee, W. J., Youn, Y. N., Yun, Y. H., & Yoon, S. D. (2007). Physical properties of chemically modified starch (RS4)/PVA blend films—Part 1. Journal of Polymers and the Environment, 15(1), 35–42.

Liu, Z. (2005). Edible films and coatings from starch. In J. H. Han (Ed.), Innovations in food packaging. London: Elsevier Academic Press.

Lourdin, D., Della Valle, G., & Colonna, P. (1995). Influence of amylose content on starch films and foams. Carbohydrate Polymers, 27(4), 261-270.

Ma, X., Chang, P.R., Yu, J., & Stumborg, M. (2009). Properties of biodegradable citric acid-modified granular starch/thermoplastic pea starch composites. Carbohydrate Polymers, 75(1), 1-8.

Mali, S., Grossmann, M. V. E., García, M. A., Martino, M. N., & Zaritzky, N. E. 2005. Mechanical and thermal properties of yam starch films. Food Hydrocolloids, 19(1), 157–164.

Mark, J., E. (1999). Polymer Data Handbook. (2nd ed.). New York: Oxford University Press, Inc.

Mathew, S., & Abraham, T. E. (2008). Characterisation of ferulic acid incorporated starch-chitosan blend films. Food Hydrocolloids, 22(5), 826-835.

Matzinos, P., Tserki, V., Gianikouris, C., Pavlidou, E., & Panayiotou, C. (2002). Processing and characterization of LDPE/starch/PCL blends. European Polymer Journal, 38(9), 1713.

McHugh, T. H., Avena-Bustillos, R., & Krochta, J. M. (1993). Hydrophobic edible films: Modified procedure for water vapour permeability and explanation of thickness effects. Journal of Food Science, 58(4), 899–903.

Olivato, J. B., Grossmann, M. V. E., Yamashita, F., Eiras, D., & Pessan, L. A. (2012). Citric acid and maleic anhydre as compatibilizers in starch/poly(butylene adipate-co-terephthalate) blends by one-step reactive extrusion. Carbohydrate Polymers, 87(4), 2614-2618.

Ortega-Toro, R., Jiménez, A., Talens, P., & Chiralt, A. (2014a). Effect of the incorporation of surfactants on the physical properties of corn starch films. Food Hydrocolloids, 38(1): 66–75.

Ortega-Toro, R., Jiménez, A., Talens, P., & Chiralt, A. (2014b). Properties of starch-hydroxypropyl methylcellulose based films obtained by compression molding. Carbohydrate Polymers, 109 (30), 155–165.

Reddy, N., & Yang, Y. (2010). Citric acid cross-linking of starch films. Food Chemistry, 118(3), 702-711.

Rindlav, A., Hulleman, S. H. D. & Gatenholma, P. (1997). Formation of starch films with varying crystallinity. Carbohydrate Polymers, 34(1–2): 25–30.

Rosa, D. S., Lopes, D. R., & Calil, M. R. (2005). Thermal properties and enzymatic degradation of blends of poly(e-caprolactone) with starches. Polymer Testing, 24(6), 756–761.

Sánchez-González, L., Cháfer, M., Chiralt, A. & González-Martínez, C. (2010). Physical properties of edible chitosan films containing bergamot essential oil and their inhibitory action on Penicillium italicum. Carbohydrate Polymers, 82(2), 277-283.

Shi, R., Zhang, Z., Liu, Q., Han, Y., Zhang, L., Chen, D., & Tian, W. (2007). Characterization of citric acid/glycerol co-plasticized thermoplastic starch prepared by melt blending. Carbohydrate Polymers, 69(4), 748-755.

Thiebaud, S., Aburto, J., Alric, I., Borredon, E., Bikiaris, D., Prinos, J., & Panayiotou, C. (1997). Properties of fatty-acid esters of starch and their blends with LDPE. Journal of Applied Polymer Science, 65(4), 705–721.

Wang, N., Yu, J., Chang, P. R., & Ma, X. (2007). Influence of citric acid on the properties of glycerol-plasticized dry starch (DTPS) and DTPS/poly(lactic acid) blends. Starch/Starke, 59(9), 409–417.

Wang, N., Zhang, X., Han, N., & Bai, S. (2009). Effect of citric acid and processing on the performance of thermoplastic starch/montmorillonite nanocomposites. Carbohydrate Polymers, 76(1), 68–73.

Xie, X. J., Liu, Q., & Cui, S. W. (2006). Studies on the granular structure of resistant starches (type 4) from normal, high amylose and waxy corn starch citrates. Food Research International, 39(3), 332–341.

Yoon, S.-D., Chough, S.-H., & Park, H.-R. (2006). Properties of starch-based blend films using citric acid as additive. II. Journal of Applied Polymer Science, 100(3), 2554–2560.

Yu, J., Wang, N., & Ma, X. (2005). The effects of citric acid on the properties of thermoplastic starch plascitized by glycerol. Starch–Stärke, 57(10), 494-504.

Yun, Y. H., Wee, Y. J., Byun, H.S., & Yoon, S.D. (2008). Biodegradability of chemically modified starch (RS4)/PVA blend films: Part 2. Journal of Polymers and the Environment, 16(1), 12-18.

CHAPTER 5

IMPROVEMENT OF PROPERTIES OF GLYCEROL PLASTICIZED STARCH FILMS BY BLENDING WITH A LOW RATIO OF POLYCAPROLACTONE AND/OR POLYETHYLENE GLYCOL

Rodrigo Ortega-Toro, Amparo Muñoz, Pau Talens, & Amparo Chiralt

Food Hydrocolloids, Accepted Manuscript

The effect of the melt blending of polycaprolactone (PCL) (5 and 10 wt. %) and polyethylene glycol (PEG 4000 D) (2 wt. %) with corn thermoplastic starch (with 30% glycerol) on film properties was studied through the characterization of the structural, thermal and physical properties of the films obtained by compression moulding, after 1 and 5 storage weeks. PCL and PEG decreased the glass transition temperature of starch, whereas no changes in PCL melting properties were observed. Starch films could incorporate 5% PCL without a notable phase separation, leading to more stretchable and stable films. Blend films with 10% PCL showed clear phase separation, without any improved tensile properties, but with lower water vapour permeability. In ternary systems, PEG reduced the PCL-starch affinity, enhancing phase separation, whereas it did not improve the film properties with respect to starch films.

VNIVERSITAT POLITECNICA
VALENCIA
EX TECHNICA
PROGRESSIO

5.1. INTRODUCTION

Synthetic polymers have been widely used for food packaging because of their accessible cost and suitable properties. However, the growth of environmental problems caused by petrochemical-based plastics has aroused interest in the use of biodegradable alternatives coming from renewable sources (Petersen *et al*., 1999; Weber *et al*., 2002).

Among the natural polymers, such as polysaccharides and proteins, starch is a promising candidate with which to develop biodegradable films due to its high film-forming capability, its low cost, its wide availability from renewable sources and its relatively easy handling (Bertuzzi *et al.,* 2007; Romero-Bastida *et al*., 2005; Talja *et al.,* 2007). Many studies have reported the development of starch-based films as a means of reducing the environmental impact of synthetic plastics (Averous & Boquillon, 2004; Park *et al.,* 2004).

Starch based-films exhibit good barrier properties to oxygen (Dole *et al*., 2004), carbon dioxide and lipids, biodegradability (Iovino *et al*., 2008) and compostability (Lörcks, 1998). However, starch itself has poor thermo-processability and exhibits some drawbacks such as a strong hydrophilic character (Teixeira *et al*., 2009), and poor mechanical properties compared to conventional synthetic polymers (Averous & Boquillon, 2004; Teixeira *et al*., 2009), which limit its use as packaging material.

The most common methods used to overcome these limitations are chemical modification (López *et al.,* 2010), plasticization and blending with other polymers and additives (Jiménez *et al.,* 2012). Plasticizers improve the processability and/or other properties required for specific applications, by establishing intermolecular bonds with polymers and promoting conformational changes, which result in an increase in deformability. Thus, plasticizers are added to reduce brittleness, increase free volume between polymer molecules and decrease the intermolecular

forces (Romero-Bastida *et al*., 2005). Both the glass transition temperature of polymer and the processing temperature decreased in the presence of a plasticizer. The most common plasticizers used on starch-based materials are polyols, principally glycerol and sorbitol (Mali *et al.,* 2002; McHugh *et al.,* 1993; Sothornvit & Krochta, 2005).

The other way to improve the properties of starch-based materials is by blending them with other polymers. The most commonly-used polymers are poly (β-hydroxyalkanoates) (PHA), obtained by microbial synthesis, Poly(lactic acid) (PLA) and poly (ε-caprolactone) (PCL), which are derived from chemical polymerization. PCL is a linear, partially crystalline, hydrophobic polyester (Li *et al.,* 1997) with good mechanical properties and high extensibility. Its elongation and tensile strength at break point was higher than 1100% and 33 MPa, respectively (Matzinos *et al.,* 2002; Ortega-Toro *et al*., 2015)

Starch and PCL blends have been extensively studied by several authors (Avella *et al*., 2000; Averous *et al.,* 2000; Matzinos *et al*., 2002; Li & Favis, 2010; Ortega-Toro *et al*., 2015; Singh *et al.,* 2003; Wu, 2003). Several disadvantages of pure starch-based films, such as their low resilience, high degree of moisture sensitivity and high shrinkage have been overcome by adding PCL to the starch matrix. With PCL addition, the impact resistance and the dimensional stability of native starch have been significantly improved (Averous *et al*., 2000). However, the main problem of the starch/PCL blend is the phase separation of both incompatible polymers and the weak adhesion between the hydrophilic polysaccharide and the hydrophobic polyester due to their different polarity, which result in poor properties. To overcome this problem, compatibilizers have been used or the polymers have been modified (Avella *et al*., 2000). Nevertheless, the incorporation of small amounts (10%) of PCL into starch films led to a very fine dispersion of PCL in the starch matrix, decreasing the starch glass transition temperature and

improving the water vapour barrier properties of starch films (Ortega-Toro *et al*., 2015).

Compatibilizers exhibit interfacial activity inside the heterogeneous polymer blends. Generally, they are amphiphilic, low molecular weight compounds (Yolesahachart & Yoksan, 2011), ionomers (Landreau *et al.*, 2009) or a third polymer at least partially miscible in both components (Parulekar & Mohanty, 2007). In this sense, Kim *et al.* (2000) have reported that the mechanical and structural properties of 40/60 (wt. %) starch-PCL blend films were greatly improved when 10% (wt.) polyethylene glycol (PEG) of intermediate molecular weight (MW: 3.400 D) was added. The films showed the highest tensile toughness and the smallest domain size of the starch dispersed phase, which implies that PEG of the proper molecular weight could effectively stabilize the interface of the starch-PCL blend, interacting with both the starch phase and the PCL phase. Considering these aspects, PEG of intermediate molecular weight could be used as a possible compatibilizer in starch-PCL blend films, while acting as a starch plasticizer.

The aim of this work was to analyse the influence of adding PEG of intermediate molecular weight on the structural, thermal and physicochemical properties of compression moulded starch films containing a low ratio (less than 10%) of PCL in order to obtain low cost starch films with improved properties.

5.2. MATERIALS AND METHODS

5.2.1. Materials

Corn starch was obtained from Roquette (Roquette Laisa Spain, Benifaió, Spain). Its moisture content was 10% w/w and amylose percentage was 14%. Glycerol was

purchased from Panreac Química, S.A. (Castellar del Vallès, Barcelona, Spain). Polyethylene Glycol (PEG) and the polycaprolactone (PCL) were provided by Aldrich Chemistry (Sigma-Aldrich Co. LLC Madrid, Spain); their molecular weights were 4000 dalton and 80000 dalton respectively. Magnesium nitrate 6-hydrate and phosphorus pentoxide were purchased from Panreac Química, S.A. (Castellar del Vallés, Barcelona, Spain).

5.2.2. Film preparation

PEG and glycerol were dissolved in water, and then native starch was dispersed in the aqueous solution. Afterwards, the respective amount of PCL was added to the mixture. The starch:glycerol ratio was 1:0.3 and the starch:water ratio was 1:05 in every case. The other components were added in different proportions depending on the blend. The starch:PEG ratio was 1:0.02 and the starch:PCL ratios were 1:0.05 and 1:0.1. Two control films (S: glycerol plasticized starch and PCL: pure PCL) and 5 blend films were prepared: S-PEG (starch, glycerol and PEG), S-PCL5 (starch, glycerol and PCL at 5%), S-PCL5-PEG (starch, glycerol, PCL at 5%, and PEG), S-PCL10 (starch, glycerol and PCL at 10%) and S-PCL10-PEG (starch, glycerol, PCL at 10%, and PEG).

The formulations were hot-mixed on a two-roll mill (Model LRM-M-100, Labtech Engineering, Thailand) at 160 °C and 8 rpm for 30 minutes. A visually good miscibility among the components was observed. When the mixing was finished, the paste sheets formed were removed from the mill and conditioned at 25 °C and 53% Relative Humidity (RH), using a $Mg(NO_3)_2$ oversaturated solution for 48 hours, to increase the blend moisture content, thus improving processability. Afterwards, films were made in a compression moulding press (Model LP20, Labtech Engineering, Thailand). Four grams of the pre-conditioned paste were put onto steel sheets and pre-heated on the heating unit for 5 min. Compression

moulding was performed at 160 °C for 2 min and 50 bars, followed by 6 min and 150 bars; thereafter, the cooling cycle was applied for 3 min. Starch-based films were conditioned at 25 °C and 53% RH for 1 week for the initial time characterization and for 5 weeks for the final time characterization.

5.2.3. Film characterization

5.2.3.1. Structural properties

The surface morphology of the films was analyzed using an atomic force microscope (AFM) (Multimode 8, Bruker AXS, Santa Barbara, USA) with NanoScope® V controller electronics. Measurements were taken from 20 μm^2 areas using the PeakForce QNM mode. Samples conditioned for 1 week at 25 °C and 53% RH were analysed. The DMT modulus maps, derived from the PeakForce QNM Mode, were obtained, showing the surface mechanical properties of the materials. Three replicates were considered for every case.

Scanning Electron Microscopy (SEM) of the cross-sections of the films was performed by means of a microscope (JEOL JSM-5410, Japan). The film samples were maintained in desiccators with P_2O_5 for 1 week to guarantee that water was not present and 2 samples per formulation were analysed. Film pieces, 0.5 cm^2 in size, were cryofractured (by immersion in liquid nitrogen and subsequent break) from films and fixed on copper stubs, gold coated, and observed using an accelerating voltage of 10 kV.

A diffractometer (XRD, Bruker AXS/D8 Advance) was used to obtain the X-ray diffraction patterns of the films. The samples (conditioned for 1 and 5 weeks at 25 °C and 53% RH) were analyzed between 2θ: 5° and 2θ: 30° using Kα Cu radiation (λ: 1.542 Å), 40 kV and 40 mA with a step size of 0.05°, using a sample holder of

quartz. For this analysis, samples were cut into 4 cm squares. Pure PEG film was also analysed, so as to identify its characteristic peaks.

Fourier Transform Infrared spectroscopy in Total Attenuated Reflection mode (ATR-FTIR) was used to study the films at initial time. Measurements were carried out using a Tensor 27 mid-FTIR Bruker spectrometer (Bruker, Karlsruhe, Germany) equipped with a Platinum ATR optical cell and an RT-Dla TGS detector (Bruker, Karlsruhe, Germany). During analysis, the diaphragm was set at 4 mm whereas the scanning rate was 10 kHz. For the reference (air) and each formulation, 100 scans were considered from 4000 to 800 cm^{-1}, with a resolution of 4 cm^{-1}. The obtained data were treated by using OPUS software (Bruker, Karlsruhe, Germany): initial absorbance spectra were smoothed using a nine-points Savitskye Golay algorithm. After, an elastic baseline correction (200 points) was applied and then centred and normalized.

5.2.3.2. Thermal properties

A Differential Scanning Calorimeter (DSC 1 Star^{e} System, Mettler-Toledo Inc., Switzerland) was used to analyse the thermal properties. Films conditioned at initial and final time were analysed. Weighed amounts of samples were placed into aluminium pans and sealed and drilled to promote the bonded moisture loss during heating. The thermograms were obtained by heating from 25 °C to 160 °C at 20 °C/min, afterwards samples were cooled till 25 ºC, and heat in a second step to 160 ºC at the same rate. In the first scan, the bonded water in the film was eliminated and the PCL fusion parameters were determined. In the second heating scan, the glass transition of starch was analysed.

5.2.3.3. Physicochemical properties

A Palmer digital micrometer was used to measure film thickness to the nearest 0.0025 mm at six random positions around the film. Every film obtained was measured. A universal test Machine (TA.XTplus model, Stable Micro Systems, Haslemere, England) was used to determine the tensile strength (TS), elastic modulus (EM), and elongation (E) of the films, following ASTM standard method D882 (ASTM, 2001). Films conditioned at 25 °C and 53% RH for 1 and 5 weeks were evaluated. EM, TS, and E were determined from the stress-strain curves, estimated from force-distance data obtained for the different films (2.5 cm wide and 5 cm long). Samples were mounted in the film-extension grips of the testing machine and stretched at 50 mm min^{-1} until breaking. At least ten replicates were obtained from each sample.

The Water vapour permeability (WVP) of films was determined according to the ASTM E96-95 (ASTM, 1995) gravimetric method, taking into account the modification proposed by McHugh *et al.* (1993). Distilled water was placed in Payne permeability cups (3.5 cm diameter, Elcometer SPRL, Hermelle/s Argenteau, Belgium) to expose the film to 100% RH on one side. Once the films were secured, each cup was placed in a relative humidity equilibrated cabinet at 25 °C, with a fan placed on the top of the cup in order to reduce resistance to water vapour transport, thus avoiding the stagnant layer effect in this exposed side of the film. The RH of the cabinets (53%) was held constant using oversaturated solutions of magnesium nitrate-6-hydrate. The cups were weighed periodically (0.0001 g) and water vapour transmission (WVTR) was calculated from the slope obtained from the regression analysis of weight loss data versus time (once the steady state had been reached), divided by the film area. From WVTR data, the vapour pressure on the film's inner surface (p_2) was obtained using eq. (5.1), proposed by McHugh *et al*. (1993), to correct the effect of concentration gradients.

$$WVTR = \frac{P \cdot D \cdot L_n \, [P - p_2 \backslash P - p_1 \,]}{R \cdot T \cdot \Delta z} \quad (5.1)$$

where P, total pressure (atm); D, diffusivity of water through air at 25 °C (m^2 /s); R, gas law constant (82.057 x 10^{-3} m^3 atm $kmol^{-1}$ K^{-1}); T, absolute temperature (K); Δz, mean stagnant air gap height (m), considering the initial and final z value; p_1, water vapour pressure on the solution surface (atm); and p_2, corrected water vapour pressure on the film's inner surface (atm). Water vapour permeance was calculated using eq. (5.2) as a function of p_2 and p_3 (pressure on the film's outer surface in the cabinet).

$$permeance = \frac{WVTR}{p_2 - p_3} \quad (5.2)$$

Permeability was calculated by multiplying the permeance by film thickness.

The Oxygen permeability (O_2P) of the films was determined at 53% RH and 25 °C using an OX-TRAN (Model 2/21 ML Mocon Lippke, Neuwied, Germany) following the ASTM standard D3985-95 method (ASTM, 2002). The samples were conditioned at the relative humidity level of the test in a desiccator using magnesium nitrate-6-hydrate over saturated solutions for 1 and 5 weeks. Three samples were placed in the equipment for analysis, and the transmission values were determined every 20 min until equilibrium was reached. The exposure area during the tests was 50 cm^2 for each sample. To obtain the oxygen permeability, the film thickness was considered. Analyses were carried out in triplicate for each sample.

The film water content (Xw) was determined in conditioned films at 53% RH by drying at 60 °C for 24h (J.P. Selecta, S.A. Barcelona, Spain) and afterwards, placing them in a desiccator with P_2O_5 (Panreac Quimica, S.A. Castellar Vallés, Barcelona) to adjust them to 0% RH and 25 °C for 2 weeks. Analyses were carried out in triplicate for each sample.

Film solubility in water was determined by keeping the samples in bidistilled water at a film: water ratio of 1:10, for 48 h. Afterwards, the film samples were transferred to a convection oven (J.P. Selecta, S.A., Barcelona, Spain) for 24 h at 60 °C to remove the free water and then transferred to a desiccator with P_2O_5 at 25 ºC for 2 weeks to complete film drying. Sample solubility was estimated from the film initial and final weights. Analysis was carried out in triplicate for each formulation.

The Kubelka-Munk theory for multiple scattering was applied to the reflection spectra to determine the film's transparency (Hutchings, 1999). The surface reflectance spectra were determined from 400 to 700 nm using a spectro-colorimeter CM-3600d (Minolta Co., Tokyo, Japan) on both a white and a black background. As the light passes through the film, it is partially absorbed and scattered, which is quantified by the absorption (K) and the scattering (S) coefficients. The internal transmittance (Ti) of the films was determined using eq. (5.3). In this equation, R_0 is the reflectance of the film on an ideal black background. Parameters *a* and *b* were calculated by means of eqs. (5.4) and (5.5), where R is the reflectance of the sample layer backed by a known reflectance, Rg. Three replicates were used for each sample on the free film surface. For this analysis, a wavelength of 650 nm was considered.

$$T_i = \sqrt{(a - R_0)^2 - b^2} \tag{5.3}$$

$$a = \frac{1}{2}\left(R + \frac{R_0 - R + R_g}{R_0 R_g}\right) \quad (5.4)$$

$$b = \sqrt{a^2 - 1} \quad (5.5)$$

The gloss was determined on the free film surface, at an 85° incidence angle by means of a flat surface gloss meter (Multi Gloss 268, Minolta, Germany), following the ASTM standard D523 method (ASTM, 1999). The measurements were carried out in triplicate in each film and three films were considered for each formulation. The results were expressed as gloss units (GU) relative to a highly polished surface of black glass standard with a value near to 100 GU.

5.2.3.4. Statistical analysis

Statgraphics Plus for Windows 5.1 (Manugistics Corp., Rockville, MD) was used to carry out statistical analyses of data through an analysis of variance (ANOVA). Fisher's least significant difference (LSD) was used at the 95% confidence level.

5.3. RESULTS

5.3.1. Structural properties

Film microstructure, determined by the structural arrangement of film components, has a great impact on the physical properties. Figure 5.1 shows the maps of the

DMT modulus of the films' surface obtained from AFM in Peak Force QNM mode.

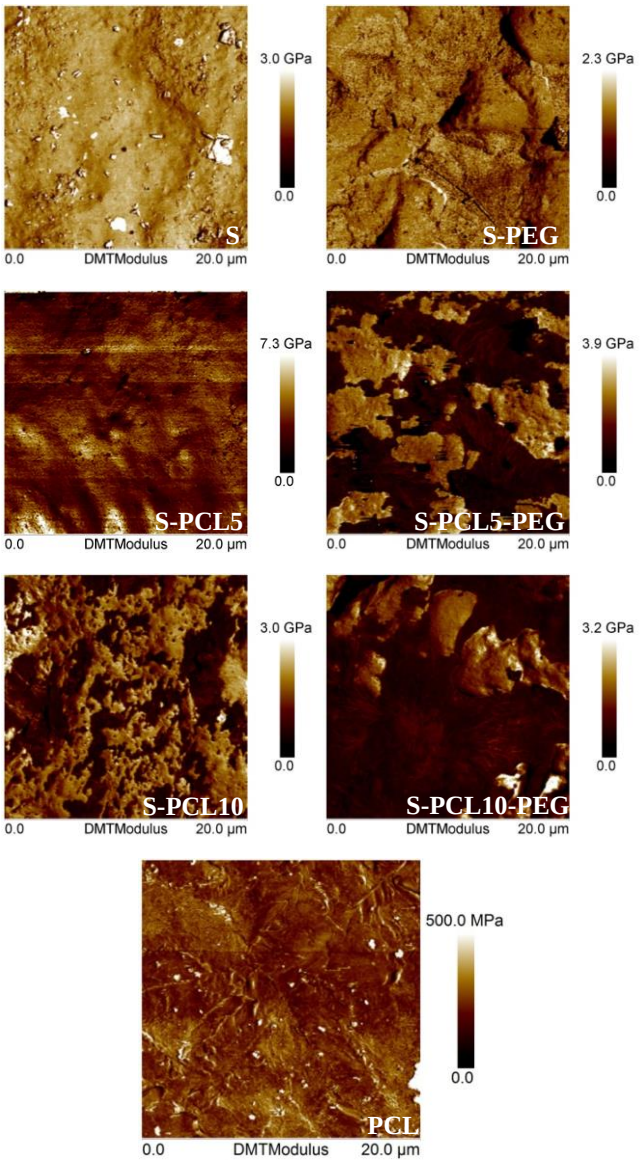

Figure 5.1.-DMT modulus maps obtained from AFM of the studied films conditioned for 1 week at 25 ºC and 53% relative humidity.

The control formulations (S and PCL) showed more homogenous values of the surface modulus than the blend films, although a great difference in their respective values could be observed for both control films. Net starch films had a much harder surface than net PCL films. The starch matrix was less homogeneous when it contained PEG, exhibiting softer zones with lower values of DMT Modulus, which suggests that PEG was not completely integrated in the glycerol plasticized starch matrix, while PEG reduced the overall rigidity of the material.

When the PCL was added to the starch matrix, the heterogeneity of the material greatly increased, showing zones with values of the modulus near to those obtained for starch films and very soft zones corresponding to the PCL domains. In the case of S-PCL5 formulations, PCL (softer zones) showed finer distribution in the starch matrix than in S-PCL10 samples. The polymer phase separation on the film surface was more evident in S-PCL10 formulations, where large, soft PCL domains could be observed. The addition of PEG to the S-PCL blends promoted the heterogeneity of the film surface; a greater differentiation of soft and hard phases could be appreciated, thus suggesting a clearer polymer phase separation at surface level.

Figure 5.2 shows the SEM micrographs of the cross section of the studied films. The structure of control formulations was more homogeneous than that of the blends. Incorporating PEG into the starch matrix hardly affected the film microstructure, although qualitative differences could be appreciated in the film matrix. The incorporation of the lowest ratio of PCL into the starch matrix led to a good dispersion in the starch continuous matrix, with very fine PCL particles. The increase in the PCL content enhanced the size of the PCL domains, coherently with the greater difficulty of dispersing a greater amount of the immiscible polymer in the starch matrix. These results indicate that the partial miscibility of PCL in the glycerol plasticized starch phase is lower than 10%, actually nearer to 5%.

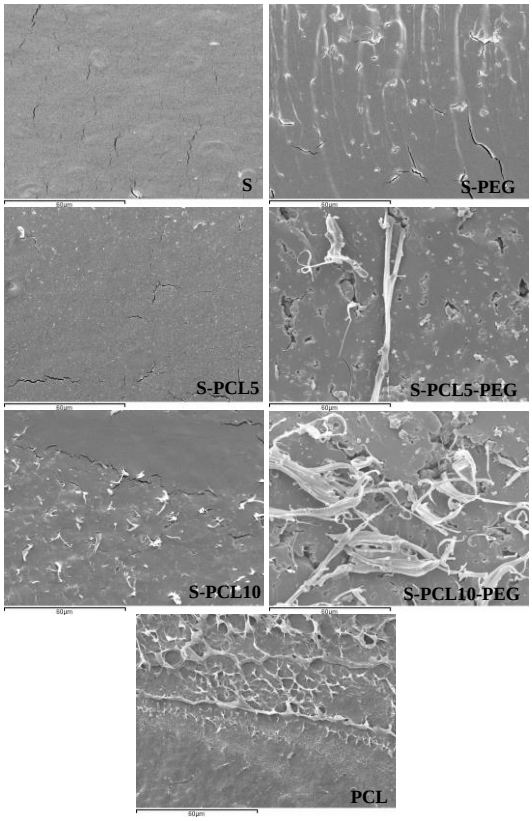

Figure 5.2.-SEM micrographs of the cross section of the studied films conditioned for 1 week at 25 ºC and 53% relative humidity.

The addition of PEG to blends clearly promoted the phase separation of polymers, since greater PCL separated domains appeared; they were separated from the starch matrix at both ratios of PCL, but especially at that of 10%. The lack of adhesion of both polymer phases could also be observed. So, the starch-PCL interactions were modified when PEG was present in the films. This could be due to the fact that PEG has a higher chemical affinity with starch than with PCL because of its predominantly hydrophilic character (HLB: 18.5, Cao & Aita, 2013) and despite its amphiphilic nature. The active points of starch able to interact with PCL could be more hindered when PEG was present in the blend.

Figure 5.3 showed the X-ray diffraction (XRD) patterns obtained for the films conditioned at 25 ºC and 53% RH for 1 and 5 weeks. The process used to obtain thermoplastic starch promoted the disruption of the typical crystallinity of native starch (type A or B) (Blanshard, 1987; Wu & Sarko, 1978) and provoked the formation of new structures with specific peaks, such as that observed at 2θ: 13.5°, which is attributed to the formation of complex between the helical conformation of amylose and endogenous starch lipids (Guilbort & Mercier, 1985). The typical forms of amylose V-type crystals were observed in starch films, with peaks at 2θ: 13.5 and 20° in the diffraction spectra, as observed by Lesmes *et al.,* 2009 and Ortega-Toro *et al.*, 2014.

On the other hand, the PCL diffractograms (Figure 5.3) showed thinner and more intense peaks than starch at 2θ: 21-22 and 24°. This indicates that the crystalline zones of PCL are bigger in size, with the amorphous region contributing much less to the diffraction pattern than in the case of starch. The addition of PEG to the starch films slightly modified the diffraction patterns of the starch films, enhancing the crystalline response (sharper peaks), especially after 5 storage weeks. This can be due to the promotion of starch crystallization or PEG crystallization, whose peaks overlap with those of starch. Characteristic diffraction spectra of PEG can be observed in Figure 5.3, showing the main peaks at 2θ: 18 and 22.6º. At final time, marked shoulders appeared at 18 and 22.6º in starch films containing PEG, while the characteristic peak at 20º splits, thus indicating changes in the starch crystallization and possible PEG crystallization, despite its low ratio in the blend.

The characteristic peaks of PCL, at 2θ 22º and 24º, appeared in the PCL-starch blends, both with and without PEG, while the amorphous response in the film diffractograms was much less pronounced when the PCL ratio increased in the film. The addition of PEG also affected the diffraction patterns of blend films in a similar way to the net starch films.

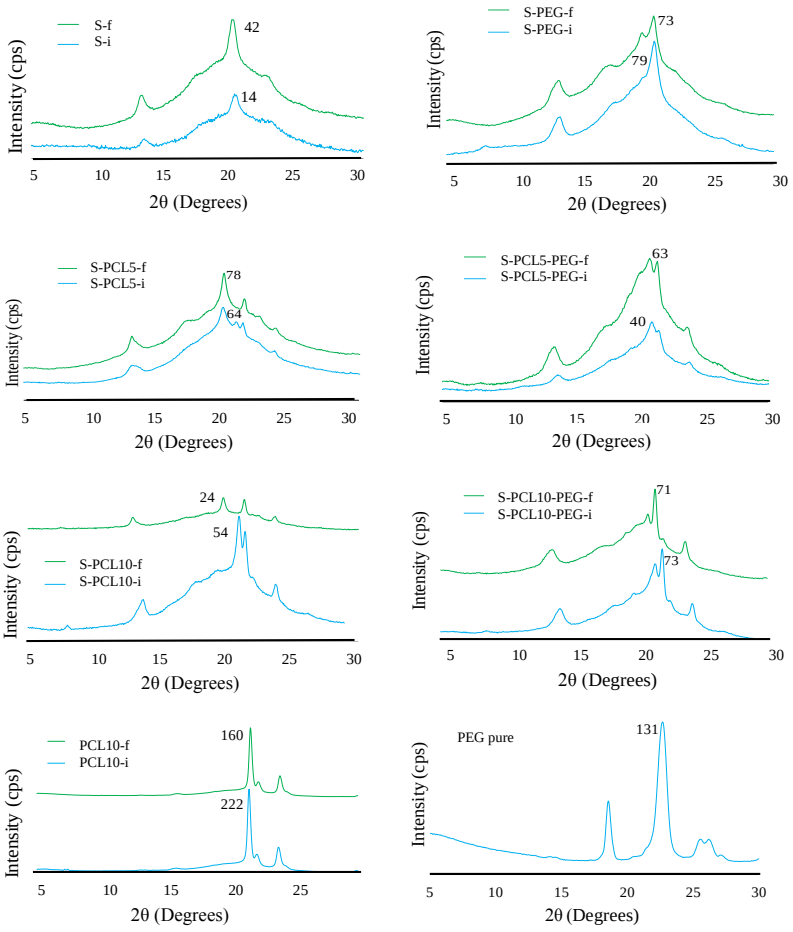

Figure 5.3.-XRD spectra of the studied films at initial (i) and final time (f) of storage at 25 ºC and 53% relative humidity. Spectra of a PEG film is also included.

FTIR spectroscopy allows us to identify molecular interactions among the components in the polymer matrix through displacement or changes in the relative intensity of the specific bands of chemical groups (Kim *et al.*, 2009; Yu *et al.*, 2013). Figure 5.4 showed the infrared spectra of studied films conditioned at 25 °C and 53% RH for 1 week, as well as that of pure PEG.

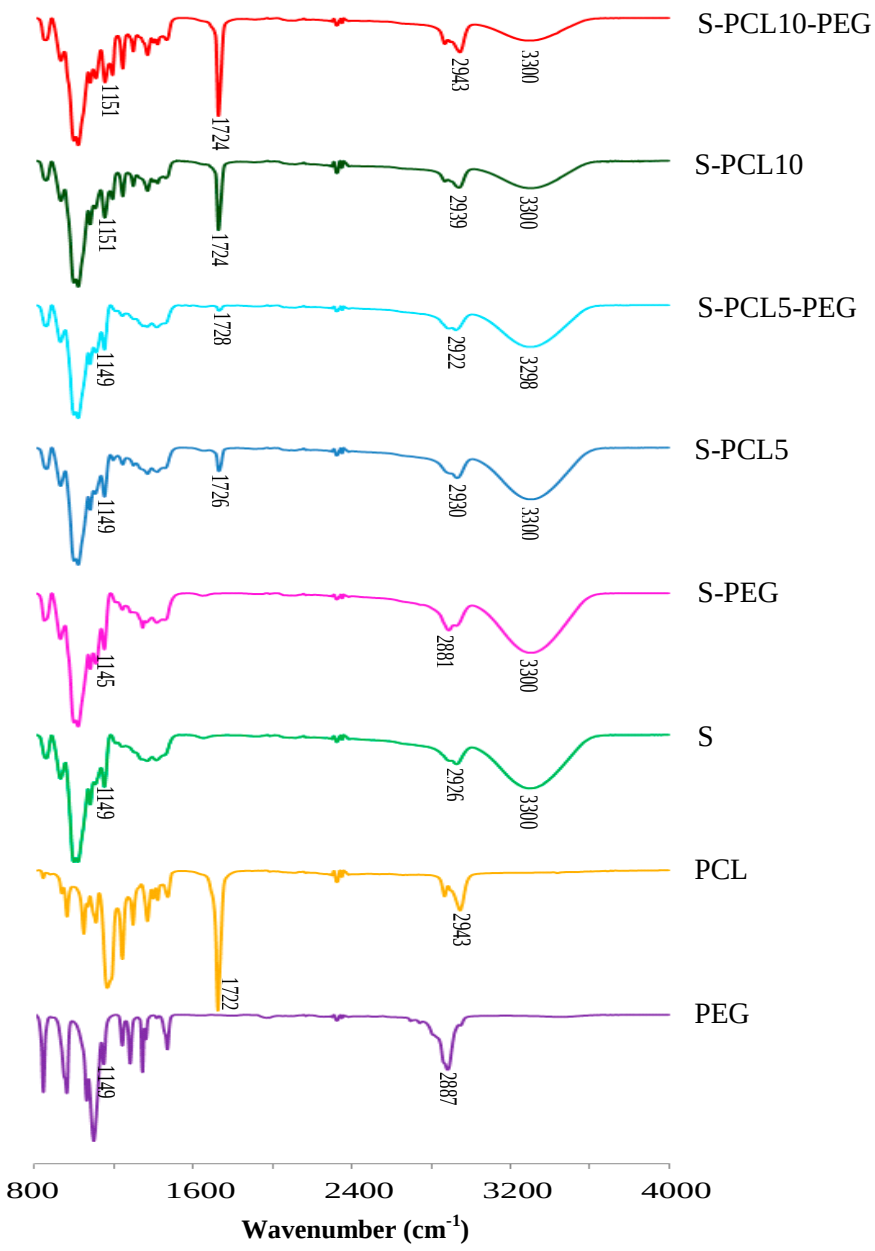

Figure 5.4.-FTIR spectra of studied films and PEG at initial time of storage at 25 ºC and 53% relative humidity.

The wavenumber of the typical vibration mode of the characteristic groups was indicated for each sample in the figure. The PCL spectrum showed the C=O stretching vibrations of the carbonyl at 1722 cm^{-1} and the (C-O-C-) stretching of the ether group at 1170 cm^{-1} and 1240 cm^{-1}, according to Elzein *et al*. (2004). The PEG spectrum showed the C-O-C- stretching at 847 $cm^{-1}$and the -C-H stretching of the methylene groups at 2887 cm^{-1}, according to Jagadish *et al*. (2012). The -OH stretching of the hydroxyl group in the region of 3000-3700 cm^{-1} was observed in the starch spectrum (Yu *et al*., 2013).

The IR spectra of blends did not show new peaks, which indicates that no new chemical bonds were formed during the film processing. However, a shift in the wavenumber of some peaks was registered in blends as compared with control formulations (S, PCL and PEG), which could indicate that molecular interactions among the components were established.

The FTIR spectra of S and S-PEG samples were very similar, with a small difference in the methylene band, with the expected higher relative intensity in the sample with PEG. In fact the -C-H stretching of methylene in PEG was observed at 2887cm-1 and in net starch films at 2926 cm-1. Likewise, the IR band at 1149 cm-1 assigned to the C-O-C stretching in starch shift to 1145 cm-1 in samples containing PEG. So, interactions between starch and PEG chains could be deduced, as reported by other authors (Kim *et al*., 2009). Nevertheless, the simultaneous use of glycerol as plasticizer could inhibit the establishment of strong interactions between starch and PEG groups (Yu *et al*., 2013).

The band of the carbonyl group of PCL was more affected when low proportions of PCL (5%) were blended, which indicates that carbonyl groups interact more effectively with the starch groups. In fact, stretching of carbonyl group shifted to 1726-1728 cm^{-1} in films containing 5% PCL and to 1724 cm^{-1} when they contained 10%, against 1722 cm^{-1} in pure PCL films. With a higher proportion of PCL, the

prevalent amount of non-interacting PCL molecules gaves rise to a less altered spectral response of the carbonyl groups. When PEG is present in the S-PCL5 blend, the carbonyl group vibration mode was more affected (1728 cm^{-1}), which suggests that carbonyls could more effectively interact with the terminal -OH groups of PEG when higher ratio PEG:PCL were present in the blend.

These results indicate that a complex balance of molecular interactions takes place in the ternary blends affecting the final arrangement of the polymer chains in matrix. As a result of the balance a clearer polymer phase separation was observed in the microstructural analyses when PEG was present in the blend.

5.3.2. Thermal properties

Table 5.1 showed the glass transition (T_g) of starch, the melting temperature (T_m) and the enthalpy (ΔH_m) of PCL in the studied films conditioned at 25 °C and 0% RH for 1 and 5 weeks. No significant differences ($p < 0.05$) between the respective T_g values of the different samples were observed for samples stored for 1 and 5 weeks, so only one value was included. The incorporation of 5% PCL in the films promoted a decrease in the T_g of starch of about 18 ºC, whereas when 10% PCL was added this was only of 12 ºC. For PCL amounts higher than 10%, a constant decrease in the starch T_g of 12 ºC was previously observed (Ortega Toro *et al*., 2015). This suggests that a greater amount of PCL was effectively miscible in the starch phase when a total of 5% is blended.

The addition of PEG also promoted a decrease in the T_g of starch (ΔT = 22 ºC), in agreement with the contribution of PEG to the polymer plasticization. Incorporating PEG was more effective than PCL because of its lower molecular weight (4000 D, against 80000 D of PCL). In the PCL-starch blends, PEG promoted an additional decrease in the T_g, but only of 4 ºC, which indicates that

PEG interactions with the starch phase are modified in the presence of PCL and *vice versa* , as previously observed from the FTIR data. The T_g values of the two blend formulations containing PEG did not exhibit significant differences. This agrees with what was previously commented on: when starch, PCL and PEG were present in the film, the total balance of molecular interactions changed, thus modifying the binary interactions between starch and PCL chains and starch-PEG molecules. This new balance reduces the starch chain's capacity to positively interact with PCL molecules leading to lower polymer compatibility, as observed in SEM and AFM images.

Table 5.1.-Mean values and standard deviation of the glass transition of starch and melting properties of PCL of the studied films equilibrated at 53% relative humidity and 25 ºC for 1 (initial time) and 5 (final time) weeks.

Films	Glass transition		Fusion on the first scan			
			Initial time		Final time	
	T_g midpoint	ΔCp (J/g K)	T_m peak	ΔH_m (J/g PCL)	T_m peak	ΔH_m (J/gPCL)
S	126.0 ± 0.3^{e}	0.112 ± 0.002^{c}	---	---	---	---
S-PEG	102.1 ± 0.8^{a}	0.028 ± 0.008^{ab}	---	---	*58.4 ± 0.5^{b}	*53 ± 2^{a}
S-PCL5	108.4 ± 0.7^{c}	0.042 ± 0.003^{b}	56.2 ± 0.5^{a1}	72.0 ± 0.6^{a1}	57.1 ± 0.4^{a1}	78.6 ± 1.5^{b2}
S-PCL5-PEG	104.4 ± 1.2^{b}	0.03 ± 0.003^{ab}	56.0 ± 0.2^{a1}	70 ± 3^{a1}	57.5 ± 0.2^{a2}	76.6 ± 0.8^{b2}
S-PCL10	114.5 ± 0.7^{d}	0.17 ± 0.02^{d}	62.4 ± 0.7^{c1}	72.4 ± 0.4^{a1}	63.9 ± 0.6^{c1}	81.9 ± 1.0^{c2}
S-PCL10-PEG	103.7 ± 0.4^{b}	0.013 ± 0.002^{a}	57.6 ± 0.2^{b1}	71.3 ± 1.4^{a1}	58.33 ± 0.04^{b2}	76.9 ± 1.3^{b2}
PCL	---	---	63.5 ± 0.6^{d1}	72.8 ± 1.4^{a1}	63.7 ± 0.6^{c1}	82.2 ± 1.5^{c2}

* Data for PEG (enthalpy in J/g PEG). Different superscript letters within the same column indicate significant differences among formulations ($p < 0.05$). Different superscript numbers within the same row indicate significant differences due to storage time ($p < 0.05$).

The melting properties of PCL are also shown in Table 5.1 for films stored for 1 and 5 weeks. Likewise, a melting endotherm, attributable to PEG, appeared in S-PEG films stored for 5 weeks at similar temperature range as PCL. The melting temperature of PEG (4000 D) was reported by Boscá et al. (2002) at 61.5 ºC, with an enthalpy value of 238 J/g. Taking into account this enthalpy value, 22% of the PEG present in the S-PEG films crystallized after 5 storage weeks. This probably corresponded to the amount of free PEG molecules, separated from the polymer matrix, as deduced from the AFM analysis. This crystallization could also occur in ternary blend films, but the endotherm would overlap with the PCL melting endotherm.

After 1 storage week, no PEG melting was observed in starch films and the PCL melting behaviour revealed very small differences among S-PCL and SPCL-PEG samples. Taking into account the melting enthalpy for totally crystallized PCL (136 J/g, Avella *et al*., 2000), the degree of crystallinity of PCL in the samples was 53%, with no significant differences between the different blend films.

Likewise, the melting enthalpy of samples stored for 5 weeks increased for both pure PCL and blend films. The progression of PCL crystallization during film storage was more marked in the case of pure PCL films, which reached a crystallinity degree of 60%, similar to that attained in blend films with 10% PCL without PEG. In the other blend films, crystallinity reached 56%. This lower crystallinity degree indicates that PCL chains were more bonded to starch or PEG molecules, thus limiting their ability to crystallize.

5.3.3. Physicochemical properties

Figure 5.5 shows the tensile behaviour of the films stored for 1 and 5 weeks and Table 5.2 shows the corresponding values of the film thickness and tensile

parameters (EM: Elastic Modulus; TS: Tensile Strength and E: Elongation at break point). A reduction in film thickness was obtained when PEG or PCL was added, in agreement with the increase in the blend flowability during compression moulding; this is due to the plasticizing effect of both components, as deduced from T_g values. The addition of PEG to the starch films led to a decrease in both the elastic modulus and tensile stress at break but increased the films' extensibility, according to the plasticizing effect of PEG.

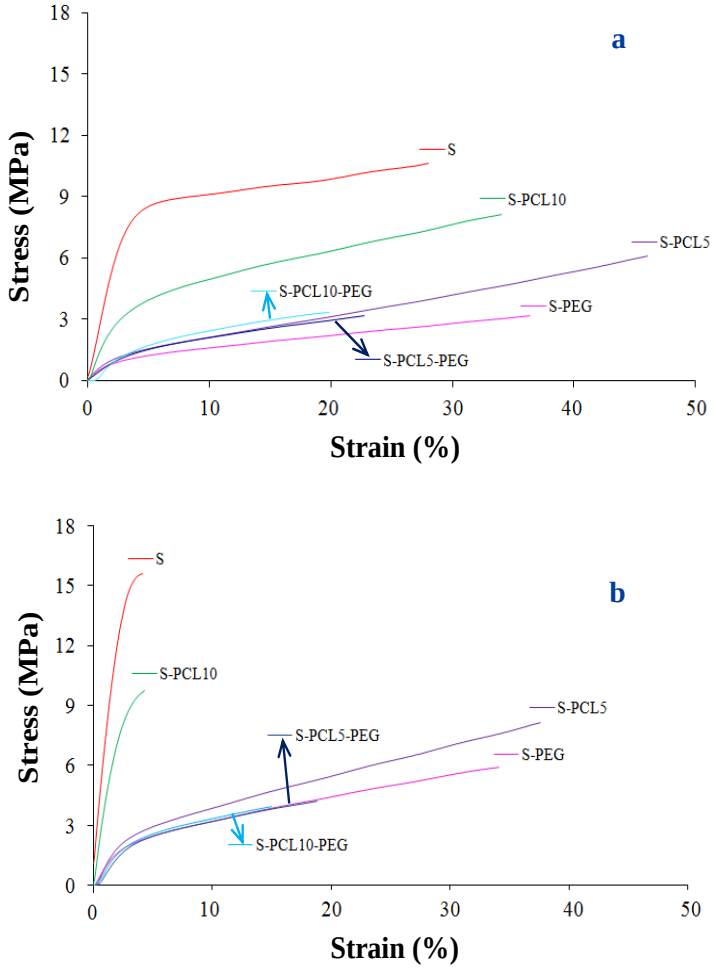

Figure 5.5.-Typical stress-strain curves of studied formulations at initial (a) and final time (b).

Table 5.2.-Mean values and standard deviation of the thickness and mechanical properties of the studied films equilibrated at 53% RH and 25 ºC for 1 week (initial) and 5 weeks (final).

Films	Thickness (µm)	EM (MPa)		TS (MPa)		E (%)	
		Initial	Final	Initial	Final	Initial	Final
S	268 ± 22^{e}	278 ± 75^{d1}	587 ± 65^{d2}	10 ± 2^{d1}	15.7 ± 1.2^{e2}	28 ± 10^{bc1}	4.1 ± 0.4^{a2}
S-PEG	243 ± 12^{d}	41 ± 12^{a1}	93 ± 16^{a2}	3 ± 0.6^{a1}	6.1 ± 1.0^{b2}	40.7 ± 6.1^{d1}	37.9 ± 6.1^{d1}
S-PCL5	261 ± 13^{e}	51 ± 13^{a1}	103 ± 10^{a2}	5.4 ± 1.5^{b1}	7.8 ± 0.7^{c2}	53.5 ± 5^{e1}	38.6 ± 4.9^{d2}
S-PCL5-PEG	219 ± 14^{c}	44 ± 10^{a1}	81 ± 12^{a2}	3.3 ± 0.5^{a1}	4.2 ± 0.7^{a2}	25.2 ± 2.7^{b1}	19.3 ± 6.7^{c2}
S-PCL10	232 ± 17^{cd}	184 ± 18^{c1}	402 ± 41^{c2}	8.4 ± 0.9^{c1}	9.1 ± 0.7^{d2}	33.5 ± 6.5^{c1}	4.2 ± 0.5^{a1}
S-PCL10-PEG	185 ± 8^{b}	69 ± 12^{a1}	92 ± 9^{a2}	3.4 ± 0.5^{a1}	4.2 ± 0.2^{a2}	18.7 ± 2.9^{a1}	14.1 ± 4.4^{b1}
PCL	149 ± 17^{a}	304 ± 11^{d1}	314 ± 51^{b1}	---	---	---	---

Different superscript letters within the same column indicate significant differences among formulations ($p < 0.05$). Different superscript numbers within the same row indicate significant differences due to storage time ($p < 0.05$).

Likewise, PEG also reduced how much the starch films harden during storage while the films maintained their stretchability better. Adding 5% PCL had a similar effect on the tensile behaviour of starch films to PEG, but with a greater increase in the film extensibility. The incorporation of PEG to this blend greatly reduced the films' extensibility coinciding with the above mentioned changes in molecular interactions. PCL at 10% provoked smaller changes in the tensile behaviour of starch films after both 1 and 5 storage weeks. The observed decrease in both the elastic modulus and tensile stress at break can be explained by the fact that the PCL dispersed domains interrupt the starch continuous matrix. The hardening of the film during storage in S-PCL10 samples was similar to what occurred in net starch films, which agrees with the fact that PCL-starch interactions were less effective in this formulation. The incorporation of PEG to S-PCL10 films led to behaviour

which was similar to that of S-PCL5-PEG films, but with slightly lowers extensibility.

According to these results, the addition of a low ratio of PCL to thermoplastic starch had a positive effect on its tensile properties, giving rise to more stretchable films with lower degree of hardening during storage. The simultaneous incorporation of PEG inhibits this effect, but also helps to maintain the stability of the tensile response of the films. This suggests that the progressive chain aggregation of starch chains during storage (Mali *et al.*, 2006) was inhibited with small amounts of PCL and/or PEG, but it progressed with a greater ratio of PCL (S-PCL10 samples).

Table 5.3 shows the water vapour permeability (WVP) and oxygen permeability (O_2P) of the studied films after 1 and 5 storage weeks. The O_2P values for S and PCL were beyond the detection limit (D. L.) (0.1-200 $cm^3 \cdot m^{-2} \cdot día^{-1}$); lower and higher, respectively.

Table 5.3.-Mean values and standard deviation of the water vapour permeability (WVP) and oxygen permeability (O_2P) of the different films after 1 (Initial) and 5 (Final) weeks of storage at 53% relative humidity and 25 ºC. D.L.: 0.1-200 cc/(m^2.day).

Films	WVP ($g \cdot mm \cdot KPa^{-1} \cdot h^{-1} \cdot m^{-2}$)		$O_2P \cdot 10^{14}$ ($cm^3 \cdot m^{-1} \cdot s^{-1} \cdot Pa^{-1}$)	
	Initial	Final	Initial	Final
S	18.1 ± 1.4^{cd1}	16 ± 2^{bc1}	< D.L.	< D.L
S-PEG	24 ± 2^{e1}	22 ± 2^{e1}	22 ± 4^{d1}	24 ± 4^{bc1}
S-PCL5	20.4 ± 0.2^{d1}	18 ± 2^{c1}	12.3 ± 0.8^{b1}	19 ± 3^{b1}
S-PCL5-PEG	16.2 ± 1.2^{bc1}	16.7 ± 0.3^{bc1}	15.4 ± 2.2^{bc1}	22 ± 5^{b1}
S-PCL10	14.5 ± 0.7^{b1}	15.8 ± 1.2^{bc1}	2.2 ± 0.9^{a1}	2.3 ± 1.5^{a1}
S-PCL10-PEG	14 ± 2^{b1}	15 ± 0.4^{b1}	19.6 ± 1.3^{cd1}	34 ± 6^{c1}
PCL	0.120 ± 0.04^{a1}	0.117 ± 0.011^{a1}	> D.L.	> D.L

D.L.: 0.1-200 $cm^3/(m^2 \cdot day)$. Different superscript letters within the same column indicate significant differences among formulations ($p < 0.05$). Different superscript numbers within the same row indicate significant differences due to storage time ($p < 0.05$).

The addition of PEG to the starch films promoted their WVP and O_2P, according to the greater plasticization of the starch matrix, with the corresponding enhancement of all diffusion dependent processes. The addition of 5% PCL did not affect the WVP of the starch films, but reduced it when incorporated at 10%. This agrees with the notable presence of a dispersed hydrophobic phase in the S-PCL10 samples, which increased the tortuosity factor for the transport of water molecules, thus limiting the water transport rate (Fabra *et al.,* 2011). At 5%, PCL was well integrated in the starch matrix (plasticizing), and so did not provoke a notable reduction in the WVP. However, the O_2P increased in this film due to both the plasticizing PCL effect and the potential increase of the film's hydrophobic character due to the PCL chains. At 10%, a smaller increase in O_2P was promoted by PCL, probably due to the lower T_g depression and the less plasticized starch matrix.

The incorporation of PEG to the binary blends led to a reduction in the WVP and an increase in the O_2P, but this was only significant in S-PCL5 and S-PCL10 samples, respectively. This can be explained by the promotion of PCL phase separation, commented on above, which gave rise to the notable increase of PCL dispersed domains in the samples. In samples with 5% PCL, this significantly increased the tortuosity factor for the transfer of water molecules, while in samples with 10% PCL this significantly increased the ratio of the hydrophobic dispersed phase, thus raising the oxygen solubility. In no formulation did any significant changes in the films' barrier properties occur during storage. This indicates that, even when structural changes occurred, these did not affect mass transport properties of the films.

Table 5.4 shows the water content (Xw) and film solubility in water of the studied films. Except those of net PCL, the water content of all the films increased during storage at 53% RH, which indicates that equilibrium moisture content was not

reached after 1 conditioning week. After 5 weeks, the moisture content of films containing PEG and 5% PCL was higher than that of the net starch films, which suggests that starch interactions with these molecules led to an increase in the active points for water sorption. This behaviour has also been observed in corn starch-carboxymethylcellulose/methylcellulose films (Arik Kibar & Ferhunde, 2013). Nevertheless, samples with 10% PCL showed values closer to those of the starch films. Likewise, the water solubility of the films was only significantly reduced when they contained 10% PCL, without PEG.

Table 5.4.-Mean values and standard deviation of the water content (g water/g dried film) and film solubility (g solubilised film/g initial dried film) of the different films stored at 53% relative humidity and 25 ºC for 1 (Initial) and 5 (Final) weeks.

Films	Xw		Film solubility	
	Initial	Final	Initial	Final
S	0.0613 ± 0.0006^{b1}	0.079 ± 0.004^{c2}	0.19 ± 0.07^{c1}	0.24 ± 0.05^{d1}
S-PEG	0.085 ± 0.002^{e1}	0.128 ± 0.005^{f2}	0.17 ± 0.04^{bc1}	0.21 ± 0.02^{cd1}
S-PCL5	0.091 ± 0.007^{f1}	0.1146 ± 0.0013^{e2}	0.18 ± 0.05^{bc1}	0.198 ± 0.004^{c1}
S-PCL5-PEG	0.0794 ± 0.0006^{d1}	0.106 ± 0.004^{d2}	0.208 ± 0.011^{c1}	0.208 ± 0.002^{cd1}
S-PCL10	0.0664 ± 0.0004^{c1}	0.074 ± 0.003^{bc2}	0.120 ± 0.009^{b1}	0.138 ± 0.002^{b2}
S-PCL10-PEG	0.0602 ± 0.0007^{b1}	0.070 ± 0.003^{b2}	0.16 ± 0.02^{bc1}	0.173 ± 0.007^{bc1}
PCL	0.003 ± 0.002^{a1}	0.0021 ± 0.0005^{a1}	0.00022 ± 0.00011^{a1}	0.0004 ± 0.0002^{a1}

Different superscript letters within the same column indicate significant differences among formulations ($p < 0.05$). Different superscript numbers within the same row indicate significant differences due to storage time ($p < 0.05$).

Table 5.5 showed the optical properties of the films: gloss and internal transmittance, related to the film transparency. No marked changes in gloss or

transparency were provoked by the addition of PEG or PCL to starch films; the least glossy and transparent sample was S-PCL10, probably due to the greater amount of dispersed PCL domains in the starch continuous matrix. This provokes both discontinuities in the refractive index through the film and irregularities at surface level, which causes light dispersion, decreasing both surface gloss and transparency.

Throughout storage, a gloss reduction occurred in every formulation, whereas transparency slightly increased in almost all cases. These changes could be attributed to the moisture gain in the films (with more open and transparent structures) which, in turn, can provoke starch crystallization at surface level (with greater molecular mobility), thus increasing surface roughness.

Table 5.5.-Mean values and standard deviation of the gloss and internal transmittance (Ti) of the different films after 1 (Initial) and 5 (Final) storage weeks at 53% relative humidity and 25 ºC.

Films	Gloss (85°)		Ti (650nm)	
	Initial	Final	Initial	Final
S	40 ± 5^{ab1}	37.2 ± 1.5^{c1}	85.1 ± 0.3^{e1}	84.2 ± 0.2^{b2}
S-PEG	49 ± 6^{bc1}	21 ± 5^{a2}	83.6 ± 0.3^{de1}	84.4 ± 0.7^{b1}
S-PCL5	47 ± 11^{b1}	25 ± 8^{a2}	80.1 ± 0.7^{b1}	83.8 ± 0.2^{b2}
S-PCL5-PEG	49 ± 12^{b1}	24 ± 12^{a2}	82.5 ± 0.3^{cd1}	84.7 ± 0.3^{b2}
S-PCL10	37 ± 9^{a1}	35 ± 6^{bc1}	77.3 ± 0.6^{a1}	79.8 ± 0.6^{a2}
S-PCL10-PEG	49 ± 7^{bc1}	28 ± 9^{ab2}	81.2 ± 0.6^{bc1}	83.77 ± 0.03^{b2}
PCL	59 ± 16^{c1}	57 ± 9^{d1}	78 ± 2^{a1}	78 ± 2^{a1}

Different superscript letters within the same column indicate significant differences among formulations ($p < 0.05$). Different superscript numbers within the same row indicate significant differences due to storage time ($p < 0.05$).

5.4. CONCLUSIONS

Glycerol plasticized starch films could incorporate 5% PCL without a notable phase separation, leading to the improved stretchability and storage stability of the films. Blend films with 10% PCL exhibited clear phase separation and poor starch-PCL interactions which did not improve the starch tensile properties, although the film water vapour permeability was reduced. In ternary systems with PEG, the total balance of molecular interactions reduced the PCL-starch affinity, enhancing phase separation. They did not exhibit improved film properties with respect to starch films. PEG partly separates from the glycerol plasticized starch matrix, crystallising after long storage times.

5.5. REFERENCES

American Society for Testing and Materials, ASTM E96-95. Standard test methods for water vapor transmission of materials. In annual book of ASTM. Philadelphia; 1995.

American Society for Testing and Materials, ASTM D523. Standard test method for specular gloss. In annual book of ASTM. Philadelphia; 1999.

American Society for Testing and Materials, ASTM D882. Standard test method for tensile properties of thin plastic sheeting. In annual book of ASTM. Philadelphia; 2001.

American Society for Testing and Materials, ASTM 3985-05. Standard test method for oxygen gas transmission rate through plastic film and sheeting using a coulometric sensor; 2010.

Avella, M., Errico, M. E., Laurienzo, P., Martuscelli, E., Raimo, M., & Rimedio, R. (2000). Preparation and characterisation of compatibilised polycaprolactone/starch composites. Polymer, 41(10), 3875-3881.

Averous, L. & Boquillon, N. (2004). Biocomposites based on plasticized starch: thermal and mechanical behaviours. Carbohydrate Polymers, 56(2), 111-122.

Averous, L., Moro, L., Dole, P., & Fringant, C. (2000). Properties of thermoplastic blends: starch polycaprolactone. Polymer, 41(11), 4157-4167.

Arık Kibar, E. A. & Ferhunde, U. (2013). Thermal, mechanical and water adsorption properties of corn Starch-carboxymethylcellulose/methylcellulose biodegradable films. Journal of Food Engineering, 114(1), 123–131.

Bertuzzi, M. A., Armada, M., & Gottifredi, J. C. (2007). Physicochemical characterization of starch based films. Journal of Food Engineering, 82(1), 17–25.

Blanshard J. M. V. (1987). Starch granule structure and function: a physicochemical approach. In: T. Galliard (Ed.), Starch: Properties and Potential, (1st ed.). New York: John Wiley & Sons.

Boscá, M., Bellver, M., & Ramos, M. (2002). Characterization and solubility study of binary mixtures of flunarizine/polyethylene glycol 4000. Ars Pharmaceutica, 43(1-2), 73-82.

Cao, S., & Aita, G. A. (2013). Enzymatic hydrolysis and ethanol yields of combined surfactant and dilute ammonia treated sugarcane bagasse. Bioresource Technology, 131, 357-364.

Dole, P., Joly, C., Espuche, E., Alric, I., & Gontard, N. (2004). Gas transport properties of starch based films. Carbohydrate Polymers, 58(3), 335–343.

Elzein, T., Nasser-Eddine, M., Delaite, C., Bistac, S., & Dumas, P. (2004). FTIR study of polycaprolactona chain organization at interfaces. Journal of Colloid and Interface Science, 273(2), 381-387.

Fabra, M. J., Pérez-Masiá. R., Talens, P., & Chiralt, A. (2011). Influence of the homogenization conditions and lipid self-association on properties of sodium caseinate based films containing oleic and stearic acids. Food Hydrocolloids, 25, 1112–1121.

Guilbort, A., & Mercier, C. (1985). The poly- saccharides, vol. 3. London: Academic Press.

Hutchings, J. B. (1999). Food color and appearance. (2nd ed.). Gaithersburg, Maryland, USA: Aspen Publishers, Inc.

Iovino, R., Zullo, R., Rao, M. A., Cassar, L., & Gianfreda, L. (2008). Biodegradation of poly(lactic acid)/starch/coir biocomposites under controlled composting conditions. Polymer Degradation and Stability, 93(1), 147–157.

Jagadish R. S, Raj B., Parameswara, P., & Somashekar, R. (2012). Structure property relations in polyethylene oxide/starch blended films using WAXS techniques Journal of Applied Polymer Science, 127(2), 1191–1197.

Jiménez, A., Fabra, M. J., Talens, P., & Chiralt, A. (2012). Edible and Biodegradable Starch Films: A Review. Food Bioprocess Technology, 5, 2058-2076.

Kim, C. H., Choi, E. J., & Park, J. K. (2000). Effect of PEG molecular weight on the tensile toughness of starch/PCL/PEG blends. Journal of Applied Polymer Science, 77(9), 2049–2056.

Kim, C. H., Kim, D. W., & Cho, K. Y. (2009). The influence of PEG molecular weight on the structural changes of corn starch in a starch/PEG blend. Polymer Bulletin, 63(1), 91–99.

Landreau, E., Tighzert, L., Bliard, C., Berzin, F., & Lacoste, C. (2009). Morphologies and properties of plasticized starch/polyamide compatibilized blends. European Polymer Journal, 45(9), 2609–2618.

Lesmes, U., Cohen, S. H., Shener, Y., & Shimoni, E. (2009). Effects of long chain fatty acid unsaturation on the structure and controlled release properties of amylose complexes. Food Hydrocolloids, 23(3), 667–675.

Li, G., & Favis, B.D. (2010). Morphology development and interfacial interactions in polycaprolactone/ thermoplastic-starch blends. Macromolecular Chemistry and Physics, 211, 321–333.

Li, S. M., Espartero, J. L., Foch, P., & Vert, M., (1997). Structural characterization and hydrolytic degradation of Zn metal initiated copolymer of L-lactide and ε-caprolactone. Journal of Biomaterials Science, Polymer Edition, 8(3), 165–187.

López, O. V., Zaritzky, N. E., & García, M. A. (2010). Physicochemical characterization of chemically modified corn starches related to rheological behavior, retrogradation and film forming capacity. Journal of Food Engineering, 100(1), 160–168.

Lörcks, J. (1998). Properties and applications of compostable starch-based plastic material. Polymer Degradation and Stability, 59(1-3), 245–249.

Mali, S., Grossmann, M. V. E., García, M. A., Martino, M. M., & Zaritzky, N. E. (2002). Microstructural characterization of yam starch films. Carbohydrate Polymers, 50(4), 379-386.

Mali, S., Grossmann, M. V. E., García, M. A., Martino, M. N., & Zaritzky, N. E. (2006). Effects of controlled storage on thermal, mechanical and barrier properties of plasticized films from different starch sources. Journal of Food Engineering, 75(4), 453-460.

Matzinos, P., Tserki, V., Gianikouris, C., Pavlidou, E., & Panayiotou, C. (2002). Processing and characterization of LDPE/starch/PCL blends. European Polymer Journal, 38(9), 1713-172.

McHugh, T. H., Avena-Bustillos, R., & Krochta, J. M. (1993). Hydrophilic edible films-Modified procedure for water-vapor permeability and explanation of thickness effects. Journal of Food Science, 58 (4), 899–903.

Ortega-Toro, R., Jiménez, A., Talens, P., & Chiralt, A. (2014). Properties of starch-hydroxypropyl methylcellulose based films obtained by compression molding. Carbohydrate Polymers, 109(30), 155–165**.**

Ortega-Toro, R., Collazo-Bigliardi, S., Talens, P., & Chiralt, A. (2015). Effect of the citric acid addition on the properties and ageing time of starch-polycaprolactone based films. Journal of Applied Polymer Science, DOI: 10.1002/app.42220.

Park, J. S., Yang, J. H., Kim, D. H., & Lee, D. H. (2004). Degradability of expanded starch/PVA blends prepared using calcium carbonate as the expanding inhibitor. Journal of Applied Polymer Science, 93(2), 911–919.

Parulekar, Y., & Mohanty, A. K. (2007). Extruded biodegradable cast films from polyhydroxyalkanoate and thermoplastic starch blends: fabrication and characterization. Macromolecular Materials and Engineering, 292(12), 1218–1228.

Petersen, K., Nielsen, P. V., Bertelsen, G., Lawther, M., Olsen, M. B., & Nilsson, N. H., (1999). Potential of biobased materials for food packaging. Trends in Food Science & Technology, 10(2), 52–68.

Romero-Bastida, C. A., Bello-Perez, L. A., García, M. A., Martino, M. N., Solorza-Feria, J., & Zarintzky, N. E. (2005). Physicochemical and microstructural characterization of films prepared by thermal and cold gelatinization from non-conventional sources of starches. Carbohydrate Polymers**,** 60(2), 235–244.

Singh, R. P., Pandey, J. K., Rutot, D., Degée, P., & Dubois, P. (2003). Biodegradation of poly(ε-caprolactone)/starch blends and composites in composting and culture environments: The effect of compatibilization on the inherent biodegradability of the host polymer. Carbohydrate Research, 338(17): 1759–1769.

Sothornvit, R., & Krochta, J. M. (2005). Plasticizers in edible films and coatings. In: J. H. Han, (ed.). London: Academic Press.

Talja, R. A., Helén, H., Roos, Y. H., & Jouppila, K. (2007). Effect of various polyols and polyol contents on physical and mechanical properties of potato starch-based films. Carbohydrate. Polymers, 67(3), 288–295.

Teixeira, E. M., Pasquini, D., Curvelo, A. A. S., Corradini, E., Belgacem, M. N., & Dufresne, A. (2009). Cassava bagasses cellulose nanofibrils reinforced thermoplastic cassava starch. Carbohydrate Polymers, 78(3), 422–431.

Weber, C. J., Haugaard, V., Festersen, R., & Bertelsen, G. (2002). Production and application of biobased packaging materials for the food industry. Food Additives & Contaminants, 19(1), 172–177.

Wu, H. C. H., & Sarko A. (1978). The double-helical molecular structure of crystalline B-amylose. Carbohydrate Research, 61(1), 7-25.

Wu, C. S. (2003). Physical properties and biodegradability of maleated-polycaprolactone/starch composite. Polymer Degradation and Stability, 80(1), 127–134.

Yokesahachart, C., & Yoksan, R. (2011). Effect of amphiphilic molecules on characteristics and tensile properties of thermoplastic starch and its blends with poly(lactic acid). Carbohydrate Polymers, 83(1), 22–31.

Yu, F., Prashanthaa, K., Soulestin, J., Lacrampea, M. F. & Krawczak, P. (2013). Plasticized-starch/poly(ethylene oxide) blends prepared by extrusion. Carbohydrate Polymers, 91(1): 253– 261.

CHAPTER 6

ENHANCEMENT OF INTERFACIAL ADHESION BETWEEN STARCH AND POLY(ε-CAPROLACTONE): STRATEGIES OF CHEMICAL COMPATIBILIZATION

Rodrigo Ortega-Toro, Gabirella Santagata, Giovanna Gomez d'Ayala, Pierfrancesco Cerruti, Pau Talens, Amparo Chiralt & Mario Malinconico

Carbohydrate Polymers, Under per rev

Grafted PCL (PCL_{-g}) materials with maleic anhydride and glycidyl methacrylate (PCL_{MG}) or only GMA (PCL_G) were obtained in order to combine them with thermoplastic starch to improve film properties. Grafted PCL materials were analysed as to their grafting degree (4 and 4.5 wt%, respectively for PCL_G and PCL_{MG}) and structural and thermal properties. Binary blends of PCL or grafted PCL with starch (0.2:1 wt ratio) and ternary blends, where grafted PCL was used as compatibilizer (at 2.5-5 wt%), were obtained by extrusion and compression moulding and characterized as to structural, thermal, mechanical and barrier properties. Properties of the starch-PCL_{-g} blend films were poorer than those of starch-PCL blends with only 2-5% PCL_{-g} acting as compatibilizer. The used of grafted PCL was effective at improving interactions between starch and PCL chains, as deduced from XRD, FTIR and thermal analysis, as well as the functional properties of the blend films. Grafted PCL compatibilizers improved the interfacial adhesion of starch and PCL, thus allowing us to obtain starch-PCL blend films with good mechanical performance and stability and high barrier properties, useful to meet the food packaging requirements.

Consiglio Nazionale
delle Ricerche

6.1. INTRODUCTION

Nowadays, the growing interest in environmental protection, the widespread use of petroleum-based polymers and the future scarcity of oil sources have increased interest in the development of biodegradable polymers. Starch, which is produced by many green plants as a store of energy (Zhang *et al.*, 2013) is an attractive alternative and offers several potential advantages as a raw material for plastics applications. It comes from renewable sources, can be obtained from a great variety of plant sources and is low-cost. In addition, starch has inherent biodegradability and the microorganisms capable of using it as a carbon source are extremely abundant in nature. These characteristics promote its potential use in biodegradable plastics (BeMiller & Whistler, 2009; Xie *et al.*, 2013; Pérez *et al.*, 2013).

The development of thermoplastic starch (TPS) from native starch and plasticizers allows the transformation of starch into a thermoprocesable material similarly to other conventional plastics (Averous *et al.*, 2000). An advantage of TPS is that it can be processed using typical melt processing equipment (Li & Favis, 2010) while starch-based films have good oxygen, carbon dioxide and lipid barrier properties. On the other hand, this material exhibited some drawbacks, such as its poor mechanical properties, high water adsorption capacity and water sensitivity, poor water vapour barrier properties and retrogradation phenomena during storage time (Wu, 2003; Arık Kibar & Us, 2013; Ortega-Toro *et al.*, 2014).

Nevertheless, both academia and industry have been developing different strategies for the purposes of improving the properties of starch-based materials. Of these, the following can be cited: blending with hydrophobic polymers and compounds (Averous *et al.*, 2000; Li & Fabis, 2010; Teixeira *et al.*, 2012; De Camargo *et al.*, 2013), blends with other biopolymers (Leroy *et al.*, 2012; Ortega-Toro *et al.*, 2014), the use of compatibilizer or cross-linking agents (Avella *et al.*, 2000; Wu,

2003; Sugih *et al.,* 2009) and the incorporation of organic and inorganic fillers (Woehl *et al.,* 2010).

Starch blending with PCL could be a potential option for improving the fucntionality of starch. Its hydrophobic character and biodegradability could help to decrease the water vapour permeability and the water uptake capacity of the starch-based films, while conserving their biodegradable properties (Ortega-Toro *et al*., 2015). However, the lack of interfacial adhesion between these polymers leads to poor mechanical properties (Avella *et al*., 2000; Averous *et al*., 2000) and the use of compatibilizers to improve the interface properties of both polymers is necessary.

In this sense, the PCL molecule can be modified by means of grafting reactions with maleic anhydride (MA) **(**Wu, 2003; Arbelaiz *et al.,* 2006**)** or glycidyl methacrylate (GMA) (Kim *et al.,* 2001; Sugih *et al.,* 2009), thus increasing its chemical affinity with the starch chains. This modified PCL could be used as a compatibilizer for TPS and PCL blends. After the grafting reaction, a purification step would be required in order to remove any excess ungrafted reagents for the purposes of avoidin the possible migration of these chemicals (residual monomers and oligomers of MA and GMA) from the developed films.

Laurienzo *et al.,* (2006), synthetized a new crosslinkable poly(ε-caprolactone) by the simultaneous grafting of MA and GMA to PCL in the melt. It has been reported (Laurienzo *et al*., 2006 and Mangiacapra *et al.,* 2007) that the addition of GMA promoted a greater grafting efficiency. Nevertheless, the use of this grafted PCL as a compatibilizer for starch-PCL systems has not yet been studied.

The aim of this work was to carry out two different strategies as to overcome the incompatibility between starch and PCL. The first one consisted of the direct blending of starch with PCL grafted with GMA (PCL_G) or both MA and GMA (PCL_{MG}). The second approach consisted of adding PCL_G and PCL_{MG} as

compatibilizers for starch-PCL blends. The structure of grafted PCL and the yield of the grafting reactions were analysed, as well as the structural, thermal, mechanical and barrier properties of binary and ternary blend films.

6.2. MATERIALS AND METHODS

6.2.1. Materials

Corn starch was purchased from Roquette (Roquette Laisa, Benifaió, Spain). Glycerol was obtained from Panreac Química, S.A. (Castellar delVallès, Barcelona, Spain). Polycaprolactone (PCL) (pellets~3 mm, average M_n 80.000 Daltons, impurities < 1.0% water) was provided by Fluka (Sigma–Aldrich Chemie, Steinheim, Germany). Glycidyl methacrylate (GMA) (purity 97%), maleic anhydride (MA) (purity 99.8%) and benzoyl peroxide (BPO) were supplied by Aldrich Chemicals and used as received. All other chemicals used in this work were reagent grade and used without further purification.

6.2.2. Chemical modification of PCL

PCL was modified using the methodology reported by Laurienzo *et al*. (2006). The grafting reaction was carried out in the melt by using a Brabender Plasticorder internal mixer equipped with two roller blades. The modification of PCL with maleic anhydride and glycidyl methacrylate, (PCL_{MG}) was performed as follows: a mixture of 45 g of PCL, 2.5 g of maleic anhydride, 0.5 g of benzoyl peroxide and 2.5 g of glycidyl methacrylate, the last one added dropwise, was fed into the mixer at 100 °C. The reaction was carried out at 100 °C for 20 min at a roller rate of 32 rpm. Modified PCL thus obtained, was dissolved in 500 mL of chloroform ($CHCl_3$) and then precipitated twice in a large excess of hexane. Samples were kept in a

desiccator under vacuum at 25 ºC for 12 h to remove possible unreacted components. Afterwards, the product was kept in a freezer at -20°C for 24 h until its use. The synthesis of PCL modified only with glycidyl methacrylate, PCL_G**,** was performed as follows: a mixture of 45 g of PCL, 0.5 g of benzoyl peroxide and 5 g of glycidyl methacrylate was fed into the mixer at 100 °C. The reaction was carried out as in the case of PCL_{MG} synthesis.

6.2.3. Characterization of the grafting rate and grafted PCL

The content of GMA grafted onto PCL was determined through the ^1H NMR spectra recorded with a Bruker Avance DPX300 apparatus operating at 300 MHz. The sample (about 12 mg) was dissolved in chloroform-deuterated ($CDCl_3$) and one dimensional ^1H NMR spectra were obtained. The relative peak area of the methylene proton of PCL α-carbon (2.30 ppm) and the methine proton of GMA (3.2 ppm) was considered to estimate the molar grafting ratio.

Due to the lack of total solubility of PCL_{MG} in $CDCl_3$, the grafting degree was evaluated through the content of grafted maleic anhydride in PCL_{MG} samples by FTIR spectroscopy (Perkin Elmer Spectrum 100 spectrometer) performed in chloroform solutions, taking the band at 1777 cm^{-1}; this corresponds to the symmetric stretching of the anhydride group, as the analytical reference band for quantitative determination. Firstly, a calibration curve was built up with different amount of succinic anhydride in chloroform. The obtained results are reported as the average of three determinations.

PCL and grafted PCL materials were also characterized as to their crystallization pattern through the XR diffraction spectra and thermal behaviour by DSC and FTIR, as described below. To this end, films of PCL and grafted PCL were

obtained by compression moulding the pellets by using the same procedure as described below for blend films.

6.2.4. Preparation of formulations

Native corn starch, previously dried overnight in an oven at 60°C under vacuum, was hand-blended with glycerol and water in a starch:glycerol:water weight ratio of 1:0.3:0.5 w/w. This formulation (S) was considered as the control. In S-PCL binary blends the polysaccharide always represents the main component (i.e., the matrix), whereas neat or functionalized PCL (PCL_{MG} or PCL_{G}) were added in a weight ratio of 0.2 g / g of starch.

For ternary blends, where grafted PCL (PCL_{G} or PCL_{MG}) was used as compatibilizer, the same ratio (0.2 g/g of starch) of net PCL was maintained and two different amounts of PCL_{G} or PCL_{MG} were incorporated: 2.5 and 5 g/g total polymer (S+PCL). Hence, four ternary blends were obtained and coded as: $S_{PCLG2.5}PCL$, $S_{PCLG5}PCL$, $S_{PCLMG2.5}PCL$, $S_{PCLMG5}PCL$.

Binary and ternary blends were processed and pelletized by means of a twin-screw extruder (Teach-Line® ZK 25T, Collin, Germany) with coaxial rotation. The temperature profile was as follows (from hopper to die): 60, 90, 110, 120 and 110 °C and the residence time was about 5 minutes.

To obtain films, pellets were compression moulded by means of a compression moulding press (Model C, Carver Laboratory Press, USA). Three grams of pellets were placed between two steel sheet frames and pre-heated at 130 °C for 2 min; kept at the same temperature, pellets were compression moulded at a pressure of 90 bars for 2 minutes and 220 bars for a further 2 minutes; lastly, a cooling cycle, applied for about 8 minutes, allowed films of about 230 µm to be obtained.

Before each test, all the films were conditioned in a climatic chamber set at 25°C and 50% Relative Humidity (RH). After one week of conditioning, a first sampling was analysed (initial time, ti) and a second group of films was characterized after 4 weeks of conditioning (final time, tf).

6.2.5. Film characterization

6.2.5.1. Fourier Transform Infrared (FTIR) spectroscopy

Attenuated Total Reflection Fourier Transform Infrared (FTIR-ATR) spectroscopy was carried out on the surface of compression moulded samples by means of a Perkin Elmer Spectrum 100 spectrometer, equipped with a Universal ATR diamond crystal sampling accessory. All the samples were analysed at room temperature. Spectra were recorded as an average of 64 scans in the range 4000–480 cm^{-1}, with a resolution of 4 cm^{-1}.

6.2.5.2. X-ray diffraction

A diffractometer (XRD, Bruker AXS/D8 Advance) was used to obtain X-ray diffraction patterns. All the samples, stored for 4 weeks in climatic chamber, were analysed at 25 °C and 50% RH, between 2θ: 5° and 30° using Kα Cu radiation (λ: 1.542 Á), 40 kV and 40 mA with a step size of 0.05°. For this analysis, 4 cm^2 samples were used. The degree of crystallinity of the samples was calculated from the integrated area of X-ray diffraction data, using OriginPro 8.5 software, for which we assumed Gaussian profiles for crystalline and amorphous peaks. The areas under the crystalline (Ac) and amorphous (Aa) phases were determined in arbitrary units and the degree of crystallinity (X_c) was obtained using the relationship reported by Monteiro *et al*. (2013).

6.2.5.3. Scanning Electron Microscopy (SEM)

A morphological analysis of the films was performed by means of a Scanning Electron Microscope (SEM) FEI Quanta 200 FEG on cryogenically fractured cross-sections. SEM observations were performed in low vacuum mode (P_{H2O}: 0.7 torr), using a large field detector (LFD) and an acceleration voltage of 5–20 kV. Before the observation, the surfaces were coated with Au–Pd alloy by means of a sputtering device (MED 020, Bal-Tec AG). The coating provided the entire sample surfaces with a homogeneous layer of metal of 18 ± 0.2 nm.

6.2.5.4. Differential Scanning Calorimetry and Thermogravimetric Analysis

Differential scanning calorimetric measurements (DSC) were performed by a TA DSC-Q2000 instrument equipped with a TA Instruments DSC cooling system. The analyses were performed under a 30 mL min^{-1} nitrogen purge gas flow. Indium was used to calibrate the temperature and energy of the calorimeter. Approximately 6 mg of the samples were placed into aluminium pans, sealed and analysed according to the following procedures. All the specimens were equilibrated at 25 ºC and heated up to 110 ºC at 20 ºC/ min. Then an isotherm step was performed at 110°C for 60 min in order to remove the free and bound water that could mask starch T_g (Russo *et al*., 2010). Afterwards, the samples were cooled to -80 ºC at 10 ºC/min, thermally stabilized for 2 min at that temperature and, finally, re-heated up to 200 ºC at 20 ºC/min, in order to erase any thermal history. A DSC cooling rate was selected in an attempt to mimic what occurs during film preparation under compression moulding, where the water chilled system allowed the samples to be cooled at about 10°C/min. For each sample, data analysis was averaged on a set of three measurements.

Thermogravimetric analyses (TGA) were carried out with a Mettler Thermogravimetric Analyzer Mod. TG 50. The measurements were performed on samples of about 8–10 mg, placed in ceramic crucibles, from 25 to 700 ºC at a heating rate of 10 ºC/min, in a nitrogen atmosphere with a nominal gas flow rate of 30 mL/min. For each composition, the thermogravimetric tests were performed in triplicate.

6.2.5.5. Tensile properties

Tensile tests were performed using an Instron machine, model 4505, equipped with a 1 kN load cell and interfaced with a personal computer for data acquisition, following the ASTM D638 test method. Dumbbell-shaped films (4 mm width, 50 mm length) were used. All the measurements were taken at room temperature, at a crosshead speed of 10 mm min^{-1}, a gauge length of 25 mm and at a nominal strain rate of 0.45 mm min^{-1}. At least 7 analysed samples were used to calculate average values of Young's modulus (EM), tensile strength (TS) and elongation at break (E)

6.2.5.6. Water vapour permeability, oxygen permeability and carbon dioxide permeability

Water vapour and carbon dioxide permeability tests were performed by means of Extra Solution Multiperm equipment, whereas the oxygen permeability analyses were carried out using an Extra Solution PermO_2 device. All the films were tested at 25°C and 50% RH. The exposed area of the film was 8.5 cm^2. The collected data were converted into water vapour, oxygen and carbon dioxide transmission rates (WVTR, O_2TR, CO_2TR), corresponding to the gas flow between two parallel surfaces under steady conditions, at a specific temperature and RH. The permeability coefficient, P, was calculated by normalizing WVTR, O_2TR, and

CO_2TR with respect to film thickness and dividing by the gas partial pressure in the bottom chamber. At least three tests were conducted for each film sample in order to confirm the reproducibility of the data.

6.2.5.7. Statistical analysis

Statgraphics Plus 5.1 (Manugistics Corp. Rockville, MD) was used to carry out statistical analyses of data through analysis of variance (ANOVA). Fisher's least significant difference (LSD) was used at the 95% confidence level. Homogeneous groups were reported as numbers or letter superscripts.

6.3. RESULTS

6.3.1. Synthesis of PCL_{MG} and PCL_G and structural characterization

In order to enhance the interfacial adhesion between starch and PCL, functional polar groups were chemically grafted on hydrophobic PCL chains. In particular, PCL was modified by inserting both maleic anhydride (MA) and glicydil methacrylate reactive molecules (GMA) (PCL_{MG}) or only GMA (PCL_G) on its macromolecular backbone, thus obtaining two differently functionalized polymers. PCL modifications were obtained by radical grafting, following the procedure described by Laurienzo *et al.* (2006). As concerns PCL_{MG}, a direct grafting of MA on PCL was inhibit due to the low reactivity and steric hindrance of maleic anhydride, as shown by John *et al.* (1997). With the aim of enhancing the functionalization degree of MA, the more reactive GMA co-monomer was added to the bulk. Being an electron donor to MA, GMA supports its insertion, thus increasing the grafting efficiency. Figures 6.1 shows the reaction mechanisms involved in the synthesis of the two functionalized PCL.

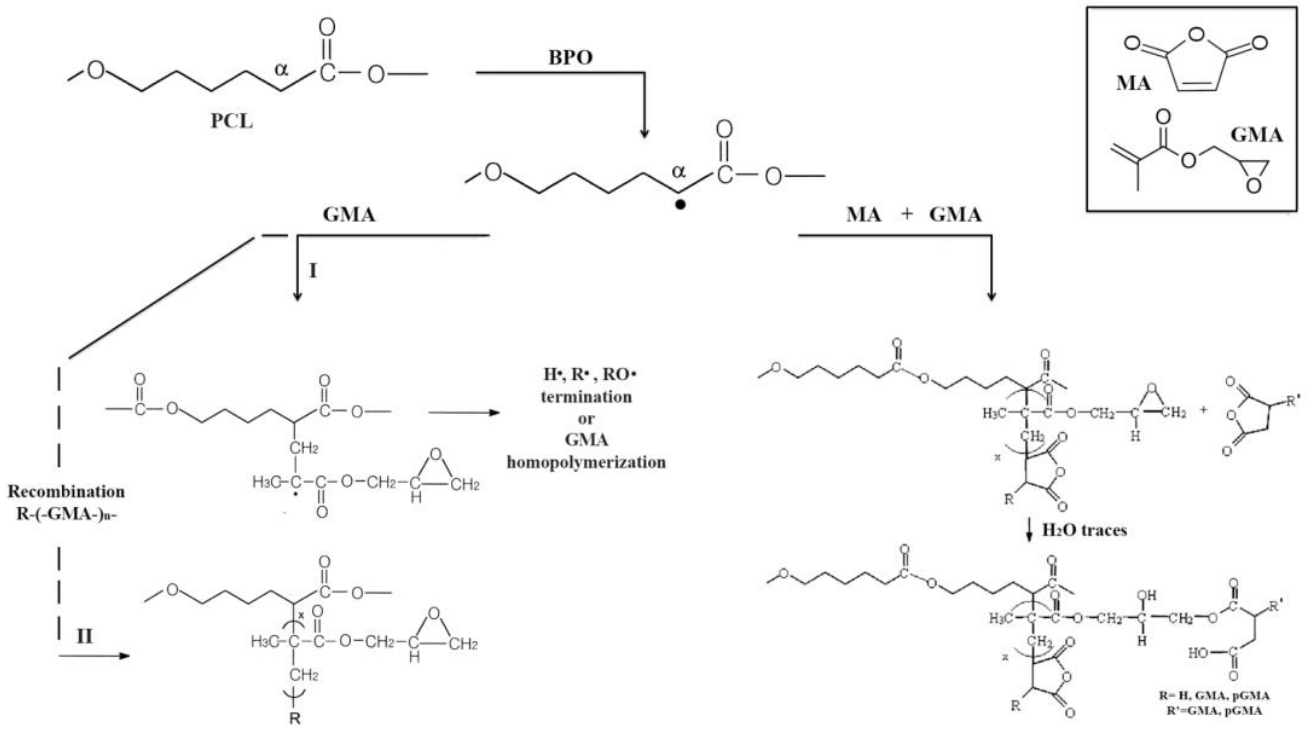

PCL_G **PCL_{MG}**

Figure 6.1.-Schematic representation of grafting reactions of PCL with maleic anhydride and glycidyl methacrylate (PCL_{MG}) and with only glycidyl methacrylate (PCL_G).

Figure 6.2 shows FTIR-ATR spectra of PCL and grafted PCL. In particular, the PCL_{MG} spectrum shows new peaks at 1780 and 1850 cm^{-1}, respectively attributed to the symmetric and asymmetric stretching of the carbonyl groups of the grafted anhydride. The quantitative determination of grafted maleic anhydride, performed by FTIR analysis as reported in the experimental section, revealed a grafting weight percentage of 4.5 ± 0.9%. Moreover, NMR analysis (spectrum not shown) confirms the occurrence of MA grafting, since the presence of the typical anhydride signal at δ = 2.5 ppm (Laurienzo *et al*., 2006).

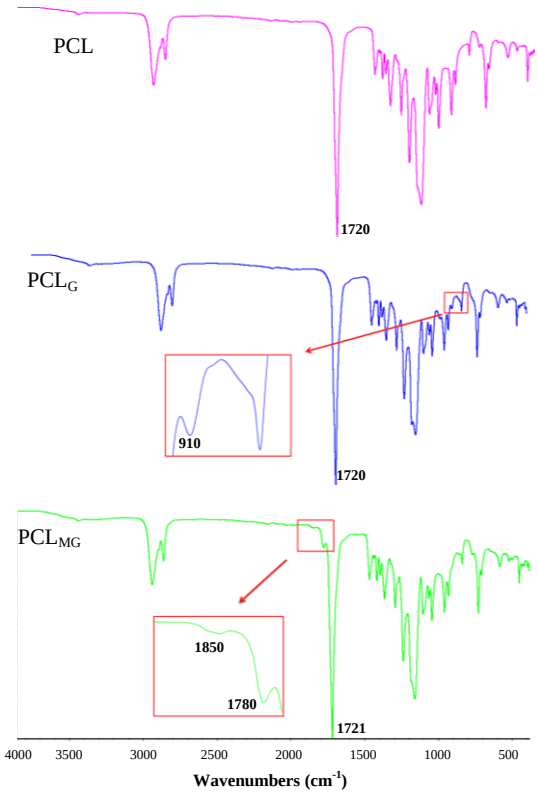

Figure 6.2.-FTIR-ATR spectra of PCL and grafted PCL (PCL_G and PCL_{MG}).

As concerns PCL_G, the FTIR-ATR spectrum displays the characteristic peak of the asymmetric stretching vibration of epoxy ring C-O bonds at 910 cm^{-1}, thus suggesting that PCL functionalization mostly involved the double bond of the methacrylate unit. This hypothesis is furthermore confirmed by NMR analysis. Indeed, the PCL_G spectrum shows characteristic signals relative to methine and methylene protons of epoxy rings of GMA, at 3.2 ppm, 2.8 ppm and 2.6 ppm (Figure 6.3). GMA molar grafting degree was evaluated from the relative peak area of the PCL proton in α–position with respect to carbonyl (δ = 2.3 ppm) and the GMA methine proton of epoxy ring (δ = 3.2 ppm) and was found to be 4.3 ± 0.4%, which correspond to a weight percentage of 5%.

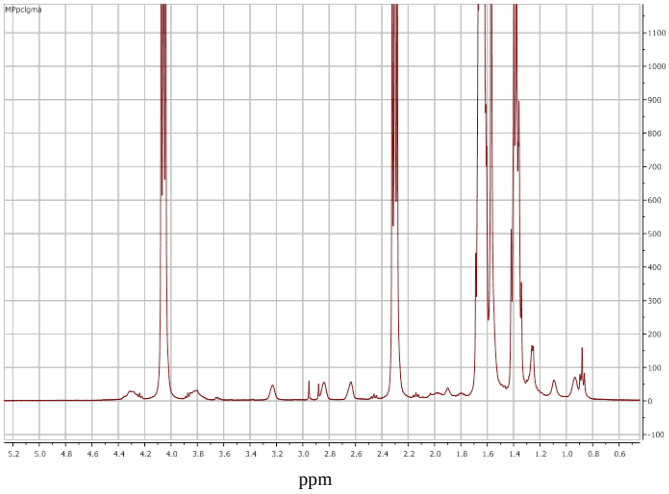

Figure 6.3.- ^1H NMR spectrum of glycidyl methacrylate grafted PCL (PCL_G).

Figure 6.4 shows XRD patterns and crystallinity degree (X_c) of all analysed films. In particular, Figure 6.4a evidences X-ray diffraction profiles of both neat PCL and grafted PCL samples.

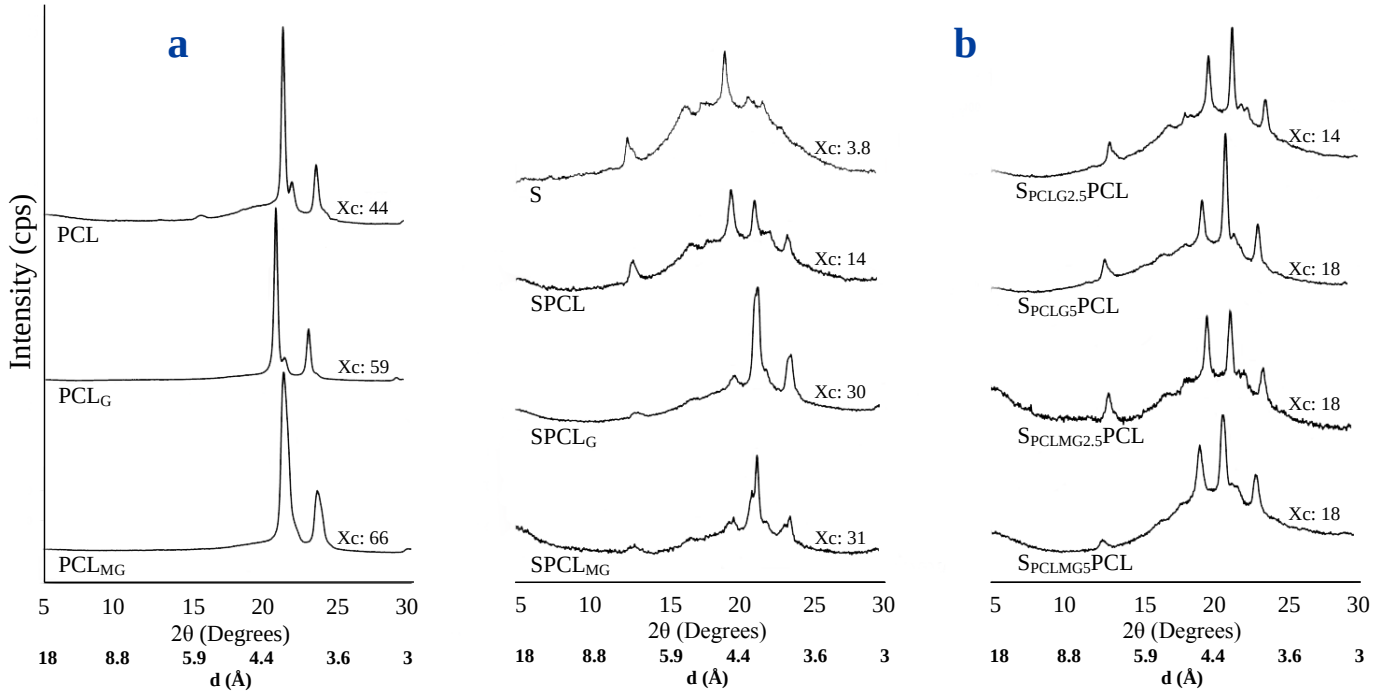

Figure 6.4.-X-Ray diffraction patterns and crystallinity degree (X_c) of: (a) PCL and PCL$_{-g}$ materials and (b) starch-based films conditioned at 50% RH and 25 ºC for 4 weeks.

In particular, three distinct crystalline peaks were observed at 2θ values of around 21.6°, 22.2° and 23.3° in the diffractograms of all three PCL-based samples, which are indexed to be (110), (111) and (200) planes, respectively, of an orthorhombic crystalline structure of PCL. The amorphous halo was fitted to a broad peak centered at 21.0° (Haque *et al*., 2012; Suzuki *et al*., 2013). Nevertheless, small displacements of the peaks could be observed for grafted PCL, thus indicating small changes in the interplanar basal spacing associated with the different packing of grafted molecules.

The crystallinity of the samples was obtained by performing a curve fitting in order to calculate the area of each peak. A linear background correction was applied to the diffraction pattern before obtaining the area of each peak, for which was assumed a Gaussian profile. As can be noticed from the data, a crystallinity value of 44% was calculated for PCL. Both functionalized PCL samples displayed a clear enhancement of crystallinity of up to 66%, although smaller crystalline formations were obtained, as deduced from the wider peaks, especially in PCL_{MG}. Hence, the presence of maleic anhydride and glycidyl methacrylate led to a more ordered polymeric matrix. This outcome could be mostly due to hydrogen bond between PCL and the polar grafted groups, responsible for a faster crystallization process during sample cooling after compression moulding. The effect was particularly marked in the case of PCL_{MG}. Actually, maleic anhydride (MA) reactivity in radical reactions is expected to be different from that of glycidyl methacrylate (GMA). Indeed, MA easily grafts onto a GMA reactive molecule, but subsequent reactions of MA onto already grafted PCL_{MG}, as previously discussed, hardly occurs. Hence, it is possible to hypothesize that, in PCL_{MG} functionalized polymers, short-grafted chains, promoting PCL structural crystallization, would be obtained. On the contrary, GMA molecules may either directly graft onto PCL radical chains, or homopolymerize by a chain transfer process, leading to longer

GMA grafted chains on a PCL backbone, this delaying PCL_G crystallization (Sugih *et al*., 2009).

XRD results are supported by the higher crystallization temperature (T_c) of grafted PCL samples with respect to PCL (less super-cooling effect), evaluated by DSC cooling ramp from the melt (as shown in Table 6.2). The polar groups grafted on PCL backbone could act as nucleating sites, providing the development of PCL small crystallization nuclei in different domains of the matrix; as a consequence the crystals growth kinetic was hampered. As a matter of fact, in Table 6.1 the melting temperature (T_m), the relative enthalpy (ΔH_m) and the crystallization degree (X_c) of neat and functionalized PCL are shown, as evaluated during the first heating run, since it better reproduces the thermal history of samples analysed by NMR, FTIR and XRD.

As shown in Table 6.1, T_m, ΔH_m and (X_c) values of functionalized PCL were lower than for pure PCL. The differences in thermal properties of the reactive PCL and plain polymer could be due to the introduction of grafted branches onto PCL backbone that induce chain structural irregularities, thus hindering PCL crystallization. Similar observations were made by Kim *et al*. (2001) for PCL-GMA. Nevertheless, in the second heating run of the DSC analysis, no differences were found between the melting behaviour (T_m and ΔH_m) of PCL and grafted PCL, which showed the same degree of crystallinity when they were thermally treated under the controlled conditions of this analysis. So, it can be concluded that GMA and MA polar molecules could act as nucleating agents in PCL matrix, but they were not able to promote the growth of crystalline domains, in this way giving rise to more amorphous material, depending on the cooling conditions.

Table 6.1.-Mean values and standard deviation of melting temperature and enthalpy and crystallization degree (X_{cm}), obtained from Differential Scanning Calorimetry on first heating scan, of studied formulation conditioned at 50% RH and 25 ºC for 4 weeks.

Films	First heating scan		
	T_m (°C)	ΔH_m (J/gPCL)	X_{cm} (%)
S	-	-	-
SPCL	$56.2 \pm 0.5a^{b}$	53.2 ± 1.4^{e}	39.1 ± 1.0^{e}
$SPCL_G$	54.3 ± 0.7^{a}	61.0 ± 0.9^{f}	44.8 ± 0.7^{f}
$SPCL_{MG}$	57.9 ± 0.9^{b}	54.8 ± 0.5^{e}	40.3 ± 0.4^{e}
$S_{PCLG2.5}PCL$	56.4 ± 1.0^{b}	49.8 ± 1.2^{d}	36.6 ± 0.9^{d}
$S_{PCLG5}PCL$	56.4 ± 0.4^{b}	53.1 ± 0.8^{e}	39.0 ± 0.6^{e}
$S_{PCLMG2.5}PCL$	56.3 ± 0.2^{b}	37.6 ± 0.8^{b}	27.7 ± 0.6^{b}
$S_{PCLMG5}PCL$	57.1 ± 0.5^{b}	53.5 ± 0.3^{e}	39.3 ± 0.2^{e}
PCL	60.8 ± 0.7^{c}	68.3 ± 0.3^{g}	50.2 ± 0.2^{g}
PCL_G	56.1 ± 0.3^{ab}	42.3 ± 0.2^{c}	31.10 ± 0.15^{c}
PCL_{MG}	56.8 ± 0.4^{b}	32.25 ± 0.3^{a}	23.7 ± 0.2^{a}

Different superscript letters within the same column indicate significant differences among formulations ($p < 0.05$).

6.3.2. Properties of starch-based blends

6.3.2.1. Structural properties of films

Infrared Spectroscopy represents a valid tool aimed to assess the physical or chemical interactions between components in polymeric blend systems. In Figure 6.5, the FTIR-ATR spectra of carbonyl stretching adsorption, related to neat PCL, SPCL and $SPCL_{-g}$ in binary and ternary blends are shown. As usually evidenced by a semicrystalline polymer, the spectrum of PCL is composed of two overlapping peaks; there is a relatively broad band centered at 1738 cm^{-1}, occurring as a shoulder of a sharper and more intense band at 1720 cm^{-1} (as shown the zoom in Figure 6.5); previously, it has been shown that the above peaks arise from the amorphous and crystalline phases of the polymer, respectively (He *et al*., 2000). After blending S with PCL and with PCL_{-g}, two interesting changes in carbonyl

stretching modes were observed: a variation of the relative intensity of the above-mentioned amorphous and crystalline peaks and a shift of the PCL crystalline band to 1724 cm^{-1}. In particular, the decrease in intensity of the crystalline carbonyl band in favour of a widening of the amorphous region, observed both in binary and ternary blends (zoom in Figure 6.5), suggests that starch chains disturb the regular packing of both PCL and functionalised PCL macromolecular structures, increasing their amorphous phases. The amorphous (Ap) and the crystalline (Cp) components of PCL carbonyl groups was quantified in the different samples by using the software package GRAMS 8.0AI, THERMO Electron Corporation. The area of each peak was calculated after performing a linear background correction and assuming mixed Gaussian-Lorentzian functions. The ratios of amorphous and crystalline areas (Ap/Cp, %) are shown in Figure 6.5 (blue square-zoom).

Furthermore, the crystalline carbonyl band moves towards higher stretching vibration frequencies, thus suggesting that a new PCL crystalline domain forms. As a matter of fact, the interaction with starch provokes both the disruption of the previous inter and intramolecular dipole interactions of carbonyl groups, responsible for both hindering local stretching vibration, and the development of a different structural organization characterized by a slight increase in the intrinsic vibration energy of the carbonyl bond (Murphy *et al*., 2012).

Another characteristic broad peak occurring about 1646 cm^{-1} is ascribed to the tightly bound water of starch (Kizil *et al*.; 2002). Santha *et al*. (1990) showed that this band concerns the vibration modes of water molecules adsorbed in the amorphous region of starch, since it is barely visible when the crystalline starch fraction increases. This peak is well discernible both in binary and ternary blends, thus suggesting that in all the investigated blends, the starch amorphous phase plays a key role in every possible polymer interactions that occur.

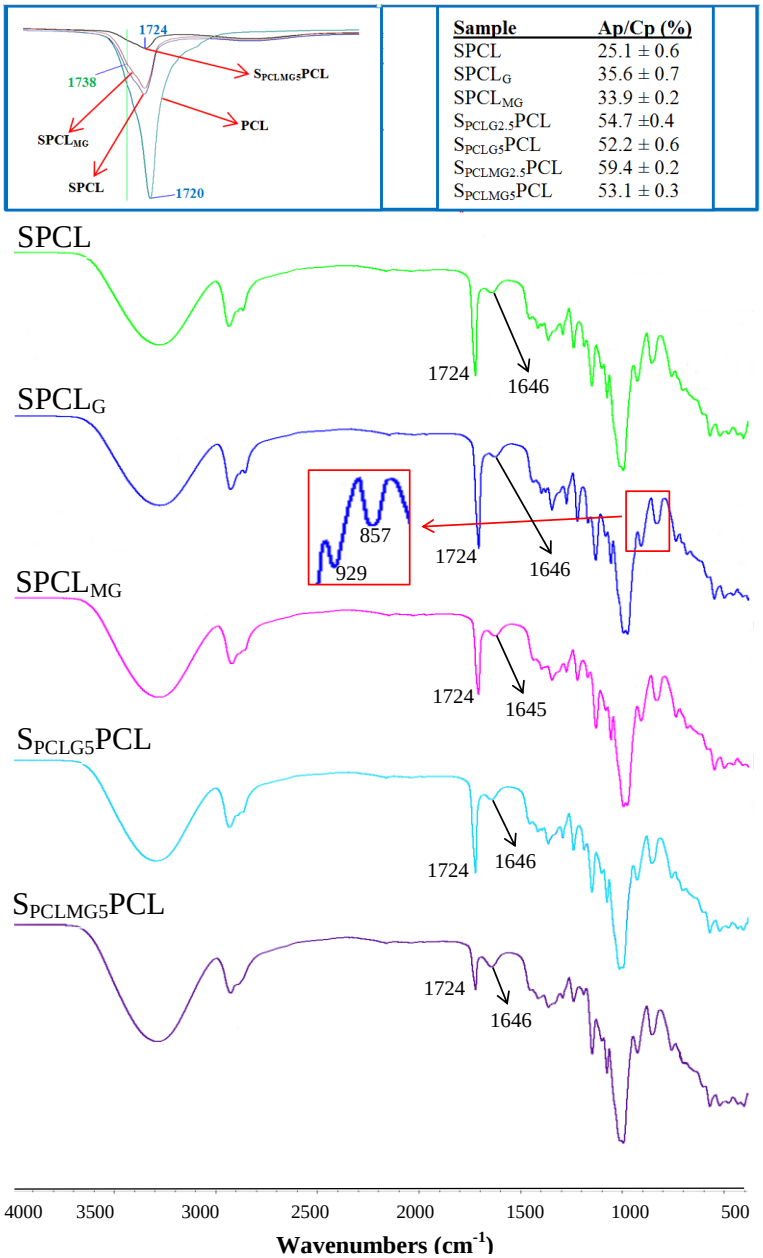

Figure 6.5.-FTIR-ATR spectra of some studied films conditioned for 4 weeks. Zooms: Blue square: carbonyl zone of some samples and the ratios of amorphous and crystalline areas (Ap/Cp). Red square: band related to the epoxy vibration C-O bonds at 910 cm^{-1} disappears.

This hypothesis is confirmed by X ray diffraction data (see Figures 6.4a,b). Indeed, all the starch-based films display lower crystallinity percentages if compared to those of PCL and PCL_{-g} samples, since the blending of all the components is sensibly affected by the amorphous phase of starch, representing the polymeric matrix of all the blends. Nevertheless, it is worth highlighting that, in binary blends, crystallinity is higher if compared to that of neat S and SPCL, as found in the case of PCL_{-g} films when compared to plain PCL. This supports the hypothesis that reactive polar groups of maleic anhydride and glycidyl methacrylate, pendant on the hydrophobic PCL backbone, can interact with –OH groups of starch chains, by means of hydrogen bond. In this way, both the interfacial association between the two polymer phases and the fast crystallization of a more packed structure are triggered.

On the other hand, the degree of crystallinity in ternary blends is comparable to that of an SPCL binary one. A likely explanation of these experimental data could be found in the low concentration of compatibilizers used (2.5-5% w/w) with respect to the SPCL blend. This implies a low ratio of polar groups to act as nucleating agents, as occurred in PCL_{-g} or binary blends. So, it could be hypothesized that, during the melting and fast cooling following the compression moulding process, the compatibilizers are not able to significantly favour polymer crystallization, the dispersion of the two polymers, hindering the development of tight interactions between the two phases. These hypotheses, strengthened by FTIR-ATR results reported in Figure 6.5 (blue square-zoom), are furthermore supported by the analysis of XRD patterns reported in Figure 6.4b, related to starch-based films. Spectrum of net starch films (S) evidences a low degree of crystallinity (3.8%) with a large amorphous region, with peaks at 2θ of 12.7º and 19.5º, which correspond to the typical crystalline forms of amylose V-type. These peaks were observed in all starch based films. According to Castillo *et al*. (2013),

the crystalline V-type can be divided into two subtypes, namely V_a (anhydrous) with peaks at 13.2º and 20.6º and V_h (hydrated) with peaks at 12.6º and 19.4º. The V_h subtype was present in net starch films, and a tendency of the peaks to shift towards higher values (typical of the V_a subtype) was observed for blends with PCL, especially in the ternary blend of $S_{PCLMG2.5}$PCL (2θ: 13.1º and 20.0º), with the subsequent decrease in the interplanar basal spacing as compared with the control formulation.

When the PCL or grafted PCL (PCL_{-g}) was blended with the starch, the characteristic peaks of PCL at about 2θ 21º and 23º clearly appeared, since overlapping with starch peaks only occurs at 2θ near 21º. Binary formulations showed a marked increase in crystallinity as compared with S, especially in blends with PCL_{-g} (up to 31%), this effect was more attenuated in ternary blends (up to 18%). As regards the interplanar spacing of PCL crystalline forms in the blends, very small differences could be observed with respect to net PCL, the exception being sample S_{PCLMG5}PCL, which showed a slight increase, coherently with a more PCL crystalline structure. The remarked upon behaviour of starch and PCL crystallization revealed that the compatibilizers have different effects on the crystallization pattern of the polymers.

6.3.2.2. Morphological properties of films

Figure 6.6 shows the micrographs of the cryogenically fractured cross-section of binary (SPCL, $SPCL_G$ and $SPCL_{MG}$), and ternary (S_{PCLG5}PCL and S_{PCLMG5}PCL) blends. From the analysis of the SEM picture of the SPCL sample, it is possible to observe some isolated but fairly dispersed PCL particles within the polymeric matrix, and some voids formed as a consequence of the debonding and pulling out of PCL fragments, following the mechanical stress applied during cryogenic fracture. This outcome suggests a poor macromolecular interconnection between

the two polymeric phases (Li & Favis, 2010; Sugih *et al.*, 2009; Cocca *et al.*, 2015).

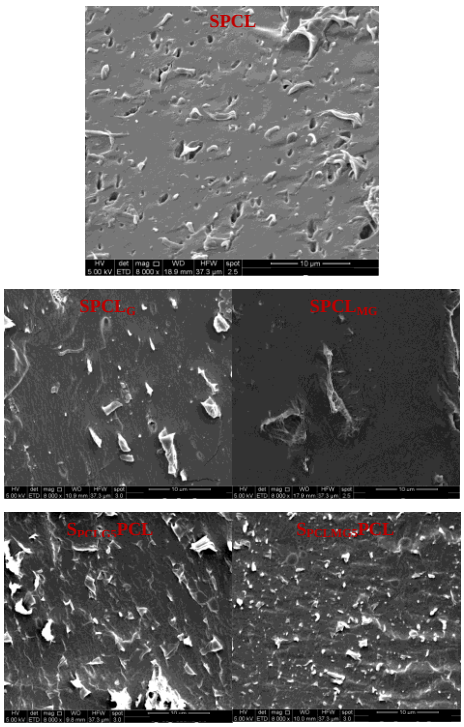

Figure 6.6.-SEM micrographs of cross-section of binary (SPCL, SPCL$_G$ and SPCL$_{MG}$) and ternary blends (S$_{PCLG5}$PCL and SP$_{CLMG5}$PCL).

However, SEM micrographs of binary and ternary blends evidenced an improved interfacial adhesion between the phases, with a diffuse halo surrounding the dispersed phase, indicating a good interaction between the polymers. As a matter of fact, the chemical interactions between hydroxyl groups of starch and polar groups of PCL$_G$ and PCL$_{MG}$ seriously affect their microstructure. Indeed, binary blends exhibited a smoother and more compact structure, resulting both in a partial coating of PCL$_G$ domains with the polymeric matrix and in a complete embedding of PCL$_{MG}$ within the starch network.

Actually, for blends containing PCL_{MG}, a greater interfacial adhesion was observed between starch and PCL. The enhancement of the interfacial adhesion is probably due to the stronger interaction between the –OH groups of starch and epoxy or the anhydride group of PCL_{MG}. Similar observations were reported by Haque *et al*. (2012) who studied PCL-based composites with cellulose micro-fibres containing PCL grafted with maleic anhydride and glycidyl methacrylate as compatibilizers.

Finally, as far as ternary blends are concerned, only $S_{PCLG5}PCL$ and $S_{PCLMG5}PCL$ micrographs are reported. Generally, it is possible to observe a fairly rough cross-section surface with a partially smooth interface between components. Nevertheless, the absence of voids and the fine dispersion of PCL, PCL_G and PCL_{MG} particles within the polymeric matrix, renders ternary blends which exhibit intermediate behaviour between SPCL blends and $SPCL_{-g}$ binary blends. In particular, in the case of $S_{PCLMG5}PCL$ sample, the presence of smaller and very finely distributed PLC domains may be noticed, thus suggesting that PCL_{MG} at 5% is a very good compatibilizer. Actually, the structure of PCL_G, as previously discussed, is quite inhomogeneous at molecular level, probably because of the homopolymerization which occurs during the grafting process on the PCL backbone. This restrains the reactive GMA groups in relatively concentrated spots, as evidenced by SEM micrographs (Haque *et al*., 2012).

6.3.2.3. Thermal properties

6.3.2.3.1. Differential Scanning Calorimetry (DSC)

The values of phase transition temperatures (Tc: crystallization peak temperature, T_m: melting peak temperature, T_g: glass transition temperature), enthalpies (ΔH_c: crystallization enthalpy, ΔH_m: melting enthalpy) and degree of crystallinity (X_c), calculated from DSC thermograms, are reported in Tables 6.1 and 6.2.

Table 6.2.-Mean values and standard deviation of crystallization temperature and enthalpy and crystallization degree (on cooling scan on DSC), melting temperature and enthalpy and glass transition temperatures (second heating scan on DSC) of studied formulation.

Films	Cooling			Second heating scan			
	T_c	ΔH_c (J/gPCL)	X_{cc} (%)	T_{mc} (°C)	ΔH_{mc} (J/gPCL)	T_g starch	T_g PCL or PCL-g
S	-	-		-	-	100.3 ± 0.2^{b}	
SPCL	27.3 ± 0.2^{a}	46.5 ± 0.8^{a}	34.2 ± 0.6^{a}	53.5 ± 0.4^{ab}	53.4 ± 0.9^{bc}	97.12 ± 0.14^{a}	-70.1 ± 0.3^{b}
$SPCL_G$	41.5 ± 0.4^{f}	74.5 ± 0.4^{h}	58.8 ± 0.3^{h}	53.0 ± 0.3^{a}	85.4 ± 1.1^{f}	131.2 ± 0.3^{f}	-62.3 ± 0.5^{c}
$SPCL_{MG}$	38.1 ± 0.2^{e}	58.2 ± 0.5^{e}	43.0 ± 0.4^{e}	54.6 ± 0.5^{abc}	66.7 ± 0.8^{e}	100.3 ± 0.4^{b}	-70.9 ± 0.3^{b}
$S_{PCLG2.5}PCL$	31.1 ± 0.3^{c} (Broad Peak)	61.0 ± 0.4^{f}	44.8 ± 0.3^{f}	54.2 ± 0.7^{abc}	52.5 ± 0.9^{b}	118.7 ± 0.3^{c}	-70.5 ± 0.9^{b}
$S_{PCLG5}PCL$	30.9 ± 0.2^{c} (Broad Peak)	65.5 ± 0.2^{g}	48.2 ± 0.2^{g}	54.5 ± 0.8^{abc}	55.3 ± 0.7^{c}	122.2 ± 0.2^{e}	-74.0 ± 0.7^{a}
$S_{PCLMG2.5}PCL$	29.2 ± 0.2^{b} 38.2 ± 0.3^{e} (Double Peak)	49.4 ± 0.5^{b}	36.3 ± 0.4^{b}	54.1 ± 0.3^{abc}	43.2 ± 0.5^{a}	119.5 ± 0.3^{cd}	-74.2 ± 0.4^{a}
$S_{PCLMG5}PCL$	32.64 ± 0.2^{d} (Broad Peak)	49.4 ± 1.0^{b}	36.3 ± 0.7^{b}	54.6 ± 0.5^{abc}	59.2 ± 1.3^{d}	120.0 ± 0.2^{d}	-75.1 ± 0.3^{a}
PCL	26.7 ± 0.3^{a}	56.1 ± 0.9^{d}	41.3 ± 0.7^{d}	55.2 ± 0.7^{bc}	68.0 ± 0.4^{e}		-61.9 ± 0.4^{c}
PCL_G	38.3 ± 0.2^{e}	52.9 ± 0.5^{c}	38.9 ± 0.4^{c}	55.4 ± 0.9^{bc}	67.7 ± 0.7^{e}		-61.3 ± 0.3^{c}
PCL_{MG}	38.4 ± 0.3^{e}	50.4 ± 0.7^{b}	37.1 ± 0.5^{b}	55.4 ± 0.6^{c}	69.3 ± 0.8^{e}		-61.0 ± 0.6^{c}

Different superscript letters within the same column indicate significant differences among formulations ($p < 0.05$).

The content of crystallinity (X_c) was calculated as the $\Delta H/\Delta H_\infty$ ratio (where ΔH is the fusion enthalpy of PCL in the samples, while ΔH_∞ refers to the hypothetically perfect crystal of PCL ΔH_∞=136 J/g-Avella *et al*., 2000). From the analysis of Table 6.2, it is possible to observe that the SPCL sample exhibited lower values of ΔH_c and X_c, due to the mixing of the components in the starch matrix amorphous phase, whereas $SPCL_{-g}$ samples of binary blends evidenced higher crystallization enthalpy, ΔH_c, and crystallinity, X_c, a noticeably improved crystallization temperature T_c (less supercooling effect) and an enhanced melting enthalpy, ΔH_m. These experimental data could be attributed to the marked interactions occurring between hydroxyl residues of starch and polar groups of functionalized PCL based samples, both able to support the nucleation process and to endorse the crystallization kinetics (Liu *et al*., 2009).

It is worth underscoring the peculiar behaviour of the $SPCL_G$ sample, exhibiting the highest values of ΔH_c, X_{cc}, ΔH_{mc}, probably ascribed to the formation of a very tight and crystalline network, able to drastically reduce the mobility of amorphous regions of S, as evidenced by the increase in the S T_g values. The proposed explanation for this behaviour may be found in the high concentration of starch hydroxyl residues available for reaction with GMA groups. As a matter of fact, this assumption could be in contrast with the previous hypothesis that long GMA branches, pending from the PCL backbone in secluded domains, could hinder its grafting efficiency. Anyway, when PCL_G is melt blended with the starch rich phase, chemical reactions between hydroxyl groups of starch and GMA occur at the expense of both reactive double bond and epoxy ring groups, by means of a steric and structural stabilization mechanism (Macosko *et al*., 1996). Actually, the FTIR-ATR analysis of the $SPCL_G$ spectrum (Figure 6.5), compared to that of the PCL_G one (Figure 6.2), points out that the band related to the asymmetric stretching vibration of epoxy ring C-O bonds at 910 cm^{-1} disappears, thus indicating GMA

epoxy ring opening as a consequence of the reaction with available starch hydroxyl groups (Odusanya *et al.*, 2000).

DSC cooling curves of all the blends are reported in Figure 6.7. Unlike binary blends, PCL melt crystallization of ternary blends generally follows a complex pattern, characterized by the presence of double or wider peaks for 2.5 or 5% of compatibilizer, respectively. This could be related to the existence of two fairly distinct crystalline domains, one related to PCL in the SPCL system, and the other associated to PCL_G and PCL_{MG} compatibilizers, as suggested by a reasonably good match between the corresponding Tc values. With 5% compatibilizer less peak separation was observed which suggest a better compatibilization degree in this case.

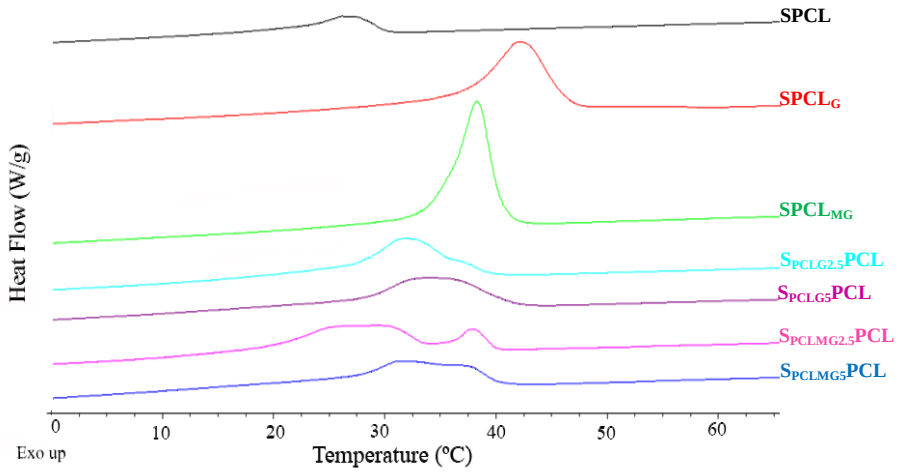

Figure 6.7.-DSC curves on cooling cycle of blends conditioned at 50% RH and 25 ºC for 4 weeks.

Actually, it could be hypothesized that the restrained amounts of compatibilizers used with respect to the S-PCL polymeric batch, induce a spot grafting process

along the macromolecular backbone, with the subsequent isolated regions of interfacial compatibilization; as a consequence, during fast cooling from melt, a homogeneous nucleation is avoided, due to different crystalline packings. Nevertheless, both ΔH_c, and X_{cc} values were higher than those of SPCL samples, particularly when PCL_G was used as compatibilizer, thus reproducing the trend previously observed in the $SPCL_G$ binary blend. As a final point, it is relevant to emphasize the mutual influence of polymers as a consequence of their better phase dispersion. Indeed, while starch T_g increases due to the stiffness of the crystalline network responsible for macromolecular free volume reduction, PCL molecules in their unstructured phase are well dispersed in the amorphous starch phase (Sarazin *et al*., 2008). The fact that the S T_g values increase while those of the amorphous PCL decrease, could indicate that, in ternary blends, the greater molecular interactions through the bonding of polar groups of both macromolecules, give rise to an increase in the mean molecular weight of starch chains, while the PCL molecules of small size remain in the amorphous PCL phase. This hypothesis is supported by the fact that, the higher the PCL chain size, the greater the probability of polar groups bonding during the grafting process.

6.3.2.3.2. Thermogravimetric analysis TGA

Table 6.3 shows the water content and thermal degradation recorded from the thermo-gravimetric analysis of the studied formulations stored for 1 and 4 weeks. All the thermograms exhibited three separate steps: a) small, broad peak due to the evaporation of bonded water between 50 and 150 °C; b) starch thermal degradation between 293 °C and 300 °C and c) PCL thermal degradation at about 373°C. The water content of samples was calculated as the weight lost between 25 ºC and 150 ºC. The blends presented a decrease in the water content compared with net starch films.

Table 6.3.-Mean values and standard deviation of water content, thermal degradation temperatures of starch and PCL of the studied formulations equilibrated at 50% relative humidity and 25 ºC for 1 (initial) and 4 (final) weeks.

Films	Water content (%) (25-150 °C)		Starch				PCL or g-PCL			
			Onset (°C)		Peak (°C)		Onset (°C)		Peak (°C)	
	Initial	Final	Initial	Final	Initial	Final	Initial	Final	Initial	Final
S	9.2 ± 0.2^{b1}	10.1 ± 0.2^{d2}	294.1 ± 0.3^{ab1}	297.0 ± 1.1^{c2}	320.3 ± 0.5^{c1}	318.1 ± 0.4^{bc2}				
SPCL	7.1 ± 0.4^{a1}	9.0 ± 0.3^{cd2}	296.1 ± 1.1b^{cd1}	294.2 ± 0.9^{b1}	317.2 ± 0.6^{a1}	319.4 ± 0.3^{c2}	370.1 ± 1.2^{a1}	369.2 ± 1.1^{a1}	402.3 ± 0.4^{a1}	406.2 ± 0.3^{b2}
$SPCL_G$	7.2 ± 0.6^{a1}	8.0 ± 0.4^{abc1}	300.2 ± 0.3^{e1}	296.1 ± 0.7^{bc2}	319.0 ± 0.3^{bc1}	317.0 ± 0.3^{bc2}	371.1 ± 0.5^{ab1}	368.2 ± 1.2^{a2}	404.2 ± 1.1^{b1}	402.2 ± 0.3^{a2}
$SPCL_{MG}$	8.0 ± 0.5^{ab1}	8.4 ± 0.4^{bc1}	295.0 ± 0.8^{abc1}	291.4 ± 0.5^{a2}	318.1 ± 0.2^{b1}	311.2 ± 0.5^{a2}	370.2 ± 0.6^{a1}	368.3 ± 0.5^{a2}	404.1 ± 0.3^{b1}	402.3 ± 0.2^{a2}
$S_{PCLG2.5}PCL$	7.4 ± 0.9^{a1}	7.6 ± 0.2^{ab1}	298.2 ± 1.2^{de1}	298.5 ± 0.5^{c1}	319.1 ± 0.5^{bc1}	319.2 ± 0.6^{c1}	373.3 ± 0.9^{cd1}	373.3 ± 0.6^{b1}	405.0 ± 0.9^{b1}	409.5 ± 0.5^{c2}
$S_{PCLG5}PCL$	7.1 ± 0.2^{a1}	7.1 ± 0.6^{a1}	297.1 ± 0.7^{cd1}	296.3 ± 0.3^{bc1}	319.2 ± 0.5^{bc1}	317.1 ± 1.1^{bc2}	372.4 ± 0.5^{bc1}	373.2 ± 0.8^{b1}	404.3 ± 0.8^{b1}	406.3 ± 0.6^{b2}
$S_{PCLMG2.5}PCL$	7.7 ± 0.3^{ab1}	8.4 ± 0.5^{bc1}	293.2 ± 0.9^{a1}	298.2 ± 0.3^{c2}	318.2 ± 0.3^{b1}	316.2 ± 0.6^{b2}	371.5 ± 0.3^{ab1}	373.2 ± 0.2^{b2}	402.0 ± 0.4^{a1}	405.0 ± 0.8^{b2}
$S_{PCLMG5}PCL$	7.11 ± 0.12^{a1}	7.9 ±0.4^{abc2}	300.2 ± 0.3^{e1}	297.2 ± 0.4^{c2}	319.2 ± 0.6^{bc1}	317.4 ± 0.9^{bc2}	374.3 ± 0.5^{d1}	370.2 ± 0.3^{a2}	412.2 ± 0.3^{d1}	412.3 ± 0.2^{e1}
PCL							373.2 ± 0.4^{cd1}	376.1 ± 0.4^{c2}	405.2 ± 0.5^{b1}	410.2 ± 0.3^{cd2}
PCL_G							377.2 ± 0.3^{e1}	380.0 ± 0.3^{d2}	411.2 ± 0.6^{d1}	411.0 ± 0.5^{de1}
PCL_{MG}							372.1 ± 0.3^{bc1}	374.0 ± 0.2^{bc2}	409.1 ± 0.4^{c1}	411.1 ± 0.6^{de2}

Different superscript letters within the same column indicate significant differences among formulations ($p < 0.05$). Different superscript numbers within the same row indicate significant differences due to storage time ($p < 0.05$).

This performance was expected as a consequence of the addition of hydrophobic polymers. Besides, the water content in the samples increased slightly throughout the storage time, which suggests that they were not in equilibrium at initial time. There is a more marked increase in the water content in SPCL through time than other blends. This fact is coherent with the more effective interactions between TPS and PCL_{-g} through the –OH groups of starch, in such a way that less active points are available for water adsorption; thus, polymeric matrices are more hydrophobic than S or SPCL.

Figure 6.8 shows TG and derivate (DTG) thermogram curves of PCL and PCL_{-g}. The derivate curve of net PCL in nitrogen displays a large peak centered at 405 ºC. Meanwhile, PCL_{-g} experience a shift in their peaks until 409 ºC and 411 ºC for PCL_{MG} and PCL_{G} respectively. Thus, the thermal stability of PCL appears to be improved by the grafting.

Table 6.3 shows the temperature of degradation onset as well as the temperature corresponding to the maximum degradation rate of neat polymers and binary and ternary blends. Plain PCL showed a very sharp degradation pattern, whose onset occurred at 393°C and the maximum degradation rate at 405°C. As regards PCL_{-g} samples, it must be underscored that, even if the presence of maleic anhydride and glycidyl methacrylate shifts T_{onset} to a fairly lower temperature, T_{max} is moved towards higher temperatures. This result coincides with DSC data, indicating that the introduction of grafted branches on the PCL backbone, in PCL_{G} and PCL_{MG}, hampered its crystallization, thus endorsing its thermal degradation at lower temperatures. On the other hand, the presence of more complex networks delayed PCL degradation kinetics, resulting in the shifting of T_{max} towards a higher temperature. As regards binary blends, it must be underlined that PCL is markedly affected by the amorphous phase of starch, as previously shown by DSC data (see Table 6.2) and spectroscopic analyses of starch-based samples. Indeed, from Table

6.3, it may be seen that the onset of PCL degradation temperature decreased by about 20°C with respect to the neat polymer. Anyway, no significant differences were recorded for compatibilized binary blends, whose PCL T_{onset} remained practically the same, whereas a slight lowering of T_{max} was observed. In ternary blends, a fairly thermal stabilization may be observed, in terms of both the T_{onset} and T_{max} of PCL. This upshot can be related to the improved efficiency of PCL_G and PCL_{MG} compatibilizers in interfacing between the two polymers, creating a strong polymer network. In particular, S_{PCLMG5}PCL is able to shift T_{max} from 402°C to 412°C, thus evidencing the formation of a very tightly-packed macromolecular association. Actually, from DSC data, it stands out that, during the cooling ramp, S_{PCLMG5}PCL showed a single crystallization peak (Figure 6.7) with the highest associated melting enthalpy (Table 6.2).

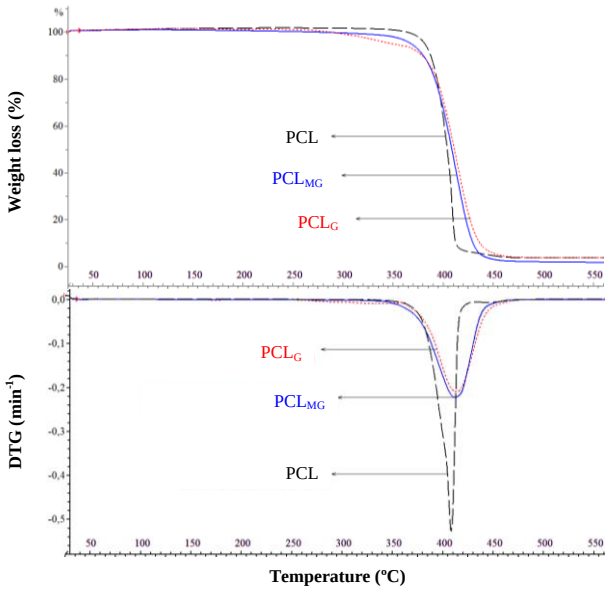

Figure 6.8.-TGA and DTG curves of PCL, PCL_G and PCL_{MG} conditioned at 50% RH and 25 ºC for 4 weeks.

As for starch, it is worthwhile highlighting a general increase in thermal stability, passing from plain polymer to binary and ternary blends, as evidenced by the increase in the onset T. This outcome is expected if the enhancement in crystallinity following the strong chemical interaction between the polar groups of the matrix and the modified PCL is considered. Moreover, it is of relevance to emphasize that thermal stability is particularly marked in $SPCL_G$ and $S_{PCLMG5}PCL$ samples, due to the formation of a very tight crystalline structure (highest melting enthalpy), as confirmed by DSC analysis.

6.3.2.4. Mechanical properties

Table 6.4 shows the tensile properties of the studied formulations at initial (1 week) and final (4 weeks) storage time. The binary blends did not show any significant changes in EM and TS with respect to net starch films, although their deformations at break are noticeable reduced (about 50%). Grafting PCL did not improve the mechanical parameters of the blend films despite the better interfacial adhesion between polymer phases observed by SEM. Nevertheless, whereas the extensibility of S films was significantly reduced during storage, the values did not significantly change in binary blends, although all the samples became harder as revealed by the significant increase in both EM and TS values. This indicates that PCL or PCL_{-g} did not inhibit the starch chain aggregation progress throughout time. The amorphous component in TPS changes fast after film forming and there appears to be some short-range ordering of the amorphous components over time. The loss of water leads to some dynamic molecular re-arrangements within the amylose fraction (Frost *et al.*, 2009). Both retrogradation and crystallization phenomena may take place in TPS/PCL or PCL_{-g} blends, but it is not clear. An increase in crystallinity may also be possible because of the interactions between the epoxy/anhydride groups of compatibilizers and the hydroxyl groups of starch.

Table 6.4.-Mean values and standard deviation of mechanical properties of films equilibrated at 50% RH and 25 ºC for 1 (initial) and 4 (final) weeks.

Films	Thickness (µm)	EM (MPa)		TS (MPa)		E (%)	
		Initial	Final	Initial	Final	Initial	Final
S	231 ± 41^{a}	131 ± 13^{a1}	221 ± 26^{a1}	2.7 ± 0.3^{ab1}	4.6 ± 0.4^{a2}	64 ± 7^{d1}	34 ± 5^{ab2}
SPCL	252 ± 42^{a}	113 ± 16^{a1}	178 ± 17^{a2}	2.7 ± 0.3^{ab1}	4.3 ± 0.3^{a2}	39 ± 5^{c1}	28 ± 6^{ab1}
SPCL$_{G}$	228 ± 48^{a}	120 ± 20^{a1}	190 ± 25^{a2}	2.8 ± 0.3^{ab1}	5.2 ± 0.9^{a2}	25 ± 6^{abc1}	25 ± 4^{ab1}
SPCL$_{MG}$	215 ± 49^{a}	126 ± 13^{a1}	219 ± 25^{a2}	2.0 ± 0.3^{a1}	4.3 ± 0.5^{a2}	30 ± 4^{bc1}	19 ± 4^{a2}
S$_{PCLG2.5}$PCL	217 ± 45^{a}	276 ± 40^{b1}	200 ± 23^{a2}	3.8 ± 0.4^{bc1}	4.5 ± 0.4^{a1}	10 ± 4^{a1}	29 ± 7^{ab2}
S$_{PCLG5}$PCL	246 ± 32^{a}	283 ± 44^{b1}	178 ± 22^{a2}	4.9 ± 0.3^{cd1}	4.6 ± 0.7^{a1}	21 ± 2^{ab1}	35 ± 7^{ab2}
S$_{PCLMG2.5}$PCL	227 ± 32^{a}	265 ± 30^{b1}	218 ± 33^{a1}	4.7 ± 0.8^{cd1}	4.7 ± 0.6^{a1}	28 ± 6^{bc1}	36 ± 5^{ab1}
S$_{PCLMG5}$PCL	243 ± 35^{a}	315 ± 32^{b1}	241 ± 22^{ab2}	5.3 ± 0.6^{d1}	5.6 ± 0.3^{a1}	36 ± 3^{bc1}	41 ± 4^{b1}
PCL	186 ± 25^{a}	304 ± 11^{b1}	314 ± 51^{b1}				

Different superscript letters within the same column indicate significant differences among formulations ($p < 0.05$). Different superscript numbers within the same row indicate significant differences due to storage time ($p < 0.05$).

As regards ternary blends, although a significant increase ($p < 0.05$) was observed in TS (up to 49% -S$_{PCLMG5}$PCL) and EM (up to 58.4% -S$_{PCLMG5}$PCL), E was seen to decrease (to 84% -S$_{PCLG2.5}$PCL). The rise in the amount of compatibilizers (from 2.5 to 5 g/100g polymers) did not significantly affect the values of tensile properties, although a tendency was observed in the sense that the greater the amount of compatibilizers, the better the matrix reinforcement. This fact suggests that the compatibility between PCL and TPS was enhanced the more compatibilizer was added. Likewise, from the point of view of mechanical behaviour, ternary blends, where PCL$_{-g}$ materials were used as S-PCL compatibilizers, exhibit a better response than binary blends.

As far as the changes experienced by ternary blends throughout time, they followed a different trend to binary ones; a decrease in EM (to 37.1% -S_{PCLG5}PCL) and an increase in E (up to 65.5% -$S_{PCLG2.5}$PCL) and TS (up to 15.5% -$S_{PCLG2.5}$PCL) were observed. The blends compatibilized with PCL_G were more unstable throughout the storage time than those compatibilized with PCL_{MG}, although, in general, minor changes could be observed for all the ternary blends. This fact, combined with the decrease in the sample rigidity and the increase in stretchability, seems to indicate that the starch retrogradation was limited in ternary blends. According to the lower degree of crystallization in these samples, as deduced from XRD and DSC analyses, the progress of this phenomenon during storage could be responsible for the observed changes in the mechanical properties. Likewise, the molecular structure (bond angles, hydrogen bonds…) of polymers may be re-ordered within time, thus reaching a new equilibrium state after the perturbation induced by extrusion and compression moulding. As a result, the films become more stretchable and tough and less rigid than at the initial time.

From the mechanical analysis, it can be concluded that the use of PCL_{-g} as a compatibilizer is more effective for improving the mechanical behaviour of starch based films with PCL than their use as a second polymer in binary blends.

6.3.2.5. Barrier properties

Table 6.5 shows the barrier properties (oxygen, carbon dioxide and water vapour) of the studied formulations stored at 25 ºC and 50% RH for 4 weeks. As concerns the binary blends, the addition of PCL causes an increase in oxygen and carbon dioxide permeability, whereas PCL_G did not cause any remarkable effects and PCL_{MG} led to a significant reduction in both parameters. Ternary blends exhibited O_2 and CO_2 permeability values in the range of the net starch films or lower.

Table 6.5.-Mean values and standard deviation of oxygen permeability (O_2P), carbon dioxide permeability (CO_2P) and water vapour permeability (WVP) of the different films stored at 50% relative humidity and 25 ºC for 4 weeks.

Films	$O_2P \cdot 10^{10}$ [$cm^3/(m \cdot s \cdot Pa)$]	$CO_2P \cdot 10^8$ [$cm^3/(m \cdot s \cdot Pa)$]	WVP [$gr \cdot mm/(m^2 \cdot h \cdot KPa)$]
S	2.00 ± 0.09^{d}	1.02 ± 0.05^{b}	4.47 ± 0.05^{d}
SPCL	2.87 ± 0.14^{e}	1.98 ± 0.12^{c}	4.30 ± 0.08^{d}
$SPCL_G$	2.07 ± 0.03^{d}	1.03 ± 0.09^{b}	3.41 ± 0.03^{b}
$SPCL_{MG}$	1.11 ± 0.11^{ab}	0.88 ± 0.05^{ab}	3.87 ± 0.13^{c}
$S_{PCLG2.5}PCL$	1.30 ± 0.03^{bc}	0.94 ± 0.08^{b}	1.35 ± 0.02^{a}
$S_{PCLG5}PCL$	0.891 ± 0.04^{a}	0.641 ± 0.09^{a}	1.26 ± 0.05^{a}
$S_{PCLMG2.5}PCL$	1.53 ± 0.05^{c}	1.04 ± 0.11^{b}	1.46 ± 0.04^{a}
$S_{PCLMG5}PCL$	1.24 ± 0.02^{b}	0.65 ± 0.06^{a}	1.39 ± 0.08^{a}
PCL	138 ± 8^{f}	120 ± 9^{d}	1.45 ± 0.04^{a}

Different superscript letters within the same column indicate significant differences among formulations ($p < 0.05$).

The gas permeability in polymeric materials stems from two contributions: the dissolution phenomenon and the interaction between the diffusing molecule and specific polymer sites (Gain *et al*., 2005). The results can be explained in terms of changes in the gas solubility in the continuous matrix and dispersed phase as well as differences in diffusion coefficients by hindrance effects provoked by dispersed PCL particles and the respective gas molecule interactions with the specific polar and non-polar polymer sites. In this sense, the increase in gas permeability when pure PCL was added to starch can be attributed to the better affinity of molecules with dispersed PCL than with S. When grafted PCL was blended with starch, both O_2 and CO_2 permeability values were reduced due to the overall increase in the PCL polarity caused by grafting polar groups (epoxy and anhydride). Likewise, if these compounds are mainly at the polymer interface, the diffusion of gas molecules into the PCL particles could be hindered. In fact, in blends where PCL_{-g} acts as compatibilizer at polymer interfacial level, gas permeability are more

reduced. Actually, samples with 5% of PCL_G and PCL_{MG} showed the lowest oxygen and carbon dioxide permeability values, below those of net starch films.

On the other hand, when the PCL and PCL_{-g} were incorporated into the starch matrix as binary blends, WVP decreases, especially for PCL_{-g}. The overall reduction of WVP in binary blends can be associated to the increase in the tortuosity factor for mass transfer when hydrophobic particles (PCL or PCL_{-g}) are dispersed. The greater WVP reduction in the starch matrix when the PCL_{-g} was incorporated may be due to the decrease in the starch matrix water affinity associated to the –OH bonding with polar groups of PCL_{-g}. Ternary blends exhibited WVP values similar to those of PCL, which represents a great improvement in the starch barrier properties. This increase in the water barrier properties of the starch based films could be attributed to the new arrangement of components in the presence of compatibilizers, which makes it more difficult for the water molecules to pass through the matrix.

In fact, ternary blends showed gas permeability values lower than those of net starch films and water vapour permeability values lower than those of PCL, which represents a noticeable improvement in the barrier properties of starch-PCL based films. In this way, these formulations met the barrier requirements for food packaging. As for WVP, all the formulations are within the requirement range for meat and MAP products (10-50 g water vapour$\cdot m^{-2}\cdot day^{-1}$) according to what is reported by Schmid *et al*., 2012. Meanwhile, the O_2P of every starch-based formulation cover the highest requirements for food packaging (less than 1 cm^3 oxygen$\cdot m^{-2}\cdot day^{-1}\cdot bar^{-1}$, Schmid *et al*., 2012). The materials developed have oxygen barrier properties comparable to Polyethylene Terephthalate (PET) and Ethylene vinyl alcohol (44% ethylene content -EVOH) and their WVTR is close to that of Polystyrene (PS) and PET (Schmid *et al*., 2012). However, despite their excellent barrier properties, the overall migration in different food simulants must be

assessed, according to the migration limits established by regulation for plastic materials in contact with food. Another alternative for the practical utilization of these materials is to develop a multilayer package in which a layer of food grade polymer forms part of the material.

6.4. CONCLUSIONS

The grafting of an MA-GMA blend or net GMA to PCL allows us to obtain good compatibilizers (PCL_{-g}) in order to obtain starch-PCL blend films with a high ratio of starch, with good mechanical performance and stability and high barrier properties, useful to meet the food packaging requirements. The grafting degree was 4.5 and 4 wt%, for the MA-GMA blend and GMA, respectively. The interfacial adhesion of both polymers was greatly improved when PCL_{-g} was present in the blends, which gave rise to tight matrices. Compatibilizers acted as nucleating agents for PCL crystallization, affecting the degree of crystallization in the blends. The properties of the starch-PCL_{-g} blend films were poorer than those of the ternary systems of starch-PCL blends with only 2-5% of PCL_{-g}, which represents an advantage from the economic point of view. The materials developed have gas and water vapour barrier properties comparable to some synthetic plastics commonly used for food packaging. The overall migration in different food simulants must be assessed, according to the migration limits established by regulation for plastic materials in contact with food.

6.5. REFERENCES

Arbelaiz, A., Fernández, B., Valea, A., & Mondragon, I. (2006). Mechanical properties of short flax fibre bundle/poly(ε-caprolactone) composites: Influence of matrix modification and fibre content. Carbohydrate Polymers, 64, 224–232.

Arık-Kibar, E. A., & Us, F. (2013). Thermal, mechanical and water adsorption properties of corn starch–carboxymethylcellulose/methylcellulose biodegradable films. Journal of Food Engineering, 114, 123–131.

American Society for Testing and Materials, ASTM D638. Standard test method for tensile properties of plastics. In annual book of ASTM. Philadelphia; 2010.

Avella, M., Errico, M. E., Laurienzo, P., Martuscelli, E., Raimo, M., & Rimedio, R. (2000). Preparation and characterisation of compatibilised polycaprolactone/starch composites. Polymer, 41, 3875-3881.

Averous, L., Moro, L., Dole, P., & Fringant, C. (2000). Properties of thermoplastic blends: starch-polycaprolactone. Polymer, 41, 4157-4167.

BeMiller, J., & Whistler, R. (2009). Starch: Chemistry and Technology. (3th ed.). Lincoln: Academic Press-Elsevier.

Castillo, L., López, O., López, C., Zaritzky, N., García, M. A., Barbosa, S., & Villar, M. (2013). Thermoplastic starch films reinforced with talc nanoparticles. Carbohydrate Polymers, 95: 664– 674.

Cocca, M., Avolio, R., Gentile, G., Di Pace, E., Errico, M. E., & Avella M. (2015). Amorphized cellulose as filler in biocomposites based on poly(ε-caprolactone). Carbohydrate Polymers, 118, 170–182.

De Camargo, A.-M., Shirai, T. P., Grossmann, M. V. E., & Yamashita, F. (2013). Active biodegradable packaging for fresh pasta. LWT- Food Science and Technology, 54: 25-29.

Gain, O., Espuche, E., Pollet, E., Alexandre, M., & Dubois, P. (2005). Gas Barrier Properties of Poly(ε-caprolactone)/Clay Nanocomposites: Influence of the Morphology and Polymer/Clay Interactions. Journal of Polymer Science: Part B: Polymer Physics, 43, 205–214.

Frost, K., Kaminski, D., Kirwan, G., Lascaris, E., & Shanks, R. (2009). Crystallinity and structure of starch using wide angle X-ray scattering. Carbohydrate Polymers, 78, 543–548.

Haque, Md. M-U., Errico, M. E., Gentile, G., Avella, M., & Pracella, M. (2012). Functionalization and Compatibilization of Poly(ε-caprolactone) Composites with Cellulose Microfibres: Morphology, Thermal and Mechanical Properties. Macromolecular Materials and Engineering, 297, 985–993.

He, Y., Asakawa, N., & Inoue, Y. (2000). Studies on poly(ε-caprolactone)/thiodiphenol blends: The specific interaction and the thermal and dynamic mechanical properties. Journal of Polymer Science Part B: Polymer Physics, 38, 1848-1859.

John, J., Tang, J., Yang, Z., & Bhattacharya, M. (1997). Synthesis and characterization of anhydride-functional polycaprolactone. Journal of Polymer Science, Part A: Polymer Chemestry, 35(6), 1139-1148.

Kim, C.-H., Cho, K. Y., & Park, J.-K. (2001). Grafting of glycidyl methacrylate onto polycaprolactone: preparation and characterization. Polymer, 42, 5135-5142.

Kizil, R., Irudayaraj, J., & Seetharaman, K. (2002). Characterization of Irradiated Starches by Using FT-Raman and FTIR Spectroscopy. Journal of Agricultural and Food Chemistry, 50, 3912-3918.

Laurienzo, P., Malinconico, M., Mattia, G., & Romano, G. (2006). Synthesis and characterization of functionalized crosslinkable Poly(ε-caprolactone). Macromolecular Chemistry and Physics, 207, 1861–1869.

Leroy, E., Jacquet, P., Coativy, G., Reguerre, A. L., & Lourdin, D. (2012). Compatibilization of starch–zein melt processed blends by an ionic liquid used as plasticizer. Carbohydrate Polymers, 89, 955–963.

Li, G., & Favis, B.D. (2010). Morphology development and interfacial interactions in polycaprolactone/ thermoplastic-starch blends. Macromolecular Chemistry and Physics, 211, 321–333.

Liu, H., Xie, F., Yu, L., Chen, L., & Li, L. (2009). Thermal processing of starch-based polymers. Progress in Polymer Science, 34, 1348–1368.

Macosko, C. W., Guegan, P., Khandpur, A. K., Nakayama, A., Marechal, P., & Noue, T. I. (1996). Compatibilizers for Melt Blending: Premade Block Copolymers. Macromolecules, 29, 5590-5598.

Mangiacapra, P., Raimondo, M., Tammaro, L., Vittoria, V., Malinconico, M., & Laurienzo, P. (2007). Nanometric dispersion of a Mg/Al layered double hydroxide into a chemically modified polycaprolactone. Biomacromolecules**,** 8, 773-779.

Monteiro, S. S. B. M, Vaca, C. F., Sebastião, P. J., & Bruno, T. M. I. (2013).^{1}HNMR relaxometry and X-ray study of PCL/nevirapine hybrids. Polymer Testing, 32, 553–566.

Murphy, S. H., Leeke, G. A., & Jenkins, M. J., (2012). A Comparison of the use of FTIR spectroscopy with DSC in the characterisation of melting and crystallisation in polycaprolactone. Journal of Thermal Analysis and Calorimetry, 107, 669–674.

Odusanya, O. S., Ishiaku, U. S., Azemi, B. M. N., Manan, D. M. A., & Kammer, H. W. (2000). On mechanical properties of sago starch/poly(ε-caprolactone) composites. Polymer Engineering Scince, 40, 1298-1305.

Ortega-Toro, R., Jiménez, A., Talens, P., & Chiralt, A. (2014). Properties of starch-hydroxypropyl methylcellulose based films obtained by compression molding. Carbohydrate Polymers, 109 (30): 155–165.

Ortega-Toro, R., Collazo-Bigliardi, S., Talens, P., & Chiralt, A. (2015). Influence of citric acid on the properties and stability of starch-polycaprolactone based films. Journal of Applied Polymer Science, DOI: 10.1002/app.42220.

Pérez, E., Pérez, C. J., Alvarez, V. A., & Bernal, C. (2013). Fracture behavior of a commercial starch/polycaprolactone blend reinforced with different layered silicates. Carbohydrate Polymers, 97: 269– 276.

Russo, R., Abbate, M., Malinconico, & M., Santagata, G. (2010). Effect of polyglycerol and the crosslinking on the physical properties of a blend alginate-hydroxyethylcellulose. Carbohydrate Polymers, 82, 1061–1067.

Santha, N., Sudha, K. G., Vijaykumari, K. P., Nayar, V. U., & Moorthy, S. N. (1990). Raman and Infrared spectra of starch samples of sweet potato and cassava. Journal of Chemical Sciences - Indian Academy of Sciences, 102, 705-712.

Sarazin, P., Li, G., Orts, W. J., & Favis, B., D. (2008). Binary and ternary blends of polylactide, polycaprolactone and thermoplastic starch. Polymer, 49, 599-609.

Schmid, M., Dallmann, K., Bugnicourt, E., Cordoni, D., Wild, F., Lazzeri, A., & Noller, K. (2012). Properties of whey-protein-coated films and laminates as novel recyclable food packaging materials with excellent barrier properties. International Journal of Polymer Science, 8, 1-7.

Sugih, A. K., Drijfhout, J. P., Picchioni, F., Janssen, L. P. B. M., & Heeres, H. J. (2009). Synthesis and properties of reactive interfacial agents for polycaprolactone-starch blends. Journal of Applied Polymer Science, 114: 2315–2326.

Suzuki, Y., Duran, H., Akram, W., Steinhart, M., Floudas, G., & Butt, H-J. (2013). Multiple nucleation events and local dynamics of poly(ε-caprolactone) (PCL) confined to nanoporous alumina. Soft Matter, 9: 9189-9198.

Teixeira, E. d.M., Curvelo, A. A. S., Corrêa, A. C., Marconcini, J. M., Glenn, G. M., & Mattoso, L. H. C. (2012). Properties of thermoplastic starch from cassava bagasse and cassava starch and their blends with poly (lactic acid). Industrial Crops and Products, 37: 61–68.

Woehl, M. A., Canestraro, C. D., Mikowski, A., Sierakowski, M. R., Ramos, L. P., & Wypych, F. (2010). Bionanocomposites of thermoplastic starch reinforced with bacterial cellulose nanofibres: Effect of enzymatic treatment on mechanical properties. Carbohydrate Polymers, 80, 866–873.

Wu, C.-S. (2003). Physical properties and biodegradability of maleated-polycaprolactone/starch composite. Polymer Degradation and Stability, 80, 127–134.

Xie, F., Pollet, E., Halley, P.J., & Averous, L. (2013). Starch-based nano-biocomposites. Progress in Polymer Science, 38, 1590– 1628.

Zhang, Y.-R., Wang, X.-L., Zhao, G.-M., & Wang, Y.-Z. (2013). Influence of oxidized starch on the properties of thermoplastic starch. Carbohydrate Polymers, 96, 358– 364.

CHAPTER 7

ACTIVE BILAYER FILMS OF THERMOPLASTIC STARCH AND POLYCAPROLACTONE OBTAINED BY COMPRESSION MOULDING

Rodrigo Ortega-Toro, Iris Morey, Pau Talens &Amparo Chiralt

Carbohydrate Polymers, 127, 282–290

Bilayer films consisting of one layer of PCL with either one of thermoplastic starch (S) or one of thermoplastic starch with 5% PCL (S95) were obtained by compression moulding. Before compression, aqueous solutions of ascorbic acid or potassium sorbate were sprayed onto the S or S95 layers in order to plasticize them and favour layer adhesion. S95 films formed bilayers with PCL with very good adhesion and good mechanical performance, especially when potassium sorbate was added at the interface. All bilayers showed excellent barrier properties to water vapour and oxygen. Bilayers consisting of PCL and starch containing 5% PCL, with potassium sorbate at the interface, showed the best mechanical and barrier properties and interfacial adhesion while having active properties, associated with the antimicrobial action of potassium sorbate.

VNIVERSITAT POLITECNICA
VALENCIA
EX TECHNICA
PROGRESSIO

7.1. INTRODUCTION

In the last few years, the need for replacing petroleum-based plastics by biodegradable polymers has led to a great number of studies focused on the design of environmentally friendly materials. In particular, starch and its derivatives have been widely studied since they could offer an inexpensive solution to such problems (Bastioli, 2001). Starch is obtained from renewable resources, is widely available and low cost and it can be used to obtain biodegradable films for food applications, as it has the ability to form films or coatings with very low oxygen permeability (Jiménez *et al.,* 2012). However, starch-based materials show several disadvantages which reduce their applicability as packaging material, such as their highly hydrophilic character, limited mechanical properties and the retrogradation phenomena that occur during ageing. The blending of starch with other, more hydrophobic, polymers is a widely studied strategy used to improve properties of starch films. The aliphatic polyesters, such as polycaprolactone (PCL) or polylactic acid (PLA), are synthetic biodegradable materials of a more hydrophobic nature that can be combined with starch in different ways to modulate the properties of mixed films. Of them, PCL has the advantage of great stretchability and low water vapour permeability (Averous *et al.*, 2000). Nevertheless, the starch-PCL materials obtained by simple blending are not adequate due to the low affinity of both polymers, which leads to polymer phase separation with limited adhesion between the polymer interfaces, thus resulting in poor film properties (Avella *et al*., 2000). To overcome this, several authors have studied the improvement in the starch-PCL compatibility by using different compounds, which can increase the polymer affinity via different mechanisms, such as PCL-co-pyromellitic anhydride (Avella *et al.*, 2000) methylene diphenyl diisocyanate (Wang *et al.*, 2001) or dioctyl maleate (Zhang & Sun, 2004). Nevertheless, the use of these kinds of compounds can compromise the use of films for food packaging due to their potential toxicity.

Other authors reported that hydrogen bonds can be established to a certain extent between the starch hydroxyls and the PCL carbonyls at the interface region, which could allow the incorporation of small amounts of PCL in starch matrices without notable polymer separation, improving film properties (Matzinos *et al*., 2002; Ortega-Toro *et al*., 2015).

The development of multilayer films using starch and PCL layers could be a good alternative for developing packaging materials for food applications. A multilayer packaging material can be defined as two or more materials with specific properties combined in a single layered structure. The multilayer films with petrochemical-based materials are already widely used in food packaging applications (Fang *et al*., 2005; Mensitieri *et al*., 2011). The PCL-starch multilayers could exhibit some advantages, such as the decrease in the overall moisture sensitivity and the improvement in the mechanical properties (Yu *et al.,* 2006), by combining the properties of each material (Fabra *et al.,* 2013). Therefore, starch-PCL multilayers could maintain the excellent gas barrier properties of the starch and the high water vapour barrier of the PCL, which would be difficult to achieve with a single biopolymer-based material. Layered structures based on biopolymers containing antimicrobial compounds have been obtained by co-extrusion (Alix *et al*., 2013) or compression-moulding (Takala *et al*., 2013).

The incorporation of antioxidant and antimicrobial agents in biodegradable films has been widely studied to obtain active packaging materials with controlled release of bioactives (Ayranci & Tunc, 2003; Wook *et al.* 2013) to enhance food stability and shelf life. These agents have often been included in the biopolymer dispersions used for casting films (Gómez-Guillén *et al.,* 2007; Jiménez *et al.,* 2013; Cian *et al.,* 2014). Nevertheless, the usual thermal processing of bioplastics make their incorporation necessary during the extrusion or other hot melting steps used at industrial level. Some losses of active compounds can occur during this

step due their thermo-sensitive. For instance, Wook *et al.* (2013) reported losses of resveratrol and α-tocopherol incorporated in PLA/starch blend films during the polymer melt blending, ranging between 4 and 26%, depending on the film formulation.

The aim of this work is to analyse the properties of starch-PCL bilayer films obtained by compression moulding by incorporating a common food antimicrobial (potassium sorbate: PS) and an antioxidant (ascorbic acid: AA) at the layers' interface. The interactions of these compounds with both phases could improve the layers' adhesion, while conferring active properties to the layered film. Bilayer films formed with starch layers containing 5% PCL was compared with those formed with pure starch layers in order to discover the potential improvement of starch-PCL interfacial adhesion when a small amount of PCL is present in the starch matrix.

7.2. MATERIALS AND METHODS

7.2.1. Materials

Corn starch was purchased from Roquette (Roquette Laisa, Benifaió, Spain). Its moisture content was 10% w/w and amylose percentage was 14%. Glycerol was from Panreac Química, S.A. (Castellar del Vallès, Barcelona, Spain). Polycaprolactone (PCL) was from Aldrich Chemistry (Sigma-Aldrich Co. LLC Madrid, Spain), with a molecular weight of 80.000 daltons. Potassium sorbate, ascorbic acid, magnesium nitrate 6-hydrate, sodium chloride and phosphorus pentoxide were from Panreac Química, S.A. (Castellar del Vallés, Barcelona, Spain).

7.2.2. Film preparation

Three kinds of monolayer films were obtained by melt blending and subsequent compression moulding: thermoplastic starch (S), thermoplastic starch with 5% (g/100g of starch) PCL (S95) and pure PCL (PCL). To prepare S films, native starch and glycerol were dispersed in water using a starch:glycerol ratio of 1:0.3 w/w. When starch films contained PCL, this was added to aqueous dispersions in 1:0.05, w/w starch:PCL ratio.

A two-roll mill (Model LRM-M-100, Labtech Engineering, Thailand) was used for the hot-mixing process where polymers were heated at 160 ºC and 8 rpm for 30 min. The resulting sheets were ground and conditioned at 25 ºC and 75% RH using NaCl oversaturated solutions for 48 h. Afterwards, the monolayer films were obtained using a compression moulding press (Model LP20, Labtech Engineering, Thailand). The following process conditions were used: a) pre-heating cycle at 160 ºC for 5 min, b) compression-moulding at 50 bar for 2 min, c) compression-moulding at 150 bar for 6 min, and d) cooling cycle at 150 bars for 3 min.

Subsequently, the bilayer films were obtained by means of a second compression-moulding step where the corresponding two layers were compressed together. The process conditions were 80 ºC and 150 bars for 4 min and cooling cycle for 2 min. The obtained bilayer films always had one PCL layer and an S or S95 layer. Before the second compression, 1 mL of distilled water (H_2O) or aqueous solutions containing ascorbic acid (AA) or potassium sorbate (PS) were sprayed onto the S or S95 layers in order to plasticize starch and promote layer adhesion. The obtained bilayer films were coded by indicating if the starch layer was S or S95 and the kind of solution sprayed onto the interface (H_2O, AA or PS); e.g. S-H_2O indicates that the bilayer film contains S plus PCL layers sprayed with pure water. AA and PS aqueous solutions were prepared in such a way that 1 mL of solution contained 0.1 g of compound/g of starch film. The bilayer films were conditioned at 25 ºC and

53% RH for 1 and 5 weeks before their characterization. The thickness of conditioned films was measured at six random positions with a digital electronic micrometer (Palmer-Comecta, Spain, ± 0.001 mm).

7.2.3. Film characterization

7.2.3.1. Scanning Electron Microscopy (SEM)

Cross-section images from resulting films were obtained by means of a scanning electronic microscope (JEOL, JSM-5410, Japan). The conditioned samples (1 and 5 weeks) were stored inside P_2O_5 desiccators for one week before the analysis. Afterwards, the samples were cryo-fractured, fixed on copper stubs, gold coated, and observed using an accelerating voltage of 10 kV.

7.2.3.2. Fourier Transform Infrared (FTIR) spectroscopy

Attenuated Total Reflection Fourier Transform Infrared (ATR-FTIR) spectroscopy was used to analyse component interactions in the films. Measurements were performed at 25 ºC using a Tensor 27 mid-FTIR Bruker spectrometer (Bruker, Karlsruhe, Germany) attached to a platinum ATR optical cell and an RT-Dla TGS detector (Bruker, Karlsruhe, Germany). The diaphragm was set at 4 mm for the analysis, and the spectra were obtained between 4000 and 800 cm^{-1} using a resolution of 4 cm^{-1}. The analysis was carried out on both the S or S95 and PCL layers. The data were analyzed using OPUS software (Bruker, Karlsruhe, Germany).

7.2.3.3. Thermal properties

Thermal degradation of the films and their components was analysed using a thermogravimetric TGA 1 Star^e System analyser (Mettler-Toledo, Inc., Switzerland), equipped with an ultra-micro weighing scale (± 0.1 μg), under nitrogen atmosphere. The analysis was carried out using the following temperature programme: heating from 25 to 500 ºC at a 10 ºC/min heating rate. Approximately 4 mg of each sample were used in each test, considering at least two replicates for each one. Initial degradation temperature (Onset) and peak temperature (Peak) were registered from the first derivative of the resulting weight loss curves.

7.2.3.4. Water content (X_w) and film solubility in water

Conditioned films were transferred to a natural convection oven (J.P. Selecta, S.A., Barcelona, Spain) at 60 ºC for 24 h. Then, these samples were stored in a P_2O_5 desiccator for 8 days. Moisture content in dry basis was obtained from the initial and final sample weights. Pieces of dry samples were transferred to glass pots, and covered with bidistilled water at a film:water ratio of 1:9 w/w. After 48 h, the samples were transferred to a natural convection oven at 60 ºC for 24 h in order to remove the water contained in bilayer films. Finally, the samples were stored in a desiccator containing P_2O_5 for 8 days to complete drying. Film water solubility was estimated from its initial and final weights. Three replicates were considered per formulation.

7.2.3.5. Water Vapour Permeability (WVP) and Oxygen Permeability (O_2P)

The Water Vapour Permeability (WVP) of films was determined according to a modification of E96-95 gravimetric method (ASTM, 1995) proposed by McHugh *et al.* (1993). The measures were carried out exposing the S or S95 layer to 100%

RH. To this end, 5 mL of bidistilled water were placed in Payne permeability cups (3.5 cm diameter, Elcometer SPRL, Hermelle/s Argenteau, Belgium). These cups were transferred to a desiccator containing oversaturated $Mg(NO_3)_2$ (53% RH) at 25 ºC. The permeability measurements were performed by weighing the cups periodically (every 1.5 h for 24 h). Eq. (7.1) proposed by McHugh *et al.* (1993) was used to calculate the vapour pressure on the film's inner surface (p_2).

$$WVTR = \frac{P \cdot D \cdot L_n[P - p_2 \backslash P - p_1]}{R \cdot T \cdot \Delta z} \quad (7.1)$$

where P, total pressure (atm); D, diffusivity of water through air at 25 ºC (m^2/s); R, gas law constant (82.057×10^{-3} m^3 atm $kmol^{-1}$ K^{-1}); T, absolute temperature (K); Δz, mean stagnant air gap height (m), considering the initial and final z value; p_1,water vapour pressure on the solution surface (atm); and p_2, corrected water vapour pressure on the film's inner surface (atm). Water vapour permeance was calculated using Eq. (7.2) as a function of p_2 and p_3 (pressure on the film's outer surface in the cabinet). Multiplication of permeance by film thickness leads to the WVP of films.

$$permeance = \frac{WVTR}{p_2 - p_3} \quad (7.2)$$

In a first approach, the WVP of S-H_2O and S95-H_2O bilayer films was determined by exposing PCL layer to both the 100% and 53% RH atmospheres in order to verify if there were significant differences among WVP values. As none were

observed, measurements were carried out by exposing the starch layer (S or S95) to 100% RH in every case. Values were obtained in triplicate for each film.

The oxygen permeability (O_2P) was determined using an Oxtran 1/50 (Mocon, Minneapolis, USA) system considering the Standard Method D3985-95 (ASTM, 2002) at 25 ºC and 53% RH. Three films were evaluated for each formulation. The assay was performed exposing the PCL layer to the highest oxygen concentration in every case. The transmission values were determined every 20 min until equilibrium was reached. The exposure area during the tests was 50 cm^2 for each sample. To obtain the oxygen permeability, the film thickness was considered.

7.2.3.6. Tensile properties

A universal test Machine (TA.XTplus model, Stable Micro Systems, Haslemere, England) was used to determine the elastic modulus (EM) and tensile strength (TS) and elongation (E) at break point of the films, following ASTM standard method D882 (ASTM, 2001). Films conditioned at 25 °C and 53% RH for 1 and 5 weeks were evaluated. EM, TS, and E were determined from the stress-strain curves, estimated from force-distance data obtained for the different films (2.5 cm wide and 5 cm long). Samples were mounted in the film-extension grips of the testing machine and stretched at 50 mm min^{-1} until breaking. At least ten replicates were obtained from each sample.

7.2.3.7. Optical properties

The films' surface gloss was determined by means of a surface gloss meter (Multi Gloss 268, Minolta, Germany) at 85º incidence angle, since films exhibit low gloss, according to D523 standard method (ASTM, 1999). Each film was measured in

triplicate on both film faces. Results were expressed as gloss units (GU), relative to a highly polished surface of black glass standard with a value near to 100 GU.

Film transparency was determined from the surface reflectance spectra (400–700 nm) obtained by a Minolta spectro-colorimeter (CM-3600d model, Minolta Co., Tokyo, Japan) on both white and black backgrounds. Kubelka-Munk theory for multiple scattering was applied in order to determine the internal transmittance (Ti). The Ti of the films was determined using eq. (7.3). In this equation, R_0 is the reflectance of the film on an ideal black background. Parameters *a* and *b* were calculated by means of eqs. (7.4) and (7.5), where R is the reflectance of the sample backed by a known reflectance, Rg.

$$T_i = \sqrt{(a - R_0)^2 - b^2} \tag{7.3}$$

$$a = \frac{1}{2}\left(R + \frac{R_0 - R + R_g}{R_0 R_g}\right) \tag{7.4}$$

$$b = \sqrt{a^2 - 1} \tag{7.5}$$

7.2.3.8. Statistical analysis

Statgraphics Plus for Windows 5.1 (Manugistics Corp., Rockville, MD) was used to carry out statistical analyses of data through an analysis of variance (ANOVA). Fisher's least significant difference (LSD) was used at the 95% confidence level.

7.3. RESULTS

7.3.1. Structural properties

Figure 7.1A shows the micrographs of the cross section of some of the studied bilayer films where the two polymer layers can be clearly distinguished. PCL layer was much thinner than that of starch, despite the fact that films of similar weight were compressed together.

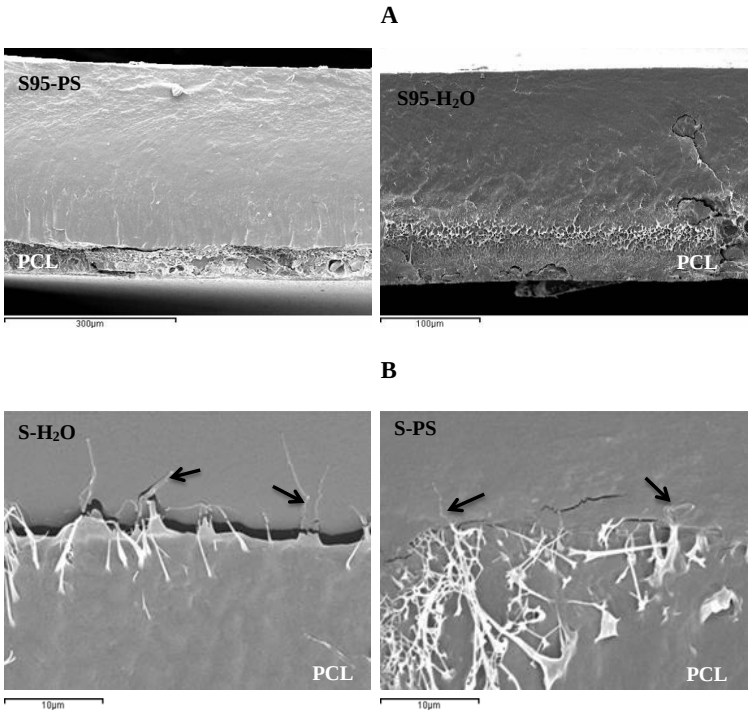

Figure 7.1.-SEM micrographs of the cross section of some bilayer films, at low (A) and high magnification levels (B) showing the layer interface.

Table 7.1 shows the thickness values of the mono- and bilayers. S and S95 bilayers showed values close to those of the initial starch monolayer, which indicated that both starch and PCL layers became thinner during the second compression.

Table 7.1.-Mean values and standard deviation of thickness, water content (g water/g dried film) and water solubility (g solubilised film/g initial dried film) of the different films stored at 53% relative humidity and 25 ºC.

Films	Thickness (µm)	X_w		Film solubility	
		Initial	Final	Initial	Final
S	261 ± 22^{bc}	0.061 ± 0.006^{b1}	0.079 ± 0.004^{d2}	0.19 ± 0.07^{d1}	0.24 ± 0.05^{d1}
S95	268 ± 13^{bc}	0.091 ± 0.007^{c1}	0.1146 ± 0.0013^{e2}	0.18 ± 0.05^{cd1}	0.198 ± 0.004^{c1}
PCL	149 ± 17^{a}	0.003 ± 0.002^{a1}	0.0021 ± 0.0005^{a1}	0.00022 ± 0.00011^{a1}	0.0004 ± 0.0002^{a1}
S-H_2O	228 ± 7^{b}	0.372 ± 0.015^{g1}	0.060 ± 0.002^{bc2}	0.30 ± 0.02^{e1}	0.21 ± 0.04^{cd2}
S-AA	236 ± 2^{b}	0.25 ± 0.02^{f1}	0.058 ± 0.008^{b2}	0.20 ± 0.05^{d1}	0.114 ± 0.010^{b2}
S-PS	234 ± 5^{b}	0.46 ± 0.04^{h1}	0.066 ± 0.004^{c2}	0.38 ± 0.05^{f1}	0.297 ± 0.014^{e2}
S95-H_2O	283 ± 30^{c}	0.20 ± 0.02^{d1}	0.067 ± 0.008^{c2}	0.114 ± 0.009^{b1}	0.107 ± 0.014^{b1}
S95-AA	322 ± 25^{d}	0.220 ± 0.012^{de1}	0.085 ± 0.002^{d2}	0.123 ± 0.012^{bc1}	0.142 ± 0.016^{b1}
S95-PS	325 ± 14^{d}	0.237 ± 0.011^{ef1}	0.0804 ± 0.0015^{d2}	0.123 ± 0.017^{bc1}	0.120 ± 0.013^{b1}

Different superscript letters within the same column indicate significant differences among formulations ($p < 0.05$). Different superscript numbers within the same row indicate significant differences due to storage time ($p < 0.05$).

However, SEM micrographs show that PCL films flow to a greater extent during the second compression step, giving rise to PCL layers of about 30-50 µm, while the starch layers barely decrease in their original thickness, especially the S95. This agrees with the higher flowability of the more plastic PCL material. At the temperature of the second compression (80ºC), the melting temperature of PCL (63.5 ºC, Ortega-Toro *et al.*, 2015) was reached, while starch (T_g: 126 ºC, Ortega-Toro *et al*., 2015) was only plasticized at surface level by the moisturising effect of the sprayed solution. The S95 bilayers were thicker which indicates that the presence of PCL in starch films decreased their ability to flow during compression. This can be attributed to the reduced water affinity of the starch phase when PCL was finely dispersed in the matrix, which inhibits the water plasticization effect of the sprayed solution. The interfacial adhesion of PCL and starch layers can be observed in Figure 7.2, where the interface of the different bilayer films is clearly

observed. Each layer shows its typical fracture appearance; pure starch exhibits a continuous and homogeneous aspect, whereas fine, well dispersed PCL particles can be observed in the S95 layer. Previous studies (Ortega-Toro *et al*., 2015) demonstrated a small degree of miscibility of PCL in starch, through the depression of the starch glass transition temperature when PCL was added.

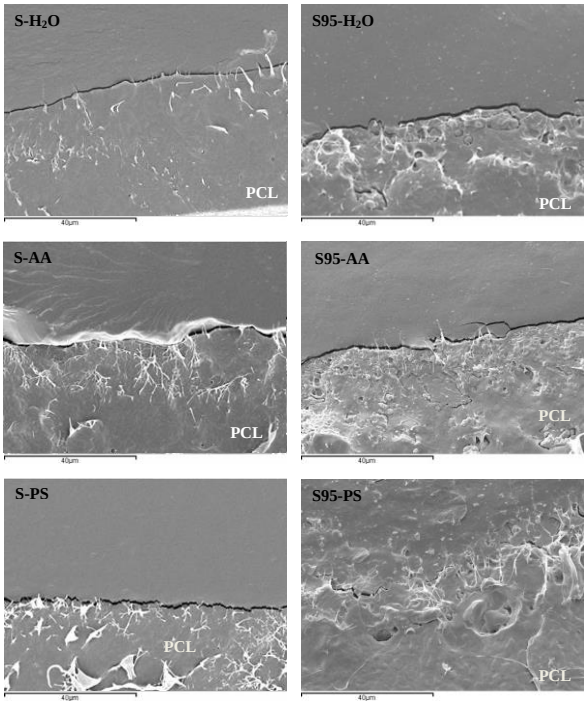

Figure 7.2.-SEM micrographs of the cross section of the different bilayer films, showing the layer interface.

PCL layers exhibit filamentous formations, associated with the plastic fracture of their amorphous zones, in agreement with the very low PCL T_g (-61.5 ºC, Averous *et al.*, 2000). At higher magnification (Figure 7.1B), the penetration of fine channels of the PCL phase (arrows) into the starch phase can be observed forming

union points between layers. This is probably favoured by the plasticization induced in the starch layer surface by the aqueous solutions sprayed before the compression step. When the starch layer contained PCL, the PCL which flows into the starch phase can bond to the dispersed, melted PCL particles, thus contributing to the layer adhesion. In Figure 7.2, greater layer adhesion can be observed in films containing S95, especially when the surface was sprayed with potassium sorbate aqueous solution, where the interface can barely be observed.

Figure 7.3 shows the infrared spectra obtained from the starch face and the wavenumber corresponding to the most characteristic peaks of the compounds. Spectra obtained from the PCL layer did not differ from that of pure PCL and they were not included. This could indicate that no significant diffusion of compounds added at the interface (AA or PS) occurred through the PCL layer, although they could act at interfacial level.

The spectra of the S95 films showed some differences with respect to those of pure starch, showing characteristic peaks of both S and PCL, with some band shifts. The carbonyl group band (C=O stretching) was shifted with respect to pure PCL, which suggests the formation of hydrogen bonds between PCL carbonyl and starch hydroxyls, as reported by other authors (Cai *et al*., 2014). Likewise, small shifts in some peaks can be detected for starch bilayers, as compared to the corresponding bands of the S or S95 monolayer films. This suggests that some changes in molecular interactions inside the starch matrix occurred, associated with the diffusion of compounds added at the interface. Shifts in bands corresponding to C-O-C (1049-1153 cm^{-1}), C=O (1724-1728 cm^{-1}) and –OH (3300-3319 cm^{-1}) can be due to the presence of small amounts of AA or PS, diffused together with water molecules inside the starch phase. The hydroxyl vibration band showed the highest shift with respect to the S or S95 films, which can be due to the higher hydration of the starch layer due to the surface wetting with the corresponding solution.

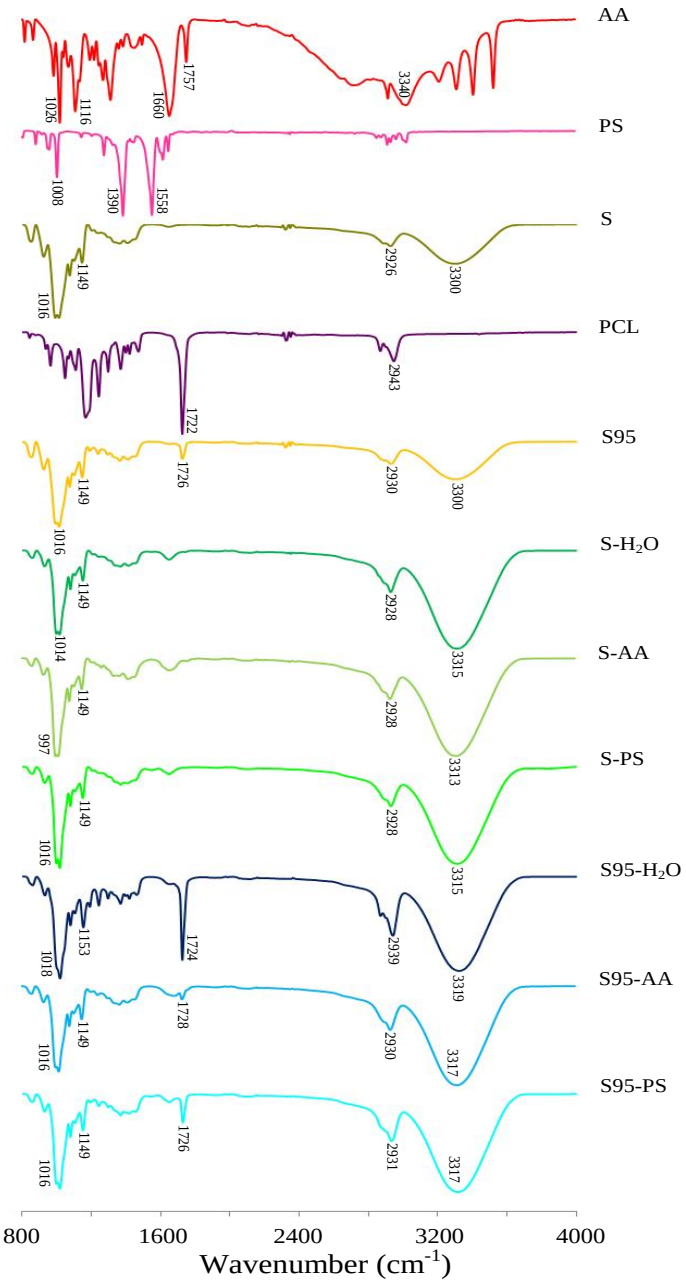

Figure 7.3.-FT-IR spectra of monolayers (S, S95 and PCL) and starch-PCL bilayers (S-H_2O, S-AA, S-SP, S95-H_2O, S95-AA, S95-SP) obtained from the starch face.

7.3.2. Thermal behaviour

Thermogravimetric analysis allows us to obtain information about the effect of compounds added at the interface on the thermal stability of polymers, due to their diffusion into the layers and potential interactions with each macromolecule. Figure 7.4 shows the DGTA curves of the bilayers, showing the peaks associated with the different weight losses caused by thermal degradation. All the curves showed three separate steps: a) small, broad peak due to evaporation of bonded water between 50 and 100 °C; b) starch thermal degradation between 283 °C and 290 °C and c) PCL thermal degradation at about 374 °C.

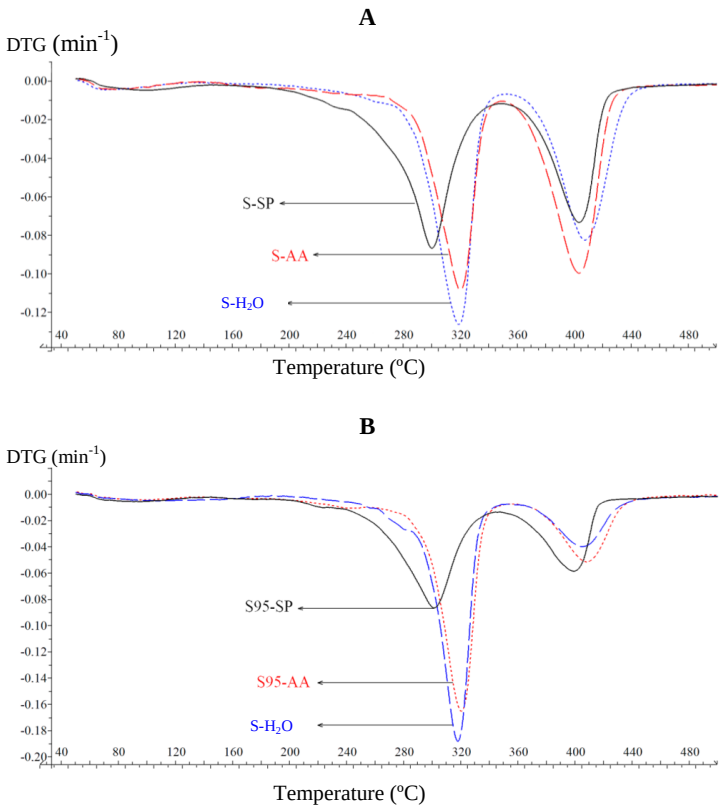

Figure 7.4.-DGTA curves of bilayer films showing peaks for starch degradation and PCL degradation. A: bilayers with S layer, B: bilayers with S95 layer.

Table 7.2 shows thermal degradation temperatures (onset and peak) of mono- and bilayer films. The PCL addition to the starch (S95 sample) provoked a significant increase ($p > 0.05$) in the starch degradation temperature (onset and peak) while the onset temperature of PCL phase also rose. This indicates that polymer interactions improved the thermal stability of both phases. In bilayers, degradation temperatures of both starch and PCL increased (more in the case of starch), except when PS was added. In these cases, the thermal degradation of polymers in bilayers occurred at a lower temperature than in the corresponding monolayer. This indicates that PS diffused from the interface inside the polymer matrices and the induced molecular interactions with both polymers affected their thermal degradation behaviour. The interactions of PS with polymer layers promoted layer adhesion, as deduced by SEM.

Table 7.2.-Mean values and standard deviation of thermal degradation of starch and PCL of the studied bilayers equilibrated at 53% relative humidity and 25 ºC.

Films	Starch		PCL	
	Onset (ºC)	Peak (ºC)	Onset (ºC)	Peak (ºC)
S	283 ± 7^{c}	313.8 ± 0.4^{b}	---	---
S95	290 ± 2^{d}	317.3 ± 1.3^{c}	383.5 ± 1.4^{e}	402.4 ± 1.1^{b}
PCL	---	---	374.1 ± 0.2^{c}	408.7 ± 0.2^{c}
S-H_2O	293.1 ± 0.8^{de}	320.92 ± 0.12^{d}	378 ± 2^{d}	410.8 ± 0.8^{d}
S-AA	293.0 ± 0.6^{de}	320.0 ± 0.2^{d}	378.0 ± 0.6^{d}	410.40 ± 0.12^{d}
S-PS	272.3 ± 0.7^{b}	299.9 ± 0.4^{a}	370.6 ± 0.6^{b}	403.4 ± 0.4^{b}
S95-H_2O	298.03 ± 0.13^{e}	319.4 ± 0.6^{d}	377.51 ± 0.11^{d}	409.90 ± 0.12^{cd}
S95-AA	295 ± 2^{de}	319.5 ± 1.2^{d}	376.5 ± 1.3^{cd}	408.9 ± 0.6^{c}
S95-PS	262 ± 2^{a}	300.9 ± 0.4^{a}	364 ± 2^{a}	399.75 ± 0.11^{a}

Different superscript letters within the same column indicate significant differences among formulations ($p < 0.05$).

As a reference, the TGA of the glycerol, AA and PS was carried out. The onset temperatures for each compound were 212 ºC, 196 ºC and 448 ºC respectively, which guarantees their stability at the temperatures used in the film

thermoprocessing (maximum 160ºC). AA and PS were only heated up to 80 ºC during the second compression. So, the antioxidant effect of AA and the antimicrobial activity of PS could be preserved after compression moulding. In fact, the pure PS showed the highest thermal stability, although it promoted the thermal degradation of starch and PCL. Flores *et al*. (2010) also reported that the PS concentration in tapioca starch–glycerol based edible films was not affected by the extrusion process and the preservative was available to act as an antimicrobial agent.

7.3.3. Physical properties

In Table 7.1, the water content and film solubility in water are also shown for all the samples conditioned at 25 °C and 53% RH for 1 and 5 weeks. At the initial time, water content of bilayers was higher than that of S or S95 films due to water absorption of the sprayed solution and their slow equilibration with the external atmosphere (53% RH). Nevertheless, after 5 storage weeks, every bilayer had similar water content (6-8%) in the range of the starch (S or S95) films.

Water solubility of S95 bilayers showed homogenous values which did not change after 5 storage weeks, whereas S bilayers showed higher solubility after 1 storage week, when they have a high moisture content, but lower solubility at 5 storage weeks when the film moisture content fell. In S95 bilayers, solubility was reduced to about half of the corresponding value of the S layer, which is coherent with the very low water solubility of the PCL layer. During the solubility test, S95 bilayers remained adhered, whereas in S bilayers, separation occurred at the edges of the films.

Figure 7.5 shows typical Stress–Hencky Strain curves of the monolayer and bilayer films after 1 week conditioned at 53% RH and 25 ºC. The S95 monolayer exhibited

lower stress values than the S layer, but greater extensibility. The addition of PCL to the starch matrix provoked a twofold effect on the mechanical response of the film: matrix plasticization effect (T_g decrease of starch) caused by the small PCL miscible fraction and matrix discontinuity due to the non-compatible PCL fraction. Both effects caused weakening of the cohesion forces of the starch phase which decreased the elastic modulus and the tensile strength, although the plasticizing effect enhanced the film stretchability. PCL is a ductile polymer with high deformability, whose deformation at break is near 500% (Averous *et al*., 2000; Matzinos *et al*., 2002), which was not reached during the tensile test.

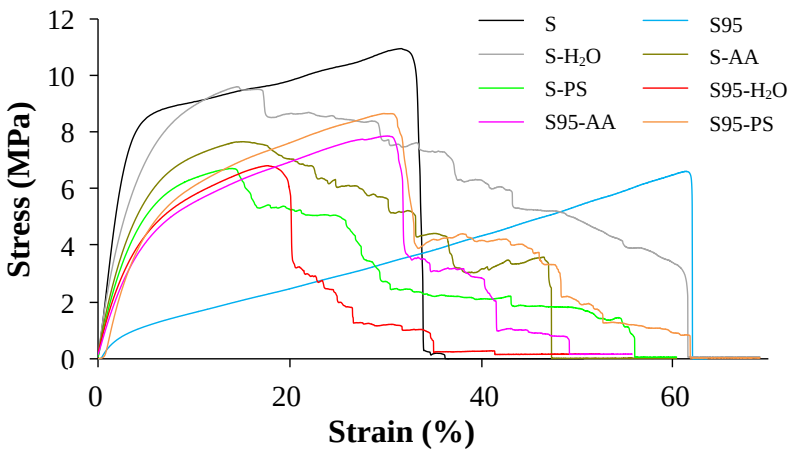

Figure 7.5.–Typical stress–Hencky strain curves of the different films conditioned at 25 ºC and 53% relative humidity for 1 week.

The bilayer films did not exhibit a net break but they showed successive micro-fractures from a determined deformation level till the total breakdown of the film. This can be associated with the progressive detachment of the film layers during the tensile test till total fracture. The value of the first fracture point was taken and

shown in Table 7.3, together with the elastic modulus and tensile strength at the first failure point.

Table 7.3.-Mean values and standard deviation of mechanical properties of films equilibrated at 53% RH and 25 ºC for 1 week (initial) and 5 weeks (final).

Films	EM (MPa)		TS (MPa)		E (%)	
	Initial	Final	Initial	Final	Initial	Final
S	324 ± 48^{e1}	587 ± 65^{e2}	10 ± 2^{d1}	15.7 ± 1.2^{e2}	28 ± 10^{c1}	4.1 ± 0.4^{a2}
S95	48 ± 10^{a1}	103 ± 10^{a2}	5.4 ± 1.5^{a1}	7.8 ± 0.7^{b2}	53 ± 5^{e1}	39 ± 5^{f2}
PCL	304 ± 11^{e1}	314 ± 51^{d1}	---	---	---	---
S-H_2O	215 ± 17^{d1}	284 ± 35^{d2}	9.1 ± 0.7^{c1}	11.9 ± 1.2^{d2}	15 ± 2^{ab1}	15 ± 5^{cd1}
S-AA	181 ± 16^{c1}	205 ± 33^{c1}	8.7 ± 1.0^{c1}	9.9 ± 0.6^{c2}	17 ± 4^{ab1}	17 ± 5^{d1}
S-PS	170 ± 16^{c1}	202 ± 18^{c2}	6.7 ± 0.6^{b1}	7.7 ± 1.0^{b2}	11 ± 5^{a1}	9 ± 4^{b1}
S95-H_2O	129 ± 17^{b1}	311 ± 14^{d2}	6.7 ± 0.6^{b1}	6.7 ± 1.0^{a1}	18 ± 5^{b1}	6.1 ± 0.6^{a2}
S95-AA	114 ± 14^{b1}	213 ± 5^{c2}	8.1 ± 0.9^{c1}	7.5 ± 0.6^{ab2}	35 ± 6^{d1}	12 ± 5^{bc2}
S95-PS	126 ± 27^{b1}	153 ± 30^{b1}	8.5 ± 1.0^{c1}	9 ± 2^{c1}	32 ± 8^{cd1}	27 ± 6^{e1}

Different superscript letters within the same column indicate significant differences among formulations ($p < 0.05$). Different superscript numbers within the same row indicate significant differences due to storage time ($p < 0.05$).

Bilayer films showed slightly lower values of EM and TS than the S or PCL monolayer but greater than the S95 monolayer, which indicates that the PCL layer reinforced the S95 bilayer films. The incorporation of AA or PS into the interface slightly decreased the EM values of bilayers, but significantly increased TS and deformation at break in the S95 bilayers. The start of layer detachment (micro-fractures) takes place at a deformation level of about 30% in S95-AA and S95-PS bilayers, which indicates that they were better adhered than in the other bilayer films when micro-fractures occurred at lower deformation levels. In S bilayers, these compounds were not so effective at promoting S-PCL adhesiveness. Therefore, the diffusion of AA and PS molecules to the PCL chains near the

interface in both PCL and S95 layers could promote stronger union forces which contribute to the layer adhesion.

After 5 weeks of storage, all the films had higher EM values, especially S monolayers, due to the phenomenon of starch retrogradation, which also reduced the film extensibility. Nevertheless, S95 maintained a deformability level of about 40% and the S95-PS bilayer did not reduce its extensibility value. This bilayer exhibited the most stable tensile behaviour, which indicates that starch chain association was mitigated by the combined effect of both PCL and PS interactions with starch chains. In general, bilayers better maintain tensile properties throughout storage time. In fact, in no case did tensile stress and deformation at break vary while EM increased in every case, except for the S95-PS samples. The increase in EM can be caused by the reduction in film water content shown in Table 7.1. The observed behaviour suggests there were positive interactions between layers inhibiting the changes in the starch phase, at least near the PCL interface.

Table 7.4 shows the water vapour permeability (WVP) and the oxygen permeability (O_2P) of the studied films conditioned at 25 °C and 53% RH for 1 and 5 weeks. In general, the WVP values of bilayers were very low, as compared with S or S95 monolayers, and similar to the PCL monolayer. This was highly positive because an effective water vapour barrier is very important in food packaging. The greater WVP of S95 than that of the S monolayer can be explained by the plasticization effect of PCL in the starch matrix, as commented on above (Ortega-Toro *et al*., 2015). After 5 weeks of storage, no notable changes in the WVP values occurred; the bilayers maintained their high water vapour barrier.

The oxygen permeability (O_2P) of starch films and bilayers was very low and in some cases they were below the sensitivity threshold of the equipment. On the contrary, the O_2P of PCL film reached the sensitivity limit. So, as expected, the barrier properties of bilayers were greatly improved with respect to the starch or

PCL films, exhibiting very low O_2P (as starch) and WVP (as PCL). As regards the influence of adding AA or PS at the interface, the most noticeable change was produced by PS, which reduces the O_2P in both S and S95 bilayers to values lower than the detection limit of the Ox-Tran® used to perform the test. This coincides with the particular interactions of PS with S and PCL, as deduced from the structural and thermal analysis.

Table 7.4.- Mean values and standard deviation of water vapour permeability (WVP) and oxygen permeability (O_2P) of the different films at 1 (Initial) and 5 (Final) weeks of storage at 53% relative humidity and 25 ºC.

Films	WVP ($g \cdot mm \cdot KPa^{-1} \cdot h^{-1} \cdot m^{-2}$)		$O_2P \cdot 10^{14}$ ($cm^3 \cdot m^{-1} \cdot s^{-1} \cdot Pa^{-1}$)	
	Initial	Final	Initial	Final
S	18.1 ± 1.4^{c1}	16 ± 2^{d1}	< D.L.	< D.L
S95	20.41 ± 0.02^{d1}	18 ± 2^{e1}	12.2 ± 0.8^{a1}	19 ± 3^{ab2}
PCL	0.120 ± 0.04^{a1}	0.117 ± 0.011^{a1}	> D.L.	> D.L
S-H_2O	0.8 ± 0.3^{ab1}	0.43 ± 0.07^{a1}	12 ± 2^{a1}	11.2 ± 1.5^{a1}
S-AA	0.71 ± 0.07^{ab1}	0.57 ± 0.07^{a1}	15 ± 2^{a1}	9 ± 3^{a1}
S-PS	0.7 ± 0.2^{ab1}	0.63 ± 0.07^{a1}	< D.L.	< D.L.
S95-H_2O	1.4 ± 0.3^{b1}	6.0 ± 0.5^{c2}	28 ± 5^{b1}	15.6 ± 1.0^{b2}
S95-AA	1.5 ± 0.6^{b1}	2.4 ± 0.9^{b1}	14 ± 3^{a1}	10 ± 2^{a1}
S95-PS	0.96 ± 0.04^{ab1}	1.24 ± 0.15^{ab2}	< D.L.	< D.L.

D.L.: 0.1-200 $cm^3/(m^2.day)$. Different superscript letters within the same column indicate significant differences among formulations ($p < 0.05$). Different superscript numbers within the same row indicate significant differences due to storage time ($p < 0.05$).

Table 7.5 shows the gloss values at 85° of both faces of the films conditioned for 1 and 5 weeks. The gloss of S and S95 films was very similar and slightly lower than that of the PCL. Likewise, the gloss of the starch and PCL faces in S bilayers was in the same range as that of the respective controls (S and PCL). However, the S95 bilayers presented lower gloss at both faces than the isolated S95 or PCL films.

This is coherent with the special role which dispersed PCL plays in S95 layers, that of favoring the layer bonding. The PCL of both S95 and PCL layers melt at 80 ºC and this contributes to compound interpenetration during the second compression, unifying itself after cooling. This melting-crystallization process of PCL at both layers could generate both more union points at the interface and micro-irregularities on each layer surface. This is a key factor in the engineering design of starch-based bilayers, because it promotes the material stability over time inhibiting the starch retrogradation, as deduced from mechanical behaviour after 5 storage weeks.

Table 7.5.-Mean values and standard deviation of surface roughness parameters and optical properties of the different films at 1 (Initial) and 5 (Final) weeks of storage at 53% relative humidity and 25 ºC.

Films	Gloss (85°). Starch face		Gloss (85°). PCL face	
	Initial	Final	Initial	Final
S	40 ± 5^{c1}	37 ± 2^{c1}	---	---
S95	47 ± 11^{cd1}	25 ± 8^{b2}	---	---
PCL	---	---	59 ± 16^{e1}	57 ± 9^{c1}
S-H_2O	41 ± 5^{c1}	38 ± 9^{c1}	52 ± 9^{cde1}	39 ± 11^{b2}
S-AA	46 ± 7^{cd1}	39 ± 6^{c2}	52 ± 7^{cde1}	38 ± 13^{b2}
S-PS	51 ± 16^{de1}	43 ± 13^{c1}	54 ± 10^{de1}	39 ± 16^{b2}
S95-H_2O	16 ± 2^{ab1}	13 ± 2^{a2}	29 ± 5^{a1}	26 ± 8^{a1}
S95-AA	13 ± 4^{a1}	15 ± 8^{a1}	24 ± 5^{a1}	19 ± 10^{a1}
S95-PS	23 ± 2^{b1}	20 ± 6^{ab1}	45 ± 7^{bc1}	41 ± 9^{b1}

Different superscript letters within the same column indicate significant differences among formulations ($p < 0.05$). Different superscript numbers within the same row indicate significant differences due to storage time ($p < 0.05$).

Figure 7.6 shows the spectral distribution curves of internal transmittance (Ti) of the films conditioned at 25 °C and 53% RH for 1 week. The results obtained, considering both starch or PCL faces as beam incidence surfaces, did not present

significant differences. So, the mean values were considered. In general, films with an isotropic structure have high Ti values since no light dispersion occurs (Villalobos *et al*., 2005; Ortega-Toro *et al*., 2014).

The S monolayer was the most transparent, whereas PCL showed a greater opacity. The S95 monolayer lost transparency with respect to the pure starch film due to the presence of a PCL dispersed phase which provoked light dispersion. Bilayers showed transparency levels in the order of those of S95, but the S95 bilayers were slightly more opaque due to the effect of dispersed PCL particles and non-isotropic bilayer formation.

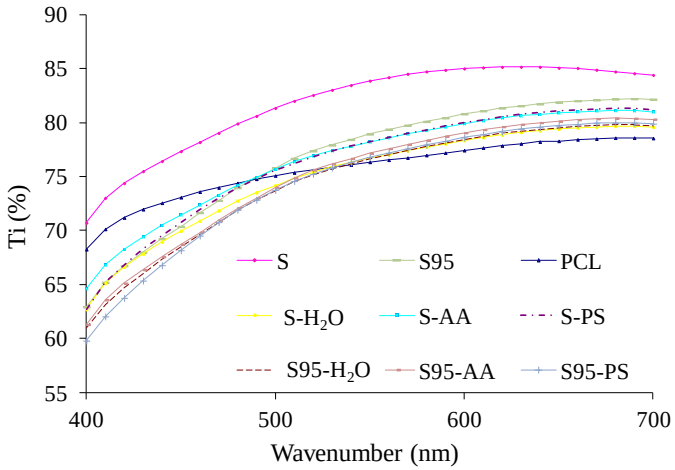

Figure 7.6.- Spectral distribution curves of internal transmittance (Ti) of the studied films conditioned at 25 °C and 53% RH for 1 week.

7.4. CONCLUSIONS

Bilayer films of thermoplastic corn starch and PCL could be obtained by compression moulding at 80ºC, by moisturising the interface with aqueous

solutions containing ascorbic acid or potassium sorbate which, in turn, can confer active properties to the films. Starch layers containing 5% PCL formed bilayers which were very well adhered with PCL and exhibited good mechanical performance, especially when potassium sorbate was added at the interface. All the bilayers showed excellent water vapour and oxygen permeability due to the association of two layers with very good barrier properties to each one. Bilayers consisting of PCL and starch containing 5% PCL, with potassium sorbate at the interface, had the best mechanical and barrier properties and interfacial adhesion while also having active properties associated with the antimicrobial action of potassium sorbate. A study of the release of this compound in different food simulants is running in order to evaluate its potential in food preservation.

7.5. REFERENCES

Alix, S., Mahieu, A., Terrie, C., Soulestin, J., Gerault, E., Feuilloley, M. G. J., Gattin, R., Edon, V., Ait-Younes, T. & Leblanc, N. (2013). Active pseudo-multilayered films from polycaprolactone and starch based matrix for food-packaging applications. European Polymer Journal, 49, 1234–1242.

American Society for Testing and Materials, ASTM E96-95. Standard test methods for water vapor transmission of materials. In annual book of ASTM. Philadelphia; 1995.

American Society for Testing and Materials, ASTM D523. Standard test method for specular gloss. In annual book of ASTM. Philadelphia; 1999.

American Society for Testing and Materials, ASTM D882. Standard test method for tensile properties of thin plastic sheeting. In annual book of ASTM. Philadelphia; 2001.

American Society for Testing and Materials, ASTM 3985-05. Standard test method for oxygen gas transmission rate through plastic film and sheeting using a coulometric sensor; 2010.

Avella, M., Errico, M. E., Laurienzo, P., Martuscelli, E., Raimo, M. & Rimedio, R. (2000). Preparation and characterization of compatibilised polycaprolactone/starch composites. Polymer, 41, 3875–3881.

Averous, L., Moro, L., Dole, P., & Fringant, C. (2000). Properties of thermoplastic blends: starch polycaprolactone. Polymer, 41(11), 4157-4167.

Ayranci, E. & Tunc, S. (2003). A method for the measurement of the oxygen permeability and the development of edible films to reduce the rate of oxidative reactions in fresh foods. Food Chemistry, 80, 423–431.

Bastioli, C. (2001). Global status of the production of biobased packaging materials. Starch/Stärke, 53, 351-355.

Cai, J., Xiong, Z., Zhou, M., Tan, J., Zeng, F., Ma, M., Lin, S., & Xiong, H. (2014). Thermal properties and crystallization behavior of thermoplasticstarch/poly(ε-caprolactone) composites. Carbohydrate Polymers, 102, 746–754.

Cian, R. E., Salgado, P. R., Drago, S. R., González, R. J., & Mauri, A. N. (2014). Development of naturally activated edible films with antioxidant properties prepared from red seaweed Porphyra columbina biopolymers. Food Chemistry, 146, 6–14.

Fabra, M. J., Busolo, M. A., Lopez-Rubio, A. & Lagaron, J. M. (2013). Nanostructured biolayers in food packaging. Trends in Food Science & Technology, 31, 79–87.

Fang, J. M., Fowler, P. A., Escrig, C., Gonzalez, R., Costa, J. A. & Chamudis, L. (2005). Development of biodegradable laminate films derived from naturally occurring carbohydrate polymers. Carbohydrate Polymers, 60, 39-42.

Flores, S. K., Costa, D., Yamashita, F., Gerschenson, L. N., & Grossmann, M. V. (2010). Mixture design for evaluation of potassium sorbate and xanthan gum effect on properties of tapioca starch films obtained by extrusion. Materials Science and Engineering C, 30, 196-202.

Gómez-Guillén, M. C., Ihl, M., Bifani, V., Silva, A. & Montero, P. (2007). Edible films made from tuna-fish gelatin with antioxidant extracts of two different murta ecotypes leaves (*Ugni molinae* Turcz). Food Hydrocolloids, 21(7), 1133-1143.

Jiménez, A., Fabra, M. J., Talens, P. & Chiralt, A. (2012). Edible and Biodegradable Starch Films: A Review. Food Bioprocessing Technology, 5, 2058 -2076.

Jiménez, A., Fabra, M. J., Talens, P. & Chiralt, A. (2013). Physical properties and antioxidant capacity of starch–sodium caseinate films containing lipids. Journal of Food Engineering, 116(3), 695-702.

Matzinos, P., Tserki, V., Kontoyiannis, A. & Panayiotou, C. (2002). Processing and characterization of starch/polycaprolactone products. Polymer Degradation and Stability, 77, 17-24.

McHugh, T.H., Avena-Bustillos, R., & Krochta, J.M. (1993). Hydrophilic edible films-Modified procedure for water-vapor permeability and explanation of thickness effects. Journal of Food Science, 58(4), 899–903.

Mensitieri, G., Di Maio, E., Buonocuore, G. G., Nedi, I., Oliviero, M., Sansone, L. & Iannace, S. (2011). Processing and shelf life issues of selected food packaging materials and structures from renewable resources. Trends in Food Science and Technology, 22, 72–80.

Ortega-Toro, R., Jiménez, A., Talens, P., & Chiralt, A. (2014). Properties of starch-hydroxypropyl methylcellulose based films obtained by compression molding. Carbohydrate Polymers, 109(30), 155–165**.**

Ortega-Toro, R., Collazo-Bigliardi, S., Talens, P., & Chiralt, A. (2015). Influence of citric acid on the properties and stability of starch-polycaprolactone based films. Journal of Applied Polymer Science. DOI: 10.1002/app.42220.

Takala, P. N., Salmieri, S., Boumail, A., Khan, R. A., Dang Vu, K., Chauve, G., Bouchard, J. & Lacroix, M. (2013). Antimicrobial effect and physicochemical properties of bioactive trilayer polycaprolactone/methylcellulose-based films on the growth of foodborne pathogens and total microbiota in fresh broccoli. Journal of Food Engineering, 116, 648-655.

Villalobos, R., Chanona, J., Hernández, P., Gutiérrez, G. & Chiralt, A. (2005). Gloss and transparency of hydroxypropyl methylcellulose films containing surfactants as affected by their microstructure. Food Hydrocolloids, 19(1), 53 – 61.

Wang, H., Sun, X. & Seib, P. (2001). Strengthening blends of poly(lactic acid) and starch with methylenediphenyl diisocyanate. Journal of Applied Polymer Science, 82, 1761-1767.

Wook, S., Kie, J., Selke, S., Soto-Valdez, H., Matuana, L., Rubino, M. & Auras, R. (2013). Migration of α-tocopherol and resveratrol from poly(L-lactid acid)/starch blends films into ethanol. Journal of Food Engineering, 116: 814-828.

Yu, L., Dean, K. & Bi, L. (2006). Polymer blends and composites from renewable resources. Progress in Polymer Science, 31, 576 – 602.

Zhang, J. F. & Sun, X. (2004). Mechanical and Thermal Properties of Poly(lactic acid)/Starch Blends with Dioctyl Maleate. Journal of Applied Polymer Science, 94, 1697-1704.

IV. GENERAL DISCUSSION

Among biodegradable materials to obtain packing films, starch is one of the most promising polymers, due to its low cost, thermo-processability, and abundance. Starch based-films exhibit some desirable properties, such as high barrier to oxygen, carbon dioxide and lipids, which represent an advantage in food packaging. However, these materials present several drawbacks such as their high water sensitivity and WVP, poor mechanical properties and retrogradation throughout storage. The improvement of these characteristics is necessary for starch applications in the plastics industry.

The present Doctoral Thesis deals with the enhancement of starch-based materials by blending with other compounds and polymers more hydrophobic than the starch in order to decrease the water sensitivity of the blends, to promote their water vapour barrier properties and time stability, while improving mechanical performance. For this purpose, different techniques of processing were used.

One of the most important parameters in food packaging is the barrier properties of the materials. The Figure IV.1 shows a map of barrier properties (WVTR vs.: O_2TR) where the studied starch film formulations, obtained by different methods, were located in order to compare them. The values are normalized at 100 µm of thickness. The values of barrier properties were affected by both the formulation and the processing method. The use of different formulations and techniques of processing resulted in enormous changes in water vapour barrier properties: from ~2500 g water vapour$\cdot m^{-2}\cdot day^{-1}$ in films prepared by casting to ~10 g water vapour$\cdot m^{-2}\cdot day^{-1}$ in bilayers and films compatibilized with PCL_{-g}. In the same way, the O_2TR decreased from ~30 $cm^3\cdot m^{-2}\cdot day^{-1}\cdot bar^{-1}$ (films by casting) until ~0.1 $cm^3\cdot m^{-2}\cdot day^{-1}\cdot bar^{-1}$ (bilayers and films obtained by melt blending and compression moulding).

The starch-based films with worst barrier properties were those obtained by casting. In these films, weaker intermolecular interactions seem to be done in line

with the film elaboration method. When the film forming dispersions were cast, water was evaporated slowly giving rise to a less compact matrix as compared with the starch matrices obtained by thermo-mechanic methods (melt blending, compression moulding and extrusion).

The starch blends with HPMC or PCL and the addition of CA and PEG promoted some changes in barrier properties, although, in most of the cases, an enhancement in WVP implied a worst O_2P. This effect was caused by the presence of more hydrophobic dispersed phases with higher oxygen permeability, which facilitated the transfer of gas molecules through the matrix.

The more efficient methods for improving the barrier properties, especially WVP, were the formation of bilayer films with starch based and PCL layers and the use of PCL_{-g} as compatibilizers between TPS and PCL phases in the blend films. In Figure IV.1 the good barrier properties of bilayer films can be observed. They maintain the low O_2TR values of the starch films, but with highly improved WVP due to the parallel arrangement of PCL and starch layers, in perpendicular sense to mass transfer rate. Likewise, the starch-PCL blends compatibilized with PCL_{-g}, obtained by extrusion and compression moulding, exhibited the best water vapour barrier properties. These results were due to the compatibilizing role of PCL_{-g} at interfacial level in starch and PCL phases, which during extrusion of the blend promoted the interfacial adhesion of both polymers.

In the Figure IV.1 the differences in barrier properties of glycerol plasticized net starch films obtained by casting (25% glycerol) melt blending (30% glycerol) and extrusion (30% glycerol) can be observed, despite that these formulations had similar composition. Dry methods (melt blending, extrusion and compression moulding) gave rise to the formation of a more compact starch matrix in comparison to casting method, which enhanced film barrier properties. This could be attributed to the compression process conditions, which leads to greater

approximation of the starch chains and more densely packed matrix. When S and S80 films obtained by melt blending in the roller mill or extrusion were compared, differences in barrier properties were also observed (Figure IV.1). Extrusion led to a notable reduction in WVP of both S and S80 films and lower oxygen permeability for S80, but higher for S films. Melt blending in the roller mill was less efficient than extrusion for defining a closer polymer matrix probably due to the higher temperature, pressure and shear in the screw which induce differences in the chain packing of the melts, thus affecting mass transfer properties.

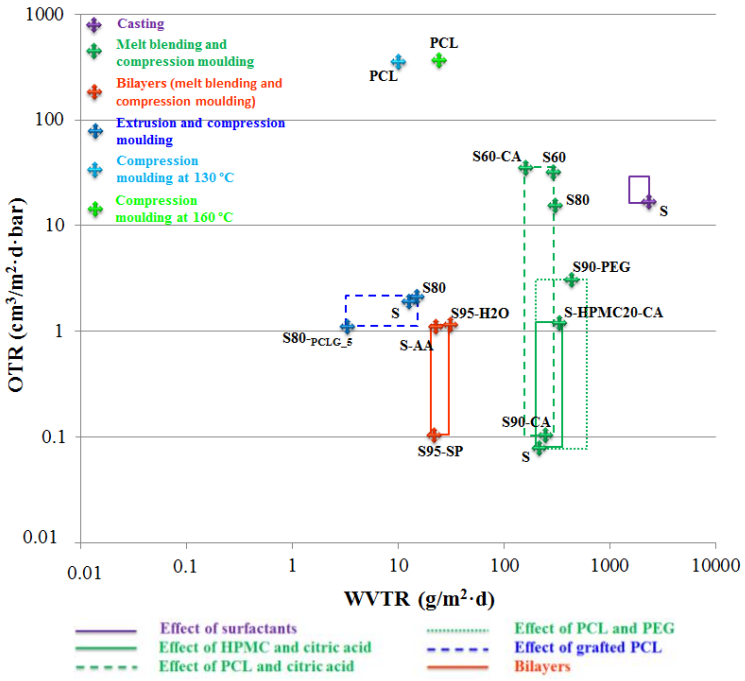

Figure IV.1.-Map showing barrier properties of starch-based films with different formulation, obtained by different methods.

Figure IV.2 shows the map of barrier properties, showing the characteristic location of some plastics commonly used in food packaging, for comparisons.

Likewise, the zones which define the requirements in barrier properties of different foods are plotted (pink dashed areas).

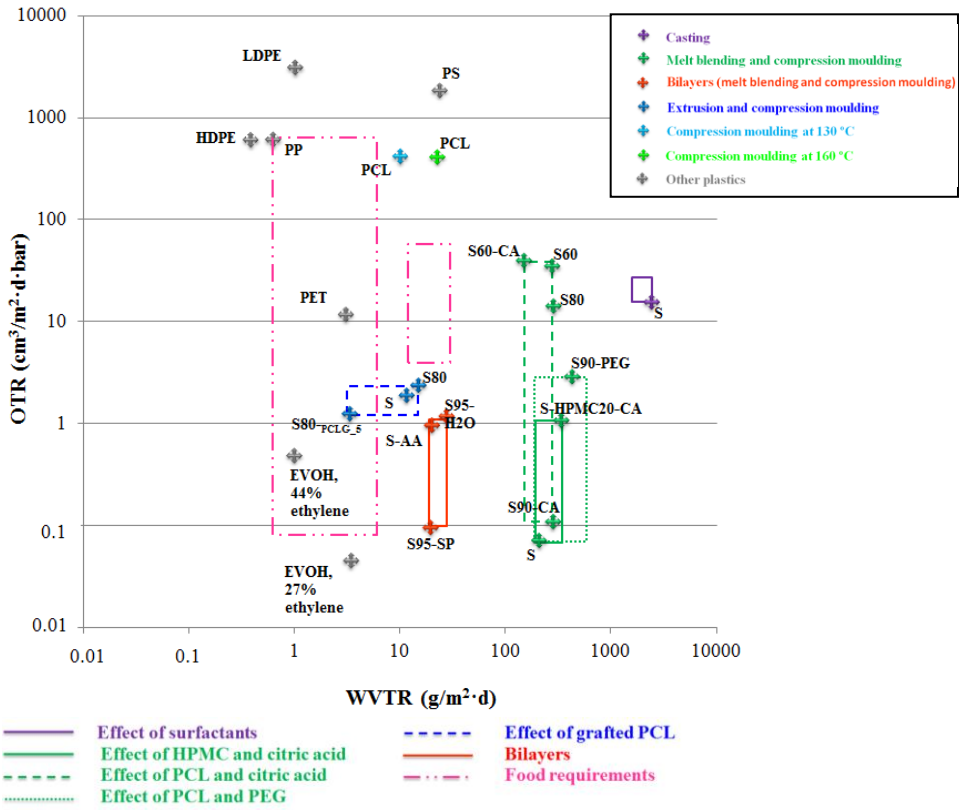

Figure IV.2.-Map of barrier properties showing the developed films, some commonly used plastics in food packaging and barrier requirement ranges for some foods.

The bilayer films and blends compatibilized with PCL_{-g} (ternary blends) showed values of barrier properties in the range of some commonly used plastics. As concerns WVTR, these films meet the packaging requirements of some foods (Schmid *et al.*, 2012) such as meat and MAP products (10-50 g water-vapour·m^{-2}·day^{-1}). Even more, some formulations exhibit WVTR values around 5 g·m^{-2}·day^{-}

[1], meeting the requirements of nuts, snacks and coffee vacuum. Meanwhile, the O_2TR of these starch-based materials reached the highest requirements for food packaging (around 1 cm^3 oxygen·m^{-2}·day^{-1}·bar^{-1}). These materials exhibited comparable O_2TR values to Ethylene Vinyl Alcohol (EVOH) and Polyethylene Terephthalate (PET) while their WVTR were close to Polystyrene (PS) and PET.

Mechanical properties of the films were also affected by the formulation and process conditions. Figure IV.3 shows a map of mechanical properties where starch-based films obtained by different methods, conditioned for 5 weeks were plotted. The principal effects of components in the different formulations were:

- Effect of surfactants: films containing surfactants were less hard, resistant and extensible than surfactant-free films.
- Effect of HPMC and CA: CA provoked a mild hardening effect in the films; while extensibility greatly decreased due to a weak cross-linking effect, which seems to increase during film storage to a greater extent in films with the highest ratio of HPMC.
- Effect of PCL and CA: the lack of interfacial adhesion of the PCL and starch phases promoted the films' fragility, although small PCL ratios increased the elastic modulus of the films. Blend films with a 90:10 starch-PCL ratio with CA exhibited high stretchability and good mechanical resistance. Plasticized starch films could incorporate 5% PCL without a notable phase separation, leading to the improved stretchability and storage stability of the films.
- Effect of PCL and PEG: the incorporation of PEG to the starch/PCL blends reduced the affinity starch-PCL, enhancing phase separation, although PEG acts as plasticizer of net starch films.
- Effect of grafted PCL: Interfacial adhesion of starch and PCL was greatly improved when PCL_{-g} was present in the blends giving rise to tight matrices.

As a result, an improvement on mechanical performance and stability was obtained.

- Effect of PCL and potassium sorbate in bilayer films: starch layers containing 5% PCL formed bilayers which were very well adhered with PCL and exhibited good mechanical performance, especially when potassium sorbate was added at the interface.

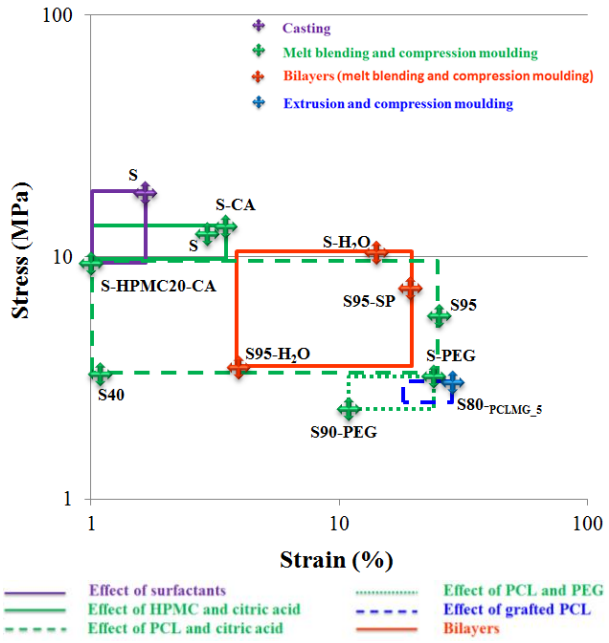

Figure IV.3.-Map of mechanical properties where starch-based films obtained by different methods and formulation are plotted.

Mechanical properties were also affected by the processing method. As an example, Figure IV.4 shows the comparison of the mechanical properties of S and S80 (S-PCL blend) formulations obtained by two different methods:

- Melt blending in a roller mill (160 ºC and 8 rpm for 30 min) and compression moulding (160 ºC for 5 min on preheating; then compressed at 160 °C for 2 min at 30 bars, followed by 6 min at 130 bars; cooling cycle applied for 4 min).
- Extrusion (temperature profile from hopper to die: 60, 90, 110, 120 and 110 °C and the residence time was about 5 min) and compression moulding (pre-heated at 130 °C for 2 min; then compressed for 2 min at 90 bares, followed by 2 min at 220 bares; cooling cycle, applied for 8 min).

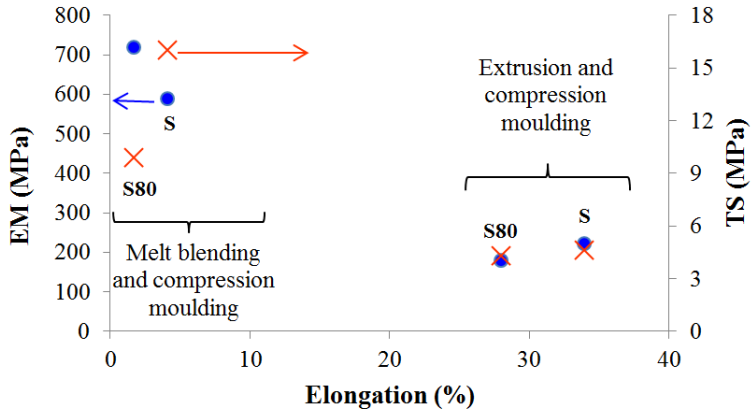

Figure IV.4.-Mechanical properties of S and S80 films obtained by different processing methods.

Melt blending in the roller mill promoted the formation of more dense and rigid matrices probably due to the greater water evaporation during blending and a different arrangement of chains according with the applied shear forces. In extrusion process, water evaporation was more limited due to the different temperature profile along the screw (closed systems), while shear forces are promoted by pressure. As a result, the higher bonded water (plasticizer) in the

matrices obtained by extrusion and subsequent compression moulding exhibited higher values of elongation and lower values of EM and TS. This fact is supported by FTIR spectra of the starch-based films: the broad peak occurring at about 1646 cm^{-1}, ascribed to the tightly bound water of starch, appeared in samples extruded (Figure 6.5) but not in films blended in the roller mill (Figure 5.4).

Figure IV.5 shows the comparison between the mechanical properties of starch-based films and some commonly used polymers for food packaging.

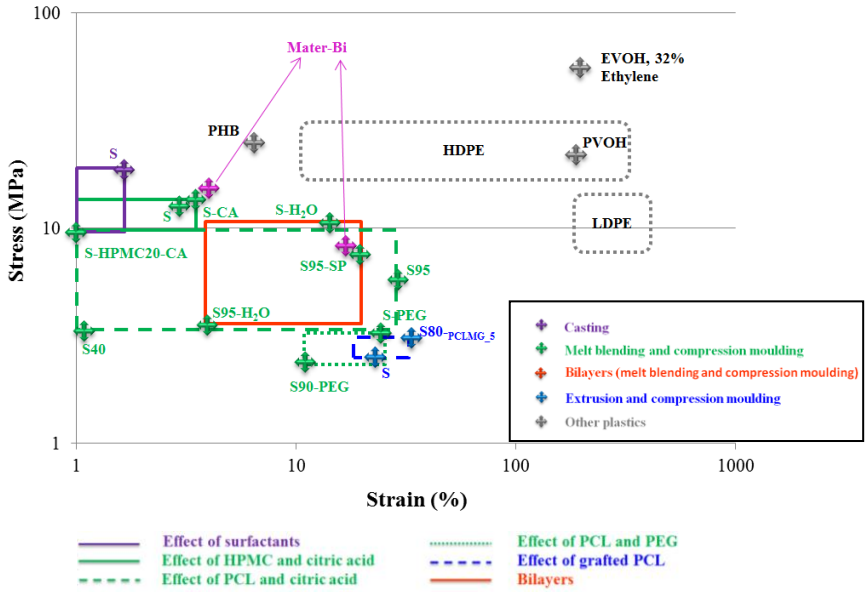

Figure IV.5- Map of mechanical properties showing the location of developed starch-based films and some commonly used polymers for food packaging.

Other polymers such as EVOH, Poly(Vinyl Alcohol) (PVOH) and Low Density Polyethylene (LDPE) exhibit greater stretchability and tensile strength than starch-based polymers. However, a fraction of High Density Polyethylene (HDPE) materials shows similar properties. On the other hand, biodegradable polymers

such as PHB and Mater-Bi (commercial starch-based polymer) have close mechanical properties. So, mechanical and barrier properties of the obtained film formulations indicate that some of them have potential applications in food packaging.

As concerns retrogradation phenomena throughout time in the developed starch films, some formulations were able to limit these undesirable changes which lead to a decrease in film elongation and an increase the film brittleness. The Figure 2.1 showed SEM micrographs of films with and without HPMC and CA at 1 and 5 weeks of storage. The retrogradation of starch chains was remarkable in net starch films while the addition of HPMC and CA promoted a decrease in the retrogradation. As concerns the PCL blends, the partial miscibility between starch and PCL led to a partial inhibition of amylose retrogradation during storage. This effect was more marked when small amounts of PCL were added (5% wt.). The Figure 5.5 showed that the S-PCL5 films did not exhibit relevant changes in their mechanical properties throughout time. In the same way, the incorporation of PEG to net starch films promoted the stability of their mechanical properties (Figure 5.5). Retrogradation was also inhibited when the S-PCL interfacial adhesion was improved by using PCL_{-g} as compatibilizer. The Table 6.4 showed the mechanical properties of starch-based films containing PCL and PCL_{-g}. In these ternary blends, the elongation increased and the elastic modulus decreased during the storage time, this behaviour being contrary to the retrogradation effects. As regards bilayer films, the addition of potassium sorbate at the interface decreased the retrogradation, as deduced from the development of mechanical properties during the film storage time.

V. CONCLUSIONS

1. Incorporation of span 40, 60 or 80 into the corn starch-glycerol film forming dispersions led to different particle size distribution, zeta potential, viscosity and extensibility on other films, depending on their hydrophobicity and melting properties (related with the unsaturation in the fatty acid chain). These aspects affected the final film microstructure and its surface morphology, since the growing of the surfactant molecule aggregates during the film drying (loss of water availability) occurred to a different extent, depending on the dispersion stability. When the surfactant melting temperature was the highest (span 60), creaming of surfactants in the film surface was not observed and the size of the final lipid aggregates in the film were lower. Likewise, the size of the type-V crystalline amylose complexes was smaller for the surfactant with the highest HLB value with saturated fatty acid (span 40). This contributed to decrease the WVP values with respect to surfactant-free film. Nevertheless, films containing surfactants were less hard, resistant and extensible than surfactant-free films, but they did not notably affect the film gloss and transparency. The use of surfactants in film formulation can be useful to incorporate non-polar bioactive compounds in the aqueous film forming dispersions. In this sense, the obtained results allow us to recommend saturated fatty acid compounds with higher melting temperature to ensure a finer microstructure in the final film which favour water barrier efficiency.

2. Corn starch films containing HPMC (10 and 20%, with respect to starch) obtained by compression molding showed a dispersed phase of HPMC in a continuous starch-rich phase with a lower glass transition than HPMC-free films. The addition of citric acid as a compatibilizer also provoked a decrease in glass transition in line with a depolymerisation effect brought about by acid hydrolysis. Both components implied a decrease in the water vapour permeability but a slight increase in oxygen permeability. Although citric acid

provoked a mild hardening effect in the films, it greatly decreased extensibility pointing to a weak cross-linking effect, which seems to increase during film storage to a greater extent in films with the highest ratio of HPMC. Starch crystallization was slightly modified by both components which induce the formation of other polymorphs mainly at initial time (1 storage week). Starch crystallization during storage was inhibited by both citric acid and HPMC. A greater ratio of citric acid could be interesting as a means of promoting both a more significant cross-linking effect and greater HPMC compatibility with starch.

3. Corn starch and PCL blend films, containing 30% glycerol with respect to starch, could be obtained by compression moulding at 160ºC and 130 bars. The films showed phase separation of the polymers, exhibiting a heterogeneous blend matrix where starch- rich regions and PCL- rich regions could be observed. Nevertheless, a small degree of PCL miscibility in the starch phase was detected through the shift in the glass transition temperature of the starch phase, which leads to the partial inhibition of amylose retrogradation during film formation and storage. The lack of interfacial adhesion of the PCL and starch phases promoted the films' fragility and reduced their elongation, although small PCL ratios increased the elastic modulus of the films, indicating its adequate properties as reinforcing filler in starch matrices. Water barrier properties of starch films were improved as the PCL increased in the blend but worsening of the oxygen barrier properties was obtained. Bilayer films with both PCL and starch blend layers could meet the requirements for packaging of some foods such as meat and MAP products. Nevertheless, the overall migration in different food simulants must be assessed, according to migration limits established by regulation for plastic materials in contact with food.

4. Citric acid improves the properties of corn starch-PCL blend films with a low PCL ratio (S:PCL ratio of 90:10), while it was not effective at compabilizing blends with higher amounts of PCL. This was observed in the microstructural analyses and deduced from the film's physicochemical properties. The incorporation of CA in the films affected both starch and PCL crystallization as deduced from the X-ray diffraction patterns of starch and PCL melting enthalpy values. The glass transition of starch was reduced by the incorporation of PCL in line with its partial solubilization in the starch phase, but lower than 10% with respect to starch. This decrease was greater in the presence of citric acid. So, citric acid promoted stronger interactions between PCL and starch chains, although this only quantitatively benefited the film properties at a low PCL ratio. In fact, blend films with a 90:10 starch-PCL ratio with citric acid exhibited the highest stretchability, with good mechanical resistance. The water solubility of the films increased when they contained citric acid, due to the acid hydrolysis of starch, although the water transfer rate was limited in blend films. Citric acid did not affect the barrier properties of the blend films which showed intermediate values, between those of net starch and PCL films, according to their ratio in the film. So, compounding starch with small amounts of PCL, using glycerol and citric acid, can supply films with better functional properties than net starch films.
5. Glycerol plasticized starch films could incorporate 5% PCL without a notable phase separation, leading to the improved stretchability and storage stability of the films. Blend films with 10% PCL exhibited clear phase separation and poor starch-PCL interactions which did not improve the starch tensile properties, although the film water vapour permeability was reduced. In ternary systems with PEG, the total balance of molecular interactions reduced the PCL-starch affinity, enhancing phase separation. They did not exhibit improved film properties with respect to starch films. PEG partly separates

from the glycerol plasticized starch matrix, crystallising after long storage times.

6. Grafting of MA-GMA blend or net GMA to PCL allow us to obtain good compatibilizers (PCL-g) to obtain starch-PCL blend films, with high ratio of starch, with good mechanical performance and stability and high barrier properties, useful to cover the food packaging requirements. Grafting degree was 4.5 and 4 wt%, for GMA-MA blend and GMA, respectively. Interfacial adhesion of both polymers was greatly improved when PCL-g is present in the blends which give rise to tight matrices. Compatibilizers acted as nucleating agents for PCL crystallization, affecting the crystallization degree on the blends. Properties of the starch-PCL-g blend films were poor than those of ternary systems of starch-PCL blends with only 2-5% of PCL-g, which represent an advantage from the economic point of view. The materials developed have comparable gas and water vapour properties usual synthetic plastics for food packaging. The overall migration in different food simulants must be assessed, according to migration limits established by regulation for plastic materials in contact with food.
7. Bilayer films of thermoplastic corn starch and PCL could be obtained by compression molding at 80ºC, by moisturising the interface with aqueous solutions containing ascorbic acid or potassium sorbate which, in turn, can confer active properties to the films. Starch layers containing 5% PCL formed bilayers which were very well adhered with PCL and exhibited good mechanical performance, especially when potassium sorbate was added at the interface. All the bilayers showed excellent water vapour and oxygen permeability due to the association of two layers with very good barrier properties to each one. Bilayers consisting of PCL and starch containing 5% PCL, with potassium sorbate at the interface, had the best mechanical and barrier properties and interfacial adhesion while also having active properties

associated with the antimicrobial action of potassium sorbate. A study of the release of this compound in different food simulants is running in order to evaluate its potential in food preservation.